Investigating the consequence of chromosome abnormalities arising during pre-implantation development of the mouse

Helen Louise Bolton

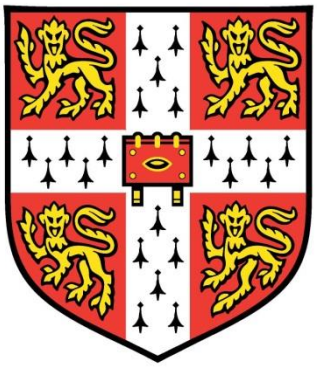

Gonville & Caius College

University of Cambridge

This dissertation is submitted for the degree of Doctor of Philosophy

Declaration

This dissertation is the result of my own work and incudes nothing which is the outcome of work undertaken in collaboration except where specifically indicated in the text. This dissertation does not exceed the word limit prescribed by the Degree Committee.

Helen Louise Bolton

Acknowledgements

I would like to thank my supervisor Magdalena Zernicka-Goetz for the opportunity to work within her laboratory and for her contribution to the project.

I am enormously grateful to my sponsor Professor David Lomas who maintained his faith in me, provided me with indefatigable support and commitment throughout the highs and lows of the Fellowship, and kept me laughing along the way. He is an exceptional individual and is the inspiration behind our youngest son's middle name. I also wish to offer my sincere gratitude for those who have informally offered mentorship and advice: in particular to my dear friend and colleague Dr Alexander Bruce. Thank you too to Dr Krzysztof Wicher for shared wisdom and calm practical support. I also wish to thank Professor Gordon Smith for mentorship and guidance and also Professor Martin Johnson for support and interest. I am grateful to the Wellcome Trust who generously sponsored the Fellowship.

I wish to thank all those who kindly helped me with the project. In particular to Alexander Bruce and Krzysztof Wicher for sharing their molecular biological expertise, both practical and intellectual; Agnieszka Jedrusik for her exceptional embryology expertise (and great friendship), Richard Butler for assisting in the development of an imaging processing plugin, Willem Rens for assistance with karyotyping, Bernhard Strauss for his help with the practical aspects of imaging (and the rest!), and to Yaron Galanty, Rimma Belotserkovskaya and Jessica Brown for their advice and assistance with the DNA damage experiments. I also wish to thank William Mansfield and Charles-Etienne Dumeau for assistance with embryo transfer experiments and their high professional standards. Finally, to all who offered help and advice with my experiments when they did not go to plan – thank you. I wish also to acknowledge the core staff in the Gurdon Institute, for being instrumental in making the Institute a first-class environment to work in. For enjoyable and productive collaborations I wish to thank Dr Thierry Voet for the array-based karyotyping experiments and also Aisha Elaimi together with Joyce Harper for FISH experiments.

Thank you to a wonderful team of laboratory companions, both past and present, many of whom have become life-long friends (in no particular order): Alexander Bruce, Agnieszka Jedrusik, Maria Skamagki, Krzysztof Wicher, Emlyn Parfitt, Bernhard Strauss, Seema Grewal, Paula Almeido Coelho, Anna Adjuk, Samantha Morris, Sarah Graham, Florencia Barrios-Abraham, Stoyana Alexandrova, Marayna Panamoarova, Rui Pires-Martin, Bedra Sharif, Monicka Bialecka, Mubeen Goolam, Chuen Yan Leung and Ivan Bedzhov. We have shared many ups and downs together, and much laughter!

This thesis would not be complete without reference to the two most exceptional embryos that developed during the course of this Fellowship; my two beautiful little sons Tobias and Cosmo. Although these embryos were unable to contribute to any of the data presented in the thesis, they provided me with indescribable joy that helped me to maintain a balance through some of the more difficult moments I experienced. Thank you boys!

To my wonderful family, in particular my parents John and Jennifer who have made me who I am today, and together with my two sisters Catherine and Rachael, I am indebted to each of you for your unfaltering support and faith in me - thank you. Finally, this thesis is dedicated to my dear husband Mark, my soul mate, who has offered me nothing but unconditional love and resolute support throughout.

INVESTIGATING THE CONSEQUENCES OF CHROMOSOME ABNORMALITIES ARISING DURING PRE-IMPLANTATION DEVELOPMENT OF THE MOUSE

SUMMARY

The majority of human pre-implantation embryos created through *in vitro* fertilization (IVF) are mosaic as they are constituted of a mixture of diploid and aneuploid cells. Chromosome abnormalities are widely believed to contribute towards the relatively low success rates of IVF treatment. Consequently major efforts have been undertaken to develop effective tools to aid the selection of embryos with minimal abnormalities with the aim of improving clinical outcomes. However, the ultimate fate of mosaic embryos is not known. Human embryo research is limited by practical and ethical constraints, and directly relevant animal studies are sparse.

To circumvent many of these limitations, a mouse model for pre-implantation chromosome mosaicism was developed. Acute chromosome segregation errors were induced in cleavage stage mouse blastomeres by bypassing the spindle assembly checkpoint (SAC). This model was used to investigate the fate of abnormal cells within the developing pre-implantation embryo, and the ultimate developmental outcome of mosaic embryos.

Time-lapse imaging of pre-implantation development revealed that cells with chromosome abnormalities were progressively depleted during blastocyst maturation; inner cell mass (ICM) cells exhibited higher rates of apoptosis, while in the trophectoderm (TE) lineage effects on the cell-cycle predominated. Depletion continued throughout post-implantation development. Significantly, the presence of a critical number of control blastomeres within the embryo could rescue the early post-implantation lethality that occurred in embryos containing high rates of abnormalities. Thus it was demonstrated that mosaic embryos can achieve full developmental potential and that abnormal cells are progressively depleted as development proceeds.

Finally, the mechanisms responsible for eliminating the abnormal cells from the embryo were investigated, revealing that embryos containing chromosome abnormalities may have increased metabolic requirements which could contribute to their clonal depletion; a feature previously characterised in aneuploid cells in the context of cancer research.

CONTENTS

LIST OF FIGURES

Chapter I - Introduction

Chapter II -Results I

Chapter III - Results II

LIST OF ABBREVIATIONS

AA – Amino Acids
ACA – Anti-Centromere Antibodies
APC – Anaphase Promoting Complex
AT – Acid Tyrode's Solution
ATM – Ataxia Telangiectasia Mutated
BAC – Bacterial Artificial Chromosome
BC - Blastocyst
53Bp1 – Tumour Protein P53 Binding Protein 1 (Tp53bp1)
BRCA1 – Breast Cancer 1 Gene
BSA – Bovine Serum Albumin
Bubr1- Budding Uninhibited By Benzimidazoles 1 (Bub1b)
Bubr1_DN - Benzimidazoles 1 (Bub1b) Dominant Negative
Casc5–Cancer Susceptibility Candidate Gene 5
C-C – Control-Control Chimeras
Cdc20 – Cell-Division Cycle Protein 20
cDNA – Complementary DNA
Cdx2 - Caudal Type Homeobox 2
CENPB – Centromere Associated Protein B
CGH – Comparative Genomic Hybridisation
CIN – Chromosome Instability
CPM – Confined Placental Mosaicism
CVS – Chorionic Villous Sampling
DAPI - 4',6-Diamidino-2-Phenylindole Dihydrochloride
DDR – DNA Damage Response
DIC - Differential Interference Contrast
DMEM – Dulbecco's Modified Eagle Medium
DMSO – Dimethyl Sulfoxide
DN – Dominant Negative
dpc – Days Postcoitum
dsDNA – Double Stranded DNA
dsRed – *Discosoma sp.* Red Fluorescent Protein
E13.5 – Embryonic Day 13.5 (substitute timings accordingly)
EAA – Essential Amino Acids
Eomes - Eomesoderm
ES cells – Embryonic Stem Cells
EPI – Epiblast
FCS - Fetal Calf Serum
Fgf4 - Fibroblast growth factor 4
FITC –Fluorescein Isothiocyanate
FISH – Fluorescent In-Situ Hybridisation
GFP – Green Fluorescent Protein
H – Histone Family Proteins
HA – Haemagglutinin
γH2AX – H2A Histone Family, Member X (phosphorylated at serine residue 139)
hCG – Human Chorionic Gonadotrophin
hES cells – Human Embryonic Stem Cells
H4K20me2 – Dimethylation of Histone4 At Lysine Residue 20
H_2O_2 – Hydrogen Peroxide
ICC - Immunocytochemistry
ICM – Inner Cell Mass
ICSI – Intra-Cytoplasmic Sperm Injection
IF – Immunofluorescence
IR – Ionizing Radiation
IRIF – Ionizing Radiation-Induced Foci
IVF – *In Vitro* Fertilization
IVT – *In Vitro* Transcription
LOH – Loss Of Heterozygosity
MII – Metaphase II
Mad2 – Mitotic Arrest Deficient –Like 2
Mad2_DN - Mitotic Arrest Deficient –Like 2 Dominant Negative
MDA – Multiple Displacement Amplification
Mdc1 – Mediator of DNA-Damage Checkpoint Protein 1
MEFs – Mouse Embryonic Fibroblasts
mES – Mouse Embryonic Stem Cells
Mps1 – Monopolar Spindle 1-Like 1
MRN - Mre-11-Rad50-Nbs1
mRNA – Messenger RNA
NEAA – Non-Essential Amino Acids
NEBD – Nuclear Envelope Breakdown
N/S – Not Significant
NZ - Nocodazole
Oct4 –Octomer Binding Protein 4
PBS – Phosphate Buffer Solution
PBS-T – Phosphate Buffer Solution Supplemented With 0.1% Tween-20
PE – Primitive Endoderm
PFA - Paraformaldehyde
PGD – Pre-Implantation Genetic Diagnosis
PGS – Pre-Implantation Genetic Screening
PHA - Phytohaemagglutinin
PMSG- Pregnant Mares' Serum Gonadotrophin
PVP - Polyvinylpyrrolidone
qRT-PCR – Quantitative Real-Time Polymerase Chain Reaction
RCT – Randomised Controlled Trial
RFP – Red Fluorescent Protein

RNAi – RNA Interference
RNF8 – Ring Finger Protein 8
ROI – Region Of Interest
ROS – Reactive Oxygen Species
Rv-C – Reversine – Control Chimeras
SAC – Spindle Assembly Checkpoint
SD - Standard Deviation
siRNA – Small Interfering RNA
SKY – Spectral Karyotyping
SNP – Single Nucleotide Polymorphisms
Sox2 – SRY Box Containing 2
Sox17 – Sex Determining Region Y Box 17
TE – Trophectoderm
Tead4 – TEA Domain Family 4
TUNEL – Terminal Deoxynucleotidyl Transferase Dutp Nick End Labelling
TFP – Tomato Fluorescent Protein
UPD – Uniparental Disomy
UTR – Untranslated Region
WB – Western Blot
WGA – Whole Genome Amplification
Yap – Yes-Associated Protein
ZGA – Zygotic Genome Activation

Italics – Reference to gene or RNA
Standard - Reference to protein

INTRODUCTION

1.1 BACKGROUND

Aneuploidy is defined as the presence of too many or too few chromosomes and is an important cause of human disease; most notably cancer, reproductive health problems and developmental disabilities.

Aneuploidy can refer to the chromosome status of a single cell, or to the genetic constitution of a population of cells such as the whole organism, specific tissues or cells in culture. The ploidy status of cell populations can be further categorized as either uniform or mosaic. In uniform aneuploidy, every cell within a single population shares an identical chromosome constitution. In contrast, mosaicism describes a population of cells containing clones with differing underlying chromosome constitutions.

A wide range of reproductive health problems can be caused by aneuploidy including subfertility, miscarriage, confined placental mosaicism (CPM) and the birth of an abnormal child. Recent technological advances in aneuploidy assessment have resulted in the increased availability of rapid diagnostic tests, and also assessment of the chromosome status at higher resolutions than could previously be achieved with the classic techniques of cytogenetic karyotyping and fluorescent in-situ hybridisation (FISH). Although these advances have led to valuable improvements in diagnostic accuracy and clinical care, they have also resulted in more embryos being diagnosed with abnormalities of uncertain significance. Chromosome mosaicism is one such situation that is clinically challenging, as the significance of mosaicism is often uncertain. This can lead to difficult decisions for couples and clinicians, and potentially unnecessary interventions which in some cases can result in harm.

1.2 EARLY PREGNANCY LOSS IN HUMANS: THE ROLE OF ANEUPLOIDY

Humans are relatively inefficient at reproduction. Even in the most optimal circumstances, the maximal chance of a clinically recognizable pregnancy is estimated to be 30-40% per

ovulatory cycle (Zinaman et al., 1996). This inefficiency is unlikely to be due to a failure to conceive; rather primarily due to a high rate of preclinical pregnancy loss, in which the conceptus fails to develop before the woman has any physical awareness that she may have been pregnant (Macklon et al., 2002). The first evidence that early pregnancy failure may be a frequent occurrence arose from studies on hysterectomy specimens acquired from fertile, ovulatory women (Hertig et al., 1956). Meticulous histological evaluation of the uterine contents was undertaken on specimens from women deemed to have the highest possible chance of conception just prior to their surgery. Clinical evidence of pregnancy was only apparent in approximately one-third of cases, and of these a further one-third were found to be abnormal. This provided the first direct evidence that early pregnancy failure was a frequent occurrence following human conception. The authors concluded that the failure to find early evidence of pregnancy in the majority of specimens could be a result of a failure of fertilization, or the early arrest of embryo development following fertilization. Further evidence for pre-clinical pregnancy losses became apparent following the introduction of biochemical assays for early pregnancy. The most widely utilized marker is human chorionic gonadotrophin (hCG), a hormone secreted by the trophoblast cells that is detectable in maternal serum or urine from the time of implantation onwards. Using hCG as a biochemical marker for pregnancy, it became possible to detect 'occult' pregnancy losses, occurring in up to 30% of detected pregnancies (Wilcox et al., 1988).

Collating all the available evidence together on early pregnancy loss, from studies on hysterectomy specimens, uterine lavage, biochemical assays and clinical miscarriage data, it has been proposed that in total approximately 70% of conceptions fail prior to birth: 30% prior to implantation, 30% following implantation but prior to delayed menstruation (ie pre-clinical), and 10% as clinical miscarriages (Macklon et al., 2002).

What could account for the high rate of early pregnancy loss in humans? This challenging question is almost impossible to address experimentally, and has consequently been described as the 'black box' of early pregnancy loss (Macklon et al., 2002). However with the advent of IVF and advances in cytogenetic techniques, the available evidence points to genetic abnormalities of the conceptus, such as aneuploidy, as the most likely cause of the majority of early pregnancy failures.

The potential importance of aneuploidy as the cause of early pregnancy loss was first recognised following the study of spontaneous miscarriage specimens. Cytogenetic analyses revealed that >50% of first trimester miscarriages are caused by aneuploidy (Hassold et al., 1980, Fritz et al., 2001). These figures may even under-represent the true contribution of aneuploidy to first trimester pregnancy loss; karyotyping tissue obtained from failed pregnancies is technically difficult and can fail to yield a result.

Further evidence for the potential role of aneuploidy in early pregnancy loss began to arise following the success of IVF in 1978 (Steptoe and Edwards, 1978); prior to this the chromosome status of pre-implantation embryos was completely unknown. The given prevalence rates of aneuploidy affecting pre-implantation embryos vary markedly between different studies due to wide variations in technical and experimental approaches, and study design. However the majority of studies conclude that aneuploidy in human pre-implantation embryos is a frequent occurrence, with diploid-aneuploid mosaicism occurring in 73% of embryos, a figure attained from the most recent systematic review of the literature (van Echten-Arends et al., 2011). More recent studies have utilized advanced array-based karyotyping techniques, enabling a more comprehensive evaluation of the chromosome constitution of IVF embryos to be undertaken (Vanneste et al., 2009, Northrop et al., 2010, Schoolcraft et al., 2010, Johnson et al., 2010, Rabinowitz et al., 2012). One such study of 23 cleavage stage embryos from young, healthy couples found that only 9% of embryos had a normal chromosome constitution in all of the blastomeres (Vanneste et al., 2009). As the study of *in vivo* conceived human embryos is not possible, the given aneuploidy rates in human pre-implantation embryos are always in the context of IVF. How closely these rates reflect the situation *in vivo* is not known.

In contrast to the pre-implantation embryo, aneuploidy in viable on-going pregnancies is infrequent, even in the first trimester. The proportion of viable pregnancies affected by aneuploidy drops from an estimated 4.2% at 8-weeks gestation, down to 2.4% at 12 weeks; figures calculated from a systematic review of five published studies evaluating the incidence of cytogenetic abnormalities in spontaneous pregnancy failures (Hook, 1981a). When tested by placental biopsy at the end of the first trimester, aneuploidy is detected in 1-2% of all samples (Ledbetter et al., 1992, Hahnemann and Vejerslev, 1997). However, in the majority of these cases the aneuploidy is constricted to the placental tissue and the

fetus has a normal chromosome constitution. This finding is known as confined placental mosaicism (CPM), and usually does not result in major adverse effect on the outcome of the pregnancy or for the future child (Kalousek and Vekemans, 1996). As gestation proceeds, the prevalence of aneuploidy continues to decrease further, affecting an estimated 1.1% of pregnancies at 16 weeks and 0.8% at 20 weeks (Hook, 1981a). Finally, a cytogenetic survey of 11,680 newborn infants detected aneuploidy in only 0.6% of all live births (Jacobs et al., 1974).

Thus, observational evidence demonstrates a dramatic decline in the prevalence of aneuploidy as gestation progresses, with the steepest drop occurring early on during the pre- and early post-implantation stages of embryo development. When viewed together with the high rates of pre-clinical pregnancy loss, it is highly probable that aneuploidy is responsible for this 'black box' of human pregnancy loss (Figure 1.1).

1.3 ANEUPLOIDY IN THE HUMAN PRE-IMPLANTATION EMBRYO

Soon after the establishment of IVF as treatment for human infertility it became apparent that the high success rates of fertilization and *in vitro* culture were countered by the low rates of established viable pregnancies following embryo transfer (Steptoe and Edwards, 1978). In view of the high rates of aneuploidy identified in first trimester miscarriages it was speculated that aneuploidy could be a major contributory cause of IVF failure, impairing embryo development beyond the pre-implantation stages.

Early investigations into this hypothesis were hampered by technical challenges of karyotyping blastomeres. Classical cytogenetic approaches rarely yielded results, and the accurate visualisation of chromosomes within a single defined cell remains a formidable task. However in 1983 one of the first successful studies evaluating the chromosome status of early human embryos was published (Angell et al., 1983). This study attempted to karyotype 8-cell stage human embryos. Full karyotyping was achieved in only three embryos, however just one of these embryos contained a normal complement of chromosomes. Further, the nature of the aneuploidy was unusual and not compatible with aneuploidies ever detected in clinical pregnancies, miscarriages or live births. By this time,

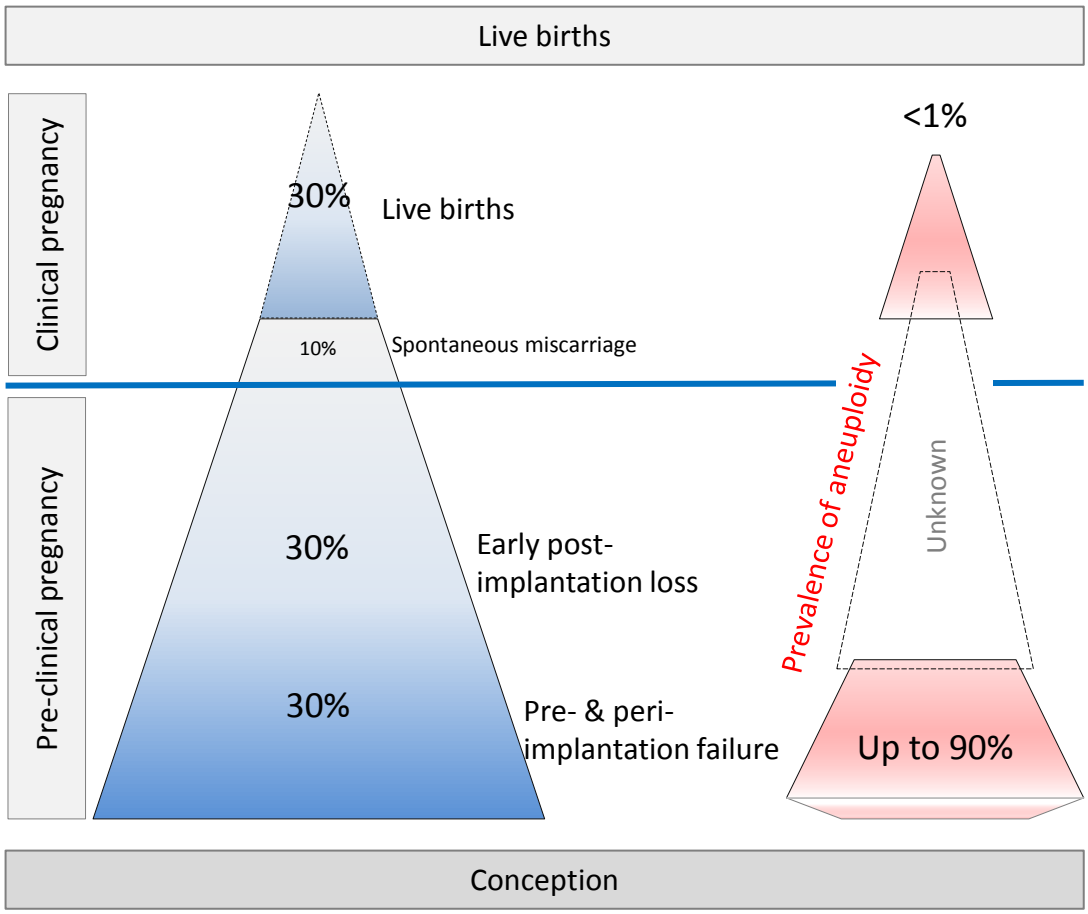

Figure 1.1 The human pregnancy loss and aneuploidy icebergs (adapted from Macklon *et al. 2002).* Approximately 30% of conceptions result in viable on-going pregnancies and live-births. The majority fail during early pregnancy, usually prior to a clinically recognised pregnancy and are therefore unrevealed. In parallel with the pregnancy loss iceberg, the prevalence of aneuploidy complicating pregnancies decreases with on-going gestation. In the pre-implantation stages of development chromosome mosaicism has been reported in up to 90% of embryos; maximal at the cleavage stages and declining thereafter. Less than 1% of live births are complicated by aneuploidy. There is virtually no data on the prevalence of aneuploidy in peri- and early post-implantation stages of pregnancy, except that >50% of spontaneous miscarriages are complicated by aneuploidy, and 1-2% of chorionic villous samples tested at the end of the first trimester are mosaic aneuploid. It is presumed that the prevalence decreases dramatically during this 'black box' stage of pre-clinical pregnancy loss.

over 100 babies had been born following IVF treatment without any reports of chromosome abnormalities. This led the authors to conclude that pre-implantation aneuploidy was the most likely cause of IVF failure following embryo transfer.

Many other studies soon followed characterising the chromosome status of human IVF embryos, and continue to be published as improved and alternative methods for detecting aneuploidy are developed: cytogenetics (Zenzes and Casper, 1992, Zenzes et al., 1992, Clouston et al., 1997, Clouston et al., 2002), FISH (Munne et al., 1993, Delhanty et al., 1993, Harper et al., 1995, Harrison et al., 2000, Magli et al., 2000), comparative genomic hybridisation (CGH) (Voullaire et al., 2000, Wells and Delhanty, 2000), array-based CGH (Vanneste et al., 2009, Northrop et al., 2010, Schoolcraft et al., 2010, Johnson et al., 2010, Rabinowitz et al., 2012). FISH quickly replaced conventional karyotyping as the investigation of choice, bypassing some of the technical obstacles associated with karyotyping. In contrast to karyotyping, FISH yielded results in the vast majority of cells tested (>90%), and did not require the cell to be arrested in metaphase. One major limitation associated with FISH is the restriction on the number of chromosomes that can be evaluated at any one time. Consequently studies utilizing FISH were largely limited to the evaluation of chromosomes 13, 18, 21, X and Y; with the rationale that these were the only chromosomes potentially responsible for human disease. More recent improvements in FISH technology have resulted in the potential to evaluate greater numbers of chromosomes simultaneously (Thornhill et al., 2005, Baart et al., 2006, Baart et al., 2007b, Munne et al., 2010). However increasing the number of FISH probes is associated with a decrease in the diagnostic accuracy of the test; this may result in an unacceptably high error rate when utilized for single cell diagnosis such as for pre-implantation aneuploidy detection (Scriven and Bossuyt, 2010).

More recently, single-cell array-based comprehensive chromosome screening technologies have been developed and used to evaluate aneuploidy in pre-implantation embryos (Harper and Harton, 2010). These technologies include array-based comparative genome hybridisation (CGH) and single nucleotide polymorphism (SNP) arrays and enable all chromosomes to be evaluated at high resolution (Treff and Scott, 2012). In CGH, DNA from a normal control genome and from the test sample are amplified separately using whole genome amplification (WGA) technologies, with each sample differentially labelled with a

fluorochrome. Both samples are then mixed and hybridised onto a bacterial artificial chromosome (BAC) DNA chip. Automated analysis of fluorescence then determines the ratio of each region of the chromosome present in the test sample compared to the normal control genome and will thus detect aneuploidies and regional chromosome losses or gains. Polyploidies and balanced translocations or inversions cannot be detected. SNP-array technologies also involve WGA however the SNP-array probes evaluate the genome at an even higher resolution than CGH. Both technologies offer the potential for rapid, comprehensive, high resolution molecular karyotyping that may be more accurate than FISH (Treff et al., 2010).

Whatever technical approach used, all studies concur with the earliest reports, that aneuploidy is a frequent finding in human cleavage stage embryos, with the most commonly reported pattern being diploid-aneuploid mosaicism. Mosaicism was first reported in human embryos in 1993 (Delhanty et al., 1993, Munne et al., 1993). Since then numerous studies have characterised the patterns of mosaicism and there is almost unequivocal agreement that mosaicism is the most commonly occurring chromosome constitution in human IVF embryos (van Echten-Arends et al., 2011). Figure 1.2 summarises the classification of chromosome constitutions in human pre-implantation embryos.

Reported prevalence rates for mosaicism have ranged from 15% (Harper et al., 1995) to more than 90% (Vanneste et al., 2009). The wide variation between studies in their reported mosaicism rates can be understood by considering the differing contexts of each study. There are multiple variables that can affect the measured rate of aneuploidy, and these differ enormously between individual studies and therefore impact upon their measured prevalence of mosaicism. Table 1.1 lists these variables and summarises their potential influence on the evaluation of aneuploidy rates. Thus, it is not representative to define an overall rate of aneuploidy or mosaicism in the pre-implantation embryo, and as such aneuploidy rates should not be declared without caveat.

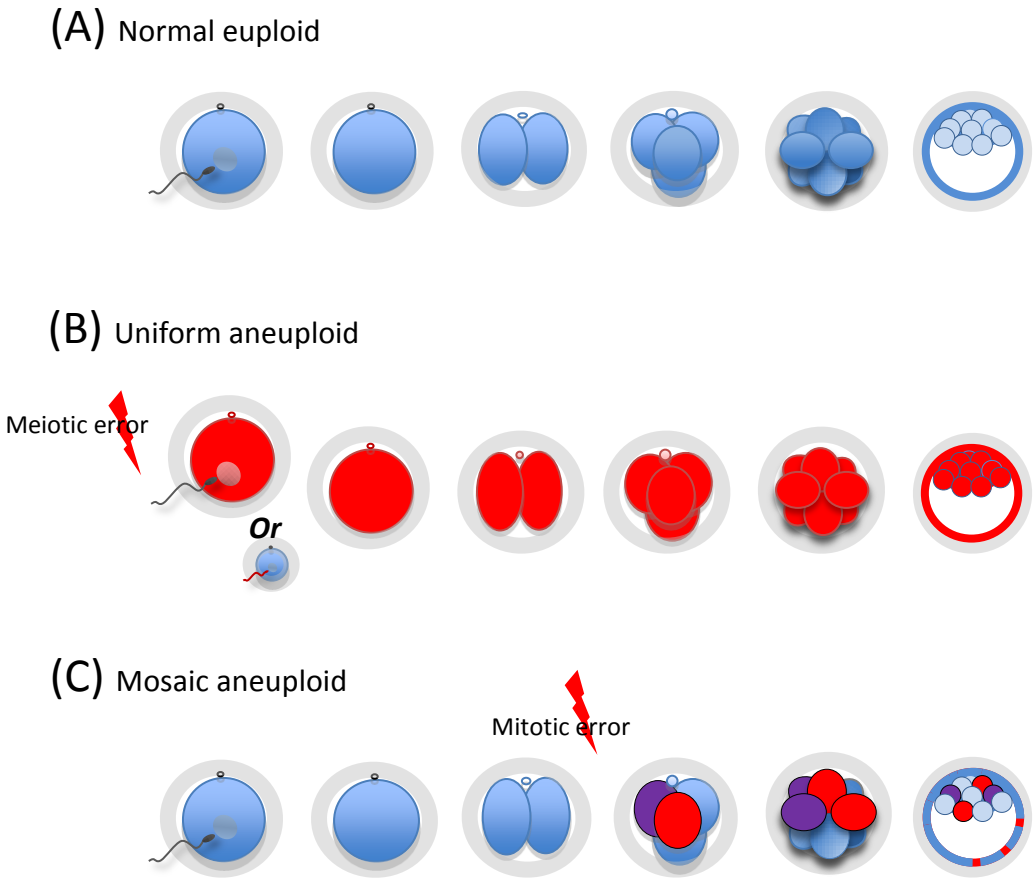

Figure 1.2. Classification of pre-implantation embryos according to their chromosome constitution. (A) Euploid embryos occur when all blastomeres contain a normal underlying chromosome constitution **(B)** Uniform aneuploid embryos contain a single identical abnormality in their chromosome status, with the abnormality affecting all blastomeres. This abnormality arises secondary to an error of meiosis in one of the gametes, usually the oocyte. **(C)** Mosaic aneuploidy occurs when the embryo contains more than one clone of blastomeres with differing chromosome constitutions, and arises secondary to an error during mitosis, post fertilization. The degree of mosaicism can be highly variable, and in some cases there are no normal cells. Aneuploidy is the most common form of chromosome abnormality, but polyploidy and haploidy can also occur, although less frequently.

Colour scheme: blue represents normal chromosome constitution; red & purple represent differing aneuploidies

Table 1.1

		Potential increase in aneuploidy rate	Potential decrease in aneuploidy rate	Additional comments
Embryo status	**Developmental history & morphology**	Abnormal or arrested embryo	Normal developing embryo	The scarcity of human embryos often results in over-representation of poor quality discarded embryos
	Timing of analysis	Cleavage stage embryos	Blastocysts	Highly dependent upon how aneuploidy is reported. Cleavage stage embryos tend to have a higher proportion of abnormal cells, while blastocysts have a lower proportion, but more whole embryos are affected
	Preservation status	Thawed following cryopreservation	Fresh embryos	With significant improvements in technology, this may be less applicable to more recent studies
Patient characteristics	**Parental age**	Increased maternal age	Younger maternal age	Uniform aneuploidies strongly related to maternal age, mosaicism less so.
	Indication for assisted reproduction	Male factor & ICSI, recurrent implantation failure, known chromosome translocation carrier	Not subfertile (for example requiring PGD for single gene disorder)	The most variable parameter and difficult to control for in studies without significantly limiting the number of embryos available for analysis
Test characteristics	**Method of analysis & number of chromosomes analysed**	High resolution tests that assess the full complement of chromosomes (e.g. array-based assays)	Fewer chromosomes assessed (e.g. FISH)	First generation tests such as interphase FISH were limited to the assessment of only a few chromosomes. However, the decreased accuracy of FISH compared to newer array-based techniques may slightly offset the potential for under-diagnosis of aneuploidy
	Number of cells assessed	Highly dependent upon true chromosome constitution of whole embryo		The greater the number of cells assessed per embryo, the greater the accuracy of the test – i.e. results representative of the true constitution of the embryo
	Blastomere characteristics	Not known	Not known	Evaluation of polar body, pluripotent cleavage stage blastomeres and trophectoderm cells have all been used to represent the embryo status
Definitions	**Classification of mosaicism**	-	Less strict criteria for abnormality	Different definitions of mosaicism in the literature: some researchers require a minimum of half assessed cells to contain errors for the embryo to be classified as abnormal

1.3.1 How does chromosome mosaicism arise?

The majority of mosaic embryos contain a mixture of diploid and aneuploid cells, and therefore are likely to arise secondary to an error occurring during mitosis, during the first few cleavage divisions following post-fertilization (van Echten-Arends et al., 2011). Uniform aneuploidy in embryos arises secondary to errors of meiosis and this phenomenon is strongly related to advanced maternal age (Hook, 1981b). In contrast, chromosome mosaicism is independent of maternal age, with no evidence of lower rates occurring in embryos from younger women (Baart et al., 2006, Vanneste et al., 2009). Why early stage embryos are error prone, and whether the IVF embryo is representative of the *in vivo* embryo, are important questions that remain to be answered.

The chaotic nature of the abnormalities observed in mosaic embryos has led to speculation that they may originate as a direct result of deficiencies in cell-cycle checkpoints during the first few cleavages (Delhanty and Handyside, 1995, Harrison et al., 2000, Ambartsumyam and Clarke, 2008, van Echten-Arends et al., 2011, Mantikou et al., 2012). If so, these deficiencies may be related to the timing of zygotic genome activation (ZGA). ZGA occurs at the 4- to 8-cell stage in the human embryo (Braude et al., 1988). Prior to ZGA the embryo is solely dependent upon maternally derived transcripts and proteins that were stored in the oocyte. Therefore, in theory, the reserves of the cell-cycle checkpoint pathway components will be maximal during the first cleavage and decrease in subsequent cleavages until the onset of genome activation, when the embryo can replenish the transcripts and proteins. Any deficiencies in maternal transcripts or proteins required for effective checkpoint function will risk the occurrence of genomic errors arising in daughter blastomeres until the onset of embryonic genome activation. In addition, further confounding factors could exacerbate maternal deficiencies such as IVF treatment-related effects including ovarian stimulation regimes (Baart et al., 2007a, Munne et al., 2007). In the case of the mouse, pre-implantation embryos cultured *in vitro* have been shown to exhibit higher aneuploidy rates than those *in vivo* derived embryos (Bean et al., 2002, Sabhnani et al., 2011). These findings suggest that in some instances culture conditions could influence the prevalence of aneuploidy.

The hypothesis that delayed ZGA may lead to deficiencies in cell-cycle checkpoint components offers a plausible explanation for how mosaicism may arise, but has not been tested directly and thus remains speculative. Does the comparison of aneuploidy rates in the embryos of other mammals add any support to this hypothesis? The timing of major ZGA varies between different species, occurring at the 2-cell stage in the mouse (Latham and Schultz, 2001), the 4- to 8-cell stage in the rabbit and cow (Manes, 1973, Schultz and Heyner, 1992, Brunet-Simon et al., 2001) and the 8- to 16-cell stage in the pig (Schultz and Heyner, 1992). Thus the mouse embryo undergoes the earliest ZGA, and aneuploidy rates in mouse pre-implantation embryos are reported as low, typically between 1 and 4% (Bond and Chandley, 1983, Glenister et al., 1987, Liu et al., 2008). Rabbit and cow embryos undergo ZGA at a similar stage to human embryos. Reported rates in rabbits range between 54.7 and 56% in cleavage stage blastomeres (Shi et al., 2004, Curlej et al., 2010), and in cows the rates range between 15% and 42% in cleavage stage embryos and blastocysts (Yoshizawa et al., 1999, Viuff et al., 2000). In pig embryos, aneuploidy rates range between 14.3% and 74% at the cleavage stage and between 4.7% and 62% at the blastocyst stage (Hornak et al., 2009, Hornak et al., 2012). The rates of abnormalities detailed above appear to show that species in which ZGA occurs later than the 2-cell stage tend to be susceptible to higher rates of aneuploidy. However, on more detailed consideration of these and other studies, this association is less conclusive. As discussed in section 1.3 above, the accurate assessment of chromosome status in human pre-implantation embryos is technically challenging, and these challenges also apply to all other mammalian embryos. Further, making direct comparisons of given aneuploidy rates between different studies is misleading as there are multiple different factors that can affect the outcome including the developmental stage and morphology of the embryo, the number of cells evaluated and the experimental techniques and classifications used to measure aneuploidy rates. These factors also influence given rates in animal studies, and with additional variables including the availability of *in vivo* conceived and cultured embryos. Finally, there are very few published animal studies that systematically characterise aneuploidy rates in embryos and thus the available data for direct comparison is sparse. Indeed the non-murine studies cited above used a range of different techniques (FISH, CGH, metaphase spreads) on *in vivo* or *in vitro* derived embryos at developmental stages ranging from the early cleavage stage through to blastocysts (Yoshizawa et al., 1999, Viuff et al., 2000, Shi et al., 2004, Curlej et al.,

2010). In the mouse, there are surprisingly few published studies that specifically evaluate aneuploidy in the pre-implantation embryo, given its widespread use as a model system for mammalian development. In addition, the frequently cited studies giving the low rates of aneuploidy were limited to embryos prior to the 8- cell stage and all used karyotyping to assess chromosome number (Bond and Chandley, 1983, Glenister et al., 1987, Liu et al., 2008). More recently, aneuploidy rates of 25% were detected in a group of 44 wild-type control mouse blastocysts evaluated by spectral karyotyping (SKY) (Lightfoot et al., 2006) and of 31% (20 of 64) in blastocysts in a study that used 2-probe FISH (Sabhnani et al., 2011). This is discussed in greater detail in Section 1.4; however these rates are significantly higher than expected and provide evidence to suggest that additional mechanisms, unrelated to ZGA, may be involved in the origins of pre-implantation aneuploidy in embryos.

1.3.2 Improving IVF outcomes by screening for aneuploidy

The first child conceived by IVF was born in 1978 (Steptoe and Edwards, 1978); a remarkable achievement recognised by the award of the Nobel Prize in 2010. Since then it is estimated that over 5 million children have been born as a result of IVF, and now account for greater than one percentage of all births in the UK. Perhaps surprisingly, over 30 years later is that IVF success rates are still considered to be relatively low, with successful outcomes expected in less than half of all cycles even in the most favourable circumstances.

Chromosome abnormalities are widely believed to play a major role in IVF failure, given the high rates identified during pre-implantation development. Aneuploidy is associated with reduced pre-implantation developmental potential in human embryos and it is considered likely that the majority of these embryos cannot develop to term (Magli et al., 2000, Sandalinas et al., 2001, Rubio et al., 2007). Therefore it was hypothesized that successful identification of abnormal embryos would result in improved IVF outcomes by enabling embryos with the best developmental potential to be selected for embryo transfer (Zenzes et al., 1992, Delhanty and Handyside, 1995, Wilton et al., 2001, Harper and Harton, 2010).

Many techniques designed to identify aneuploid embryos have been pioneered but have largely produced disappointing results. Non-invasive methods include embryo morphology

grading and, more recently time-lapse imaging (Wells, 2010, Racowsky et al., 2010, Machtinger and Racowsky, 2013). Human pre-implantation embryos vary widely in their morphological development and various grading systems have been devised in an attempt to classify embryos and correlate morphology with likelihood of IVF success (Fisch et al., 2001, Boiso et al., 2002). Embryos may be scored according to the number of cells, symmetry of blastomere size, degree of fragmentation, presence of compaction, blastocyst cavitation and expansion, hatching and morphology of the ICM and TE (Racowsky et al., 2010, Machtinger and Racowsky, 2013). Many studies have evaluated the relationship between embryo morphology and aneuploidy, and most conclude that while an association exists, it is weak (Wells, 2010, Alfarawati et al., 2011). Aneuploid embryos frequently undergo apparently normal development, and likewise, a normal chromosome complement does not always ensure normal development (Rubio et al., 2007, Magli et al., 2007, Munne et al., 2007, Eaton et al., 2009, Alfarawati et al., 2011). An extension of morphology assessment is the more recent application of time-lapse imaging systems, enabling the dynamic evaluation of embryo development in real-time (Cruz et al., 2011). Several early studies have reported promising correlations between early developmental kinetics and successful blastocyst formation (Wong et al., 2010, Hashimoto et al., 2012) and with implantation rates (Meseguer et al., 2011). To date, only one published study has directly evaluated the association between developmental kinetics and chromosome status (Chavez et al., 2012). Zygotes were imaged until the 4-cell stage. Precise cell-cycle parameter timings were observed in all euploid embryos; in contrast, only 30% of aneuploid embryos exhibited timings within that same window. Further and more detailed studies on greater numbers of embryos are still required to characterise the link between aneuploidy and abnormal developmental kinetics. If confirmed, whether these differences will be specific enough to translate into a clinically useful tool remains to be seen.

In contrast to the non-invasive approaches used, pre-implantation genetic screening (PGS) is an invasive test designed to detect abnormal embryos. The fundamental principle of PGS is the removal of one or more cells from the embryo for assessment of the chromosome status; embryos that are identified as aneuploid are discarded, and those identified as normal are selected for transfer.

In 1990 the first pregnancies were reported after embryo biopsy and genetic testing for couples at risk of X-linked recessive diseases (Handyside et al., 1990). Pre-implantation genetic diagnosis (PGD) soon became an established clinical test for single gene disorders (Sermon et al., 2004). As technologies for aneuploidy assessment evolved, pregnancies following PGS were soon reported (Verlinsky et al., 1995, Wilton et al., 2001, Wilton, 2002). Early PGS protocols involved cleavage stage embryo biopsies and used FISH to assess chromosome status. Thus, there were limitations on the number of chromosomes that could be evaluated although subsequent improvements in FISH technology soon enabled greater numbers to be assessed simultaneously (Thornhill et al., 2005, Baart et al., 2006, Baart et al., 2007b). PGS was embraced with enthusiasm, and has since been widely used within IVF clinics. However, its rapid introduction into the routine clinical setting has resulted in perhaps the fiercest academic debate within the IVF community during the last two decades (Donoso P, 2007, Jansen et al., 2008, Fauser, 2008, Harper et al., 2008, Gleicher et al., 2008, Ly et al., 2011, Gleicher and Barad, 2012, Hens et al., 2012).

The aim of PGS was to improve implantation rates, decrease spontaneous miscarriages, and ultimately increase the success of IVF by increasing live birth rates. More specifically, patients with a poor prognosis after IVF were those anticipated to gain the most; such as those with advanced maternal age, recurrent IVF failures, severe male factor infertility and unexplained recurrent miscarriages. Indeed, some of the first few observational studies were encouraging, with improvements reported in implantation rates, live births (Gianaroli et al., 1999, Munne et al., 1999, Munne et al., 2003) and fewer miscarriages (Munne et al., 2006). As a consequence of early promising results, PGS was advocated as a tool to improve IVF outcomes, although there was still limited evidence of its clinical efficacy.

Multiple studies have subsequently been published attempting to address the impact of PGS on IVF outcomes (Twisk et al., 2006, Mastenbroek et al., 2007, Jansen et al., 2008, Meyer et al., 2009, Schoolcraft et al., 2010, Forman et al., 2012, Scott et al., 2012). It is almost impossible to reach definitive conclusions regarding efficacy of PGS from single studies alone due to the multiple variables that could potentially influence the outcome of PGS. Patient characteristics, stage of biopsy, number of cells assessed, diagnostic test applied, number of chromosomes assessed, criteria for embryo transfer, superovulation regimes are just some examples of the many variables that potentially influence PGS outcome results,

and also vary widely between the different individual studies. However, despite the early promising reports from small observational studies, evidence soon began to emerge that PGS may not be as beneficial as initially hoped (Staessen et al., 2004). In 2006 a Cochrane Review of published randomised controlled trials (RCTs) was conducted to evaluate the effectiveness of PGS in improving live birth rates following IVF or ICSI treatment (Twisk et al., 2006). Only nine trials met the inclusion criteria; however analysis of the available evidence showed that PGS was actually associated with a decrease in live birth rates, rather than the improvement that was intended, and as a result recommended that PGS should not be routinely used in clinical care. Shortly afterwards a large, multicentre, double-blinded RCT also concluded that PGS was detrimental to IVF outcome, and presented data showing a significant association between PGS and lower pregnancy and live birth rates (Mastenbroek et al., 2007). Further, the negative impact of PGS on IVF outcome was confined to patients with the poorest prognosis; the same group for which PGS was anticipated to help. Even in patients with good prognosis, PGS was not shown to provide any additional improvement in their outcomes (Staessen et al., 2008, Meyer et al., 2009). The routine role of PGS in IVF treatment was reassessed following these publications, with calls for the withdrawal of use in routine clinical practice and urgent recommendations for further well conducted clinical trials (Mastenbroek et al., 2007, Gleicher et al., 2008, Practice Committee of Society for Assisted ReproductiveTechnology and Practice Committee of American Society for Reproductive Medicine, 2008, Harper et al., 2010).

A number of potential reasons to explain why PGS failed to deliver the anticipated improvements in IVF outcome are possible. These include technical limitations of the test, differing technical competencies between laboratories, detrimental effects of biopsy, timing of the test and the presence of embryo mosaicism (van Echten-Arends et al., 2011). PGS requires embryo biopsy and the removal of one or more blastomeres, and this in itself may be detrimental to the embryo (Cohen et al., 2007, De Vos et al., 2009). Both the developmental stage at the time of biopsy and the number of blastomeres removed may have an impact upon future developmental potential of the biopsied embryo. When PGS is conducted on cleavage stage embryos the aim is usually to evaluate only one blastomere. However, in some cases diagnosis is not technically possible from that blastomere and it may be necessary to remove a second blastomere, which may be further detrimental to

future pregnancy rates (Cohen et al., 2007). Indeed, when compared with single cell, two cell biopsy has been shown to have small but significant detrimental effects on blastocyst formation (Goossens et al., 2008), and live birth rates (De Vos et al., 2009). In addition to embryo biopsy, the type of test used to evaluate chromosome status may be responsible for the poor outcomes following IVF. Any clinical test has intrinsic limitations, the potential for failure and an error rate; all of which could offset the desired benefits of the test. The majority of PGS studies published to date have used interphase FISH to interrogate chromosome status. FISH requires the use of fluorescently-labelled DNA probes that are then hybridised to DNA segments specific to individual chromosomes. Chromosome copy number is determined by the number of probe-specific fluorescent signals detected visually using a fluorescent microscope. FISH can fail during biopsy, fixation or analysis; and unlike the analysis of most other clinical biological samples where hundreds of cells are readily accessible, usually only one or two cells are available for evaluation, significantly increasing the chances of error (Scriven and Bossuyt, 2010). Reported failure rates vary between studies, but tend to be around 10% (Munne et al., 1993, Munne et al., 1998). In addition, a major intrinsic limitation of FISH is the number of chromosomes that can be assessed simultaneously. Although technological advances have enabled greater numbers of chromosomes to be tested, the potential benefits may be offset by a concomitant decrease in efficiency secondary to an increased error rate; each chromosome probe has an accuracy rate between 92-99% due to signal errors, hybridisation failure and probe inefficiencies (Ruangvutilert et al., 2000, Daphnis et al., 2005, Scriven and Bossuyt, 2010). Additionally, the optimum chromosome probe combination to use is unknown. More recently array-based molecular karyotyping techniques have been used instead of FISH, and these allow a more comprehensive evaluation of chromosome status, and may be less error prone (Treff et al., 2010, Treff and Scott, 2012). The potential impact of replacing FISH with these newer techniques is currently unknown, although early reports are promising (Schoolcraft et al., 2010, Forman et al., 2012, Scott et al., 2012).

Another major factor that may significantly impact upon the efficacy of PGS is the high prevalence of chromosome mosaicism. PGS was routinely carried out on cleavage stage embryos, with the permanent removal of a single cell for aneuploidy assessment. The results obtained from that one individual cell are used to infer the underlying chromosome

status of the entire remaining embryo. In the case of mosaicism the principle of this strategy is erroneous, as clinical decisions are based on the findings from a cell that no longer contributes to the embryo (illustrated in Figure 1.3). By definition, mosaicism requires there to be a minimum of two different clones within the embryo therefore evaluation of just one cell is insufficient to draw any justifiable conclusions on the likelihood of mosaicism in the remaining embryo. Moreover, removal of the cell may fundamentally alter the constitution of the remaining embryo, either by increasing or decreasing the proportion of aneuploid cells, with the potential to alter the long term developmental potential of that embryo. In the case of mosaics comprising a clone of diploid and aneuploid cells, biopsy of an aneuploid cell will lead to discarding a potentially viable embryo. Conversely, biopsy of a diploid cell may result in transfer of an embryo with curtailed developmental potential secondary to its removal. This may be the underlying reason why those patients with the poorest IVF prognosis have the least to gain from PGS; they have fewer embryos in total and in addition a greater proportion of these are abnormal. Diploid-aneuploid mosaicism is the most commonly reported pattern of mosaicism, and therefore may be the most significant factor contributing to the inefficiency of PGS (van Echten-Arends et al., 2011).

The failure of PGS to improve clinical outcomes has prompted a re-evaluation of clinical strategy. New efforts are focussing on the role of blastocyst biopsy combined with comprehensive molecular karyotyping approaches instead of FISH. Unlike FISH, comprehensive molecular karyotyping techniques enable every chromosome to be evaluated simultaneously and thus improve the scope of aneuploidy screening. In addition, early reports suggest that these may be more accurate tests than FISH thus minimising the risk of inaccurate results (Treff and Scott, 2012). Blastocyst biopsy involves the removal and analysis of trophectoderm (TE) cells from the embryo, and offers several potential advantages compared to biopsy at the cleavage stage. Blastocyst biopsy allows for several cells to be removed for analysis, without significantly altering the constitution of the embryo; therefore there may be less impact upon future developmental potential. Hence a greater number of cells can be assessed from the same embryo and thus the presence of mosaicism evaluated with greater certainty. Mosaicism may also be less problematic at blastocyst biopsy than in the cleavage stage embryo, as the degree of mosaicism in the

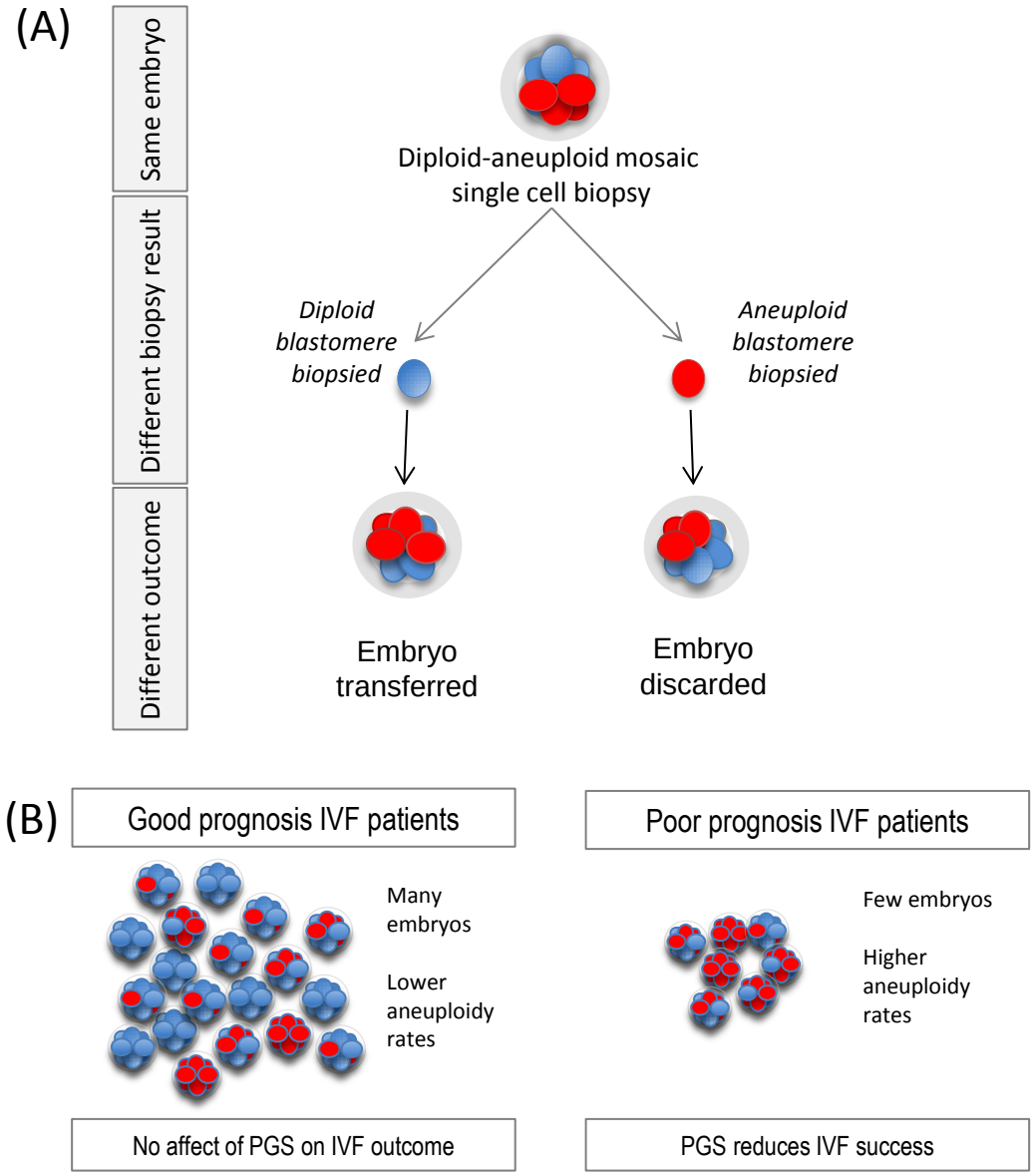

Figure 1.3. Pre-implantation aneuploidy screening in diploid-aneuploid mosaic embryos. (A) Single cell biopsy of cleavage stage mosaic embryos can yield different results depending upon the cell assessed by biopsy. For example, embryos containing a 1:1 ratio of normal to aneuploid blastomeres are equally likely to be diagnosed as normal or abnormal, and transferred or discarded respectively. The removal of the cell for diagnosis results in a change in the constitution of the remaining embryo, potentially altering its developmental prospects in the opposite direction than predicted by biopsy result. **(B)** Embryo profiles of different IVF groups. The impact of the effects of PGS is greater in poor prognosis patients who are likely to have higher prevalence of aneuploidy, and fewer embryos than those with a good prognosis.

Colour scheme: blue represents normal chromosome constitution; red represents aneuploidy

blastocyst is significantly lower than at the cleavage stage (Evsikov and Verlinsky, 1998, Clouston et al., 2002, Coonen et al., 2004, Santos et al., 2010, Johnson et al., 2010, Capalbo et al., 2012, Fragouli et al., 2008).TE biopsy offers theoretical advantages for future fetal development, as biopsy does not interfere with the inner cell mass (ICM), and hence the future fetal lineage. Conversely, it is possible that biopsy from the TE could also reduce the accuracy of the test, as the biopsy results will not be directly reflective of the future fetus. However, there is no experimental evidence that aneuploid cells are enriched within the TE lineage when compared with the ICM. This will be further investigated experimentally in this thesis.

Despite the theoretical advantages of these new clinical approaches to PGS, it is essential that they are subject to robust clinical evaluation before being introduced widely into clinical practice (Gleicher and Barad, 2012).

1.3.3 The developmental fate of mosaic embryos

Despite the high prevalence of mosaicism in human pre-implantation embryos and their proposed impact upon IVF outcomes, the ultimate developmental potential or fate of these embryos is poorly understood. The major research aim of this thesis is to investigate the developmental fate of mosaic embryos, using a mouse model of chromosome mosaicism.

It is reasonable to suppose that mosaic embryos containing no normal cells may share a similar fate to uniformly aneuploid embryos; it is highly improbable that they will result in a viable on-going pregnancy, with developmental arrest occurring at the very early stages of pregnancy. However many mosaics contain a complement of diploid cells (van Echten-Arends et al., 2011). The outcome for these embryos is less certain. No study has directly evaluated this question in human embryos; however useful inferences can be drawn from scrutinising data attained from less direct questions. How does the prevalence of mosaicism change as gestation proceeds? How does the prevalence of mosaicism compare with the prevalence of uniform aneuploidy? What are the overall success rates of IVF in comparison to the prevalence of chromosome abnormality?

Peaking at the cleavage stage of pre-implantation development, chromosome mosaicism declines as gestation proceeds, and despite the high prevalence of pre-implantation mosaicism, mosaicism in post-implantation embryos is rare. Less than <10% of first trimester spontaneous miscarriages are mosaic (Warburton et al., 1978, Hassold, 1982, Robberecht et al., 2009, Martinez et al., 2010); significantly lower than the prevalence of uniform aneuploidy (Hassold et al., 1980, Fritz et al., 2001). Chromosome mosaicism is identified in 1-2% viable pregnancies when tested by chorionic villous sampling (CVS) at the end of the first trimester (Ledbetter et al., 1992, Hahnemann and Vejerslev, 1997). Finally, the reported prevalence of mosaicism in live births is extremely rare at less than 0.2% (Hansteen et al., 1982) and notably less prevalent than uniform aneuploidy (Jacobs et al., 1974). In those individuals born with trisomy 21 (Down's syndrome), the mosaic variation accounts for a less than 4% of all cases (Devlin and Morrison, 2004). Further, it is worthwhile noting that the majority of chromosomal aberrations identified in pre-implantation embryos are never detected in clinical pregnancies, spontaneous miscarriages or in live births (Nagaoka et al., 2012).

However it is possible that the true prevalence of mosaicism in post-implantation pregnancies and live births is underestimated; diagnoses are usually based upon the aneuploidy status of a small number of cells obtained from an accessible tissue, usually a blood sample. Identification of low level mosaicism by classic cytogenetic techniques or FISH is technically challenging as many cells have to be examined. At least 20 cells must be assessed to detect a mosaicism level of 14% with 95% confidence (Hook, 1977). Greater numbers of cells are not usually assessed unless there is a clinical reason to suspect mosaicism. In addition, cytogenetic analysis techniques that require cell culture may underestimate the true rates of mosaicism if the aneuploid cells proliferate less efficiently than their euploid clone, with metaphase assessment resulting in a biased view of the true chromosome constitution. Therefore occult mosaicism affecting other tissues, or low level mosaicism, is likely to be missed.

Despite the potential shortcomings in evaluating the prevalence of mosaicism, the observational evidence presented above demonstrates an apparent rise and fall of mosaicism, confined to the very early stages of development. Does this shift away from mosaicism towards normality arise secondary to the developmental failure of the whole

embryo? Alternatively, could this occur through the elimination of aneuploid cells from the mosaics resulting in a normal, on-going gestation? It is not possible to investigate these questions directly in the human embryo; however reviewing mosaicism levels in IVF embryos and comparing them with IVF success rates may be informative. One important study analysed 21 cleavage stage embryos using an array-based technology providing a comprehensive, high resolution assessment of the chromosome status of each blastomere within the embryo (Vanneste et al., 2009). Embryos were obtained from young, healthy couples with normal fertility that required IVF treatment for genetic conditions unrelated to fertility. Despite these favourable characteristics, the majority of embryos contained no normal blastomeres at all, 39% were mosaics containing at least one normal blastomere, but only 9% of embryos had a normal karyotype in every blastomere. IVF success rates in the authors' clinic were reported to be in line with the average across IVF centres worldwide (>20% baby-take-home-rate per embryo transferred). A more recent study used the same array-based analysis of the chromosome status of 14 good quality embryos, and determined that 10 (71.4%) of these were diploid-aneuploid mosaics (Mertzanidou et al., 2013). Significantly, these embryos obtained from a cohort of young women who achieved a live birth using sibling embryos attained during the same IVF cycle. Therefore, these findings strongly suggest that some mosaic embryos have the potential to develop into viable, on-going pregnancies.

What mechanisms could account for the dramatic decline in the prevalence of mosaicism as gestation proceeds? Is mosaicism incompatible with on-going development, ultimately resulting in pregnancy failure? Alternatively, can mosaic embryos normalise through the elimination of the abnormal clone of cells as development proceeds, and thus result in a normal, non-mosaic, viable pregnancy? These important questions are difficult to address directly, however the observational evidence presented above suggests that both mechanisms are likely to occur. It is reasonable to speculate that if both outcomes are possible, then the ultimate outcome could depend upon the specific nature and degree of abnormality, particularly the number or proportion of normal cells present in the embryo at the peak of mosaicism. The major aim of this thesis is to address these questions directly, and determine the developmental fate of mosaic embryos, using a mouse model of mosaicism.

1.3.4 Self-limiting mosaicism & potential correction mechanisms

As discussed above, it is possible that some mosaic embryos may develop into viable on-going pregnancies with the initial mosaicism being self-limiting. If this is the case, how could the aneuploid cells become eliminated from the embryo? Leaving aside those mosaics that arrest, a number of potential mechanisms have been proposed to account for the normalisation of mosaic embryos, and can be categorised as either clonal-normalisation or cellular self-correction mechanisms (Figure 1.4). In the case of clonal-normalisation aneuploid cells may be eliminated from the future fetal lineage, either through apoptosis or senescence, and / or by the active segregation to the future placental tissue as the embryo develops and establishes the extra-embryonic lineages. In contrast, the cellular self-correction hypothesis proposes that abnormal cells may self-correct their abnormality, either through trisomic rescue or chromosome duplication mechanisms.

Providing direct evidence of self-limitation in human embryos is difficult. Several studies have attempted to address this issue through the sequential analysis of chromosome status at different stages of pre-implantation development in the same embryos (Li et al., 2005, Munne et al., 2005, Barbash-Hazan et al., 2009, Santos et al., 2010, Northrop et al., 2010). Although experimental approaches varied between studies, the overall findings were comparable; a significant proportion of embryos classified as aneuploid at cleavage stage biopsy were found to be euploid when re-assessed in culture at the blastocyst stage or beyond. Despite similar findings, the interpretation of the results varied between each study. Li *et al.* deemed FISH inaccuracies and embryo mosaicism as the most plausible explanations for their findings. Both Munne *et al*. and Barbash-Hazan *et al.* favoured cellular self-correction of chromosome abnormalities, although neither groups provided any direct evidence to support this conclusion. Santos *et al.* proposed that their data provided indirect support for the clonal-normalisation hypothesis. Finally, Northrop *et al.* concluded misdiagnosis by cleavage-stage FISH as the most likely explanation for their findings, and provided experimental data to rule-out alternative hypotheses of cellular self-correction or preferential segregation to the trophectoderm lineage.

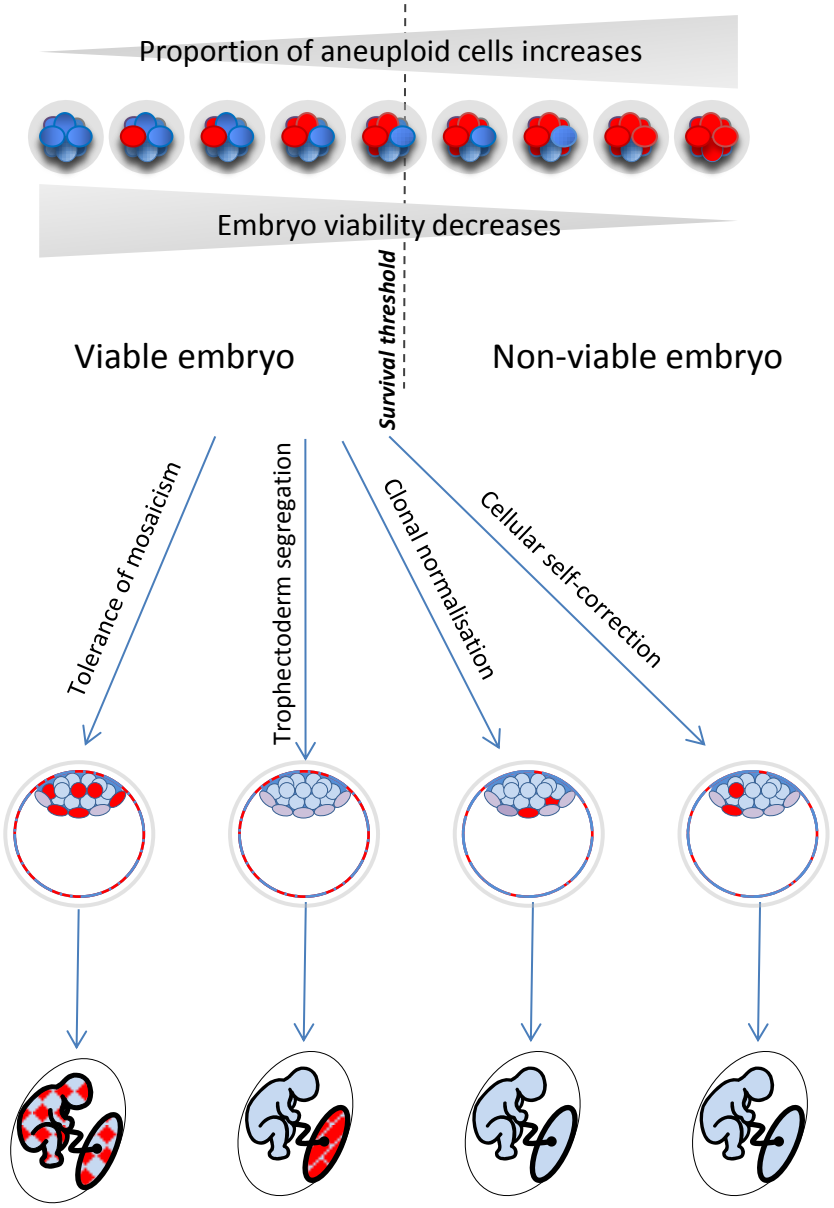

Figure 1.4 Proposed hypotheses for the developmental fate of mosaic embryos. The viability of mosaic embryos may depend upon a threshold of abnormality related to the proportion and nature of the aneuploid cells. Four potential outcomes may be possible, either singly or in combination: **i) Tolerance of mosaicism**, where the conceptus continues to develop with mosaic clones. Tolerance may be global, or restricted to specific lineages. **ii) Trophectoderm segregation** – aneuploid cells are actively segregated to the TE lineage at the first fate decision during embryogenesis. **iii) Clonal normalisation**, where the normal clone has a growth advantage, and the aneuploid clone becomes eliminated by senescence or apoptosis. **iv) Cellular self-correction**, whereby aneuploid cells convert to euploidy by trisomic or monosomic rescue.
Colour scheme: blue represents normal chromosome constitution; red represents aneuploidy

Further evidence for self-limiting mosaicism has been attained from studies on the derivation of human embryonic stem cell (hES) lines from IVF embryos. Several hES lines have been derived successfully from embryos diagnosed as chromosomally abnormal by embryo biopsy, and in the majority of cases the established hES line is euploid, rather than aneuploid (Munne et al., 2005, Peura et al., 2008, Lavon et al., 2008). When tested, earlier passages of stem cells during the derivation process were more frequently mosaic than later passages. In addition, stable aneuploid hES lines were much more difficult to establish than euploid lines, even from embryos diagnosed with aneuploidy, suggesting a selective growth advantage of diploid cells in the case of diploid-aneuploid mosaic embryos (Biancotti et al., 2010). As described in the previous section, the results of these studies on hES cells may also be influenced by the presence of mosaicism and the inaccuracies of FISH.

1.3.4.1 Preferential segregation of aneuploid cells to the TE lineage

Confined placental mosaicism (CPM) was first described in 1983 (Kalousek and Dill, 1983) and is defined by the presence of one or more clones of cells with differing chromosome constitutions confined to the chorionic or placental tissues, and not present within the fetus. Mosaicism confined to the fetus is rarer, with reported rates at less than 0.2% (Hahnemann and Vejerslev, 1997).

The origin of placental mosaicism is often attributed to events occurring during pre-implantation development, when the ICM and TE lineages are established (Wolstenholme, 1996, Kalousek and Vekemans, 1996). A more detailed discussion of pre-implantation development is presented in Section 1.6. In brief, the TE lineage gives rise to all of the fetal cells of the future placenta and the ICM segregates further into the epiblast (EPI) and primitive endoderm (PE). The EPI is the major lineage from which the embryo proper develops; and hence future fetus. By the time the blastocyst is formed, the outer TE cells are committed to their fate and their progeny do not contribute to the future fetus. Therefore, mosaicism exclusively confined to the placental tissues would occur if the aneuploid cells were confined to the outer TE lineages and absent from the ICM. This could arise through two potential mechanisms; either the preferential allocation of abnormal cells to TE lineages or by elimination of cells from the ICM, or a combination of both.

In animal models it is well established that tetraploid-diploid chimeric embryos develop with a restricted lineage distribution; tetraploid cells are excluded from the epiblast lineage by mid-gestation but are maintained within the placental tissues (Tarkowski et al., 1977, James et al., 1995, Goto et al., 2002, Viuff et al., 2002). One study evaluated the distribution of tetraploid cells within mouse diploid-tetraploid chimeras at the late blastocyst stage (Mackay and West, 2005). Tetraploid cells were present in all lineages, but were relatively depleted from the ICM when compared to the TE, and in addition the blastocyst cavity tended to form with the clone of tetraploid cells. Although not investigated experimentally, the authors proposed that such pre-implantation biases in lineage allocation of abnormal cells could also occur in human embryo development and thus provide a possible explanation for how confined placental mosaicism arises. However, the majority of chromosome abnormalities in human pre-implantation embryos are aneuploid, rather than tetraploid, and different mechanisms may underlie their respective fates. Indeed, the same group generated mouse trisomy3-diploid chimeras and triploid-diploid chimeras and did not find the classic confined trophectoderm fate that may be unique to tetraploid-diploid embryos (Everett et al., 2007). Therefore tetraploid-diploid chimeras are unlikely to be a representative model for aneuploid mosaic embryos, or for the pathogenesis of human confined placental mosaicism, which is usually trisomic (Ledbetter et al., 1992, Wolstenholme, 1996, Hahnemann and Vejerslev, 1997).

Other studies have taken a different approach to address this hypothesis. Detailed analyses of human blastocysts were undertaken, using FISH to evaluate the chromosome constitution of cells within the TE and ICM. ICM mosaicism rates were equivalent to the rates within the blastocyst overall (Evsikov and Verlinsky, 1998, Magli et al., 2000) and also comparable between the ICM and TE (Derhaag et al., 2003). More recent studies have repeated these experiments in more detail, evaluating the chromosome constitutions of blastocysts using high resolution array-based karyotyping (Johnson et al., 2010, Northrop et al., 2010). The findings were complimentary to the earlier FISH-based studies; TE and ICM karyotypes from the same embryos were concordant, and aneuploidy rates were equivalent with no evidence of enrichment with the TE lineage.

Thus there is indirect evidence against the hypothesis proposing the preferential allocation of aneuploid cells to the TE lineage. This hypothesis will be evaluated more directly in this thesis.

1.3.4.2 Cellular self-correction

The cellular self-correction hypothesis proposes that aneuploid cells can revert to a euploid cell status, either by losing the extra chromosome in the case of trisomy (trisomic rescue), or by duplication of the single chromosome in the case of monosomy. Cellular self-correction is considered to be responsible for rare genetic disorders that result from the presence of two copies of a chromosome from a single parental origin (Kotzot, 2004, Conlin et al., 2010). How self-correction may occur at the cellular level is not known; a further mitotic error that happens by chance to act in the opposite direction to the original error is one possibility. Alternatively, anaphase lag and chromosome demolition have both been proposed as additional mechanisms for trisomic rescue.

Is there any evidence of cellular self-correction occurring in human embryos? Most cases of cellular self-correction will be impossible to detect. However, some cases of self-correction will result in whole chromosome uniparental disomy (UPD) which can be detected, albeit by non-routine cytogenetic analyses. UPD describes a cell, or population of cells, that contain the correct number of chromosomes, but both copies of the chromosome originate from one parent. In the case of monosomic duplication, UPD is inevitable as all chromosomes will be copies of the single chromosome. In the case of trisomic rescue, one-third of rescues will result in UPD, and in two-thirds there will be bi-parental disomy. Whole chromosome UPD affecting fetuses has been reported from prenatal diagnosis biopsies, and is cited as evidence that cellular self-correction can occur; however it is extremely rare, highly chromosome specific and often lethal (Kotzot, 2004). The low prevalence of UPD may reflect the low frequency with which cellular self-correction occurs; however it is possible that given UPD rates could significantly underestimate the frequency of self-correction for three reasons. First, the majority of trisomic rescue events will not result in UPD and are therefore impossible to detect. Second, UPD is often lethal due to effects of imprinting and recessive mutations. Finally, UPD cannot be identified by classic cytogenetic techniques and specific

testing is usually undertaken only if there is any underlying clinical suspicion. Therefore many cases of UPD may never be detected, especially in the case of mosaicism.

However, there are a few studies in embryos that have investigated the cellular self-correction hypothesis directly by assessing prevalence of UPD using SNP-array technologies (Lavon et al., 2008, Vanneste et al., 2009, Northrop et al., 2010). As both chromosomes are derived from the same parent, the DNA sequences on each chromosome will be identical and will be lacking in heterozygous SNPs. The absence or loss of heterozygosity (LOH) in a chromosome is diagnostic of UPD. Northrup *et al.* assessed 50 blastocysts for LOH and did not identify a single case of UPD, and Lavon *et al.* also failed to detect any cases of UPD in euploid stem cell lines that had been derived from aneuploid embryos. Both groups concluded that cellular self-correction mechanisms were unlikely to account for the normalisation of aneuploid embryos. However, when Vanneste *et al.* evaluated cleavage stage embryos, they found two embryos with UPD in their cohort of 23, a rate of 9%. One embryo was diploid with uniform UPD, likely to represent a gamete complementation event, rather than self-correction. The other was mosaic in two of its blastomeres for two chromosomes, but surprisingly the UPDs were of different parental origin in each of the blastomeres. Taken together, these studies provide significant evidence that if cellular self-correction does occur, it is likely to be an infrequent occurrence and therefore to account for a small minority of self-limiting mosaic aneuploidies.

1.3.4.3 Clonal-normalisation

In the absence of evidence to support a major role for cellular self-correction or preferential segregation to the trophectoderm lineage, the most plausible explanation for self-limiting mosaicism is clonal-normalisation. This occurs when the constitution of the embryo changes from a mosaic containing a mixture of normal and aneuploid cells, to a uniform clone of chromosomally normal cells. These normal cells have a growth advantage over the aneuploid cells, which become progressively depleted either through senescence or apoptosis, until the aneuploid clone is virtually eliminated. Clonal-normalisation would require a mosaic embryo to contain a minimum proportion of normal euploid cells to establish both a functional TE and sufficient cells within the ICM to develop into a normal

embryo. In theory, it could also occur in a two-step process from an embryo with no normal cells; the first step generating euploid cells through cellular self-correction, although this is unlikely (as discussed above).

The exact proportion of normal cells required for embryo viability is unknown. Several articles quote a figure of two-thirds (Lavon et al., 2008, Frumkin et al., 2008, Barbash-Hazan et al., 2009) citing Li *et al.* (Li et al., 2005). Indeed, in their discussion the authors state 'if two-thirds of the cells of these *(mosaic)* embryos are normal, the embryo can continue to divide, overwhelming the abnormal cells, resulting in a blastocyst or even a live birth' (Li et al., 2005). This study assessed the chromosome status of single blastomeres in cleavage stage embryos, re-evaluated at day six, and correlated the aneuploidy status at cleavage stage with blastocyst formation and aneuploidy status at day six. No experimental data was presented to support the claim and nor is there other published direct evidence in the literature to date. As such, the concept of a minimum proportion of cells remains hypothetical, supported indirectly by observational data alone.

Currently, the non-invasive identification of aneuploid cells within an embryo is not possible. The current evidence offers only snap-shot approaches, and does not allow for follow-up of abnormal cells to determine their individual fates or their effect on the development of the embryo as a whole. Consequently, clonal normalisation is a plausible hypothesis, supported by significant weight of observational evidence, but remains untested. This study aims to investigate the fate of abnormal cells within the developing embryo in real-time, using a four-dimensional time-lapse imaging approach, in a mouse model of chromosome mosaicism.

1.4 THE FATE OF ANEUPLOID MOUSE EMBRYOS

Research on human embryos is challenging; in addition to the major ethical, legal and technical limitations, human embryos are a scarce resource, especially those of good quality. Pre-implantation research is also restricted to embryos derived from IVF, and *in vivo* early post-implantation study is not possible. Therefore, much of our knowledge of early mammalian development has arisen through the study of other mammals, most notably the

mouse. Mouse embryos are readily available, with the possibility to study *in vivo* conceived embryos, and the peri and post-implantation embryos are accessible. Further, the potential for genetic manipulation opens the scope for a wide range of different research questions. Although there are notable differences between mouse and human development, studies conducted on mouse embryos have provided key insights into early mammalian development, including humans.

In contrast to humans, the prevalence of aneuploidy in mouse pre-implantation embryos is estimated to be low at around 1-4% (Bond and Chandley, 1983, Glenister et al., 1987, Liu et al., 2008). Perhaps surprisingly, there are very few studies that specifically assess the level of aneuploidy in mouse embryos, most likely due to technical challenges unique to the pre-implantation mammalian embryo. Newer array-based and genome-sequencing technologies are able to provide efficient, accurate and comprehensive evaluation of chromosome status in single cells, and are now increasingly used in human blastomeres (Schoolcraft et al., 2010, Alfarawati et al., 2011, Treff and Scott, 2012, Capalbo et al., 2012). However, these techniques are still relatively expensive and need to be specifically adapted for use in non-human species and their application in mouse studies is still limited at present (including non-embryonic studies).

However, the result of several recent studies evaluating the chromosome status of mouse embryos using established techniques, have reported higher prevalence rates of aneuploidy than previous given estimates. The prevalence of mosaic aneuploidy in wild-type control embryos was found to be 25% in blastocysts assessed by classic cytogenetics (Lightfoot et al., 2006), and 17 and 31% in *in vitro* cultured cleavage stage embryos and blastocysts respectively, by two-probe FISH (Sabhnani et al., 2011). Interestingly, the latter study also found higher rates of aneuploidy in their in-vitro cultured embryos compared to the in-vivo controls; in-vivo cleavage and blastocyst stage embryos had abnormality rates of 2 and 8% respectively. This finding suggests that the *in vitro* culture environment could be a critical factor in the prevalence of aneuploidy.

In view of the high prevalence of aneuploidy in human embryos, its presumed role in reproductive failure, together with challenging research constraints, it is perhaps surprising that there are very few publications that use a mouse or other animal model to investigate

the effect of aneuploidy on early embryo development. Insights may be gained from animal models that could potentially have a direct relevance to human embryo development.

The following section summarises some key findings from relevant animal studies. The research questions in the majority of these studies do not directly relate to the fate of aneuploid or mosaic embryos; however, it is pertinent to review their findings in the context of this study. Collectively, the studies provide strong evidence that aneuploidy in mouse embryos is embryonic-lethal at around the time of early implantation, and that pre-implantation development is relatively unimpaired. In addition, there is some evidence to support the hypothesis that aneuploid mosaic embryos may have the ability to develop into viable, stably euploid offspring.

In their paper entitled 'The fate of mosaic aneuploid embryos during mouse development' Lightfoot *et al.* used *Sycp3*$^{-/-}$ null females to generate aneuploid embryos (Lightfoot et al., 2006). Sycp3 is a protein subunit of the meiotic synaptonemal complex, and its inactivation results in increased rates of meiotic errors, thus high rates of meiotic aneuploidy and hence aneuploid embryos (Yuan et al., 2002). Compared to wild-type controls, Sycp3 females had smaller litter sizes, despite producing an equal number of fertilized eggs. The majority of embryos developed to the blastocyst stage, at which point karyotyping was undertaken. As expected (Yuan et al., 2002), nearly two-thirds of blastocysts were aneuploid, however the majority displayed chaotic mosaic aneuploid karyotypes. The aneuploid embryos implanted but underwent p53-independent apoptotic death at the onset of gastrulation while the remaining viable embryos showed no evidence of mosaicism when assessed at embryonic day 12 (E12). The authors concluded that aneuploid embryos can undergo normal pre-implantation development but are non-viable beyond early implantation. One of the surprising findings in this study was the high incidence of chaotic mosaic aneuploidy, leading the authors to propose that a primary state of aneuploidy can render the embryo susceptible to chromosomal instability resulting in chaotic mosaic aneuploidies (Lightfoot et al., 2006).

Additional evidence of early post-implantation failure can be gained from the study of genetic knockout mouse models of chromosome instability (CIN). Chromosome instability is defined as a genetically unstable state arising from frequent chromosome segregation

errors occurring during mitosis, and is a highly aneuploid state (Holland and Cleveland, 2009). CIN can be the result of a multitude of different mechanisms including defects of the spindle assembly checkpoint (SAC) and aberrant kinetochore-microtubule attachments amongst others (Thompson et al., 2010). Genetic mouse knockout models have been created for many mitotic checkpoint genes, and for several other mitotic regulators and kinetochore components (Foijer et al., 2008). Consistently, all homozygous null knockout embryos shared the universal phenotype of early post-implantation lethality between E6.5 & E8.5. In contrast, heterozygotes exhibited a mild phenotype with no apparent developmental defects: *Cenpc* (Kalitsis et al., 1998), *Bub3* (Kalitsis et al., 2000), *Mad2* (Dobles et al., 2000), *Cenpa* (Howman et al., 2000), *Cenpe* (Putkey et al., 2002), *BubR1* (Wang et al., 2004a), *Bub1* (Jeganathan et al., 2007), *Mad1* (Iwanaga et al., 2007). In those studies where pre-implantation embryo development was specifically assessed (assaying the role of the *Mad2*, *BubR1*, *Bub3*, *Cenpc* and *Cenpa* genes), there was evidence of increased chromosome segregation characterised by high rates of micronuclei and other chromatin abnormalities, together with reduced proliferation in culture from E3.5 onwards, preferentially affecting the ICM, rather than the TE. With the exception of *Cenpc*, no studies evaluated embryos prior to the early blastocyst stage, however the homozygous embryos were recovered at the expected Mendelian ratios, therefore earlier lethality seems unlikely. *Cenpc* null embryos were morphologically normal at the 8-cell stage, but abnormalities started to manifest from the morula stage onwards (Kalitsis et al., 1998).

Collectively, these studies provide compelling evidence that embryonic aneuploidy is lethal at around the time of implantation or early post-implantation. Phenotypes secondary to gene knockouts can be attributed directly to the specific function of the gene, or may be an indirect result of a secondary downstream effect. In this series of genetic knockout mice, it is most likely that the early post-implantation lethality is a secondary effect, caused by aneuploidy; a direct effect would require that all genes have a critical role in embryo survival around the time of implantation. The effect of aneuploidy on pre-implantation development however is less conclusive. All genetic knockout mice underwent apparently normal pre-implantation development, however there were no attempts to evaluate the chromosome status of the blastomeres prior to the blastocyst stage. It cannot be assumed that chromosome segregation errors occurred in the first few cleavages as the presence of

maternally inherited factors may potentially have countered the knockout effects on chromosome segregation during the first few cleavages, with errors not arising in the earlier stages of pre-implantation development. Finally, although these animal studies provide convincing evidence that mosaic aneuploidy is likely to be lethal at or just after the time of implantation, they are unlikely to be representative of the majority of human pre-implantation mosaics. In the case of human mosaicism, the embryo is likely to be error-prone for the first few cleavages only, as the proportion of aneuploid cells within the embryo declines beyond the cleavage stage (Evsikov and Verlinsky, 1998, Clouston et al., 2002, Coonen et al., 2004, Santos et al., 2010, Johnson et al., 2010, Capalbo et al., 2012). Thus, many mosaics contain a complement of diploid cells and as development continues, further errors become less likely. In the mouse models discussed above, the underlying pre-disposition to aneuploidy is permanent affecting all cells, and consequently the phenotype is likely to be more severe with cumulative aneuploidy occurring as development proceeds.

One other animal study is of particular interest (Eggan et al., 2002). In this study viable mice were created from karyotypically unstable mosaic mouse embryonic stem cell (mES) lines using a tetraploid complementation approach. ES cell-tetraploid complementation is an experimental technique used to generate mice exclusively derived from the ES cell line, as the tetraploid cells remain confined to the extra-embryonic lineages (Tam and Rossant, 2003). ES-tetraploid embryos were constructed from a range of ES-cell lines with unstable mosaic karyotypes. Viable mice with stable karyotypes were generated from all ES cell lines tested, including those with high proportions of aneuploid cells (up to 80%) (Eggan et al., 2002). In addition, no correlation was found between the efficiency of the cell line to produce mice and the proportion of abnormal cells, or type of abnormality, within the cell line. Although interesting from a proof-of-principle point of view that normal offspring can be derived from mosaic mES cells, the direct relevance to unperturbed development is questionable. The generation of mice from ES cell-tetraploid complementation is far removed from naturally developing embryos, and thus not a representative model of normal development. The number of ES cells available for embryogenesis is likely to be far greater than there would be under normal developmental conditions, and the presence of tetraploid cells may further increase the availability of the normal cells to the future embryonic lineage. This may mask the requirement for a critical number of normal cells

necessary for the future potential of a mosaic embryo, as it is plausible that it is the number of normal cells available, rather than the proportion, that has greatest impact upon future viability. In addition the use of tetraploid cells may bypass any potential embryonic lethality that may occur as a direct result of aneuploidy affecting the extra-embryonic lineage.

1.5 NON-EMBRYONIC ANEUPLOIDY

Aneuploidy is most widely studied in the context of cancer research. Indeed, it has been branded as the hallmark of cancer as the majority of malignant tumour cells have an abnormal chromosome constitution (Holland and Cleveland, 2009). Consequently, there is a vast resource of literature characterising the potential causes and consequences of aneuploidy from the perspective of cancer. As discussed in the previous section, human embryo studies are largely limited to descriptive studies, with mechanistic biological questions almost impossible to study. Therefore, in addition to reviewing animal models of aneuploid embryogenesis, it is worthwhile reviewing the cancer-focused literature to collate what is currently known in the non-developmental context, and to identify any areas that may be potentially relevant to human embryogenesis. This may be beneficial to assist the collective understanding of human embryogenesis in the context of mosaic aneuploidy, and consequently focus the direction of future research programmes.

Aneuploidy in the context of cancer is a paradox; cancer is a state of uncontrolled cellular proliferation and tumour cells are almost always aneuploid, however the majority of aneuploid cells proliferate poorly. Transformation, defined as the acquisition of cancer-like properties, is believed to occur in only a small minority of aneuploid cells. Therefore the cellular consequences of the aneuploid state have been studied in great detail, in an effort to understand how aneuploidy-related alterations in cellular physiology may ultimately result in cancer. Whole-organism, uniform aneuploidy arising during gamete formation is frequently incompatible with life, with early developmental failure in most studied species ranging from the sea urchin, fruit fly, nematode, mouse, through to humans (Siegel and Amon, 2012). In those cases where aneuploidy is not lethal, the consequences are usually severe. In humans, the only whole chromosome autosomal aneuploidies that are potentially compatible with life are trisomy 21, 18 & 13 (Down, Edwards and Patau

syndromes respectively); the majority are lethal in-utero, however those that do survive have profound, multi-system developmental abnormalities and significantly shortened life-expectancies. Autosomal monosomies are never compatible with life. Thus, it is irrefutable that aneuploidy is significantly detrimental at the cellular and organism level; but precisely how aneuploidy affects individual cells is less well understood.

A detailed evaluation of how aneuploidy impacts upon fundamental cellular physiology is often hampered by the poor cellular fitness of these cells. Whole animal studies are rarely achieved as the establishment and maintenance of viable animal lines is expensive and practically challenging. Therefore, many cancer research studies are undertaken on immortalized cell culture lines. These are not directly relevant to the more frequently occurring, benign aneuploidies arising during mitosis that likely constitute the vast majority of human pre-implantation embryos. However, several studies have been published recently focussing more directly on the consequences of aneuploidy *per se*, and shed interesting light on the potential behaviour and fate of aneuploid cells (Torres et al., 2007, Williams et al., 2008, Li et al., 2010, Sheltzer et al., 2012).

Aneuploidies can be broadly categorised into two groups (Pfau and Amon, 2012): (a) chronic defined aneuploidies, where each cell contains the same, known abnormal chromosome constitution; or (b) acute random aneuploidies that arise secondary to frequent chromosome segregation errors, usually resulting in a pattern of complex and unstable, chaotic mosaicism. Several methods have been applied to derive aneuploid yeast strains and mammalian cell culture lines to study the effects of both types of aneuploidy at the cellular level (Torres et al., 2007, Williams et al., 2008, Li et al., 2010, Sheltzer et al., 2012). These studies have revealed that aneuploidy can disturb cellular physiology in a variety of different ways. Aneuploid cells have been shown to exhibit genetic dosage expression levels, transcribing and translating genes in proportion to their gene copy number (Mao et al., 2003, Lyle et al., 2004, Torres et al., 2007, Williams et al., 2008). By definition, aneuploid cells contain an abnormal proportion of genes; consequent imbalances in gene products are often detrimental and result in specific phenotypes directly related to the particular chromosome imbalance present in the cell. However, in addition to chromosome-specific effects, there are a number of phenotypes shared between different aneuploidies, indicating that there may be a common generic cellular response to aneuploidy (Torres et

al., 2007, Williams et al., 2008, Sheltzer et al., 2012). Further, there is also evidence that chromosome missegregation itself may affect cellular physiology, giving rise to a cellular response that may alter the fate of the cell regardless of the underlying aneuploidy (see below).

A key phenotype shared by aneuploid cells is impaired proliferation relative to euploid cells. This has been demonstrated in several chronic, defined aneuploidies: human trisomy 21 fibroblasts (Segal and McCoy, 1974), budding yeast disomic for different chromosomes (Torres et al., 2007), and aneuploid mouse embryonic fibroblasts (MEFs) trisomic for chromosomes 1, 13, 16 and 19 (Williams et al., 2008). Slower proliferation has also been characterised in cell lines with acutely arising random aneuploidies: MEFs bearing random aneuploidies secondary to impaired SAC function (Baker et al., 2004, Li et al., 2010) and human cell lines treated with different drugs to induce chromosome segregation errors (Thompson and Compton, 2008) also proliferate poorly relative to their wild-type or untreated euploid controls. Beyond proliferation rates, detailed studies of chronic defined aneuploidies have characterised a set of shared phenotypes that have been described as an 'aneuploidy stress response' (Torres et al., 2010): defects in cell growth, altered metabolism and proteotoxic stress (Torres et al., 2007, Williams et al., 2008). The slow growth and high energy demands arise secondary to the additional gene products that result from the presence of the additional chromosome. Protein stoichiometry imbalances arise secondary to excessive protein complexes; the cell attempts to compensate for the imbalance by increasing protein turnover, increasing the energy burden on the cell, and impairing proliferation (Jallepalli and Pellman, 2007). The aneuploidy stress response has only been characterised in cells with additional chromosomes, not for those with chromosome losses, such as monosomies. However, the consequences of chromosome loss are usually more severe than gain, and are more likely to result from an insufficiency of gene products critical for cell survival.

In contrast to chronic aneuploidies, acutely arising random aneuploidies may be associated with additional alterations in cellular physiology, as a direct consequence of the acute chromosome missegregation. Several studies have demonstrated that p53 is activated in response to chromosome missegregation, potentially resulting in cell-cycle arrest or apoptosis (Li et al., 2009, Li et al., 2010, Thompson and Compton, 2010). In two mouse

models of CIN, where chromosome missegregation occurs frequently, depletion of p53 has been shown to postpone early embryonic lethality by several days, and improve the viability of cultured MEF cell lines (Burds et al., 2005, Li et al., 2009).

A number of different mechanisms have been proposed to account for p53 activation in response to aneuploidy, including activation of the DNA damage response pathway and elevated reactive oxygen species (Li et al., 2010, Janssen et al., 2011, Crasta et al., 2012). Several recent studies have reported an association between abnormal mitosis and the acquisition of DNA damage, albeit through a variety of different mechanisms (Quignon et al., 2007, Dalton et al., 2007, Guerrero et al., 2010, Janssen et al., 2011, Crasta et al., 2012). This is an attractive hypothesis as it potentially unifies the paradox of how aneuploidy and tumorigenesis may be linked. Acute chromosome segregation errors resulting in whole chromosome aneuploidy may incur further genomic instability secondary to the associated DNA damage. In most instances the result will be a cell with impaired fitness that may undergo cell-cycle arrest or apoptosis. However, in a minority of cases the DNA damage may result in the acquisition of tumour-promoting mutations. The potential mechanisms of how DNA damage may be attained during mitosis are discussed in detail in a recent comprehensive review (Ganem and Pellman, 2012). In brief, these include: prolonged mitotic arrest (Quignon et al., 2007, Dalton et al., 2007), aberrant kinetochore-microtubule attachments at the mitotic spindle (Guerrero et al., 2010) or physical damage during cytokinesis (Janssen et al., 2011). Further, DNA damage occurring at or during mitosis activates a more limited cellular response than if it occurs during any other stage of the cell-cycle; although sites of DNA damage are marked by early DNA damage response (DDR) factors, the cell-cycle proceeds and the full DDR and repair pathway is not activated until completion of division, during the subsequent G1 phase (Giunta et al., 2010, Giunta and Jackson, 2011). This risks the propagation of unrepaired chromosome fragments to the resultant daughter cells. Finally, micronuclei resulting from chromosome segregation errors are vulnerable to further significant DNA damage that arises secondary to replication stress within the micronucleus (Crasta et al., 2012). The consequences of DNA damage in these micronuclei may be further confounded by inefficient nuclear importation of the essential DDR and repair agents (Terradas et al., 2010). Further, DNA replication within micronuclei has been demonstrated to be asynchronous and delayed when compared to its

corresponding primary nucleus, and as a result may enter subsequent mitosis whilst still in S-phase, increasing the risk of further substantial DNA damage (Crasta et al., 2012).

The significance of DNA damage arising secondary to chromosome missegregation is still uncertain, with several studies finding no direct evidence of DNA damage following missegregation events (Burds et al., 2005, Thompson and Compton, 2010, Li et al., 2010). Experimentally, the degree of double stranded DNA (dsDNA) damage is frequently quantified by assessing the recruitment of various DDR factors to the site of the damaged chromatin. Using these techniques, no evidence of increased DNA damage was identified in a chromosomally unstable human cell line (Thompson and Compton, 2010), or in the highly aneuploid and unstable SAC-mutant MEFs (Burds et al., 2005, Li et al., 2010). In contrast, the SAC-mutant MEFs were found to activate p53 via the ataxia telangiectasia mutated (ATM) protein kinase pathway secondary to elevated levels of reactive oxygen species (ROS) (Li et al., 2010). The finding of elevated ROS levels provides further evidence that suggests that aneuploid cells may experience increased metabolic burdens.

Therefore there is evidence from cancer-focused studies that the aneuploid state is associated with reduced cellular fitness secondary to a range of different potential mechanisms, both acute and chronic. These mechanisms have not been directly studied in human pre-implantation embryos. If the aneuploid cells in mosaic embryos are also affected by reduced cellular fitness relative to their diploid counterparts it is likely that aneuploid cells could be readily outcompeted by the surrounding diploid cells as development proceeds. The work presented in Chapter IV of this thesis investigates the potential role of these mechanisms in a mouse model of pre-implantation embryonic chromosome missegregation.

1.6 AN OVERVIEW OF PRE-IMPLANTATION MOUSE DEVELOPMENT

The study presented in this thesis uses the mouse as a model for mammalian development in the context of pre-implantation chromosome mosaicism. Therefore, the purpose of this section is to summarise the key features of pre-implantation mouse embryo development (Figure 1.5).

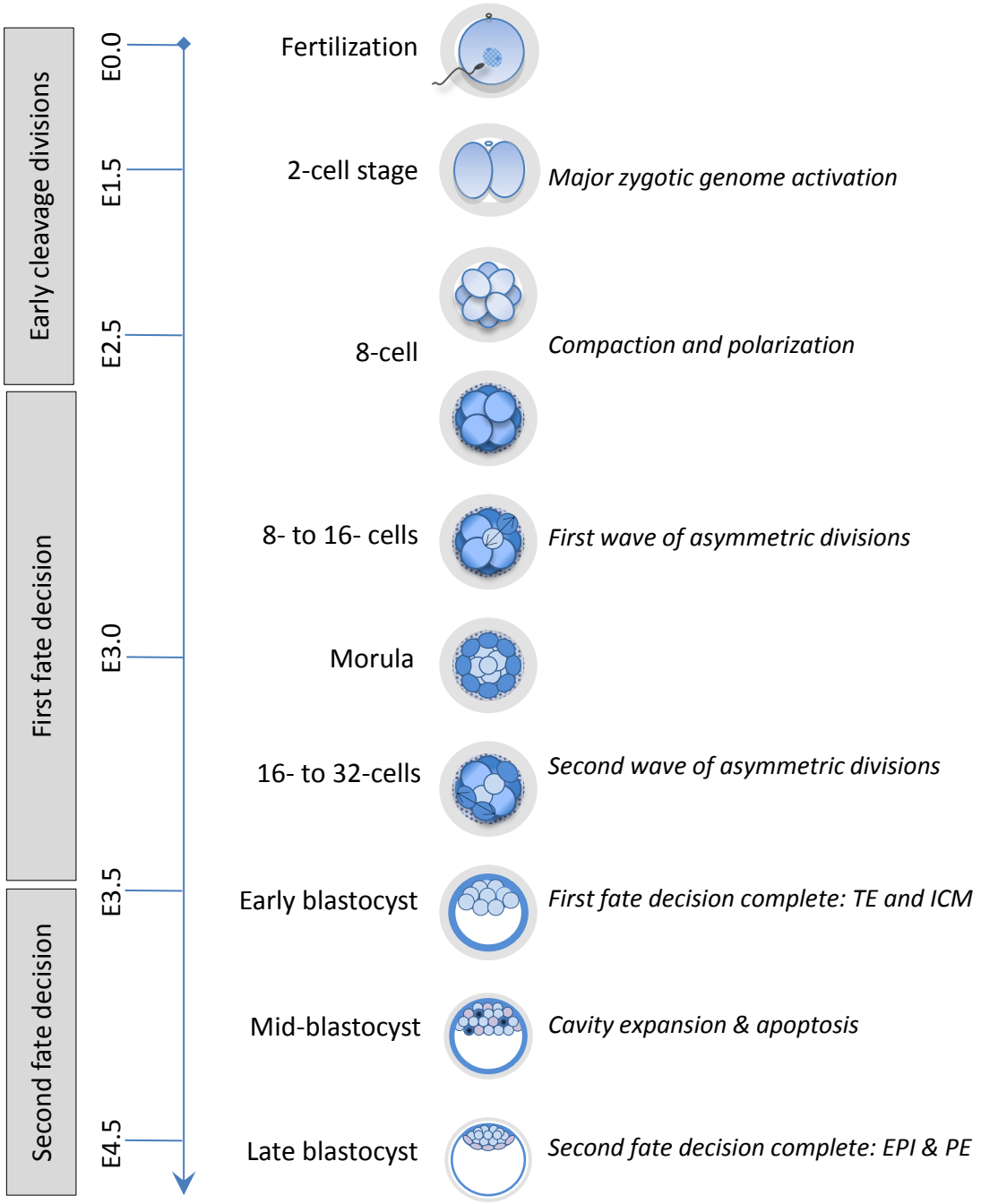

Figure 1.5. An overview of pre-implantation mouse development. Following fertilization, major ZGA occurs at the 2-cell stage and the embryo undergoes successive cleavage divisions until the 8-cell stage when compaction and polarisation occur. Two waves of asymmetric divisions occur, during which time the inner and outer populations are established. The first fate decision, segregation of the TE and ICM, is complete by E3.5 at the early blastocyst stage. The blastocyst cavity expands during which time cell lineages segregate further and apoptosis occurs within the ICM. By E4.5 the blastocyst cavity is expanded and the second fate decision is complete – segregation of the PE and EPI. The embryo is now ready for implantation.

In the mouse, pre-implantation development takes place over a period of approximately four and a half days, during which time the uterine tissue prepares to receive the embryo. Mammalian development is viviparous; the embryo develops within the mother, who gives birth to live young at the end of gestation. A key necessity of viviparity is the development of a highly specialised set of extra-embryonic membranes and placenta located at the materno-fetal interface. These function to facilitate the effective transfer of essential nutrients from the mother to the developing offspring. Consequently, a major function of pre-implantation development is the establishment of the extra-embryonic lineages that are vital for successful uterine implantation and hence post-implantation development.

Following implantation there is a dramatic increase in the growth rate of the embryo, particularly within the epiblast cells; the progenitors of the future fetus. Gastrulation occurs around two days later as the endoderm, mesoderm and ectoderm lineages emerge from the primitive streak. Gestation in the mouse is usually completed within 19 to 20 days.

Pre-implantation development begins at the moment of fertilization and ends with the formation of the mature blastocyst, at which time the embryo is ready to implant into the uterine wall. Fertilization takes place within the ampulla of the oviduct, near the ovary. The embryo travels along the oviduct as development proceeds, and passes into the uterine cavity at around three days post-fertilization. As the blastocyst cavity expands, it hatches from the zona pellucida, the glycoprotein membrane that surrounds the earlier embryo, ready for implantation. Pre-implantation development is complete at the mature blastocyst stage at which point the first three cell lineages are segregated; the TE, PE, and EPI. The TE gives rise to the embryonic component of the future placenta, the PE gives rise to a set of extra-embryonic membranes, the visceral and parietal endoderm which later contribute to the yolk sac, and the EPI gives rise to the future fetus.

1.6.1 Early cleavage divisions

Upon fertilization, the zygote first undergoes a series of cleavage divisions, resulting in an increase in cell number; the resulting daughter cells become progressively smaller but without any accompanying growth or change to the size of the embryo (Aiken et al., 2004).

1.6.2 Zygotic genome activation

The early mouse embryo initially relies on maternal factors, RNA and proteins stored in the oocyte, to support its development until ZGA occurs. ZGA is defined as the time point at which transcription of mRNA coded by the zygotic genomic DNA begins. This occurs in two waves in the mouse; a minor wave of zygotic transcription at the late 1-cell stage (minor ZGA), followed by a second major wave at the 2-cell stage (major ZGA) (Latham and Schultz, 2001, Hamatani et al., 2006, Wang et al., 2004b). Accompanying the major wave of ZGA is the degradation of the majority of maternal transcripts (Schultz, 2002, Hamatani et al., 2006) although some maternal factors may persist beyond the blastocyst stage (Bachvarova and De Leon, 1980).

1.6.3 Compaction and polarization

During first few cleavage divisions, the developing embryo consists of individually distinct, morphologically identical, symmetrical blastomeres. During the 8-cell stage there is dramatic reorganisation of the cells within the embryo as they compact, and within the cells themselves as they polarise along their apical-basolateral cell axis. Although polarisation and compaction are temporally linked and occur at the same time during normal unperturbed development, they are different and distinct processes. Compaction can occur without polarisation (O'Sullivan et al., 1993), and likewise polarisation without compaction (Johnson and Maro, 1984).

Compaction occurs when the 8-cell stage blastomeres adopt a more flattened morphology, secondary to an increase in intercellular adhesion. The embryo transforms into the morula; a tightly packed structure with the loss of distinctive cell outlines. Compaction maximises intercellular contacts, concomitantly minimising the amount of contact each blastomere has with the outside environment.

Polarisation occurs when the 8-cell stage blastomeres lose their intracellular symmetry, usually at the time of compaction. At the early 8-cell stage each blastomere is symmetrically organised with an even distribution of microvilli over the entire cortex. Following compaction, when polarisation occurs, this symmetry is lost at all levels of organisation; the cell nuclei reposition basally, the cytoplasm and cytoskeleton reorganise, and the surface

microvilli become restricted to the apex of the blastomeres, polarity proteins Par3, Par6 and aPCK localise apically, and Par1 localises basolaterally (Johnson and McConnell, 2004). Polarity is organised axially with respect to the centre of the embryo; outward facing apical regions become distinct from the inward facing baso-lateral regions.

1.6.4 Symmetric and asymmetric divisions

Following compaction and polarisation the blastomeres in the embryo undergo a further two rounds of division that generate the 16- and then 32-cell stage embryo generating two distinct cell populations, the inner and outer cells. At the 8-cell stage, every blastomere is an outside cell and there is no inside cell population. However, when an 8-cell blastomere divides, it can give rise to outer or inner daughter cells, depending upon the orientation of the cleavage plane. These divisions can be classified as either symmetric or asymmetric, and are highly relevant in determining the future fate of their daughter cells (Johnson, 1981). Symmetric divisions occur when the blastomere divides along the apical-basolateral axis; both daughter cells will remain on the outside of the embryo. In contrast, asymmetric divisions occur when the blastomere divides perpendicular to the apical-basolateral axis; one daughter cell will remain on the outside of the embryo, while the other will be located on the inside. Symmetric divisions give rise to two identical, polarized daughter cells. In contrast, the two daughters arising from an asymmetric division are different, based on their differential inheritance of the apical and basal domains established during polarisation of their mother blastomere. The outer cell predominantly inherits the apical polarised domain, while the inner cell predominantly inherits the baso-lateral domain. The two distinct populations of cells differ not only in their physical position within the embryo, but also in their polarity, and characteristics that anticipate their future fate as either TE or ICM cells (Johnson and McConnell, 2004). Symmetric or asymmetric divisions occur in two waves during the fourth and fifth cleavage divisions, or 8- to 16- and 16- to 32-cell divisions respectively (Pedersen et al., 1986). Both types of division will always result in the formation of an outer cell, however only asymmetric divisions will give rise to an inside cell. Thus, every outside cell in the 8 and 16-cell stage embryo will contribute to the future TE, however only those that undergo asymmetric divisions will contribute to the ICM, and

hence the future fetus. More recently a third although rarely observed wave of asymmetric division has been described, occurring at the sixth cleavage (Morris et al., 2010). This study used a time-lapse imaging approach to track the ultimate fate of the inside progeny that arose from these asymmetric divisions and found that these progeny invariably contributed to the PE population of cells. In addition, this study also found that inside cells arising during the 8- to 16-cell cleavage were significantly more likely to give rise to future EPI cells, while those arising at the 16- to 32- cell division were strongly biased towards a PE fate. These findings led to the authors proposing a model in which the future cell fate of the PE or EPI is influenced by the amount of time the ancestral parent cells reside with an outer surface; the earlier the cell is internalised the more likely it is to retain its pluripotent properties and thus contribute to the EPI lineage (Morris et al., 2010). However, in contrast to these results, another study also employing a time-lapse imaging approach, albeit on experimentally manipulated embryos, found no clear linkage between the timing of ICM progenitor cell internalisation and subsequent developmental fate (Yamanaka et al., 2010). A possible reason for the discrepancy in results between the two studies, relating to experimental artefacts on blastomere apical-basolateral polarisation, has been suggested (Morris, 2011). This study also demonstrated that modulating Fgf4 (Fibroblast growth factor 4) signalling during blastocyst maturation could shift the fate of ICM cells towards either EPI or PE fate, by inhibition of, or addition of exogenous Fgf4 respectively. These results were in accord with a previously reported study (Nichols et al., 2009). Accordingly, Yamanaka et al., proposed an alternative developmental model in which stochastic and progressive specification of the EPI and PE lineages occurs during maturation of the blastocyst, in an Fgf4 signal-dependent manner (Yamanaka et al., 2010).

Therefore, between the 8- and 32- cell stage the embryo has transformed from a morphologically uniform population of cells into two distinct populations. This first fate decision segregates the ICM from the TE lineage. Cells on the outside of the embryo contribute to the TE lineage, while inside cells contribute to the ICM and will later segregate to form the EPI and PE blastocyst lineages.

1.6.5 Formation of the blastocyst, cavity expansion and apoptosis

At the 32-cell stage, as the TE differentiates into a functional epithelium, fluid filled cavities begin to form within the embryo. These coalesce into a single, expanding cavity known as the blastocoel and its presence now defines the embryo as a blastocyst. As the blastocyst cavity expands the inner cell population cluster together and are displaced to one end of the blastocyst. The location of the cluster of ICM cells defines the embryonic-abembryonic axis of the blastocyst. The embryonic pole comprises the ICM and its surrounding trophectoderm, now known as the polar TE; the abembryonic pole is demarked by the blastocoel cavity and its surrounding TE, now known as the mural TE. The early blastocyst is usually formed by three and a half days post fertilization, and coincides with the establishment and segregation of the ICM and TE lineages which remain distinct from here onwards (Dyce et al., 1987).

The progressive expansion of the blastocyst cavity continues for a further 24 hours as the embryo undergoes a further two rounds of cell division. During this time the ICM cells further diverge into two separate lineages with different fates, the PE and EPI. The PE gives rise to a set of extra-embryonic membranes, and is a superficial epithelial layer of cells that lines the embryonic pole of the blastocyst cavity. In contrast, the EPI remains as a deep population of non-polarised cells that remains pluripotent.

As the blastocyst cavity expands some cells within the ICM usually undergo apoptosis (Copp, 1978, Fabian et al., 2005). Cell death is rarely observed prior to cavitation, or within the TE lineage. Apoptosis is observed in the majority of *in vivo* derived embryos, and affects up to 10-20% of ICM cells, in contrast to just 1-3% of TE cells (Hardy, 1997). Maximal cell death occurs at the late-32 to early 64-cell stage, at around the same time that the ICM segregate into EPI and PE lineages (Copp, 1978, Pampfer and Donnay, 1999). The function of apoptosis within the pre-implantation embryo is not fully understood; increased levels have been reported on exposure to hyperglycaemia (Moley et al., 1998), however it also occurs during apparently normal, *in vivo* development (Copp, 1978, Brison and Schultz, 1997, Pampfer and Donnay, 1999). Apoptosis is a well-established characteristic of normal embryogenesis and can usually be understood in terms of its morphogenic role, for example in sculpting the shape of digits during limb development. However, the location and apparent randomness

of apoptosis within the ICM favour an alternative, non-morphogenic function. In non-developmental settings, a major role of apoptosis is the elimination of abnormal or potentially deleterious cells. Therefore it has been widely hypothesized that apoptosis within the ICM may serve to eliminate cells with underlying abnormalities such as aneuploidy or DNA damage, or with inappropriate developmental potential, such as the presence of cells with TE identity within the ICM lineage (Hardy, 1997, Pampfer and Donnay, 1999, Fabian et al., 2005).

The potential role of apoptosis in the elimination of abnormal cells from the ICM is addressed in this study.

During blastocyst cavity expansion, the ICM cells further segregate themselves into the deep, pluripotent EPI lineage, or differentiate into the PE. The PE is an epithelial layer of cells that line the surface of the blastocyst cavity by the late blastocyst stage.

1.6.6. Developmental plasticity

A key feature of early mammalian development is its highly regulative nature. During the first few cleavages the embryo is able to tolerate significant experimental perturbations without adverse effects on subsequent development, including the removal, addition and rearrangement of blastomeres (Tarkowski and Wroblewska, 1967, Hillman et al., 1972). This phenomenal resilience provides irrefutable evidence that early blastomeres share similar developmental potencies, and are able to alter their developmental pathway if necessary.

However the highly regulative nature of the early embryo with its remarkable ability to adapt to change, does not exclude the possibility of naturally occurring asymmetries that may bias cell fate during normal, unperturbed development. Indeed there is plenty of experimental evidence to support the presence of such early developmental bias, even occurring as early as the first cleavage division (Gardner, 1997, Piotrowska et al., 2001, Piotrowska and Zernicka-Goetz, 2001, Gardner, 2001, Plusa et al., 2005, Plachta et al., 2011, Tabansky et al., 2013).

The developmental flexibility of the embryo diminishes as development proceeds. As lineages become established the blastomeres become progressively committed to their prospective developmental fate losing their developmental potency, becoming unable to adapt to perturbations. At which developmental time point do blastomeres restrict their developmental potency? The transition from the 8- to 16-cell stage marks first milestone at which point there are two subpopulations of cells that can be distinguished by their properties, position and their prospective fate. In unperturbed development outside cells contribute progeny to the TE, some outside cells contribute progeny to the ICM, and inside cells contribute progeny exclusively to the ICM. However, experimental manipulation of embryos at this stage has demonstrated that there is still considerable developmental plasticity of both cell populations. If outer cells are removed, exposing the inner cells to the outside environment, they undergo polarisation and develop TE-like properties (Ziomek and Johnson, 1982, Johnson and Ziomek, 1983). Further, when aggregation chimeras are constructed exclusively from the outside cells of 16-cell stage embryos (outside-only chimeras), or conversely exclusively from inside cells (inside-only chimeras), both are able to develop into blastocysts and healthy mice, although the implantation rates for inside-only chimeras are lower (Suwinska et al., 2008). In contrast, if this experiment is repeated at the 32-cell stage, neither outside-only nor inside-only chimeras develop into viable mice, although inside-only chimeras are able to organise into recognisable blastocysts. In contrast, outside-only chimeras were unable to compact. Thus, these studies demonstrate that 16-cell stage blastomeres retain developmental plasticity and hence potency, but that this is lost by the 32-cell stage. What still remains unknown is whether every cell within the 16-cell stage embryo retains pluripotent potential, or if this is restricted to a subpopulation of cells.

1.6.7 Pre-implantation development in the human embryo

The majority of what is known about mammalian pre-implantation development has arisen through study of the mouse embryo. Due to limited availability of human embryos for research, far less is known about pre-implantation development in humans. At the morphological level the human embryo is similar to the mouse undergoing cleavage, compaction, blastocyst cavity formation and hatching prior to implantation. However,

where studies on human embryos have been possible it is clear that there are differences between human and mouse development, most notably in the timing of developmental events and mechanisms of lineage specification (Cockburn and Rossant, 2010, Niakan et al., 2012, Oron and Ivanova, 2012). In addition, the high rates of developmental arrest, aneuploidy and abnormal morphology encountered in human pre-implantation embryos are rare in the mouse embryo. A more detailed discussion of the relative merits and limitations of using the mouse embryo as a model for the human embryo is presented in the following chapter.

1.7 AIMS OF THIS STUDY

Aneuploidy is a major cause of human reproductive failure, and widely believed to be responsible for the relatively low success rates of *in vitro* fertilization (IVF). The majority of human pre-implantation embryos are mosaics, due to chromosome segregation errors occurring during the first few cleavages. Pre-implantation genetic screening (PGS) was developed with the goal of improving IVF outcomes by identifying and discarding aneuploid embryos, and thus transferring those embryos with the greatest developmental potential. Despite intense efforts, PGS failed. Until aneuploidy can be assessed non-invasively, mosaicism will always prove problematic for PGS. However, due to the technical and ethical limitations of human embryo research, the ultimate fate of mosaic embryos remains elusive. Therefore the first aim of this study was develop a mouse model of human embryo chromosome mosaicism. This model was then used to investigate the fate of abnormal cells within the embryo, and then the ultimate developmental potential of the embryo as a whole. Finally, the model was used to investigate the potential mechanisms accounting for the ultimate fates of the abnormal cells, drawing parallels between abnormal embryo development and cancer biology.

DEVELOPING A MOUSE MODEL OF CHROMOSOME MOSAICISM

2.1 INTRODUCTION TO RESULTS I

The major aim of this chapter was to create a mouse model for human pre-implantation chromosome mosaicism that could then be used to evaluate the consequences of mosaic aneuploidy during development.

The majority of mosaic embryos in human development are diploid-aneuploid mosaics (van Echten-Arends et al., 2011). Therefore to investigate the fate of aneuploid cells within diploid-aneuploid mosaic embryos it was necessary to create a mouse model that contained a clone of cells that were likely to be normal. The mouse is usually considered a poor model of the human pre-implantation embryo development due to the low reported incidence of aneuploidy in the mouse embryo. However in this study this characteristic could be utilized to experimental advantage, as it would indeed be possible to ensure that the mouse model embryo contained a proportion of cells that were likely to be normal, and thus enable the fates of both normal and abnormal clones to be compared directly.

Two potential experimental approaches for creating mosaic embryos were possible as illustrated in Figure 2.1. Mosaic embryos could either be true or chimeric mosaics, depending on the source or origin of the abnormal blastomeres. In true mosaics the abnormal blastomeres would originate as direct progeny arising from a clone of cells within a single intact embryo (Figure 2.1a). This would be the ideal model for mosaicism as the normal and abnormal clones would act as near-perfect controls for each other and there would be minimal disruption to the embryo. However some experimental approaches are not suitable for this model. In these cases an alternative approach would be to create chimeric mosaics, whereby single mosaic-type embryos are generated by aggregating blastomeres together that originate from two different embryos (Figure 2.1b).

In developing a mouse model for chromosome mosaicism it was necessary to generate or acquire a source of aneuploid blastomeres. Two experimental approaches were considered; abnormal blastomeres could be obtained from embryos with chronic defined aneuploidies (as defined in the previous chapter), or alternatively generated experimentally by inducing

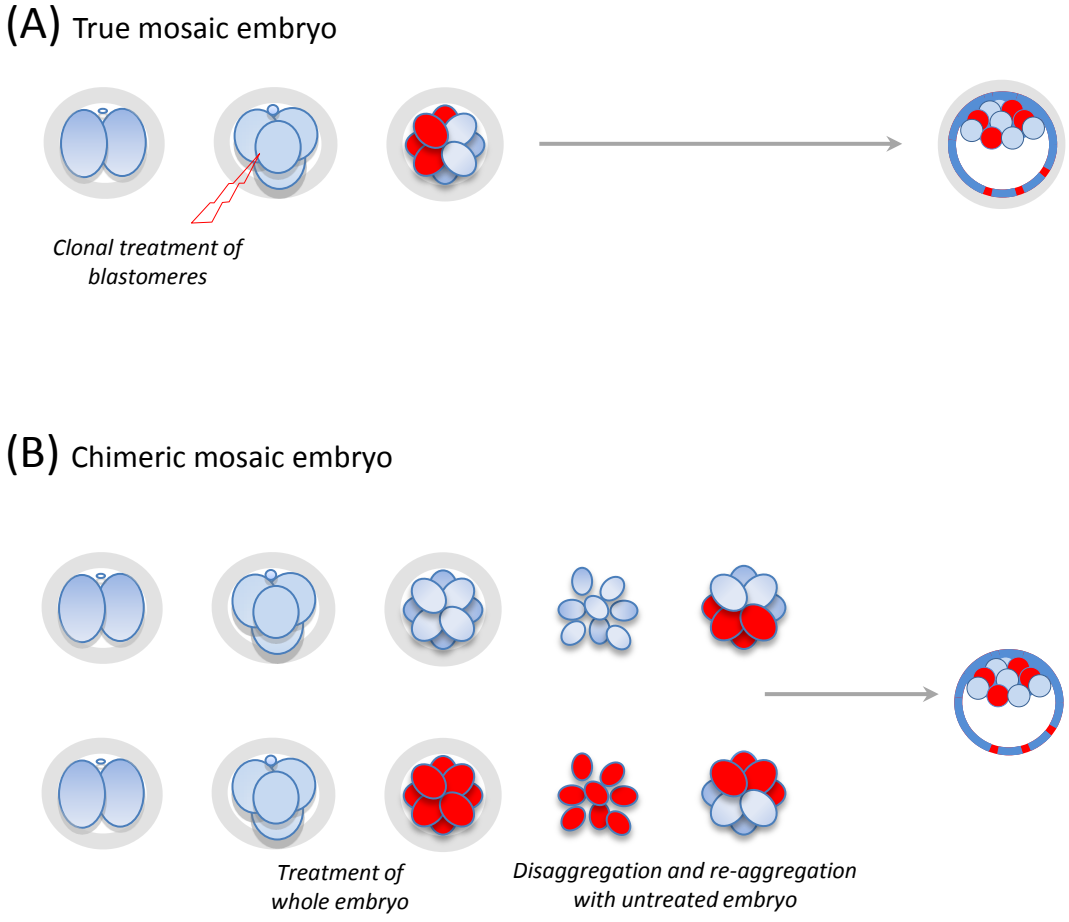

Figure 2.1 Experimental strategies for generating mosaic embryos. (A) In a true mosaic embryo, treatment is restricted to a single clone of blastomeres. This technique is limited to treatments or manipulations that can be carried out in one blastomere, without altering the others **(B)** In chimeric mosaic embryos the final embryo is constituted of cells obtained from two different embryos aggregated together. The embryos have been subjected to different treatments or are of a different genetic background. This method is employed when clonal treatment options are not technically possible.
Colour scheme: Blue denotes euploid and red denotes aneuploid blastomeres

chromosome segregation errors in blastomeres during mitosis. In the first instance the experimental strategy focused on generating abnormal blastomeres secondary to acutely arising chromosome segregation errors occurring during mitosis. Of the two potential approaches, this was considered to be the most representative model for human pre-implantation aneuploidy. Unlike chronic defined aneuploidies, chromosome segregation errors that arise during mitosis usually result in a pattern of complex, unstable chaotic mosaicism with a range of aneuploidies in different cells (Pfau and Amon, 2012), and resemble the patterns of aneuploidy that have been described in human cleavage stage embryos (Vanneste et al., 2009, Ledbetter, 2009). Human embryo aneuploidies are frequently chaotic with a wide range of different chromosomes affected and variable abnormalities often identified within the same embryo, even within the same blastomere (Vanneste et al., 2009, Rabinowitz et al., 2012). An additional important factor to take into consideration was the possibility that chromosome segregation errors arising during mitosis may directly trigger acute cellular responses that could have a significant impact upon the future fate of the cell, as discussed in section 1.5 of the previous chapter. In the context of the pre-implantation embryo, such acute cellular responses could play a critical role in determining the fate of the abnormal blastomeres and the embryo. If so, such effects may be missed if blastomeres containing chronic defined aneuploidies were used in the model embryo.

To create a mouse model of acutely arising chromosome mosaicism it was necessary to induce transient chromosome segregation errors in cleavage stage blastomeres. When any cell undergoes division it must faithfully segregate its duplicated chromosomes between each daughter cell and any errors occurring during this process can result in aneuploidy. Such errors may arise as a result of disruption of the spindle assembly checkpoint (SAC), defects in chromosome attachments to the mitotic spindle, abnormalities in chromosome cohesion, failures of error correction mechanisms or centrosome abnormalities (Holland and Cleveland, 2009, Fang and Zhang, 2011). The mechanism underlying the origin of aneuploidy in the human embryo is not known. However the relaxation or absence of cell-cycle checkpoints, or the proteins involved, during the first few cleavage divisions of the human pre-implantation embryo has been speculated as a possible cause of chromosome mosaicism (Delhanty and Handyside, 1995, Harrison et al., 2000, Los et al., 2004,

Ambartsumyam and Clarke, 2008, van Echten-Arends et al., 2011, Mantikou et al., 2012). The experimental perturbation of any of these pathways is likely to result in aneuploidy and therefore this strategy was applied to cleavage stage embryos in this study. Described further in this chapter are a range of experimental techniques that were applied with the intention of either abrogating the SAC or disrupting kinetochore structure, in order to cause chromosome segregation errors in the clone of treated blastomeres.

The SAC is the primary surveillance mechanism that acts to prevent a cell from entering mitosis in the presence of unattached chromosomes (Musacchio and Salmon, 2007). During pro-metaphase chromosomes align along the mitotic spindle and attach via direct interactions between their kinetochores and the spindle microtubules. As chromosomes align the SAC is active and prevents the cell from entering anaphase until every single kinetochore is attached to the spindle (Rieder et al., 1995). The SAC acts through a complex biochemical pathway involving interactions between kinetochores and multiple SAC proteins that concentrate at the site of unattached kinetochores, generating a signalling cascade that ultimately inhibits the onset of anaphase (Musacchio and Salmon, 2007). SAC proteins that accumulate at unattached spindles become depleted by microtubule attachment to kinetochores, and when all kinetochores are attached this ultimately results in the onset of anaphase, and mitosis proceeds (Hardwick and Shah, 2010). Core SAC components include Mad2, Bubr1, Bub3, Mad1, Mps1 and Aurora B, together with a multitude of other and additional regulatory proteins (Kops et al., 2005, Musacchio and Salmon, 2007). Cells without a functional SAC exhibit high rates of chromosome segregation errors, a shortening of the time from metaphase to anaphase (Gorbsky et al., 1998, Canman et al., 2002, Meraldi et al., 2004), and a failure to undergo arrest in mitosis under conditions that would usually prevent satisfaction of the checkpoint such as drug treatment with spindle poisons (Rieder and Palazzo, 1992, Rieder and Maiato, 2004).

Central to the formation of stable attachments between the chromosomes and spindle microtubules is the kinetochore, a complex multi-protein structure assembled on the centromeric regions of the chromosomes at the time of mitosis (Cheeseman and Desai, 2008). The outer kinetochore proteins are required for the formation of stable attachments to the spindle microtubules and several of the key SAC proteins bind directly to the kinetochores (Kline-Smith et al., 2005, Ciferri et al., 2007). Kinetochore structure is

intricately related to the function of the SAC (Musacchio and Salmon, 2007). Defects in key outer kinetochore components result in chromosome segregation errors mediated through unstable attachments of the chromosomes to the microtubules or through bypass of the SAC (Kline-Smith et al., 2005). Of the many proteins that constitute the kinetochore, the highly conserved Ndc80 complex is a key component of the outer kinetochore that has an essential role in maintaining stable kinetochore-microtubule connections (Kline-Smith et al., 2005, Ciferri et al., 2007).

In this chapter the development of a mouse model of pre-implantation diploid-aneuploid mosaicism is presented.

2.2 MATERIALS AND METHODS

2.2.1 Pre-implantation embryo collection and culture

F1 (C57B16xCBA) female mice were injected with 10IU of PMSG (Intervet) followed by 10IU of hCG (Intervet) 48 hours later to induce superovulation. Females were paired with stud males for mating. Unless specifically stated, females were paired with F1 males. In a subset of time-lapse imaging experiments females were mated with H2B-GFP transgenic males (Hadjantonakis and Papaioannou, 2004).

Embryos were recovered into M2 medium from sacrificed females at the required developmental stage depending upon the experiment. All experimental manipulations were carried out in M2 medium, but any prolonged culture or imaging was undertaken in KSOM medium under mineral oil, equilibrated to 37^0C in atmospheric oxygen and 5% carbon dioxide.

M2 and KSOM media were prepared from stocks within the laboratory according to standard protocols (Nagy et al., 2003).

2.2.2 Generating metaphase spreads

Embryos at different stages of development were treated with demecolcine or colchicine (Sigma) to induce metaphase arrest. They were treated with a hypotonic solution of sodium citrate (Sigma), followed by fixation in methanol and acetic acid solutions (Sigma). Following fixation the embryos were dropped onto clean glass slides, and evaluated for metaphase spreads on a phase microscope, or a Deltavision fluorescent widefield microscope following 4',6-diamidino-2-phenylindole dihydrochloride (DAPI) (Invitrogen) staining of the DNA. As a protocol control, metaphase spreads were generated from MEF cells. MEF cells were obtained from E13.5 fetuses following natural mating, and cultured overnight in Dulbecco's Modified Eagle Medium (DMEM) (Invitrogen) supplemented with 10% fetal calf serum (FCS) and penicillin-streptomycin (Invitrogen).

2.2.3 Immunocytochemistry

Embryos were treated with acid Tyrode's (AT) solution (Sigma) to remove the zona pellucida and left to rest in M2 for 20 minutes. Unless otherwise stated all reagents were diluted in

phosphate buffer solution (PBS), incubations carried out room temperature, and washes were for a minimum of five minutes in PBS-T (0.1% Tween-20 (Sigma) in PBS).

For anti-centromere antibody (ACA) staining, embryos were fixed in methanol (Sigma) at -20^{o}C for one hour. For haemagglutinin (HA) tag staining, embryos were fixed in 4% paraformaldehyde (PFA) solution (EMS) for 20 minutes in the dark. Embryos were then permeabilized for 20 minutes in 0.6% Triton X-100 (Sigma), washed and then incubated in blocking solution for a minimum of four hours at 4^{0}C. Blocking solution comprised of 3% bovine serum albumin (BSA) (Sigma) in PBS.

Embryos were then incubated in the required primary antibodies diluted in blocking solution for a minimum of six hours at 4^{0}C. Primary ACA antibodies were supplied ready-conjugated with fluorescein isothiocyanate (FITC). For HA-tag antibodies, embryos were washed and incubated in secondary antibody for one hour, washed again and then incubated in DAPI for five minutes. Embryos were transferred into M2 for imaging on an Olympus FV1000 or Leica SP5 inverted confocal microscope and captured with Olympus Fluoview FV10-AW or LAS AF software respectively.

FITC-labelled ACA antibodies (human antisera, Antibodies Incorporated) were diluted at 1:100; anti-HA antibodies at 1:250 (mouse monoclonal, Covance); and secondary Alexa-Fluor 488-conjugated anti-mouse antibody at 1:500 (Invitrogen).

2.2.4 Plasmid construction and mRNA synthesis

A plasmid vector (pCDNA3) containing the full length DNA sequence of human CENPB (centromere associated protein B) tagged with GFP (CENPB-GFP) was obtained as a gift from Jonathan Pines (Principal Investigator, Gurdon Institute, University of Cambridge). This was subcloned into plasmid pBluescript RN3P (pRN3P:CENPB-GFP) ready for *in vitro* transcription (IVT) of recombinant mRNA. The pRN3P vector was used because it allowed for the inserted CENPB-GFP to be transcribed *in vitro* from the upstream T3 RNA polymerase II promoter whilst incorporating the 5' and 3' untranslated regions (UTRs) of the frog β-globin gene locus, which provided transcript stability following microinjection into embryo blastomeres. The CENPB-GFP insert was isolated from pCDNA3 using *EcoRI* and *NotI* restriction enzymes

(New England Biolabs), alongside preparation of the pRN3P vector with the same enzymes. The prepared vector and inserts were then ligated using T_4 DNA ligase (Roche), followed by chemical transformation into DH5-α *E. coli* (Stratagene). Successful transformants were selected by overnight incubation on LB agar plates with ampicillin. Purified DNA plasmids were then digested with *EcoRI* and *NotI* and run on a 1% agarose gel to confirm the presence of the desired CENPB-GFP insert. Successful plasmid clones were sent for sequencing, yielding a sequence verified pRN3P:CENPB-GFP plasmid.

A Mad2 dominant negative construct (Mad2_DN) containing an N-terminus HA-tag was obtained from Bedra Sharif (then a PhD student in David Glover's laboratory, Department of Genetics, University of Cambridge). This construct was obtained already cloned into the pRN3P plasmid, ready for linearization and IVT.

A mouse Bubr1_dominant negative construct (Bubr1_DN) was designed to contain an N-terminus HA-tag. The cDNA was amplified from a sequenced IMAGE clone obtained from GeneService using Phusion High-Fidelity PCR (Thermoscientific). Primers were designed to incorporate *BamHI* and *XbaI* restrictions sites, a Kozak sequence, HA-tag, start and stop codons (Table 2.1). The resulting PCR product was sub-cloned into pRN3P prepared with *BamHI* and *XbaI* (New England Biolabs), as described above. The purified plasmids were digested with *BamHI* and *XbaI* and run on a 1% agarose gel to confirm the presence of the Bubr1_DN insert, and sequenced to confirm successful cloning.

All mRNAs were transcribed from pRN3P vectors linearized by the restriction enzyme *SfiI* (Roche), as pRN3P contained a unique *SfiI* recognition site not present in any of the inserts, and then purified using a standard phenol-chloroform extraction protocol. The mMessage mMachine T3 Kit (Ambion) was used to transcribe and cap mRNA *in vitro*. The mRNA was dissolved in nuclease-free water to the desired working concentrations and microinjected into blastomeres as required. Microinjections were carried out in M2 on a glass concaved slide using a Femtojet micro-injection system (Eppendorf).

In this chapter the following mRNAs were microinjected at the given concentrations: *CENPB-GFP* 0.04 μg/μl; *dsRed* 0.5 μg/μl; *Histone-RFP* 0.02 μg/μl; *Mad2_DN* 0.8 & 2.0 μg/μl; *Bubr1_DN* 0.8 & 1.75 μg/μl.

2.2.5 Preparation of short interfering RNAs (siRNA)

Pre-designed siRNAs for *Mad2*, *Bubr1* and *Ndc80* were purchased from Invitrogen (Stealth RNAi™), together with a universal negative control siRNA (medium GC content; catalogue number 12935-112). For each gene, three non-overlapping pre-annealed 25-nucleotide dsRNA oligos were supplied and mixed together in equal proportions and diluted in nuclease-free water at the required concentration, ready for microinjection. The sequences are given in Table 2.2.

2.2.6 Drug treatments

Nocodazole (NZ) (Sigma) was used at a concentration of 0.33μM diluted in culture medium. Reversine (Cayman chemicals) was dissolved in DMSO and used at concentrations of 0.5 or 1.0μM. Where required, control embryos were incubated in the equivalent DMSO concentration in the absence of the active drug. The final concentration of DMSO was 0.005%.

2.2.7 Time-lapse imaging and analysis

For imaging embryos were transferred into a glass bottom culture dish (MatTek) customised to contain a finely weaved adherent nylon mesh. Embryos were placed within individual interstices of the mesh that served to keep them in position throughout the duration of the imaging.

Time-lapse movies were generated using a spinning disk confocal microscopy system (3i Intelligent Imaging Innovations, Marianas, Intelligent Imaging Innovations), consisting of an inverted confocal microscope (Axiovert Observer Z1, Carl Zeiss, Inc.) and camera (QuantEM 512SC; Yokogawa), with images captured using SlideBook software (Intelligent Imaging Innovations 3i). The microscope set-up included a multi-position stage function which enabled each embryo to be imaged individually at every time point, using a 63x water objective. Brightfield and fluorescent images were captured in 15 z-planes at 3.5μM intervals. Images were captured every seven to ten minutes, for 10 to 16 hours according to the specific experiment. Images were analysed using SlideBook software.

2.2.8 Real-Time Quantitative Reverse Transcriptase-Polymerase Chain Reaction

Real-time quantitative reverse transcriptase-polymerase chain reaction (qRT-PCR) was used to determine the degree of gene knockdown in siRNA experiments. Total RNA was prepared from embryos 40 hours after injection with siRNA at the zygote stage using the PicoPure RNA isolation kit (Arcturus Bioscience). Between 30 and 50 embryos per experimental group were collected into a total of 20μl of RNA extraction buffer and snap frozen on dry ice. Total RNA was extracted following the manufacturers protocol, and then DNase treated to remove any contaminating DNA using the DNA-free kit (Ambion). Next cDNA was synthesized using SuperScript III Reverse Transcriptase (Invitrogen) with Oligo-$dT_{(20)}$ priming. The cDNA was then used as a template in real-time PCR reactions using the SYBR Green Master Mix (Applied Biosystems) in optical 96-well reaction plates. Reactions were performed in technical triplicate for each primer pair (Table 2.1) using the StepOne™ Real-Time PCR System (Invitrogen).

The degree of gene knockdown was calculated in Microsoft Excel software using the $\Delta\Delta$Ct quantification method (Livak and Schmittgen, 2001), normalised against the housekeeping gene *Actin B (ActB).*

2.2.9 FISH analysis of blastocysts

A group of control and reversine-treated early blastocysts were analysed for their chromosome constitution using FISH probes for chromosomes 2, 11 and 16. The FISH procedure and analysis was carried out by Aisha Elaimi (then a PhD student in Joyce Harper's laboratory, University College London) as previously described in her recent publication (Elaimi et al., 2012).

2.2.10 Array-based karyotyping

To collect individual blastomeres for array-based karyotyping 8-cell stage embryos (control and reversine-treated) were treated with AT to dissolve the zona pellucida. After 30 minutes they were incubated in calcium- and magnesium-free M2 media for five minutes and then disaggregated into single cells by gentle pipetting with a flame-polished glass pipette.

Individual cells were serially washed through four large drops of freshly prepared 1x PBS (Cell Signalling). Single blastomeres were collected into 2μl of the 1x PBS solution in a 200 μl PCR tube, and immediately frozen on dry ice and kept at -80^{o}C. Cells were shipped on dry ice to Dr Thierry Voet (University of Leuven) for array-based karyotyping (Konings et al., 2012).

2.2.11 Statistical analysis

To compare categorical data the Chi-square test was used, unless the numbers were small in which case Fisher's exact test was used. The Mann-Whitney U or Kruskall-Wallis tests were used to compare median timings of mitosis or time to mitotic slippage. In all cases the two-tailed version of the test was used to evaluate statistical significance. Calculations were carried out in Microsoft Excel or with GraphPad software.

Table 2.1 Primer sequences

Gene	Forward Sequence - (5' to 3')	Reverse Sequence - (5' to 3')	Application
Bubr1	GACTATGGATCCGCCACCATGGGCTACCCATACGATGTTCCTGACTATGCTATTGAGCCTAGTATCAACCATGTTCTC	GACTATTCTAGATTAATTAGTCAGCTCCAGCTTTTCCAG	BubR1_DN
Mad2	GGGACCGCAATTTATTACCA	TTGACAGGGGTTTTGTAGGC	qRT-PCR
BubR1	GAAGGAGCGTCTGAATGAGG	TCTGAAGGGTGGAGCAGTTT	
Ndc80	TGTATGCACCGCTCAAAGAG	GCTTTCCGTTTTCATGGTGT	
ActB	GCTCTTTTCCAGCCTTCCTT	CGGATGTCAACGTCACACTT	

Table 2.2 siRNA sequences

Target gene	siRNA Sequences
Mad2	GAGCUGAACCAGUACAUCCAGGACA
	UCAGCCUCCCUUGCUGUCCAUCAAU
	UCCUGGCAGAUGAACAGGAUGUCCA
Bubr1	GGAAGACAAUCAGCCCGGAAGCUUU
	CCAGUACACGGUAAUCGCAGGAUCA
	UGGGACAUUUGUGCAAUGAACCUUU
Ndc80	GAGUACACACAAACCGACAUCGGAA
	GCUCUUGAAUGAAAGCGAAGAAGAA
	CAGGAAUAGUCAACUUGGUAUAUUU

2.3 RESULTS I

2.3.1 Evaluating the chromosome status of mouse pre-implantation embryos

In the first instance it was necessary to develop a protocol to evaluate the chromosome status of cells within the pre-implantation mouse embryo. This protocol was then used to establish the success of the experimental approaches aimed at generating a clone of aneuploid blastomeres. A range of approaches were investigated including classic cytogenetic techniques, evaluation of centromeres and time-lapse imaging.

2.3.1.1 Classical cytogenetic approaches

First the classical cytogenetic technique of generating chromosomes spreads for analysis was attempted. Although this approach in pre-implantation embryos is widely acknowledged to be technically challenging (Delhanty and Handyside, 1995, Macklon et al., 2002), successes have been reported (Garside and Hillman, 1985, Roberts and O'Neill, 1988, Yoshizawa et al., 1990, Roberts et al., 1990, Kola and Wilton, 1991, Jamieson et al., 1994, Clouston et al., 1997, Clouston et al., 2002, Lightfoot et al., 2006). To begin with a detailed review of the practical techniques used in the above mentioned studies was undertaken. In particular there were noted to be a wide range of variations at every step in the procedure including the metaphase arrest protocol, hypotonic solution, fixation technique and spreading methods. The salient experimental details were summarised together and subsequently used as a guide in developing and optimising a protocol that could be used for this study.

Despite multiple attempts and variations of the protocol it was not possible to produce a single good quality metaphase spread in mouse embryos ranging from the 2-cell stage through to the blastocyst stage. Parameters that were varied (as guided by literature evaluation) included: metaphase arrest protocol (drug used – demecolcine or colchicene, doses, length of exposure), hypotonic treatment (water or sodium citrate, incubation time and temperature), fixation step (composition of fixative, dropping onto slide approach) and spreading techniques (disaggregation, drying and further fixative). Following several failed attempts further practical expertise was then sought on collaboration with Dr Willem Rens,

at that time a senior scientist with extensive experience in the preparation of metaphase spreads in cells obtained from a wide range of animals and within a variety of different tissues (Molecular Cytogenetics Laboratory Department of Veterinary Medicine, University of Cambridge). Further trouble-shooting of the protocol in great detail still did not produce any good quality chromosome spreads. In those cases where metaphase was achieved, most were not suitable for analysis due to inadequate chromosome spreading, and clumping of the chromosomes over each other (Figure 2.2a). In contrast obtaining suitable metaphase spreads was relatively easy in MEF cells, and as a result the failure was attributed to the cellular characteristics specific to the pre-implantation embryo rather than a failure to master the technique of cytogenetic preparation itself (Figure 2.2b).

Therefore it was concluded that the cytogenetic analysis of the mouse pre-implantation blastomeres could not be adequately optimised and hence would not be suitable for this study. This technique was abandoned in pursuit of alternative potential strategies.

2.3.1.2 Evaluating centromere number

Classic cytogenetic techniques enable cells to be karyotyped. In addition to evaluating chromosome number, the karyotype provides a detailed visual map of every chromosome within the cell, with abnormalities defined by the specific chromosome involved in the abnormality together with the presence or absence of major structural abnormalities. However, for the purposes of this study it was considered sufficient to determine the number of chromosomes per cell and to classify the chromosome status as either normal or abnormal based on chromosome number. Therefore an alternative experimental approach was considered, based upon the evaluation of centromere number as a surrogate marker of chromosome number within mouse blastomeres. In the mouse, every chromosome contains a single centromere, and thus if the centromere number could be determined with accuracy this number could be extrapolated to determine the rates of aneuploidy.

Two experimental approaches were evaluated; either the detection of centromeres using anti-centromere antibodies (ACA) followed by IF and image analysis, or the microinjection of a GFP-tagged centromere protein mRNA, *CENPB-GFP* which would, when translated into

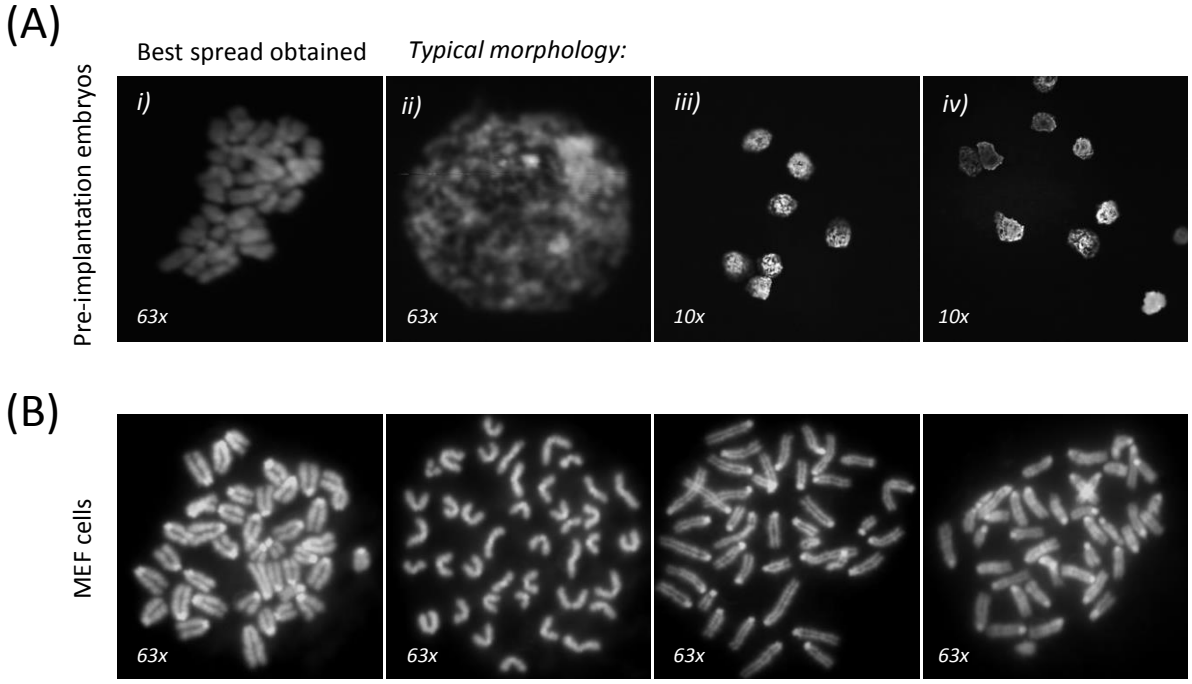

Figure 2.2 Chromosome spreads in pre-implantation embryos compared with MEF cells. (A) Achieving chromosome spreads suitable for analysis was not possible in pre-implantation embryos. In the few cases where metaphases containing relatively normal looking chromosomes were identified, the chromosomes spread poorly, exhibiting clumping and were unsuitable for accurate chromosome counting (i). The majority of nuclei were either not arrested in metaphase or contained very contracted chromatin (ii to iv). **(B)** In contrast chromosome spreads were easily achievable from MEF cells, with multiple well-spread metaphases suitable for chromosome analysis and counting if required.

protein, localise to the site of every centromere and could be detected during time-lapse imaging of mitosis.

Technically the immunostaining for ACA appeared successful. Fluorescent signal was clearly visible in the expected distribution although significant background staining was present (Figure 2.3a). However the imaging conditions required to accurately detect all centromeres were unachievable. Multiple small z-sections were necessary to capture all centromeres resulting in almost complete bleaching of the fluorochrome during image capture. The centromeres were also well visualised following injection of *CENPB-GFP* mRNA into blastomeres and with less background staining than the ACA images. However, this approach met with the same technical limitations as for the antibody associated approach; the imaging parameters required were unachievable even when using a spinning disk confocal microscope (Figure 2.3b). It also became further apparent that labelling of the centromeres with the same fluorescent probe would almost certainly never be suitable for counting chromosome number with any accuracy due to the close proximity of the chromosomes and overlapping centromere signals.

Therefore this approach was also abandoned in pursuit of a more suitable alternative technique.

2.3.1.2 Evaluating chromosome segregation errors using time-lapse imaging

The aim of this part of the study was to induce chromosome segregation errors, and hence aneuploidy, through experimental perturbation of the SAC or disruption of kinetochore structure. In view of the technical challenges encountered in assessing for chromosome status described above, an alternative strategy was established to evaluate the effectiveness of SAC bypass or disruption of kinetochore structure, rather than specifically evaluating aneuploidy in individual blastomeres *per se*.

As discussed in Section 2.1, bypass of the SAC results in chromosome segregation errors, a shortening of the time to anaphase (Gorbsky et al., 1998, Canman et al., 2002, Meraldi et al., 2004, Musacchio and Salmon, 2007), and a failure to undergo mitotic arrest in response to spindle poisons such as NZ (Rieder and Palazzo, 1992, Rieder and Maiato, 2004). These

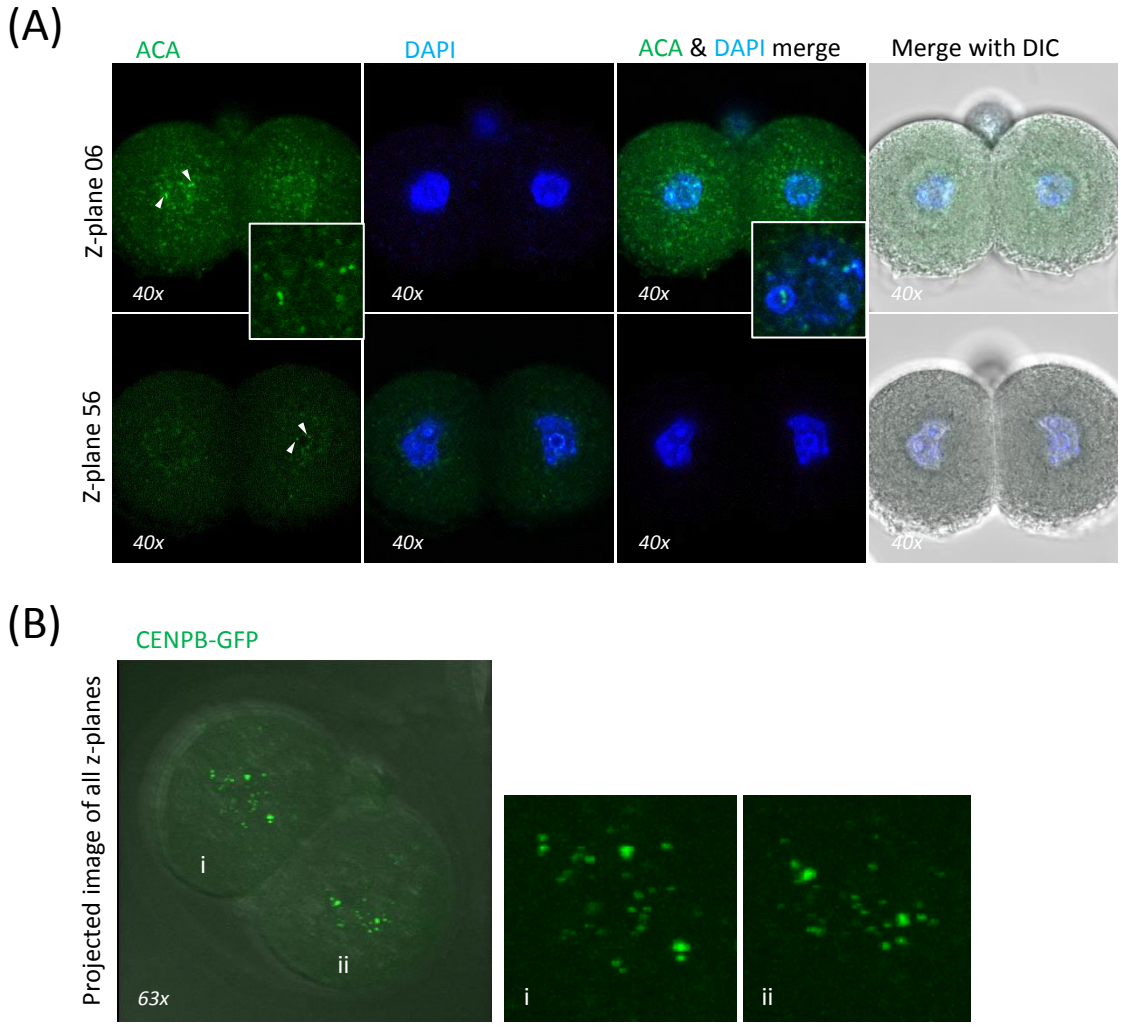

Figure 2.3 Evaluation of chromosome number by assessment of centromeres (A) Anti-centromere antibody (ACA) staining of centromeres in 2-cell stage embryos, shown in z-plane 06 and 56. Centromere staining is achieved (white arrowheads) however the relatively high background staining and significant bleaching during imaging render centromere number assessment impossible. **(B)** Labelling of endogenous centromeres with CENPB-GFP minimised issues with background staining, but still did not result in images of sufficient resolution to accurately evaluate centromere or chromosome number. Images i) and ii) are cropped and magnified views of the nuclei in the 2-cell stage embryo shown in the main image.
Inset images in lower right corners are close up views of single representative nuclei.

effects could potentially be evaluated using high resolution time-lapse imaging of chromatin dynamics during mitosis.

Therefore an imaging strategy was developed and optimised to enable the chromatin morphology to be evaluated in blastomeres undergoing cleavage. Embryos were microinjected with *histone-red fluorescent protein (RFP) mRNA* to label the chromatin and thus enabled the chromosomes to be visualised during mitosis. Embryos were imaged on a spinning disk confocal microscope during cleavage in two channels, RFP and bright-field. Imaging parameters were optimised to gain maximal chromatin morphology while still enabling the cells to undergo the next two cleavage divisions as expected. The effects of imaging on subsequent development were not assessed, as the embryos were then to be discarded. Embryos were imaged undergoing cleavage at different stages of development and evaluated for the length of metaphase and the presence of major chromosome segregation abnormalities during mitosis. Metaphase length was defined as the time from nuclear envelope breakdown (NEBD) to the onset of anaphase (Figure 2.4). Chromosome segregation was classified as abnormal if there were major segregation errors resulting in the formation of a micronucleus or nucleo-cytoplasmic bridges (Figure 2.5).

This imaging protocol was then used to evaluate the effectiveness of the experimental attempts to bypass the SAC or disrupt kinetochore structure, as presented in the following section.

2.3.2 Inducing chromosome segregation errors in cleavage stage blastomeres

Having established a protocol that could be used to detect acutely arising chromosome segregation errors in the embryo, the next aim was to experimentally induce missegregation errors in mouse blastomeres. Several experimental strategies were attempted including dominant negative approaches, siRNA mediated gene knockdowns and drug treatment, targeting key components of the SAC or kinetochore structure.

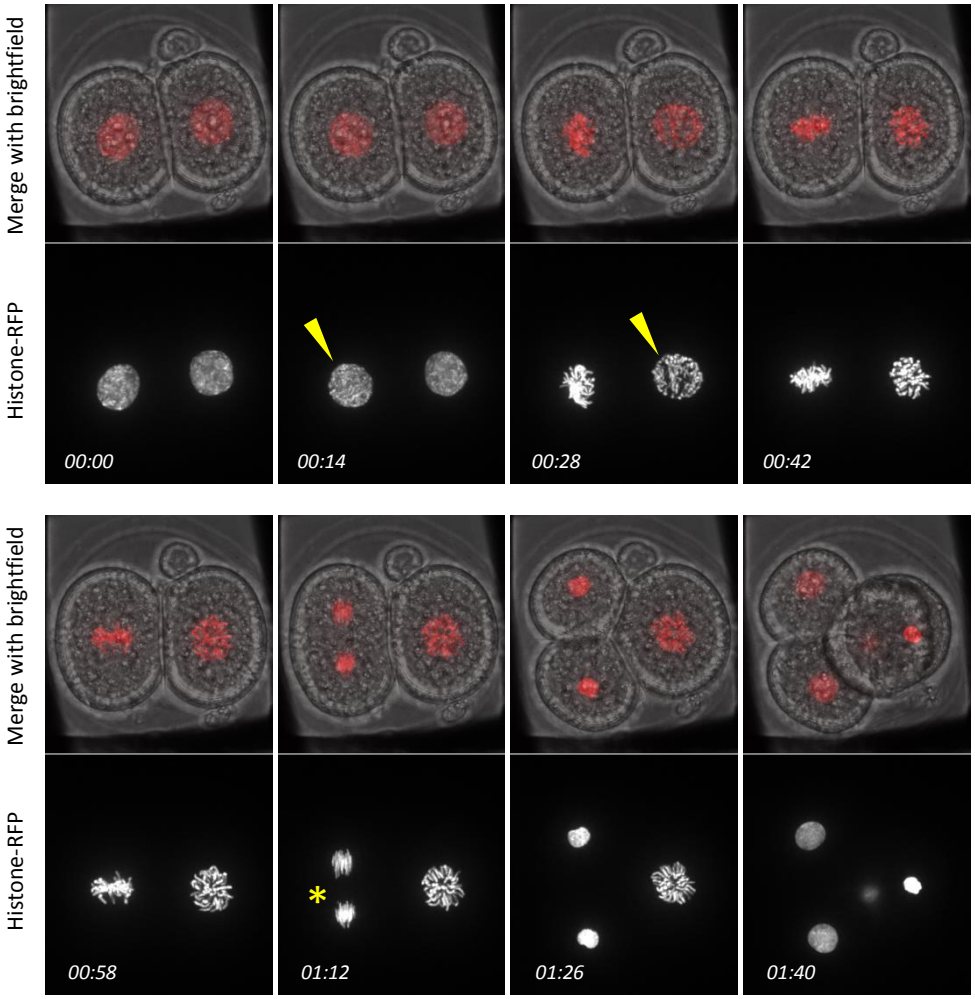

Figure 2.4 Time-lapse imaging of normal mitosis in a 2-cell stage embryo. Embryos were injected with *histone-RFP* mRNA to enable visualisation of chromosome morphology during spinning disk confocal imaging. Images were captured at 7-minute intervals in 15 z-planes, shown as a projected image in the panels above. The length of metaphase was defined as the time from nuclear envelope breakdown (NEBD) (arrowheads) to the onset of anaphase (asterisks), identified by morphological features of the chromatin. In this example there were no chromosome segregation errors and the mitosis was classified as normal.
Timings are given in hours and minutes (hh:mm)

All images at 63x magnification

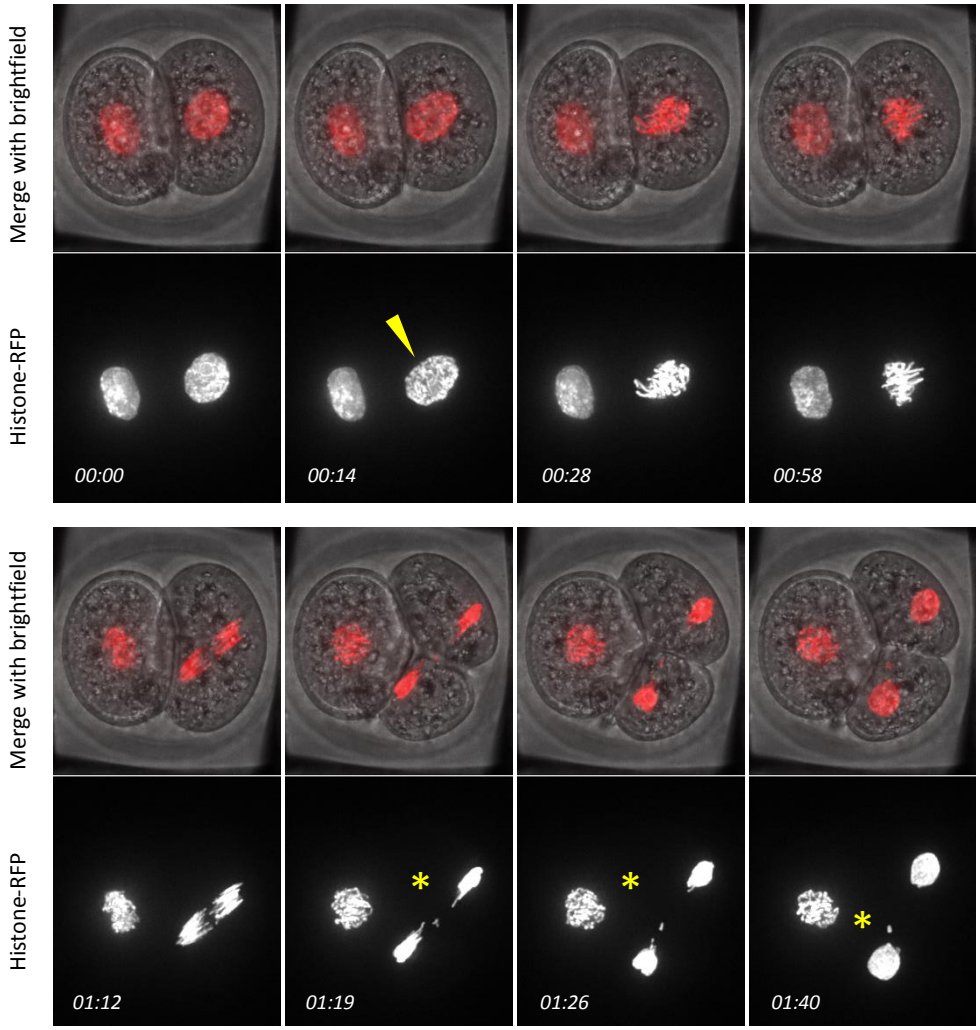

Figure 2.5 Major chromosome missegregation occurring during the 2- to 4-cell stage cleavage. Time-lapse imaging sequences reveal a lagging chromosome during mitosis that results in the formation of a discrete micronucleus within one of the daughter blastomeres. This mitosis would be classified as abnormal. NEBD is shown by the arrowheads and the asterisks denote the presence of a lagging chromosome that ultimately forms a micronucleus in a daughter blastomere.

Timings are given in hours and minutes (hh:mm)

All images at 63x magnification

2.3.2.1 Dominant negative approaches

The generation of DN constructs was carried out in close collaboration with Dr Alexander Bruce, a post-doctoral researcher within the laboratory.

Two constructs were used: a DN construct for Mad2 (Mad2_DN) and Bubr1 (Bubr1_DN), both key proteins required for SAC function (Musacchio and Salmon, 2007). These two particular proteins were selected because Mad2 and Bubr1 DN constructs have previously been used to successfully bypass the SAC in mouse oocytes (Tsurumi et al., 2004) and thus considered likely to be effective in the early embryo.

The Mad2_DN construct contained the mouse DNA sequence but lacked 10 amino acids at the C-terminus preventing its interaction with cell-division cycle protein 20 (Cdc20,) an essential regulator of cell division, and thus preventing the essential cell-cycle delay mediated by a functioning SAC.

An effective human BUBR1_DN construct was first characterised in Hela cells and consisted of a truncated protein containing amino acid residues 351 to 700, unable to inhibit the anaphase promoting complex (APC) and thus also preventing the cell-cycle delay mediated by a functioning SAC (Tang et al., 2001). Since then, an equivalent mouse Bubr1_DN construct had subsequently been used to successfully bypass the SAC in mouse oocytes (Tsurumi et al., 2004). Therefore an equivalent Bubr1_DN construct for amino acid residues 351 to 700 was generated. The Bubr1_DN construct was also designed to contain an N-terminus HA-tag, to enable the protein to be identified by IF as required.

Mad2_DN or *Bubr1_DN* mRNA was microinjected into 2-cell stage embryos between 42 and 44 hours post hCG injection. Successful injection was confirmed at the late 2-cell stage by checking for the expression of a co-injected fluorescent marker and only those embryos expressing the marker strongly were used in the subsequent experiment. Control embryos for comparison were injected with the lineage marker alone. For time-lapse imaging experiments the lineage marker was histone-RFP and for all other experiment dsRed.

In the first instance immunostaining for the HA-tag was carried out in a subset of embryos in order to check for successful expression of the DN protein following mRNA injection. The HA-tag was detected clearly in embryos injected with either *Mad2_DN* or *Bubr1_DN* mRNA

thus confirming successful translation of the mRNA into protein by the late 2-cell stage. Additionally, when checked at the 8-cell and mid-blastocyst stage the protein was still present in abundance (in both Mad2_DN and Bubr1_DN groups) thus demonstrating that the injected constructs generated recombinant proteins that remained present in the embryo over several cell-cycles.

In the following experiments presented in this section two concentrations of *Mad2_DN* and *Bubr1_DN* mRNA were evaluated. Concentrations of 0.8 or 2.0μg/μl of *Mad2_DN* were injected, and for *Bubr1_DN* the concentrations were 0.8 or 1.75 μg/μl. Subsequently these concentrations will be referred to as low or high concentrations accordingly for clarity. These particular concentrations were selected based upon their previous use in mouse oocytes (Tsurumi et al., 2004, Sharif, 2011), and also on consideration of the concentrations of mRNA usually used within the laboratory for microinjection of pre-implantation embryos. Within the laboratory the vast majority of mRNAs are effective at concentrations significantly lower than 1.0μg/μl. Further, the microinjection of mRNA becomes technically more challenging as the concentration of mRNA increases and thus limits the use of higher concentrations of mRNA.

Following successful microinjection of either *Mad2_DN* or *Bubr1_DN* mRNA into both blastomeres of 2-cell stage embryos, a series of experiments were conducted to assess pre-implantation developmental potential or to evaluate evidence of successful bypass of the SAC within individual blastomeres. The results for each set of experiments are presented in detail individually in Figures 2.6 (Mad2_DN) and 2.7 (Bubr1_DN), and also summarised together in Table 2.3.

For clarity of the following text, some details of the numbers and statistics are omitted from the section below but can be found clearly within the given figures and tables.

(A)

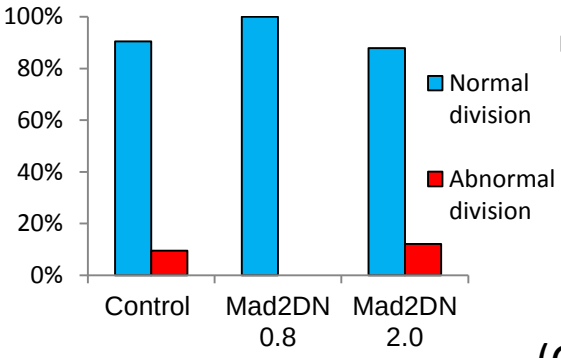

Data for **(A)** *Chromosome segregation during mitosis*

Mitosis	**Normal division**	**Abnormal division**	*Total blastomeres assessed*
Control	19 (91%)	2 (9%)	*21*
Mad2DN 0.8	26 (100%)	0 (0%)	*26*
Mad2DN 2.0	29 (88%)	4(12%)	*33*

(B)

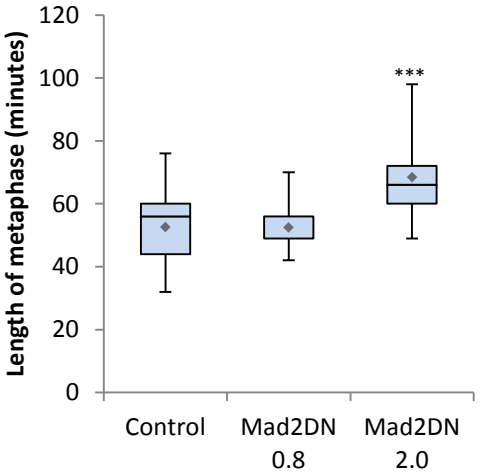

(C)

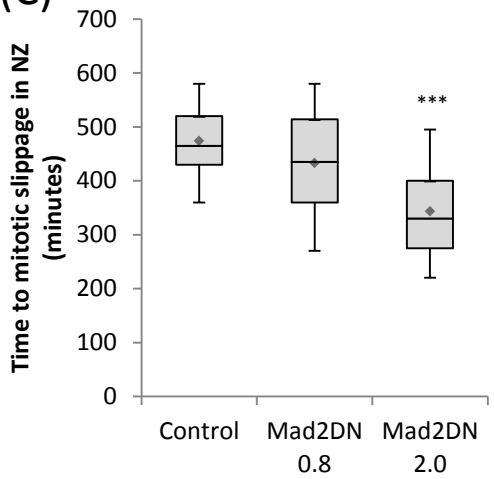

Developmental potential table

	Expanded BC	**Arrest**	*Total embryos*
Control	24 (96%)	1 (4%)	*25*
Mad2DN 0.8	18 (90%)	2 (10%)	*20*
Mad2DN 2.0	18 (90%)	2(10%)	*20*

(D)

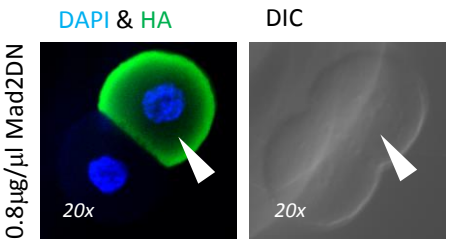

Figure 2.6 Effect of Mad2_DN on the SAC in the embryo (A) Blastomeres injected with low or high concentrations of *Mad2DN* mRNA had equivalent rates of chromosome segregation errors as controls (Fisher's test; p=0.19 & 1.0 respectively) **(B)** Metaphase lengths measured in control and low concentration Mad2DN blastomeres were equivalent, but prolonged in blastomeres injected with the high concentration (Mann-Whitney U; ***p<0.001) **(C)** Mad2DN injection did not bypass metaphase arrest induced by NZ, however injection with 2.0µg/µl of *Mad2DN* mRNA was associated with a significantly shorter time to mitotic slippage (Mann-Whitney U; ***p<0.001). **(D)** Representative image of a 2-cell stage embryo following single blastomere injection with the low concentration of *Mad2DN* mRNA, clearly demonstrating strong expression of the protein in the injected blastomere (arrowhead shows injected blastomere and HA-tag). **(Developmental potential table)** Development to the blastocyst stage was equivalent to controls in both low and high concentrations of *Mad2DN* (Fisher's test; p=0.57 & 0.57 respectively).
Diamond symbols on the box-plot charts represent the mean.

(A)

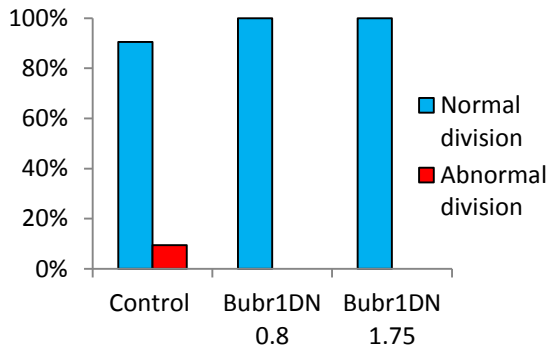

Data for **(A)** *Chromosome segregation during mitosis*

Mitosis	Normal division	Abnormal division	*Total blastomeres assessed*
Control	19 (91%)	2 (9%)	*21*
Bubr1DN 0.8	24 (100%)	0 (0%)	*24*
Bubr1DN 1.75	23 (100%)	0 (0%)	*23*

(B)

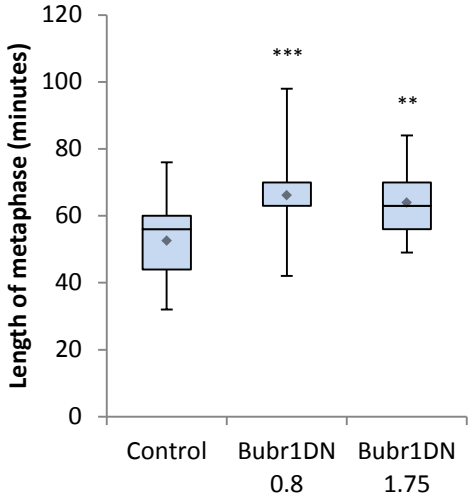

(C)

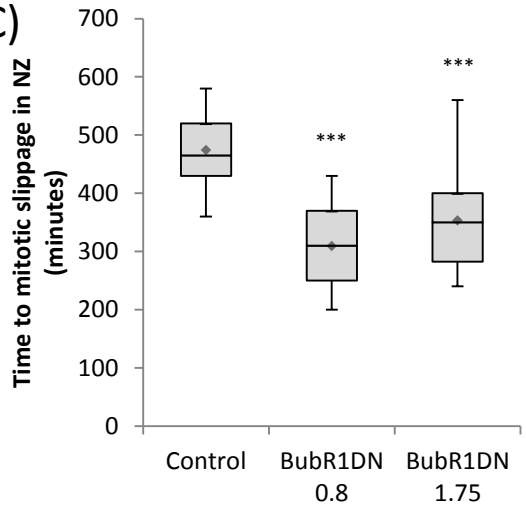

(D)

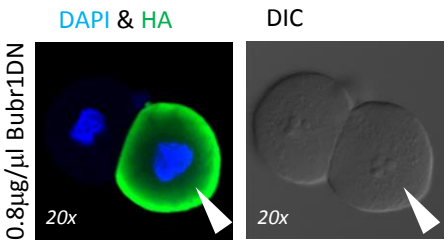

Developmental potential table

	Expanded BC	Arrest	*Total embryos*
Control	24 (96%)	1 (4%)	*25*
Bubr1DN 0.8	20 (100%)	0 (0%)	*20*
Bubr1DN 1.75	19 (95%)	1 (5%)	*20*

Figure 2.7 Effect of Bubr1_DN on the SAC in the embryo (A) Blastomeres injected with low or high concentrations of *Bubr1DN* mRNA had equivalent rates of chromosome segregation errors as controls (Fisher's test; p=0.21 & 0.22 respectively) **(B)** Metaphase lengths were prolonged in blastomeres injected with the low and high concentrations of *Bubr1_DN* (Mann-Whitney U; ***p<0.001 low, **p<0.01) **(C)** *Bubr1DN* injection did not bypass metaphase arrest induced by NZ, however both concentrations were associated with a significantly shorter time to mitotic slippage (Mann-Whitney U; ***p<0.001 for both high & low). **(D)** Representative image of a 2-cell stage embryo following single blastomere injection with the low concentration of *Bubr1DN* mRNA, clearly demonstrating strong expression of the protein in the injected blastomere (arrow head shows injected blastomere and HA-tag). **(Developmental potential table)** Developmental to the blastocyst stage was equivalent to controls in both the low and high concentrations of *Bubr1DN* (Fisher's test; p=1.0 & 1.0 respectively).
Diamond symbols on the box-plot charts represent the mean.

The injection of either Mad2_DN or Bubr1_DN had no apparent effects on pre-implantation developmental potential assessed by morphology

Both blastomeres of 2-cell stage embryos were injected with the DN constructs, cultured and then evaluated for their morphological appearance at the expanded blastocyst stage. When compared with control embryos, microinjection of *Bubr1_DN* or *Mad2_DN* mRNA at either high or low concentrations did not have any apparent adverse effects on morphological pre-implantation development; between 90 and 100% of DN-injected embryos reached the expanded blastocyst stage, compared with 96% of control embryos (Fisher's tests; not significant Figures 2.6 and 2.7). In addition there were no differences in morphology noted between the control and DN-injected embryos such as fragmentation.

Neither Bubr1_DN *or* Mad2_DN *proteins successfully bypassed the SAC or increased the rate of chromosome segregation errors in cleavage stage blastomeres*

Successful bypass of the SAC was evaluated in three ways: the rate of chromosome segregation errors occurring during mitosis, the length of metaphase, and the response to incubation in the spindle poison nocodazole (NZ).

Embryos were imaged during the 2- to 4-cell cleavage and scored for the presence of chromosome segregation errors during division. In control embryos major chromosome segregation errors were identified in 9.5% (2 of 21) of blastomeres. Embryos injected with Mad2_DN or Bubr1_DN mRNA revealed similar chromosome missegregation rates in blastomeres, ranging from 0 to 12%, at both low and high concentrations of both DN constructs (Fishers tests; not significant, Figures 2.6 and 2.7).

Time-lapse images were also analysed for the length of metaphase, defined as the time between NEBD and the onset of anaphase. The mean length of metaphase in control blastomeres was 52.5 minutes (n=21). Embryos injected with the low dose of Mad2_DN embryos had similar timings (52.5 minutes, n=28 blastomeres, Mann-Whitney U test; p=0.91), however the higher dose was associated with a significant increase in the length of metaphase to 68.4 minutes (n=24 blastomeres, Mann-Whitney U test; p=0.0001). Findings in Bubr1_DN embryos were similar, however both the low and high doses were associated

with a significant lengthening of metaphase when compared with controls (low dose – mean 66.0 minutes, n=23 blastomeres, Mann-Whitney U test; p=0.0002, and for high dose – mean 63.9 minutes, n=23 blastomeres, Mann-Whitney U test; p=0.002). Although significant differences following DN injections were identified in a subgroup of blastomeres, these changes were in the opposite direction than would be expected if the SAC had been successfully bypassed, and were not associated with detectable chromosome segregation.

Finally, embryos were incubated in 0.33μM NZ at the 2- to 4-cell cleavage to determine if there was any evidence of bypass of the SAC-mediated metaphase arrest induced by spindle poisons. All embryos in the control and DN groups underwent arrest, and eventually fragmented many hours later. It was difficult to quantify any differences in the response to NZ by morphology alone therefore the time to mitotic slippage was evaluated using time-lapse imaging of the chromatin. Mitotic slippage occurs when the cell exits mitosis despite the presence of a functioning checkpoint, although the time to mitotic slippage can be shortened if the SAC is compromised (Rieder and Maiato, 2004). Mitotic slippage was measured as the time between the formation of the mitotic plate until de-condensation and fragmentation of the chromatin. Control blastomeres underwent mitotic slippage at an average of 474 minutes post metaphase arrest (n=15 blastomeres). Embryos injected with the low dose of Mad2_DN had similar timings (433 minutes, n=26, Mann-Whitney U test; p=0.19), however the higher dose was associated with a significant shortening in the time to mitotic slippage (343 minutes, n=17, Mann-Whitney U test; p=0.0001). Findings in Bubr1_DN embryos were similar, however both the low and high doses were associated with a significant shortening of the time to mitotic slippage when compared with controls (low dose – mean 309 minutes, n=43, Mann-Whitney U test; $p<<0.001$, and for high dose – mean 353 minutes, n=31, Mann-Whitney U test; $p<<0.001$).

In addition to the data presented here, several other small pilot experiments were performed evaluating the rates of chromosome segregation errors at different stages (4- to 8-cell stage), and following injection of zygotes rather than 2-cell stage. The findings of these pilot experiments were in keeping with the experiments presented above, with no evidence of chromosome segregation errors. Therefore these experiments were not pursued further.

Considering all of these results together, it was concluded that there was minimal evidence that injection of low or high doses of either *Mad2_DN* or *Bubr1_DN* mRNA resulted in successful bypass of the SAC, or increases in chromosome segregation errors. Although incubation in NZ was associated with a shortened time to mitotic slippage, which does occur in the absence of a functional SAC, this isolated finding was insufficient to conclude that the SAC had been bypassed. Therefore an alternative strategy for inducing chromosome segregation errors was pursued.

2.3.2.2. RNA interference (RNAi) approaches

In view of the failure to bypass the SAC using DN approaches an RNAi strategy was adopted with the aim of inducing an effective silencing of gene expression, and hence silencing of the gene product. RNAi has previously been used effectively for this purpose in the mouse oocyte and pre-implantation embryos (e.g (Wianny and Zernicka-Goetz, 2000, Jedrusik et al., 2010, Morris et al., 2010)). Pre-designed mouse-specific Stealth RNAi™ was purchased from Invitrogen for the SAC genes *Mad2* and *Bubr1*. In view of the difficulty in abrogating the SAC using the DN approach, siRNA specific to Ndc80, an essential kinetochore protein required for the faithful segregation of chromosomes during mitosis (Kline-Smith et al., 2005, Ciferri et al., 2007) was also purchased thus providing an alternative strategic approach. Each gene-specific siRNA mix consisted of three different synthetic 25-nucleotide non-overlapping sequences. An appropriate siRNA negative control mix was also used.

The effect of siRNA knockdown of these genes was evaluated using similar approach to that described in the DN experiments. In brief, zygotes were injected between 21 to 23 hours post hCG injection, together with the required lineage marker, and only those strongly expressing the marker were selected for use in the subsequent experiments. Embryos were evaluated for their pre-implantation developmental potential, chromosome segregation errors and for evidence of bypass of the SAC.

For clarity of the following text, some details of the numbers and statistics are omitted from the section below but can be found clearly within the given figures and tables. Figures 2.8

(*Mad2* siRNA), 2.9 (*Bubr1* siRNA) and 2.10 (*Ndc80* siRNA), and Table 2.3 summarise the results of these experiments.

For all three genes a siRNA concentration of 5μM was injected, however in the preliminary Ndc80 experiments the effects of 0.01 and 0.2μM concentration were also evaluated. The manufacturer recommends a concentration between 0.0001 to 0.2 μM for use in cultured cell lines. At the time these experiments were conducted the experience of siRNA use within the laboratory was limited. In a general literature search for publications using siRNA in pre-implantation embryos, siRNA concentrations ranging between 5 and 100 μM had been used (Cui et al., 2007, Morris et al., 2010, Jedrusik et al., 2010, Kawamura et al., 2010). Based on these findings a maximum concentration of 5μM was used in the subsequent experiments in order to minimize the potential risk of cell-toxicity secondary to non-specific effects of siRNA.

The degree of knockdown by siRNA was evaluated using qRT-PCR to detect the transcript levels of the genes of interest. The levels of each gene's mRNA were normalised against beta-actin (a constitutive 'housekeeping' gene, expressed in all cells at relatively constant levels). Percentage knockdowns in target gene mRNA expression were calculated by directly comparing normalised transcript levels between control siRNA and target gene siRNA microinjected embryos. When injected at a concentration of 5μM, all siRNAs showed depleted expression of their specific gene with expression decreasing by 96% for Ndc80, 42% for Mad2 and 52% for Bubr1 relative to control siRNA levels (Figures 2.8D, 2.9D and 2.10D).

The injection of Mad2, Bubr1 or Ndc80 siRNA had no apparent effects on pre-implantation developmental potential assessed by morphology

In the first instance, zygotes were injected with 5μM siRNA, cultured and determined if there were any significant effects on developmental potential to the expanded blastocyst stage. When compared with control embryos, all three experimental groups of embryos underwent equivalent pre-implantation development; between 85 and 95% of experimental embryos reached the expanded blastocyst stage, compared with 100% of control embryos

(A)

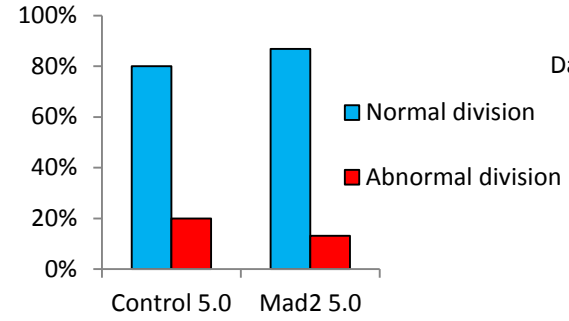

Data for **(A)** *Chromosome segregation during mitosis*

Mitosis	Normal division	Abnormal division	*Total blastomeres assessed*
Control 5.0	32 (80%)	8 (20%)	*40*
Mad2 5.0	33 (87%)	5 (13%)	*38*

(B)

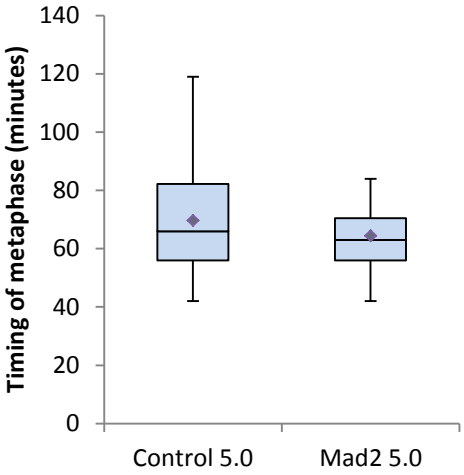

(C)

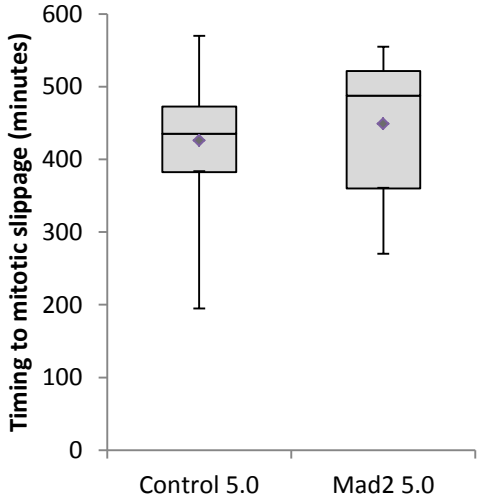

(D)

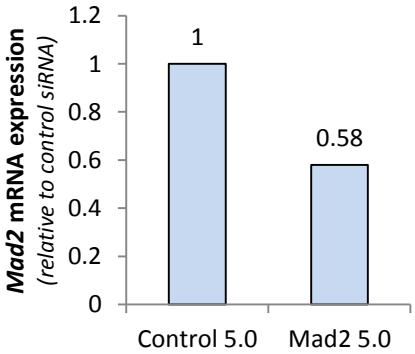

Developmental potential table

	Expanded BC	Arrest	*Total embryos*
Control 5.0	22 (100%)	0 (0%)	*22*
Mad2 5.0	20 (87%)	3 (13%)	*23*

Figure 2.8 Effect of *Mad2* siRNA on the SAC in the embryo (A) Blastomeres injected with *Mad2* siRNA had equivalent rates of chromosome missegregation errors compared to controls (χ^2 test; p=0.42) **(B)** Injection with *Mad2* siRNA did not have any effect on the length of metaphase compared with controls (Mann-Whitney U; p=0.5), and **(C)** did not result in bypass of metaphase arrest induced by nocodazole, or in any shortening of the time to mitotic slippage (Mann-Whitney U; p=0.3) **(D)** Injecting embryos with 5μM of *Mad2* siRNA reduced the expression of *Mad2* mRNA by 42% when compared to those injected with control siRNA, as assessed by qRT-PCR. **(Developmental potential table)** Development to the blastocyst stage was equivalent in control and *Mad2* siRNA injected embryos (Fisher's test; p=0.23).

Diamond symbols on the box-plot charts represent the mean.

(A)

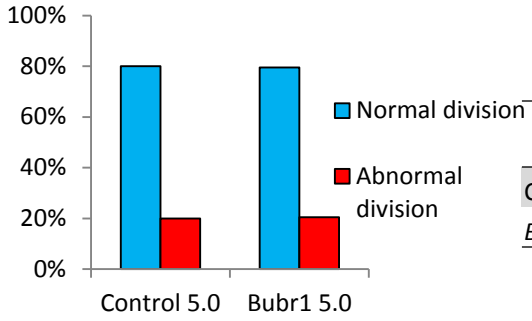

Data for **(A)** *Chromosome segregation during mitosis*

	Normal division	**Abnormal division**	*Total blastomeres assessed*
Control 5.0	32 (80%)	8 (20%)	*40*
Bubr1 5.0	35 (80%)	9 (20%)	*44*

(B)

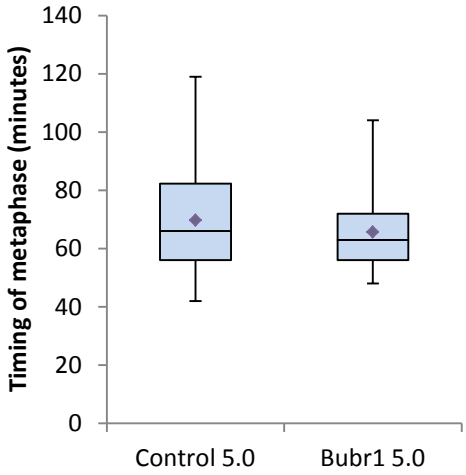

(C)

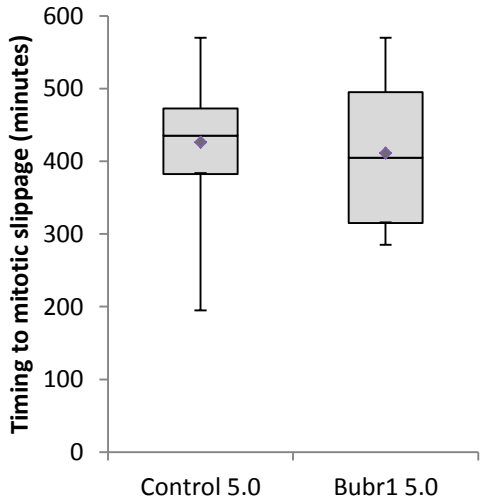

(D)

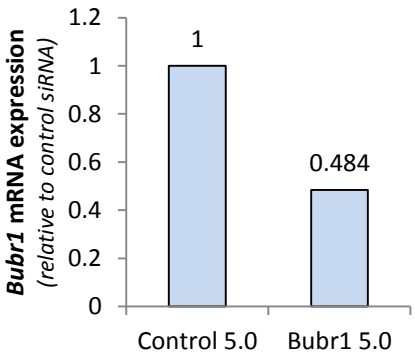

Developmental potential table

	Expanded BC	**Arrest**	*Total embryos*
Control 5.0	22 (100%)	0 (0%)	*22*
Bubr1 5.0	18 (95%)	1 (5%)	*19*

Figure 2.9 Effect of *Bubr1* siRNA on the SAC in the embryo (A) Blastomeres injected with *Bubr1* siRNA had equivalent rates of chromosome missegregation errors compared to controls (χ^2 test; p=0.96) **(B)** Injection with *Bubr1* siRNA did not have any effect on the length of metaphase compared with controls (Mann-Whitney U; p=0.6), and **(C)** did not result in bypass of metaphase arrest induced by nocodazole, or in any shortening of the time to mitotic slippage (Mann-Whitney U; p=0.5) **(D)** Injecting embryos with 5μM of *Bubr1* siRNA reduced the expression of *Bubr1* mRNA by 52% when compared to those injected with control siRNA, as assessed by qRT-PCR. **(Developmental potential table)** Development to the blastocyst stage was equivalent in control and *Bubr1* siRNA injected embryos (Fisher's test; p=0.46).

Diamond symbols on the box-plot charts represent the mean.

Data for **(A)** *Chromosome segregation during mitosis*

Mitoses	**Normal division**	**Abnormal division**	*Total blastomeres assessed*
Control 0.01	24 (80%)	6 (20%)	*30*
Control 5.0	32 (80%)	8 (20%)	*40*
Ndc80 0.01	16 (89%)	2 (11%)	*18*
Ndc80 0.2	22 (81%)	5 (19%)	*27*
Ndc80 5.0	30 (79%)	8 (21%)	*38*

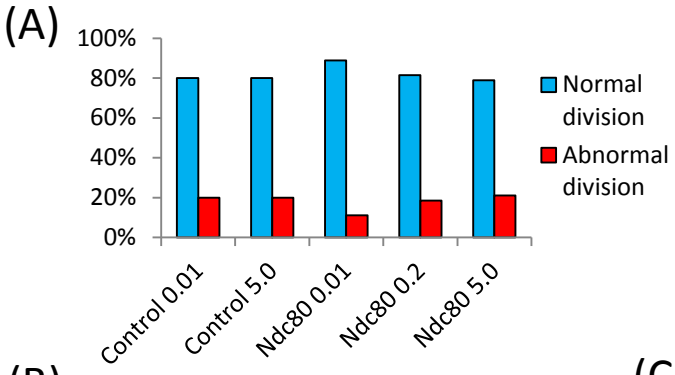

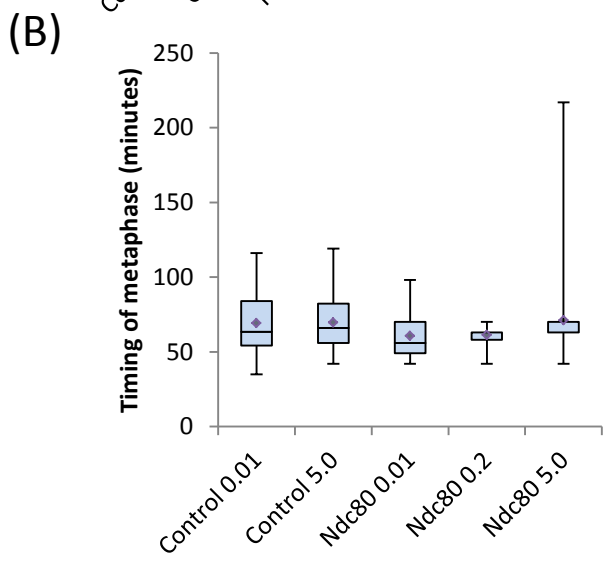

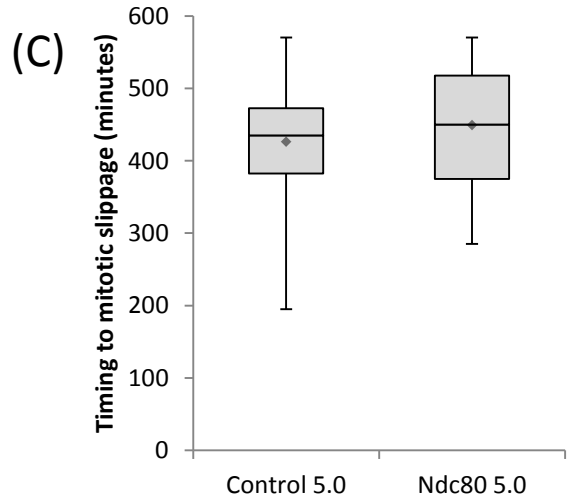

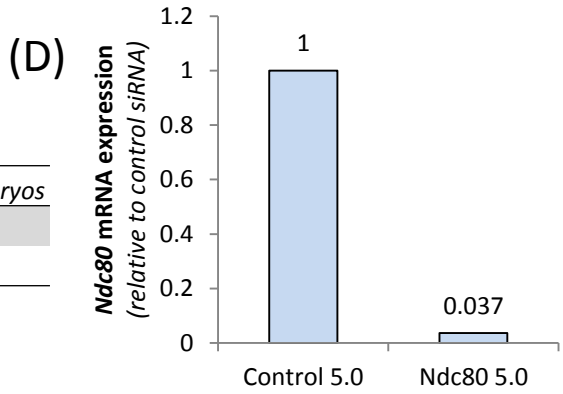

Developmental potential table

	Expanded BC	**Arrest**	*Total embryos*
Control 5.0	22 (100%)	0 (0%)	*22*
Ndc80 5.0	17 (85%)	3 (15%)	*20*

Figure 2.10 Effect of *Ndc80* siRNA on the SAC in the embryo (A) Blastomeres injected with differing concentrations of *Ndc80* siRNA all had equivalent rates of chromosome missegregation errors compared to both concentrations of controls (Fisher's test; p=0.95) **(B)** Injection with *Ndc80* siRNA did not have any effect on the length of metaphase compared with controls (Kruskall-Wallis test; p=0.4), and **(C)** did not result in bypass of metaphase arrest induced by nocodazole, or in any shortening of the time to mitotic slippage (Mann-Whitney U; p=0.4) **(D)** Injecting embryos with 5μM of *Ndc80* siRNA reduced the expression of *Ndc80* mRNA by 96% when compared to those injected with control siRNA, as assessed by qRT-PCR. **(Developmental potential table)** Development to the blastocyst stage was equivalent in control and *Ndc80* siRNA injected embryos (Fisher's test; p=0.10).
Diamond symbols on the box-plot charts represent the mean.

(Fisher's tests; Figures 2.8, 2.9 & 2.10). In addition there were no other differences in morphological features noted between the groups such as the presence of blastomere asymmetry or embryo fragmentation.

Injection of Mad2, Bubr1 or Ndc80 siRNA did not result in the bypass of the SAC or increase the rates of chromosome segregation errors in cleavage stage blastomeres

Bypass of the SAC and evaluation of chromosome segregation was evaluated during the 2- to 4-cell stage as described for the DN experiments above in Section 2.3.2.1.

The rates of chromosome segregation errors in all experimental groups of siRNA injected embryos were found to be equivalent to error rates in the control siRNA blastomeres. Missegregation occurred in 20% of control siRNA blastomeres (n=40), and between 11 and 21% in blastomeres injected with experimental siRNA (χ^2 & Fisher's tests; p= not significant, Figures 2.8, 2.9 & 2.10).

Next the timing of metaphase was assessed. In control siRNA blastomeres the mean length of metaphase was 69.7 minutes (n=40). In all groups of experimental siRNAs evaluated, the mean length of metaphase was not significantly different from that in the control blastomeres: *Ndc80* 71.2 minutes (n=33, Mann-Whitney U; p=0.90); *Mad2* 64.4 minutes (n=38, Mann-Whitney U; p=0.50); and *Bubr1* 65.7 minutes (n=43, Mann-Whitney U; p=0.60).

Finally, embryos were incubated in 0.33μM NZ at the 2- to 4-cell cleavage. All embryos in the control and injected groups underwent arrest, and eventually fragmented many hours later. The mean time to mitotic slippage in control siRNA blastomeres was 426 minutes (n=17). In all groups of experimental siRNAs, the mean time to mitotic slippage was not significantly different from that in the control blastomeres: *Ndc80* 449 minutes (n=17, Mann-Whitney U; p=0.36); *Mad2* 449 minutes (n=16, Mann-Whitney U; p=0.25); and *Bubr1* 411 minutes (n=15, Mann-Whitney U; p=0.48).

In addition to the data presented here, several small pilot experiments were performed evaluating the rates of chromosome segregation errors at later stages (4-to 8-cell & 8- to 16-

cell stage) and with higher concentrations of siRNA (20μM). The results of these pilot experiments were in keeping with the findings presented above and were therefore not pursued any further (data not shown).

Considering all of these results together, it was concluded that there was minimal evidence that injection of *Mad2*, *Bubr1* or *Ndc80* siRNA resulted in successful bypass of the SAC, or increases in chromosome segregation errors compared to control siRNA.

Therefore an alternative strategy for inducing chromosome segregation errors was employed.

2.3.3.1 Bypassing the SAC with a small molecule inhibitor of Mps1

During the course of the siRNA and DN experiments a series of papers were published characterising the effects of several small molecule inhibitors of Monopolar spindle 1-like 1 (Mps1) (Lan and Cleveland, 2010, Santaguida et al., 2010, Hewitt et al., 2010, Kwiatkowski et al., 2010). Mps1 is another highly conserved key enzyme critical for the effective functioning of the SAC (Weiss and Winey, 1996, Abrieu et al., 2001, Stucke et al., 2002). The Mps1 inhibitors were all shown to override the SAC block secondary to microtubule poisons and to increase the rates of chromosome misalignment and segregation errors in cultured cell lines (Lan and Cleveland, 2010, Santaguida et al., 2010, Hewitt et al., 2010, Kwiatkowski et al., 2010). Of all the Mps1 inhibitors available, the drug reversine is the most potent, and its effects on Mps1 inhibition rapidly reversible following the removal of the drug from the culture medium (Santaguida et al., 2010).

There is no evidence in the published literature to suggest that the effects of reversine have previously been described in pre-implantation mouse embryos. Therefore a series of experiments were conducted to characterise the effects of reversine treatment in the pre-implantation embryo, in particular evaluating its impact on developmental potential together with its effect on the SAC and effects on chromosome segregation during mitosis. The results of these experiments are summarised in Figure 2.11 and Table 2.3.

(A)

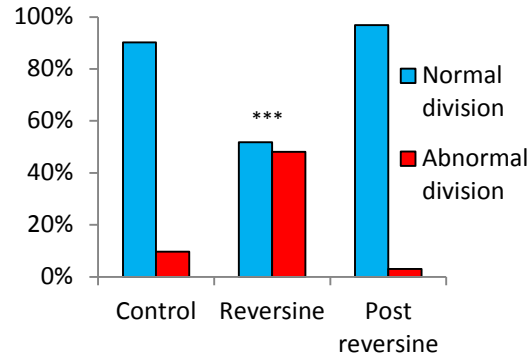

Data for **(A)** *Chromosome segregation during mitosis*

	Normal	**Abnormal**	*Total blastomeres*
Control	65 (90%)	7 (10%)	*72*
Reversine	42 (52%)	39 (48%)	*81*
Post-reversine	31 (97%)	1 (3%)	*32*

(B)

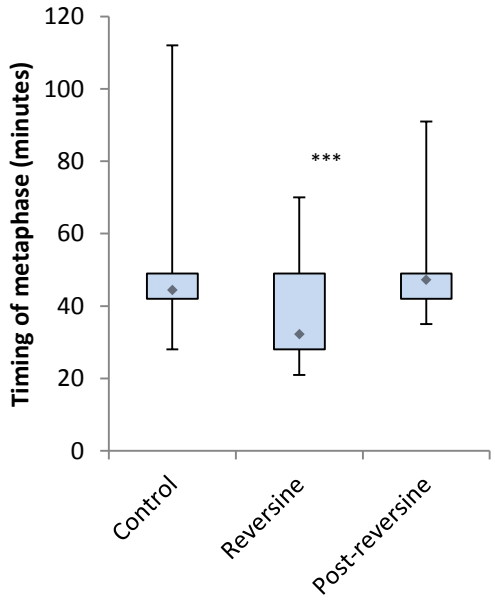

Response to incubation in NZ

	Arrest and fragment	**Divide as expected**
Control	5	0
Reversine 0.5μM	8	2
Reversine 1.0μM	2	8

Developmental potential table

	Expanded BC	**Arrest**	***Total embryos***
Control	33 (92%)	3 (8%)	*36*
Reversine	28 (93%)	2 (7%)	*30*

Figure 2.11 Effect of reversine treatment on the SAC in the embryo (A) Blastomeres incubated in 0.5μM of reversine had significantly greater rates of chromosome missegregation during mitosis than controls ($\chi 2$; ***p<0.001), however on washout of the drug (post-reversine), the function of the SAC was completely restored with chromosome missegregation rates equivalent to controls **(B)** Blastomeres incubated in reversine had a significant shortening of metaphase when compared with controls (Mann-Whitney U; ***p<0.001). On washout of the drug (post-reversine), the length of metaphase returned to the same as control blastomeres **(Incubation in NZ)** The majority of embryos incubated in 1.0μM of reversine were able to overcome metaphase arrest induced by nocodazole treatment **(Developmental potential table)** Development to the blastocyst stage was equivalent in control and reversine treated embryos (Fisher's test; p=1.0).
Diamond symbols on the box-plot chart represent the mean.

In contrast to the DN and siRNA approaches detailed above, reversine treatment required incubation of the embryos in culture media containing the drug. In DN and siRNA treatments embryos were injected hours in advance of assessing their potential effect as the blastomeres required time to synthesize the required protein (DNs) or for depletion of mRNA expression (siRNAs) and subsequent protein. In contrast, the effect of reversine on Mps1 inhibition was expected to be immediate upon the cells' entry into mitosis. Therefore in these experiments, embryos were incubated in reversine just prior to the expected mitotic division in order to keep the exposure to the drug to a minimum. Mitoses were evaluated at either the 8- to 16 cell cleavage or 4- to 8-cell cleavage as these were the cleavages most likely to be targeted in subsequent experiments. As a starting point, a drug concentration of 0.5μM was used for experiments. Previously, one study had systematically characterised the effects of a range of concentrations in human cell lines (HeLa and U2OS); and as a result a working concentration of 0.5μM was recommended as the optimal concentration for maximal Mps1 inhibition; at doses >5μM reversine has been shown to have an inhibitory effect on the Aurora kinases (Santaguida et al., 2010). Reversine was dissolved in DMSO, and all control embryos were incubated in the equivalent concentration of DMSO in the absence of reversine, but otherwise treated in the same manner to the experimental embryos.

Reversine treatment of mouse embryos had no apparent adverse effects on pre-implantation developmental potential assessed by morphology

In the first instance, the effects of reversine on developmental potential to the expanded blastocyst stage were evaluated. Of the reversine-treated embryos, 93% developed into expanded blastocysts (n=30), equivalent to the rate in the controls (92%, n=36) (Fisher's test; p=1.0) (Figure 2.11). In addition there were no differences in morphological features noted between the groups such as embryo fragmentation.

Reversine treatment increased the rates of chromosome segregation errors secondary to successful bypass of the SAC

Chromosome segregation rates and the length of mitosis were evaluated in embryos incubated in 0.5μM of reversine. As microinjection of mRNA or siRNA was not required, these experiments were conducted on transgenic embryos expressing H2B-GFP (Hadjantonakis and Papaioannou, 2004) to enable the chromosomes to be visualised during live imaging. Major chromosome segregation errors were found to occur during mitosis in 48% of blastomeres (n=81) within embryos incubated in reversine; significantly more frequent than in controls (9.7%, n= 72) (χ^2 test; p=0.0003) (Figure 2.11B). The length of metaphase in reversine-incubated blastomeres also differed from controls, being significantly shorter with a mean length of 32.2 minutes and 44.4 minutes in reversine (n=81) and control (n=72) blastomeres respectively (Mann-Whitney U; p<<0.001) (Figure 2.11B). These experiments were then repeated but this time the embryos were incubated in reversine during the 4- to 8-division only. The drug was then washed out and the subsequent 8- to 16-cell division was evaluated by time-lapse imaging as above. In these blastomeres (n=32), both the chromosome segregation rates and lengths of metaphase were equivalent to those in the control blastomeres; with a missegregation rate of 3.1% and average metaphase length of 47.2 minutes (Fishers test; p=0.43, and Mann-Whitney U test; p=0.25 respectively) (Figure 2.11). Thus this experiment confirmed that reversine treatment only exerted an effect on the SAC during the period of drug incubation, and that the function of the SAC was completely restored on washout of the drug. This finding was in keeping with the previously described characteristics of reversine in other cell culture systems (Santaguida et al., 2010).

Finally, embryos were incubated in 0.33μM NZ at the late 4-cell cleavage. As observed in the control embryos at the 2-cell stage in the experiments detailed above, all control embryos underwent prolonged arrest before eventually fragmenting with no embryos at all dividing to the 8-cell stage. In contrast, two of eight embryos incubated in 0.5μM of reversine with NZ were able to divide to the 8-cell stage, and this increased to eight of 10 embryos in 1.0μM of reversine (Figure 2.11). These results provided strong evidence that the SAC was inactivated in these embryos.

Taken together it was concluded that the results of these experiments demonstrate that reversine is an effective and reversible inhibitor of the SAC in the mouse pre-implantation embryo.

2.3.3 Evaluating aneuploidy rates using FISH

A collaboration was then established with Aisha Elaimi, then a PhD student at University College London in the Centre for PGD, who kindly agreed to evaluate levels of aneuploidy in these embryos using FISH, a technique that was well established in mouse embryos within their laboratory. A group of control and reversine-treated embryos were analysed for their chromosome constitution using FISH analysis for chromosomes 2, 11 & 16. In total, 38 control and 43 reversine-incubated early blastocysts were analysed, with a total of 1376 and 1076 blastomeres analysed in each respective group.

Reversine-treated blastomeres had significantly higher rates of aneuploidy for chromosomes 2, 11 & 16 than in control blastomeres, with abnormalities detected in 35% of all reversine-treated blastomeres compared with 17% of controls (χ^2 test; $p << 0.001$) (Figure 2.12).

2.3.4 Evaluating aneuploidy rates using an array-based karyotyping approach

A collaboration was also established with Dr Thierry Voet (Principal Investigator, Laboratory of Reproductive Genomics KU Leuven, and The Wellcome Trust Sanger Institute, University of Cambridge). Dr Voet specialises in the microarray analysis of copy number variation in single cells; a technique that is used to detect aneuploidy in single cells, as detailed in Konings *et al.* 2012. The technique has recently been established in human samples; however the protocol required specific adaptation and optimisation for analysis of the mouse genome. In brief, whole genome amplification (WGA) is performed using a multiple displacement amplification (MDA) approach. Amplified DNA is then hybridized to a bacterial artificial chromosome (BAC) array and to a SNP array. The copy number analysis, and hence karyotype, is based upon comparing the BAC-hybridisation probe intensities with a reference model for diploid chromosomes, together with the SNP-copy number results estimated by statistical modelling.

(A)

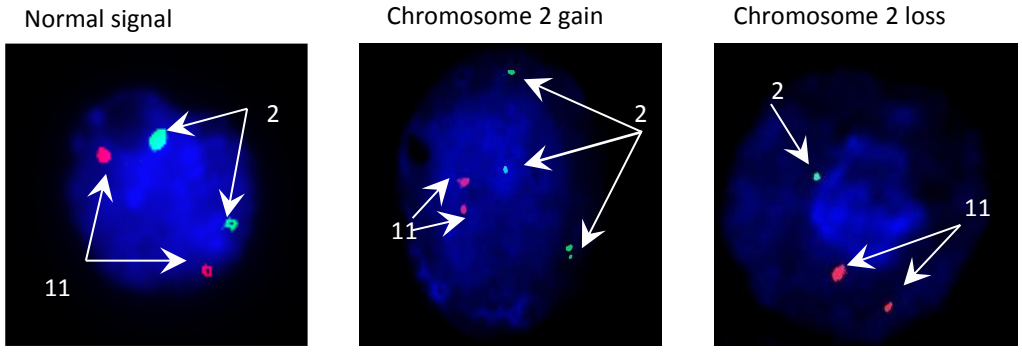

Images from Aisha Elaimi, who performed the procedure and analysed the images

(B)

Blastomere classification in control and reversine-treated embryos

	Normal	Aneuploid
Control (n=1376)	83%	17%
Reversine (n=1076)	65%	35%

Figure 2.12 FISH analysis of embryos (A) Representative images of FISH signals in reversine-treated blastomeres. A normal chromosome number is confirmed by the presence of two probe signals from each chromosome assessed; in this example two green signals for chromosome 2 and two red signals for chromosome 11. Chromosome loss and gain are scored by the loss or gain of signals. Note – the analysis of embryos in this study also included an additional probe for chromosome 16 evaluated during a second round of FISH. **(B)** Blastomeres were classified as normal or aneuploid based on FISH analysis for chromosomes 2, 11 and 16. Reversine-incubated embryos had significantly higher rates of aneuploidy compared with controls (χ^2 test, ***p<0.0001).

All images at 100x magnification

To date (May 2013), preliminary results from three 8-cell stage embryos are available; one control and two reversine-treated embryos (Figure 2.13). Of the eight cells assessed in the control embryo, seven were found to be euploid and one showed an unusual pattern of abnormality. The significance of this abnormality is yet to be determined and it may be a result of artefact, further analysis and conclusive results are still pending. Of the two reversine-treated embryos a total of 14 cells were evaluated, of which ten were aneuploid and four were euploid. As illustrated in Figure 2.13B, where abnormalities were detected there were reciprocal trisomies and monosomies present in sister blastomeres, a finding which was consistent with the abnormalities that would be expected through abrogation of the SAC.

Analyses of further embryos are still pending however these preliminary results demonstrate high levels of aneuploidy following treatment with reversine.

2.3.5 Summary of results and the mouse model

Table 2.3 summarises the major findings for all siRNA, DN and reversine-treatment experiments. When considered together, it was clear that reversine-treatment was the only experimental approach that successfully bypassed the SAC resulting in an increased rate of chromosomal instabilities in treated mouse blastomeres. Therefore reversine-treatment was chosen as the experimental technique which would be used to generate a source of abnormal blastomeres that would then be used in the mouse model of chromosome mosaicism.

Reversine is a highly soluble small molecule rendering it unsuitable for microinjection into single blastomeres as the drug would readily diffuse into the neighbouring blastomeres and surrounding culture medium. Thus the ‘true mosaic embryo’ model could not be generated using reversine treatment (illustrated in Figure 2.1A). However the ‘chimeric mosaic embryo’ is suitable and will be used to generate the mouse model for chromosome mosaicism in future experiments (Figure 2.1B).

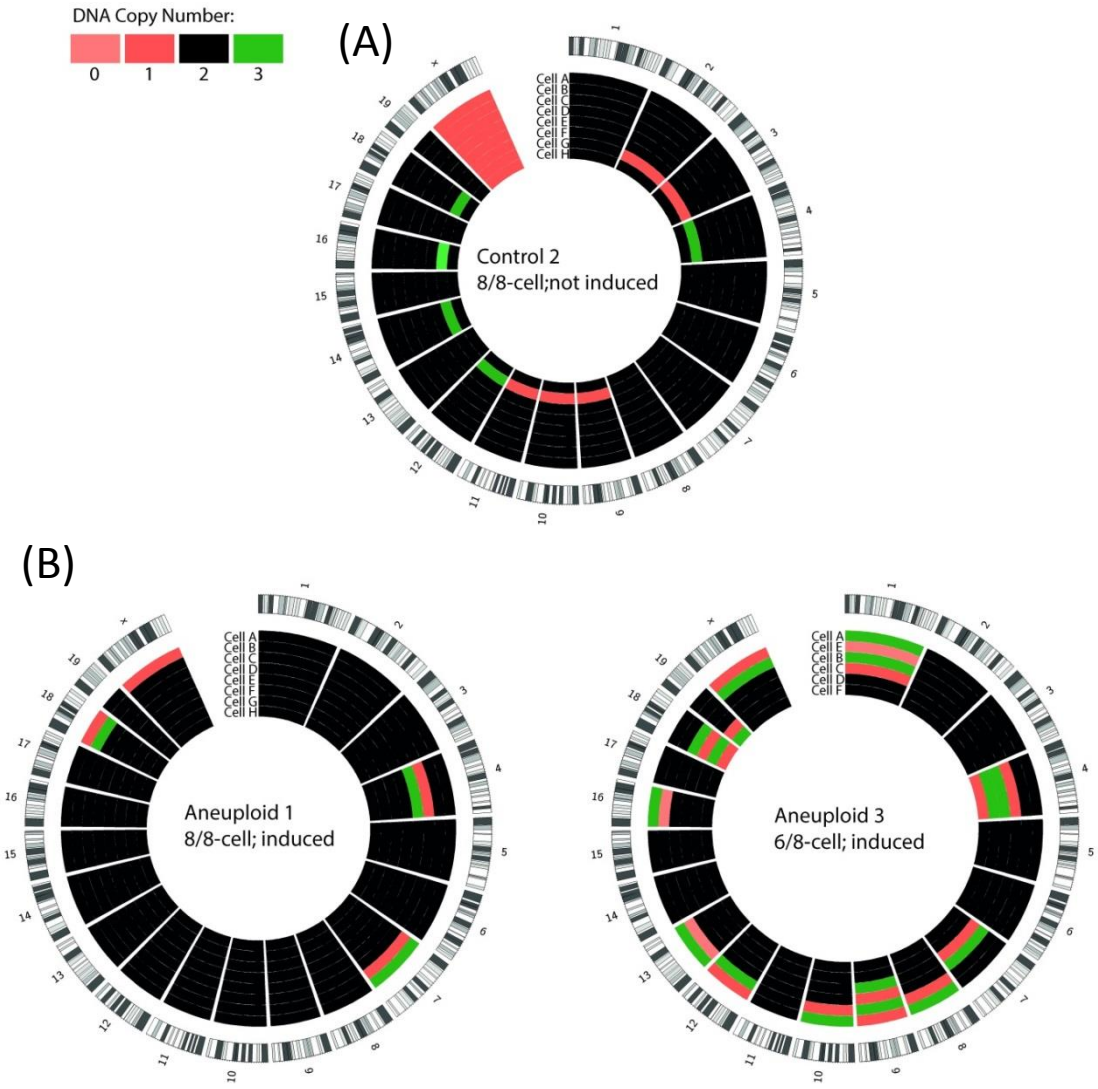

Figure 2.13 Circo plots summarising chromosome status of embryos evaluated by array-based karyotyping. Each circo plot represents an embryo, with individual blastomeres each presented as a single ring within the donut, annotated as cells A-H. Along the outer edge of the donut each whole chromosome is annotated as a barcode which represents chromosomal segments. Coloured bars represent chromosome copy number as given in the accompanying key. **(A)** Control embryo showing an euploid chromosome constitution in 7 of 8 cells. Cell G has an unusual pattern of abnormality and may be secondary to experimental artefact rather than aneuploidy – further analysis is awaited. **(B)** Both reversine-treated embryos (annotated as Aneuploid 1 and Aneuploid 3) show high levels of aneuploidy. Four of eight blastomeres in 'Aneuploid 1' are aneuploid, as are six of six in 'Aneuploid 3'. Note the reciprocal abnormalities between sister blastomeres – for example in 'Aneuploid 1' cell A is trisomic for chromosome 7 while cell B is monosomic. There are several examples of reciprocal losses and gains in both reversine-treated embryos.

Images and analysis courtesy of Dr Thierry Voet.

		Check for expression or knockdown	Development to BC (%)	Chromosome missegregation rates at 2- to 4- cleavage (%)	Length of metaphase (mins)	Time to mitotic slippage (mins)
Dominant negative	Controls	N/A	96	9.5	52.5	474
	Mad2_DN 0.8	HA-tag ICC	90	0	52.5	433
	Mad2_DN 2.0	-	90	12	68.4***	343***
	Bubr1_DN 0.8	HA-tag ICC	100	0	66.0***	309***
	Bubr1_DN 1.75	-	95	0	63.9**	353***
siRNA	Controls	N/A	100	20	69.7	426
	Ndc80 5	mRNA 4%	85	21	71.2	449
	Mad2 5	mRNA 52%	87	13	64.4	449
	Bubr1 5	mRNA 42%	95	20	65.7	411
Drug	Control	N/A	92	9.7	44.4	Arrest
	Reversine	N/A	93	48***	32.2***	Bypass

Indicates significant findings in opposite direction to expected phenotype

Indicates significant findings consistent with expected phenotype

****p<0.001*

*****p<0.01*

Table 2.3 Summary of all experimental approaches to attempted to induce chromosome missegregation in blastomeres. Neither dominant negative approaches or siRNA treatment were shown to bypass the SAC or induce increased rates of chromosome segregation errors in mouse blastomeres. In contrast, treatment with reversine significantly increased chromosome missegregation rates and displayed a phenotype consistent with abrogation of the SAC.

2.4 RESULTS I DISCUSSION

The primary aim of the work described in this chapter was to develop a mouse model for chromosome mosaicism that could be used in future experiments to investigate the fate of abnormal cells within mosaic embryos and the ultimate fate of the embryo. This required a source of abnormal blastomeres together with the ability to evaluate the chromosome status of cells within the pre-implantation embryo.

2.4.1 Evaluation of chromosome status in the mouse embryo

Evaluation of the chromosome status in pre-implantation embryos was technically challenging. Initially attempts were made to prepare metaphase spreads that would be used to count the number of chromosomes present in each blastomere. A protocol for the cytogenetic analysis of mouse pre-implantation embryos using metaphase spreads was first reported in 1966 (Tarkowski, 1966). Subsequently multiple studies have been published that used classic cytogenetic techniques to evaluate the chromosome status of mouse or human pre-implantation embryos (Garside and Hillman, 1985, Roberts and O'Neill, 1988, Yoshizawa et al., 1990, Roberts et al., 1990, Kola and Wilton, 1991, Jamieson et al., 1994, Clouston et al., 1997, Clouston et al., 2002, Lightfoot et al., 2006). Many of these studies discuss the technical challenges specific to pre-implantation embryos that are not encountered in other types of cells, and it is widely acknowledged that the cytogenetic evaluation of pre-implantation embryos is difficult (Delhanty and Handyside, 1995, Macklon et al., 2002). Yet in spite of these challenges successes have been reported, hence the classic cytogenetic analysis of mouse pre-implantation embryos is technically possible. In view of these published successes together with the fact that the technique requires no specialist equipment or reagents, it was considered worthwhile attempting to optimise a protocol that could then be used in this study. Despite multiple attempts and varying multiple parameters within the protocol it was concluded that it was not possible to consistently generate good quality spreads that would be suitable for the analysis of chromosome number during this study. Problems arose secondary to the lack of mitoses, overlapping or shattered chromosomes at metaphase or poor quality chromosomes. This result was not unexpected given the acknowledged challenges in this approach as evidenced by the

number of studies specifically proposing optimised protocols (Garside and Hillman, 1985, Roberts et al., 1990, Yoshizawa et al., 1990, Kola and Wilton, 1991, Clouston et al., 1997) and the fact that this technique has never been routinely introduced into IVF clinics for use in PGS.

As an alternative strategy the assessment of centromere number was considered as a potential technique. Two experimental approaches were evaluated; either the detection of centromeres using IF or detection of a GFP-linked centromere protein (CENPB) expressed following mRNA microinjection into the embryo. Although not a classical approach to chromosome analysis, this strategy was deemed worthwhile of experimental investigation as it offered the potential advantage of being a relatively quick technique that could be used to evaluate large numbers of cells and required no additional expertise or equipment that was not readily available within the laboratory. A similar principle has been applied to FISH chromosome analysis; cenM-FISH is a multicolour centromere-specific technique that can analyse the entire set of chromosomes (Nietzel et al., 2001). This technique requires the arrest of the cell in metaphase but when tested in human oocytes had a low efficiency secondary to the failure of adequate chromosome spreading (Gutierrez-Mateo et al., 2005). By using antibody binding to the centromere protein in the case of IF, or by endogenous synthesis following mRNA microinjection, it was considered that some of the technical errors associated with FISH may be overcome. However, despite the successful detection of the centromeres with both experimental techniques it was clear that neither approach could be used in this study due to the limitations of the imaging technology.

As a consequence of the failure to evaluate chromosome status in blastomeres, a time-lapse imaging approach was developed. This strategy was developed as a modified version of the micronucleus assay test; an assay frequently used as a comprehensive screening system for the measurement of genomic damage in dividing cells (Fenech, 2007). There are several potential origins of spontaneously arising micronuclei, ranging from whole chromosomes to chromosome breaks (Rao et al., 2008). However, in the context of this study any increase in the rates of micronucleus formation were assumed to be due to whole chromosome errors secondary to the successful abrogation of the SAC or disrupted kinetochore structure. By directly visualising chromatin dynamics during metaphase and beyond it was possible to detect chromosome segregation errors and newly arising micronuclei. Additionally the

movies could also be used to evaluate the length of metaphase and thus provide an additional and assayable parameter for successful bypass of the SAC, where the length of metaphase would be shortened.

Although the time-lapse imaging assay did not directly evaluate aneuploidy *per se*, its application in this study was essential for the accurate evaluation of chromosome missegregation rates and for determining if bypass of the SAC was successful. When time-lapse imaging studies did confirm the successful bypass of the SAC in the case of reversine treatment, these embryos were then evaluated for aneuploidy using more specific techniques (see section 2.4.3).

2.4.2 Experimental induction of acute chromosome segregation errors

A variety of experimental approaches were attempted with the aim of inducing chromosome segregation errors in blastomeres secondary to either abrogation of the SAC or disruption of the kinetochore structure. In the first instance DN and RNAi approaches were attempted, however these strategies were unsuccessful. The SAC is functional in the early cleavage stages of the mouse pre-implantation embryo (Wei et al., 2011) and incubation in NZ resulted in metaphase arrest, an effect mediated through activation of the SAC (Rieder and Palazzo, 1992, Rieder and Maiato, 2004). Thus the successful bypass of the SAC or disruption through the alteration of kinetochore structure was expected to result in increased levels of acutely arising aneuploidy. The failure to bypass the SAC can be attributed to a failure of experimental strategy or hitherto unknown properties relating to the SAC that are unique to pre-implantation mouse embryo development.

The consistent failure to induce chromosome segregation errors in blastomeres through a DN strategy is difficult to explain. DN mutant proteins are frequently used as tools to investigate protein function and act to block the function of the gene at the protein level (Herskowitz, 1987). The cloned gene is specifically designed to encode a mutant protein that acts to disrupt or inhibit the function of the wild-type protein when over-expressed, therefore resulting in a loss-of-function phenotype. In this study DN constructs for Mad2 and Bubr1 were used; both constructs had been previously been reported to induce bypass

of the SAC in studies undertaken in mouse oocytes, including within our own laboratory in the case of Mad2_DN (Tsurumi et al., 2004, Sharif, 2011). It was therefore expected that both DNs would bypass the SAC in cleavage stage embryos and the failure to achieve this in spite of the high concentrations of mRNA injected was surprising. Sequencing was used to confirm that both constructs contained the correctly aligned DNA insert. Successful expression of the protein was also confirmed following microinjection using IF to detect the HA-tag.

With any experimental interference of gene or protein function in early stage mouse embryos it is always necessary to consider the potential effect of maternally inherited transcripts and proteins present in the oocyte (Braude et al., 1979). By their nature the potential interference from the presence of maternal proteins is less likely to be problematic in the case of DN experiments, as the DN protein is specifically designed to exert a dominant effect over any residual wild-type protein, provided sufficient DN protein is present. In this study, although the presence of maternal factors could still account for the failure to induce the expected SAC-deficient phenotype, this explanation seems less likely considering the previously reported successes when used in mouse oocytes (Tsurumi et al., 2004, Sharif, 2011).

The failure of DN approaches to achieve a phenotype in this study thus remains unexplained. As the primary aim of the experiments was to induce chromosome abnormalities in mouse blastomeres the strategy was re-evaluated and an RNAi approach was pursued. However the RNAi approach also failed to achieve the desired phenotype. In contrast to the DN approach, the failure of RNAi may be more easily attributed to the role of several possible factors including the presence of maternally inherited mRNA / proteins, an inadequate concentration of effective siRNA, and / or suboptimal siRNA oligo sequences.

In the time since the RNAi experiments were carried out during 2009 and 2010 a study has been published that specifically characterised the role of the SAC during mouse pre-implantation development using a similar RNAi approach (Wei et al., 2011). The effects of siRNA depletion of Bub3, Bubr1 or Mad2 were evaluated individually. The key findings and conclusions of this study were that the depletion of each of these SAC components in the pre-implantation embryo did result in bypass of the SAC as characterised by a shortening of

metaphase time, bypass of metaphase arrest in NZ, and increased levels of micronuclei and aneuploidy in the daughter blastomeres. Thus in contrast to the study presented in this thesis, the authors were able to abrogate the SAC of pre-implantation embryos using an RNAi approach. It is most probable that differences in the experimental details may account for the different outcomes between the two studies. In this thesis *in vivo* conceived zygotes were injected with siRNA and the second cleavage division (2- to 4-cell stage) was evaluated approximately 26 hours later. The first cleavage (1- to 2-cell stage) was not assessed as it was considered that there would have been insufficient time for the siRNA to exert its effect on gene or protein expression by that time. In contrast, the published study did evaluate the first cleavage division but instead injected metaphase II (MII) stage oocytes with siRNA which were then fertilized *in vitro*, an approach which provided sufficient time for the siRNA to take effect prior to the first cleavage, as confirmed by Western blot (WB) depletion of the target proteins. For each gene targeted in this thesis a mixture of three siRNA sequences were injected at a concentration of 5μM, in contrast to the single sequence injected at a given concentration of 25μM in the published study. The specific oligo sequences were different between the two studies, which could have had differing efficacies, although the mixture of three used in this study would be expected to have a greater chance of efficacy than using a single oligo alone. Nonetheless the higher concentration of siRNA injected in the published study compared to this study may have been a major factor in the effectiveness of gene knockdown and resultant phenotype. Although both studies confirmed the effectiveness of the siRNA gene knockdown two different methodological approaches were used. Protein levels were evaluated by WB in the published study confirming effective down-regulation of protein levels for each gene targeted, however it is pertinent to note that residual protein was still clearly present. In this thesis the effectiveness was determined using qRT-PCR, confirming 42% & 52% knockdown of *Mad2* and *Bubr1* mRNA transcripts respectively. Although the degree of knockdown was suboptimal, it has previously been shown that MEFs heterozygous for either Mad2 (*Mad2*$^{+/-}$) or Bubr1 (*Bubr1*$^{+/-}$) exhibit high rates of aneuploidy, affecting 55% of *Mad2*$^{+/-}$ MEFs (Michel et al., 2001) and 35% of *Bubr1*$^{+/-}$ MEFS (Baker et al., 2004). This suggests that even a 50% reduction in gene expression could result in defective SAC function, chromosome segregation errors and aneuploidy. However although a degree of transcript depletion did occur in this study, qRT-PCR does not evaluate the effect on protein level. Thus it was not

known how the protein levels were affected by the siRNA, and it was therefore considered likely that the protein levels were insufficiently depleted to induce a phenotype in these blastomeres, despite a reduction in transcript levels.

In the case of Ndc80, injection of 5μM siRNA resulted in a 96% reduction in mRNA transcript levels. Despite this reduction there was also no evidence of increased chromosome segregations errors compared to controls. This is also likely to reflect the presence of sufficient residual maternal Ndc80 protein, insufficient time for the transcript depletion to effect protein levels, or that a higher concentration of siRNA was required for even higher knockdown effects.

The decision to inject a maximum concentration of 5μM siRNA in zygotes was taken after careful consideration, based upon concentrations used in other publications and also in view of the experience within the laboratory. In particular, at that time there was some experimental evidence emerging from siRNA studies conducted in oocytes that high concentrations of siRNA could in itself induce experimental artefact, with major chromatin and spindle defects apparent on injection of concentrations at and above 60μM (Sharif et al., 2010). Although considerably lower than 60μM, it is possible that similar effects that could be occurring at lower concentrations albeit too subtle to detect experimentally. Adverse effects on the spindle or chromatin could have major implications for the results of this study. If siRNA were to be used as a strategy for inducing aneuploidy, it would be necessary to inject control blastomeres with equivalent negative control siRNAs. These concerns regarding potential siRNA-induced artefact in control blastomeres were difficult to dismiss. In addition, the injection of 20μM of Mad2 siRNA or Bubr1 into a small number of embryos during a pilot experiment did not reveal preliminary results consistent with abrogation of the SAC.

However, the major aim of this part of the study was to induce chromosome segregation errors in the mouse embryo model. As the siRNA experiments failed to achieve this goal this experimental strategy was concluded in pursuit of an alternative approach.

In a final set of experiments, the pharmacological inhibition of the key SAC protein Mps1 with the drug reversine successfully achieved bypass of the SAC and induced high rates of chromosome segregation errors in treated blastomeres. In addition, the effect of the

treatment was transient and the SAC function was restored on washout of reversine. An important point worthy of emphasis here is that once an error has occurred, reinstating the function of the SAC after the completion of mitosis will not result in the detection of the resulting aneuploidy or trigger of the checkpoint at the next cell division; the SAC functions to delay mitosis only in the presence of unattached kinetochores irrespective of the chromosome constitution within the cell (Rieder et al., 1995, Khodjakov and Rieder, 2009). Therefore the transient nature of reversine treatment refers to its effect on the SAC within the cell-cycle that it was administered in and not the abnormalities already induced by the drug applied in previous cell-cycles.

Reversine treatment was the only experimental approach that was successful in inducing acute chromosome segregation errors and was thus selected as the method for generating abnormalities in blastomeres that were to be used in the mouse model of mosaicism.

2.4.3 Aneuploidy evaluation using FISH, array-based karyotyping and future perspectives

A subset of control and reversine-treated blastocysts underwent aneuploidy analysis using interphase FISH probes for chromosomes 2, 11 and 16. As FISH evaluation of chromosome status in mouse blastomeres requires specialist expertise and reagents these experiments were conducted by a laboratory that routinely performs this procedure. FISH evaluation did indeed confirm that reversine-treated blastomeres exhibited significantly higher rates of aneuploidy as expected, with rates of 17 and 35% for control and reversine-treated blastomeres respectively. Yet it was of some concern that the abnormality rates in the control blastomeres were so high. Although this could reflect true differences between control and reversine-treated blastomeres, the inaccuracies of FISH may result in errors and thus erroneous rates of aneuploidy. Until recently interphase FISH was widely used in the clinical setting for PGS (see previous chapter). However, the diagnostic accuracy of FISH for aneuploidy assessment in the pre-implantation embryo has always been an area of concern (Delhanty and Handyside, 1995, Scriven and Bossuyt, 2010, Mantikou et al., 2012) and in the light of recent advances in array-based karyotyping techniques used for comprehensive chromosome screening the accuracy of FISH is under renewed scrutiny (Treff and Scott, 2012). FISH was initially developed as a technique to evaluate the chromosome status of

large populations of cells. Therefore, when applied at the single cell level the technical inaccuracies of the test may be magnified and with the potential for significant inaccuracies. One recent study developed a theoretical model to investigate FISH errors in human embryos and concluded that the diagnostic accuracy rate of FISH was unacceptably high for the analysis of several autosomes (Scriven and Bossuyt, 2010). Further, comparisons between FISH and SNP-microarray based technologies demonstrated markedly higher rates of mosaicism diagnosed by FISH than with the SNP-microarray technology; presented as further evidence of the inherent inaccuracies of FISH (Treff et al., 2010, Treff and Scott, 2012), although the diagnostic accuracy of these newer technologies still requires additional confirmation (Wells et al., 2008, Harper and Harton, 2010, Treff and Scott, 2012). Finally, very few studies have applied interphase FISH for the analysis of mouse embryos, and thus far less is known about the potential for inaccuracy when FISH is used in the mouse (Sabhnani et al., 2011, Elaimi et al., 2012).

In view of the potential uncertainties surrounding the FISH analysis, an additional method of aneuploidy evaluation was desirable. For that reason the collaborative project with Dr Thierry Voet was established with the aim of evaluating the control and reversine-treated embryos using a single-cell microarray analysis of copy number variation approach (Konings et al., 2012). To date (May 2013) the protocol is still being established and only three embryos have been evaluated, however these preliminary results look promising. There is a high rate of aneuploidy in the reversine-treated embryos, and the finding of reciprocal losses and gains add credibility to the results. Additional embryos are awaiting analysis, together with further analysis for the identification of structural variations.

In addition to the analysis of aneuploidy levels for the purposes of this study, a future study is also underway to determine the naturally occurring baseline rate of aneuploidies in the mouse embryo using this array-based karyotyping approach. As discussed in the previous chapter, the literature regarding the rates of aneuploidy in the mouse embryo is limited, and it is intended that this on-going study will establish these rates with greater certainty.

2.4.4. The mouse model for chromosome mosaicism

As a result of the experiments presented in this chapter, the mouse model that would be used to investigate diploid-aneuploid mosaicism was to be a chimeric mosaic embryo composed of a complement of control and reversine-treated blastomeres aggregated together (Section 2.3.4; Figure 2.1B). This model is used throughout the rest of this thesis to investigate the key questions and hypotheses. In the following chapter the results of a small series of experiments using a diploid-tetraploid mosaic model are presented. Although this could be considered a second model of mosaicism, tetraploidy and aneuploidy are quite different and not directly comparable. Like aneuploidy, tetraploid cells also contain an abnormal number of chromosomes (4n) however in tetraploidy there is an extra copy of all chromosomes and thus the gene dosage is also balanced. In contrast, aneuploid cells contain an unbalanced abnormality in chromosome number (2n +/-x) and are thus comprised of an unbalanced genetic constitution with potentially very different consequences for cellular physiology (King, 2008). Tetraploidy mosaicism has been identified in human pre-implantation embryos (Evsikov and Verlinsky, 1998, Sandalinas et al., 2001, Clouston et al., 2002, de Boer et al., 2004). However the clinical significance of tetraploidy is uncertain and has even been proposed to be a normal finding within the TE lineage (Angell et al., 1987, Krieg et al., 2009). Hence while the diploid-tetraploid mosaic model offers useful insights into pre-implantation development in the presence of abnormal chromosome constitution, a further model of diploid-aneuploid mosaicism remains highly desirable.

During the course of this study alternative options for a source of aneuploid cells were considered in detail. Several transgenic mice lines containing Robertsonian translocations are commercially available (for example Jax^{R} Mice; www.jax.org). As such it is possible to attain embryos with defined aneuploidies through breeding of these mice. However, this experimental approach was not pursued for two reasons. First, this type of abnormality would not resemble the complex and variable aneuploidies characteristic of the human embryo (Vanneste et al., 2009, Fragouli et al., 2010, Rabinowitz et al., 2012). In addition it was also hypothesized that the ultimate fate of abnormal cells in the pre-implantation embryo may be influenced directly by an acute cellular response to chromosome missegregation itself. Consequently any such effects would be missed in a model with

containing a stable aneuploid clone of cells, not arising secondary to acute chromosome segregation errors. This hypothesis will be considered in greater detail in Chapter IV.

Thus the experimental efforts were focused on inducing acute missegregation errors in blastomeres. When RNAi and DN strategies failed other experimental approaches were considered. One possible option was to use blastomeres obtained from transgenic embryos known to be highly susceptible to acute chromosome segregation, such as those used to study CIN phenotypes: for example *Mad2*, (Dobles et al., 2000); *BubR1*, (Wang et al., 2004a); *Bub1* (Jeganathan et al., 2007); *Bub3*, (Kalitsis et al., 2000); *Mad1*, (Iwanaga et al., 2007), *Cenpe*, (Putkey et al., 2002); *Cenpc*, (Kalitsis et al., 1998); *Cenpa*, (Howman et al., 2000) or embryo mosaicism (*Sycp3*$^{-/-}$ (Lightfoot et al., 2006)). Although these embryos would have very high rates of chromosome segregation, they were deemed an unsuitable source of abnormal blastomeres for the model as the susceptibility to errors would be permanent and inherited in every single daughter cell indefinitely. In the human embryo the susceptibility to chromosome segregation errors is considered to be transient, with aneuploidy peaking during pre-implantation development (as discussed in the previous chapter). Thus a model containing a clone of cells with an on-going permanent susceptibility to aneuploidy was considered likely to be unrepresentative and therefore discounted as a first line model.

A further experimental option reviewed was the use of drugs such as NZ or monastrol to induce chromosome segregation errors; a strategy that is sometimes utilized in studies using cell culture lines (Thompson and Compton, 2008, Crasta et al., 2012, Thompson and Compton, 2010). These drugs induce missegregation errors and aneuploidy through their ability to generate abnormal merotelic kinetochore attachments at the spindle during mitosis; merotelic meaning that chromosome kinetochores attach to spindle microtubules from opposite poles rather than just one pole, which can result in abnormal chromosome segregation during division (Cimini et al., 2001). There were several reasons why this approach was considered unsuitable for this study. In the first instance the frequency of reported errors in cell culture studies was relatively low, ranging between 10 to 30% (Thompson and Compton, 2008, Crasta et al., 2012). A significantly higher rate was desirable for the mouse model otherwise potential differences between control and treated blastomeres may have been too difficult to detect. In addition, both drugs would require an incubation step over a period of several hours, inducing a prolonged metaphase arrest.

Gene transcription is silenced during mitosis and this effect could compromise viability and trigger additional alterations in cellular physiology unrelated to any resulting aneuploidy (Gottesfeld and Forbes, 1997). Additionally, prolonged mitotic arrest in itself is associated with DNA damage (Dalton et al., 2007, Quignon et al., 2007, Orth et al., 2012) and the consequent damage to the genome together with activation of the DNA damage response could further alter cellular viability and fate secondary to effects independent of chromosome segregation or aneuploidy.

The treatment of blastomeres with reversine was found to be effective at inducing acute chromosome segregation errors, and was thus chosen as the method by which abnormal blastomeres would be generated for the model. Until further models of mosaicism are developed, it will always be of concern that any phenotype revealed in the subsequent studies could be a consequence of other effects independent of acute chromosome segregation or aneuploidy *per se*; as it is possible that the inhibition of Mps1 or non-specific off-target effects of the drug itself could induce a phenotype. These potential effects are discussed in greater detail in the following chapter. However this fact does not invalidate the potential usefulness of the presented model, rather it means that all results and conclusions should be considered in this context and that efforts should be made to continue to develop additional models. In addition it was not possible to accurately determine which cells became aneuploid as a consequence of reversine treatment. Major chromosome segregation errors were visualised in nearly half of all treated blastomeres, resulting in micronuclei formation. However, the absence of visualised errors does not exclude the possibility that errors were also occurring in other apparently normal mitoses, as it was not possible to determine if each daughter cell inherited the correct number or complement of chromosomes. Both FISH analysis and the preliminary results of array-based karyotyping did reveal higher rates of aneuploidy in reversine-treated blastomeres compared to controls. However, as experimental limitations prevent the real-time measurement of aneuploidy within reversine-treated cells, a comparative approach to analysis has been adopted for the subsequent experiments presented in Chapter III.

When compared with other potential sources of abnormal blastomeres reversine treatment conferred several advantages. Of paramount importance was the finding that reversine treatment was highly effective at abrogating the SAC and inducing chromosome segregation

errors in blastomeres during mitosis. Incubating embryos in reversine ensured a consistent and penetrant phenotype that can be difficult to achieve using a clonal approach which requires microinjection. Technically the microinjection of embryos is an experimental approach that can be associated with difficulties in achieving a perfectly consistent dose delivery to each injected blastomere, and thus variations in the penetrance of phenotype can occur, and in addition it can be complicated by the risk of RNA degradation; none of which would be problematic in reversine treatment. In addition, the transient nature of reversine treatment was a particularly beneficial characteristic as it enabled the induction of acute chromosome segregation to be tightly restricted and thus limited to a defined and desirable developmental-window, similar to that believed to occur during human pre-implantation development.

The primary goal of this section of the study was to generate a mouse model for diploid-aneuploid chromosome mosaicism. This aim arose as a consequence of the limited knowledge of the ultimate developmental fates of human mosaic embryos. IVF is now a well-established and widely used treatment for infertility worldwide and thus it is of paramount importance that efforts are made to increase our understanding of early embryo development. Given this, it may be surprising that there are limited reliable animal models for embryo mosaicism, however non-human primates and other larger mammals are expensive, difficult to maintain and present additional practical challenges. Thus there is a need to develop more practical animal model systems that can be used to complement and guide future human embryo research programs. The mouse is an attractive model system as it overcomes many of the logistical, ethical and financial challenges of working with human or larger mammalian species. In addition, in contrast to other systems, the mouse offers the unique advantage of a wealth of knowledge of mouse genetics and the potential for genetic modification, not as readily possible with other model animals. The mouse genome is remarkably similar to the human with 99% of mouse genes having human orthologs, and mutations in mouse genes often have similar consequences to their human homologues (Waterston et al., 2002). Mouse and human embryos are morphologically alike and undergo a similar developmental process of cleavage, cavity formation, hatching followed by implantation and the establishment of the first three lineages. Despite these apparent similarities there are also major differences that must be taken into consideration. The

timing of events varies between human and mouse embryos; ZGA occurs at the 2-cell stage in the mouse (Latham and Schultz, 2001) compared to 4- to 8- cell in the human (Braude et al., 1988), cleavage divisions are slower and compaction, blastocyst formation, hatching and implantation occur at a later stage in humans compared to the mouse (Niakan et al., 2012). Much of what is known about mammalian pre-implantation development is as a result of studies on the mouse. However, in the case of chromosome mosaicism the mouse is usually viewed as a poor model due to its low level of aneuploidy together with the infrequent occurrence of embryo fragmentation, poor morphology and developmental arrest; common characteristics of human embryos. While these are notable and important differences they should not exclude the potential use of the mouse as a model system to explore developmental questions that are impossible to address in human embryos, or otherwise impractical in larger mammals. Provided all results are interpreted in the context of these known differences, the mouse model can be successfully employed to gain further insight into human pre-implantation embryo development.

To date, the model presented in this chapter is the first mouse model of acutely arising aneuploid-diploid mosaicism in the pre-implantation embryo. Despite the potential limitations of this model, it offers a unique and novel opportunity to explore developmental questions that up until now have only been speculated upon. In the next chapter, this model will be used to explore the fate of abnormal cells within the developing embryo together with the developmental outcome of the embryo as a whole.

INVESTIGATING THE FATE OF EMBRYOS WITH CHROMOSOME ABNORMALITIES

3.1 INTRODUCTION TO RESULTS II

The previous chapter described the development of a mouse model for pre-implantation diploid-aneuploid mosaicism. The work presented in this chapter utilizes that mouse model to investigate the fate of abnormal cells within the developing embryo and to determine the developmental potential of mosaic embryos as a whole.

The majority of human pre-implantation embryos are mosaic with the most common pattern being diploid-aneuploid mosaicism, where the embryo contains a complement of both normal and abnormal cells (van Echten-Arends et al., 2011). Aneuploidy is widely believed to be directly responsible for high rates of early human pregnancy failure in both spontaneous conceptions (Macklon et al., 2002) and following IVF treatment (Magli et al., 2000, Sandalinas et al., 2001, Rubio et al., 2007, Mantikou et al., 2012). As a consequence there have been intense efforts to develop clinical tests that can identify abnormal embryos during IVF treatment prior to embryo transfer. By pre-selecting only those embryos containing a normal chromosome constitution for uterine transfer, the ultimate goal is to improve IVF outcomes and ultimately increase live birth rates. Embryo biopsy followed by PGS was widely adopted for this reason but failed to deliver the anticipated improvements in IVF outcome (Twisk et al., 2006, Mastenbroek et al., 2007). Although there are many potential reasons underlying the failure of PGS, the high prevalence of chromosome mosaicism is likely to be a significant factor.

The developmental fate of mosaic embryos is not known. Mosaicism peaks at the cleavage stage of pre-implantation development, declining rapidly as gestation progresses (see section 1.3.3). Whether this shift away from mosaicism towards normality results from developmental failure of the whole embryo, or alternatively through elimination of abnormal cells from the mosaic embryo is not known. Observational findings comparing mosaicism levels with IVF outcomes are suggestive that some mosaic embryos have the potential to develop into viable, on-going pregnancies (Vanneste et al., 2009).

If it is the case that some mosaic embryos have full developmental potential then important questions remain outstanding. What confers viability to mosaic embryos? Does this depend upon the proportion of abnormality within the embryo? How do mosaic embryos normalise? Several hypotheses have been proposed and can be categorised into either clonal depletion or self-correction hypotheses, summarised in Figure 1.4 and discussed in section 1.3.4. These hypotheses are difficult to investigate directly in the human pre-implantation embryo and thus published data is largely limited to supportive evidence from observational studies. Therefore the major aim of this study was to directly investigate developmental outcome of mosaic embryos using the mouse model. By using the mouse model it was possible to approach these questions using novel methodological strategies that would not be achievable in human embryos.

In this chapter time-lapse imaging technology was applied to evaluate the pre-implantation development of mosaic embryos at single cell resolution, enabling the behaviour and fate of normal and abnormal blastomeres to be compared directly within the same embryo. An additional model of diploid-tetraploid mosaicism was developed and used to determine if the fates of aneuploid and tetraploid cells were equivalent. Finally the peri- and post-implantation developmental potential of diploid-aneuploid mosaics was investigated through the uterine transfer of embryos into recipient mothers.

3.2 MATERIALS AND METHODS

3.2.1 Pre-implantation embryo collection and culture

As described in Section 2.2.1 of Chapter II.

3.2.2 Treatment with reversine and equivalent controls

Embryos were incubated in reversine (Cayman Chemicals) at a concentration of 0.5μM diluted in KSOM during the 4- to 8-cell cleavage. To minimise the exposure of embryos to reversine, embryos were selected for incubation at the late 4-cell stage and removed as soon as all four blastomeres had divided, at the 8-cell stage. Any embryos from the batch that had already commenced the third cleavage in any of its blastomeres were discarded. Alongside, an equivalent group of control embryos were treated in an identical manner cultured in KSOM containing an equivalent concentration of DMSO (0.005%) (Sigma) in the absence of reversine.

3.2.3 Immunocytochemistry

With the exception of expanded blastocyst stage embryos, the zona pellucida was first removed using acid Tyrode's solution (Sigma) 20 minutes prior to fixation. Embryos were fixed in 4% PFA (EMS) for 20 minutes in the dark and then washed through three drops of PBS where they were stored at 4^0C until required.

Immunocytochemistry was then carried out as detailed in section 2.2.3 in Chapter II.

Imaging was carried out on an Olympus FV1000 (Fluoview FV10-AW software) or Leica SP5 (LAS AF software) inverted confocal microscope. For experiments that required cell counting, serial Z-planes were taken at a minimum of every 3μM intervals throughout the depth of the embryo. Image files were viewed in ImageJ (www.rsb.info.nih.gov/ij) or FIJI (www.fiji.sc/wiki/index.php/Fiji) software and cells were counted manually using the ROI manager tool.

In this chapter the following antibodies were used at the given concentrations: Cdx2 (1:200; mouse monoclonal, BioGenex), Nanog (1:200; rabbit polyclonal, Abcam), Sox17 (1:200; goat

polyclonal, R&D systems). All secondary antibodies were AlexaFluor Dye conjugates (Invitrogen) and used at a concentration of 1:500.

3.2.4 Generation of chimeric mosaic embryos

Aggregation chimeric mosaics containing reversine-treated and control blastomeres were created at the 8-cell stage. First the zona pellucida was removed by brief incubation in acid Tyrode's solution (Sigma) at 37^0C under direct vision. Immediately on dissolution of the zona pellucida the embryos were washed through at least three drops of M2 medium, and left to recover in M2 for a minimum of 30 minutes before proceeding to the next step. Zona-free 8-cell stage embryos were incubated in individual drops of Ca^{2+}- and Mg^{2+}-free M2 medium for five minutes at 37^0C to aid embryo disaggregation. Embryos were then washed into individual drops of M2 media where they were disaggregated into single cells by gentle mouth pipetting through a flame-polished glass pipette.

Chimeric mosaics were generated by aggregating blastomeres together in drops of M2 containing phytohaemagglutinin (PHA) (Sigma) at a concentration of 0.1mg/ml to enhance blastomere stickiness and hence aid aggregation. Each chimera was created in an individual drop and after several minutes washed through M2 media, and then cultured in KSOM.

The constitution of the chimeras varied according the experiment. In the majority of experiments, chimeras were constructed in a 1:1 ratio and thus constituted of four blastomeres from each of the reversine-treated and control groups. In a set of further experiments 3:1 chimeras were used, comprising six reversine-treated and two control blastomeres.

In one experiment, true 'half-mosaic' embryos were generated from control blastomeres. These were created exactly as described above, except that they were comprised of four control blastomeres rather than eight.

3.2.4.1 Blastomere labelling for time-lapse imaging

For time-lapse imaging experiments all embryos used were from H2B-GFP matings to enable nuclear visualisation and cell tracking. Because the chimeras contained two different populations of cell clones that needed to be distinguished at the start of the movie, it was necessary to mark one of the clones with an additional red label.

For chimeras imaged from the 8-cell stage, one clone of blastomeres was labelled with the vital dye FM4-64 (Invitrogen). Blastomeres were labelled immediately following disaggregation by a ten minute incubation containing a 1:100 dilution of FM4-64 in M2 in the dark. Following labelling, blastomeres were washed through three drops of M2 and used to make aggregation chimeras as described above.

For chimeras imaged from the mid-blastocyst stage, half of the embryos were labelled at the 2-cell stage by micro-injection of *Tomato-fluorescent protein* (TFP) mRNA for (a gift from Samantha Morris) into both blastomeres. Embryos were checked for expression several hours later, and only those expressing TFP were selected to use for one clone. Un-injected embryos were used for the second clone, and chimeras were generated as described above.

3.2.4.1 Lineage marking for uterine transfer experiments

For several uterine transfer experiments chimeras were constructed from clones with two different genetic backgrounds: H2B-GFP and F1. H2B-GFP clones could be identified by the presence of GFP labelled chromatin and thus the two clones could be readily distinguished.

3.2.5 Time-lapse imaging of mosaic embryos

For imaging, embryos were transferred into individual interstices of a finely weaved polypropylene mesh which was firmly adhered within a glass bottom dish (Matek). This customisation of the glass bottom dish ensured the embryos stayed in position throughout the duration of the imaging, an adaptation invented by Dr Bernhard Strauss (a Post-doctoral researcher in the laboratory).

Time-lapse movies were generated using a spinning disk confocal microscopy system (Axiovert Observer Z1, Carl Zeiss, Inc.) with images captured in SlideBook software (Intelligent Imaging Innovations 3i). The multi-position stage enabled each embryo to be imaged individually, using a 40x air objective. Labelled clones were identified at the start of the movie by capturing a single 3D frame in the RFP, GFP and bright-field channels. Subsequently bright-field and GFP-fluorescent images were captured in 25- to 30- Z-planes at 2.5 to 3μM increments, for each embryo at 15 minute time intervals over a 48 hour period from the 8-cell stage through to blastocyst cavity expansion. For the subset of embryos that were imaged during blastocyst cavity expansion only, imaging continued over a period of 24 hours and did not require re-adjustment.

3.2.5.4 Analysis of time-lapse movies

Every cell in each embryo was tracked using SimiBiocell software (Bischoff et al., 2008) creating cell-lineage trees for each individual embryo. Cell-lineage trees included all data regarding the origin, history, cell behaviour and ultimate fate of each blastomere. Cell-cycle lengths were defined as the length between two anaphases, identified by changes in chromatin morphology. Major chromosome segregation errors such as lagging chromosomes and the formation of micronuclei were recorded. Symmetric and asymmetric divisions were assessed during the 8- to 16- and 16- to 32-cell stage cleavages by evaluating the position of the daughter cells in relationship to the embryo surface, as previously described (Bischoff et al., 2008, Jedrusik et al., 2008, Jedrusik et al., 2010). Apoptosis was recorded based on the presence of characteristic chromatin morphology and nuclear fragmentation (Kerr et al., 1972) as described in previous time-lapse studies (Plusa et al., 2008, Meilhac et al., 2009), and final lineage allocation by the position of the cell at the end of the imaging, and on consideration of its division history as previously described (Bischoff et al., 2008, Jedrusik et al., 2008, Jedrusik et al., 2010). Cell tracking was carried out blind to the origin of the blastomere, with identification of cell origin revealed only on completion of tracking of the entire embryo, when the RFP-channel in the original SlideBook file was opened.

3.2.6 Generating tetraploid embryos and mosaics

Whole tetraploid embryos were created by electrofusion at the 2-cell stage using an Electro Cell Manipulator 2001 (BTX) (Kubiak and Tarkowski, 1985). Electrofusion was carried out in a freshly prepared 0.3M solution of mannitol (Sigma) in ultrapure water containing 3% BSA filtered through a 0.22μM filter. Embryos were placed between the chamber electrodes and subjected to an AC pulse of 2V for 10 seconds to align the embryos, followed by three 10ms pulses of DC 50V. The DC voltage was reduced to 30 or 40V for some experiments as the sensitivity of the embryos to electrofusion was variable. Embryos were immediately washed through three drops of fresh M2 media, and observed 30 to 60 minutes later. Embryos that had fused successfully were selected for use in the subsequent experiments.

This technique was also used to create true diploid-tetraploid mosaic embryos. Electrofusion was carried out as described above but on early 4-cell stage embryos. Between 30 to 60 minutes later the embryos were re-assessed and those that had become 3-cell embryos were selected for use in the subsequent experiment, and the remainder discarded.

3.2.6.1 Time-lapse imaging of diploid-tetraploid mosaics

True diploid-tetraploid mosaics were generated from H2B-GFP embryos. Imaging was commenced shortly after fusion, using a Zeiss widefield microscope, Hamamatasu camera and Kinetic Imaging software. Images were captured using a 20x air lens with GFP and DIC z-stacks were recorded every 15 minutes, in 15 z-stacks at 3μM intervals. Imaging was continued for 48 hours by which time the embryos had developed into early blastocysts. SimiBiocell software was used to analyse the images, as described above. Tetraploid blastomeres were identifiable by their cell size at the start of imaging so there was no requirement for additional cell labelling.

3.2.7 Blastocyst transfer into recipients

Uterine transfers into prepared female recipients were performed by William Mansfield or Charles-Etienne Dumeau from the Transgenic Facility of the University of Cambridge Stem

Cell Institute. E3.5 stage early blastocysts were transferred into the uterine horn of 2.5 days postcoitum (dpc) pseudo-pregnant females that had been mated with vasectomized males. Embryo recoveries were undertaken as required according to the specific experiment.

3.2.8 Early post-implantation embryo recovery, imaging and TUNEL staining

Early post-implantation embryos were recovered at E6.5 or E7.5 into PBS on ice as required. The number of implantation sites was recorded and then the embryos were dissected from the maternal decidua. Viable embryos were fixed in 4% PFA at 4^{o}C for one hour followed by washes through PBS, and incubation in DAPI. Confocal images were captured on either a Leica SP5 or Olympus FV1000 inverted confocal microscope into LAS AF or Olympus Fluoview FV10-AW software respectively.

For terminal deoxynucleotidyl transferase dUTP nick end labelling (TUNEL) staining (Roche), embryos were fixed, washed and then permeabilized for 30 minutes in 0.5% triton-100 on ice, and then washed through three drops of PBS/PVP (PBS containing 1mg/ml of polyvinylpyrrolidone (Sigma). Embryos were then incubated in 50μl of TUNEL reaction mixture consisting of 5μl of enzyme with 45μl of the fluorescein label (supplied with the TUNEL kit), in the dark for one hour at 37^{o}C. Embryos were then washed through PBS/PVP and incubated in DAPI for 5 minutes at room temperature prior to imaging.

3.2.9 E13.5 recovery and placental and fetal biopsies

Embryos were recovered at E13.5 individually into PBS on ice keeping the fetus together with its corresponding placenta and whole mount images were captured. Both placental and fetal biopsies were taken from several sites in all H2B-GFP-:-F1 chimeras recovered at E13.5. These were fixed in 4% PFA in PBS for one hour at 4^{0}C. The specimens were rinsed in PBS and then incubated in serial 15%, 20% and 30% sucrose (Sigma) solutions for one hour each, followed by a further overnight incubation in a 1:1 30% sucrose : OCT embedding solution mix at 4^{0}C. The samples were then embedded in OCT media (Tissue-Tek) and frozen on dry ice. Cryosections were cut at approximately 12μM sections and slides were stained with NucView DAPI (Invitrogen) and mounted with Vectashield^{R} mounting medium (Vector

laboratories). Images were taken using a Deltavision widefield microscope with a 20x objective.

3.2.10 Statistical analysis

To compare categorical data the Chi-square test was used, unless the numbers were small in which case the Fisher's exact test was used. The Student's paired or unpaired t-test was used to compare mean values between samples. The binomial test was used to evaluate the clonal distributions of chimeras at the blastocyst stage, based upon the known constitution of the clones at the 8-cell stage. In all cases the two-tailed version of the test was used to evaluate statistical significance. Calculations were carried out in Microsoft Excel or GraphPad software.

3.3 RESULTS II

3.3.1 The pre-implantation development of reversine-treated embryos

The developmental potential of reversine-treated embryos (treated during the 4- to 8-cleavage) was compared with a group of equivalent control embryos. Both groups of embryos were cultured until E4.5 when the developmental outcome was evaluated. Successful morphological development was defined as a hatching or well expanded blastocyst with a large blastocoel cavity. In total 30 reversine-treated and 35 control embryos were evaluated. There were no significant differences in between the two groups; 28 of 30 (93%) reversine-treated embryos underwent successful development, compared to 33 of 35 (91%) of control embryos (Fishers test; p=1.0).

To determine if reversine treatment had any adverse effects on lineage establishment or segregation, embryos were fixed at E4.5 and immunostaining was undertaken for three lineage-specific transcription factors: Cdx2 to mark the TE, Nanog to mark the EPI, and Sox17 to mark the PE. The number of cells in each lineage was counted and reversine-treated embryos were compared with controls. Reversine-treated embryos comprised of significantly fewer cells than the control embryos, with an average of 80.5 cells per embryo, compared to an average 96.8 for control embryos (n= 17 & 23 embryos respectively; Student's t-test; p=0.012) (Figure 3.1A). Immunostaining for the three lineage markers Cdx2, Nanog & Sox17 showed that there was a significant reduction of cells in the TE and EPI lineages (Cdx2 p=0.006 & Nanog p=0.019 respectively, Student's t-test) compared to control embryos, with the exception of the PE lineage which was equivalent to controls (Sox17 p=0.43, Student's t-test).

However there were no significant differences in the overall relative allocation of cells to the ICM and TE lineages, with Cdx2-positive TE cells comprising 82.5% of control and 82.1% of the reversine-treated embryos respectively (χ^2 test; p=0.49). In addition, the lineages were segregated normally with expression of Cdx2 restricted to the outside cells, Nanog restricted to within the deep layer of ICM cells, and Sox17 forming a monolayer of ICM cells, adjacent to the blastocyst cavity (Figure 3.1B).

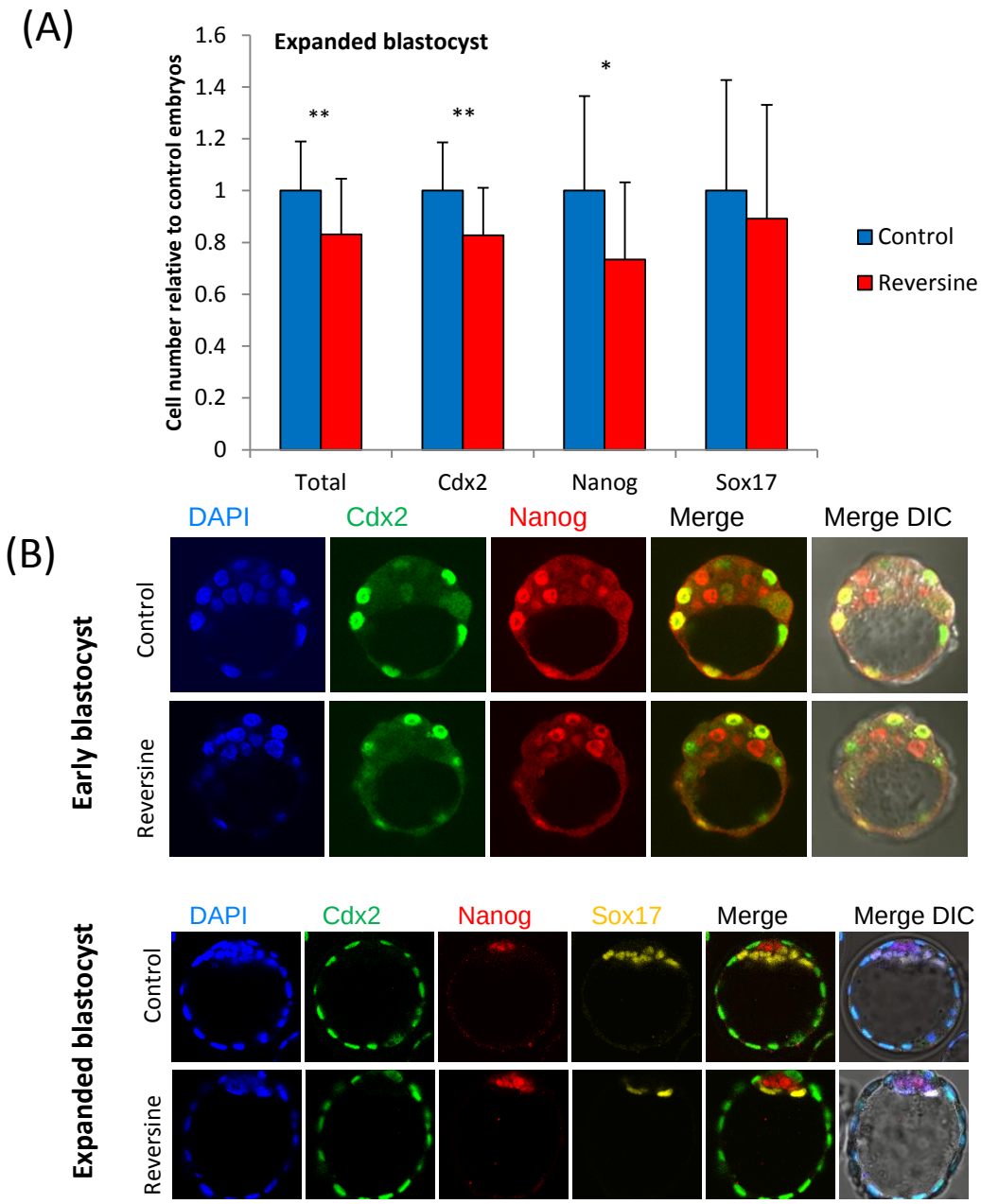

Figure 3.1 Effect of reversine treatment on embryo development. (A) By the expanded blastocyst stage reversine-treated embryos contained significantly fewer cells than controls, with a significant depletion of Cdx2 and Nanog positive cells relative to control embryos (n=17 & 23 embryos respectively, Student's t-test p=0.01). Error bars = SD * p<0.05, ** p<0.01 **(B)** Immunofluorescence staining for transcription factors showed no significant differences in expression patterns in reversine embryos at the early and expanded blastocyst stages. Note the correct sorting into three distinct lineages by the expanded blastocyst stage: Cdx2 marking the TE, Nanog marking the EPI, and Sox17 marking the PE.

All images at 40x magnification

To determine the timing of divergence in cell number between reversine-treated embryos and controls the experiment was repeated but embryos were evaluated at the early blastocyst stage, E3.5. In contrast to the late blastocyst stage, there were no significant differences in cell numbers between reversine-treated and control embryos (containing a mean of 41 and 43 cells per embryo respectively; Student's t-test $p = 0.64$; $n = 6$ reversine and 7 control embryos). Further, there were no significant differences in the distribution of Cdx2 or Nanog positive cells; reversine-treated embryos showed the expected restriction of Cdx2 expression to the outer cells, together with increasing confinement of Nanog positive cells to the inside lineage (Figure 3.1B).

Therefore it was concluded that reversine-treatment of embryos had a detrimental effect on total cell number that became manifest between the early to late-blastocyst stage. Despite this finding, embryo morphology remained unchanged and the TE cells maintained functional capacity and epithelial integrity manifest by the formation of the blastocyst cavity. Additionally the establishment and segregation of the three lineages appeared to be unperturbed.

3.3.2 Time-lapse imaging of chimeric mosaic embryos

The depletion in cell number occurring between the early to late blastocyst stage could arise secondary to differences in cell-cycle lengths, cell-cycle arrest rates, an increase in cell death rates by apoptosis, or a through a combination of some or all of these factors. To investigate this, high resolution time-lapse imaging was used to evaluate the development of chimeric mosaic embryos, comprising of a mixture of reversine-treated and control blastomeres.

Figure 3.2 summarises the experimental strategy. In brief, mosaic chimeras were created at the 8-cell stage by aggregating four control and four reversine-treated blastomeres together thus creating a chimeric embryo containing a one to one ratio of control to treated blastomeres. These experiments were performed on H2B-EGFP transgenic embryos (Hadjantonakis and Papaioannou, 2004) to enable individual nuclei to be visualised throughout the period of imaging. The reversine-treated and control blastomeres within each embryo were distinguished from each other at the start of the imaging by detecting

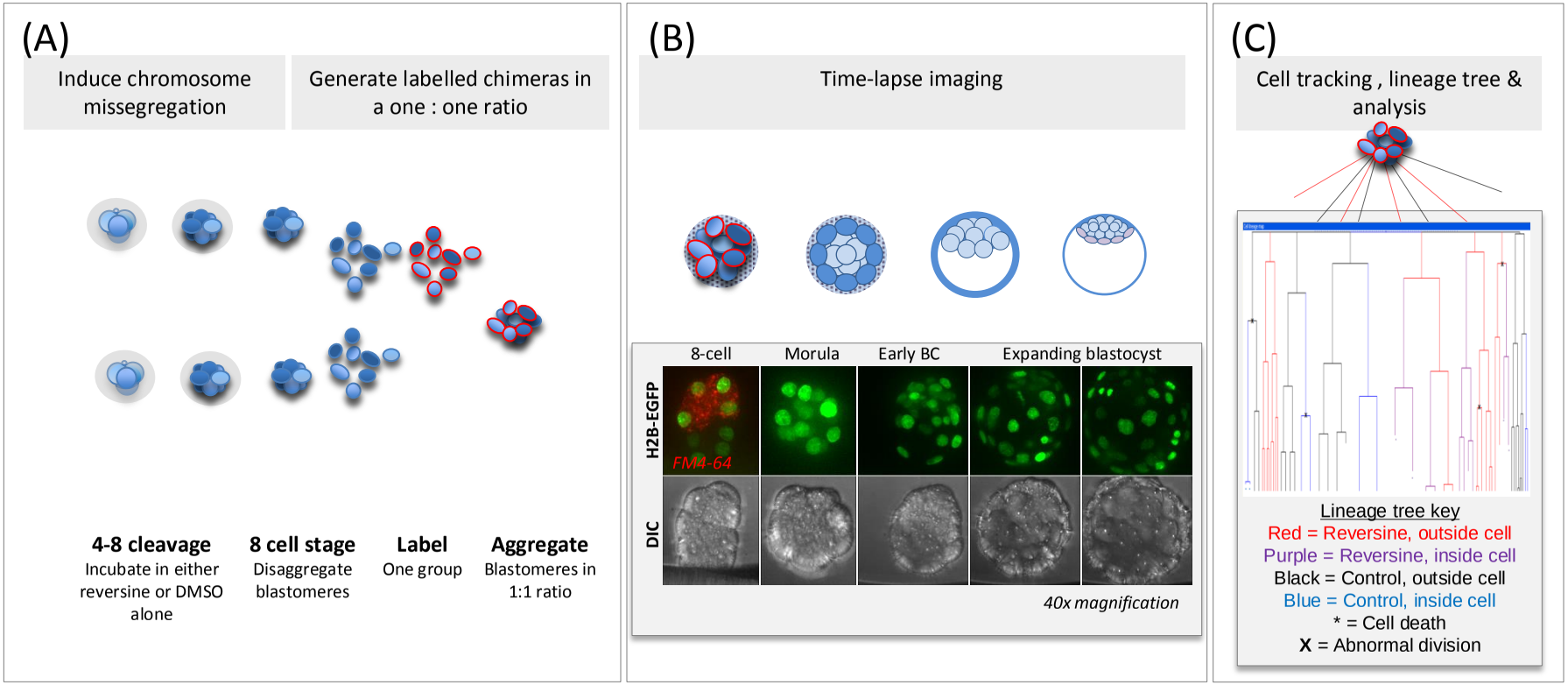

Figure 3.2. Experimental outline for time-lapse imaging and analysis of chimeric mosaics. (A) Embryos expressing H2B-EGFP were incubated in reversine or vehicle (DMSO) alone throughout the 4- to 8-cell stage cleavage. After removal of the zona pellucida, 8-cell stage embryos were disaggregated and one group of blastomeres was labelled with FM4-64. Chimeras were generated by aggregating control and reversine blastomeres together in a 1:1 ratio thus creating 8-cell chimeric mosaics. **(B)** Chimeras were then subjected to 4D time-lapse microscopy from the 8-cell to expanded blastocyst stage, immediately following a single 3D scan to detect the labelled blastomeres. The images show an example of the development of a single embryo. **(C)** Images were then analysed and data recorded as lineage trees (example shown above), with each tree representing a single embryo containing the origin, behaviour and fate of each cell within that embryo.

those blastomeres labelled with the red fluorescent vital dye FM4-64 on a single 3D scan with the red laser immediately prior to commencing 4D time-lapse imaging. Time-lapse imaging was continued for 48 hours until the majority of embryos had developed into expanded blastocysts. In a subset of experiments a group of chimeras were imaged only during a 24 hour period encompassing blastocyst cavity expansion.

20 suitable embryos from several experiments were selected for cell tracking and analysis. Embryos were deemed suitable for analysis if their orientation during imaging was conducive to cell tracking throughout the period of development.

Every single blastomere in each of these embryos was tracked manually using SIMI Biocell Software until its ultimate fate was known, or it was not possible to accurately track the blastomere any further. Most embryos contained a small minority of blastomeres that were lost during tracking. This mostly occurred during blastocyst cavity expansion when the embryos underwent rapid enlargement or when the limitations of imaging had been reached as the cavity expanded out of the imaging plane. For these blastomeres it was not possible to accurately determine the ultimate fate of that individual cell beyond a certain time point. In such cases these cells were tracked up until the time-point of uncertainty, and were recorded as lost to tracking. There were no significant differences between reversine-treated and control blastomeres in the proportions of cells that were lost to tracking, occurring in 11% and 12% of reversine-treated and control blastomeres respectively (n=1938 blastomeres from a total of 34 embryos; χ^2 test; p=0.35). Therefore the loss of these cells did not invalidate or bias the findings for the rest of the embryo, nor their behaviour prior to their loss. Hence embryos were not discarded if they contained a few cells that were lost to tracking, and such cells were included in the analysis up until the time-point at which they could no longer be tracked further.

The 20 embryos tracked from the 8-cell stage onwards consisted of two reciprocally labelled groups of ten embryos; one group in which reversine-treated blastomeres were labelled with FM4-64 (classified as group one) and another in which the control blastomeres were labelled with FM4-64 (classified as group two). This was to ensure that any differences in behaviour of the blastomeres could be attributed solely to their origin (control or reversine-treated) and to rule out the possibility of any differences being masked or detected being a

direct and unexpected consequence of the labelling procedure itself. To be certain that both groups of embryos were comparable, a systematic comparison of the two groups was undertaken to compare all potential variables of interest. This included patterns of lineage allocation, patterns of cell division (symmetric or asymmetric), cell-cycle timings and behaviour, and the frequency of cell death. The results are summarised in detail in Tables 3.1 to 3.4. This analysis confirmed that there were no significant differences detected in the variables between the two groups of embryos secondary to the labelling procedures, but with just one exception. The cell-cycle lengths of the 5th cleavage (16- to 32-cell stage) were found to be significantly longer in control-FM4-64-labelled embryos than reversine-labelled (by 210 and 222 minutes, inside and outside cells respectively, Student's t-test; p=0.015). This difference was unexpected but could be explained by the variation in the exact timing of constructing of the chimeras. Although pre-implantation embryos are relatively robust and readily survive disaggregation, chimera construction and subsequent imaging, it is plausible that the process of disaggregation itself might result in a temporary delay or slowing of cell-cycle length. The two labelled groups were created during completely different experiments and it may be that control-labelled chimeras were created at a slightly later developmental time-point that the reversine-labelled embryos. There were no significant differences between the two groups in the subsequent cell-cycle (32- to 64-cell stage). Overall these comparisons were reassuring, and therefore for all subsequent analyses the data obtained from both groups of embryos was amalgamated and considered together as a single group.

In total 1079 blastomeres were tracked from 20 embryos, comprising 348 ICM cells and 731 outer TE cells. In addition to the 20 chimeras imaged from the 8-cell stage, a further 14 embryos were imaged and tracked from the early blastocyst stage onwards for analysis of ICM apoptosis rates (see section 3.3.2.4). These embryos also comprised of two reciprocal groups, labelled with the fluorescent lineage marker TFP, injected at the 2-cell stage. A comparison between the two groups also revealed no effects attributable to the labelling procedure (Table 3.4).

Limitations of experimental procedure meant that it was not possible to accurately determine the chromosome status of each individual blastomere, as discussed in section 2.4.4 of the previous chapter. Reversine treatment had previously been shown to induce

Table 3.1 Lineage distribution

Early BC	% of Control cells inside	% of Control cells outside
Fm4-64 labels reversine blastomeres	38	63
Fm4-64 labels control blastomeres	30	70

Late BC	% of Normal clone inside	% of Normal clone outside
Fm4-64 labels reversine blastomeres	28	72
Fm4-64 labels control blastomeres	29	71

Table 3.1 shows the lineage distribution of all control blastomeres at the early and expanded blastocyst stage (inside position or outside position), and demonstrated no differences between the labelled and unlabelled cells (χ^2 test p=0.2 & p=0.9).

Table 3.2 Division pattern

	% of Symmetric divisions	% of Asymmetric divisions
Fm4-64 labels reversine blastomeres	36%	64%
Fm4-64 labels control blastomeres	43%	57%

Table 3.2 shows the proportion of blastomeres that underwent symmetric or asymmetric divisions during the 8- to 32-cell stage. There were no significant differences between the labelled and unlabelled blastomeres (χ^2 test p=0.2).

Table 3.3 Cell cycle timings & behaviour

Cleavage (minutes)	5 outside **	5 inside **	6 outside	6 inside
Fm4-64 labels reversine blastomeres	750	853	707	778
Fm4-64 labels control blastomeres	960	1075	721	808

Cell cycle category	Slow outliers	Normal
Fm4-64 labels reversine blastomeres	10%	90%
Fm4-64 labels control blastomeres	8%	92%

Table 3.3 summarises the mean cell-cycle length, and cells classified as 'slow outliers'. 5th cleavage cell-cycle length was significantly longer in FM4-64 blastomeres than labelled unlabelled (t-test **p<0.01), but no differences were observed during the 6th cleavage (t-test, p=0.3). There were differences in the proportions of slow outliers between the labelled and unlabelled blastomeres (χ^2 test p=0.2).

Table 3.4 Apoptosis

Inner cell mass (ICM)	Abnormal cells die	Abnormal cells survive
Fm4-64 labels reversine blastomeres	41%	59%
Fm4-64 labels control blastomeres	34%	66%
TFP labels control blastomeres	31%	69%
TFP labels reversine blastomeres	35%	65%

Trophectoderm (TE)	Abnormal cells die	Abnormal cells survive
Fm4-64 labels reversine blastomeres	4%	96%
Fm4-64 labels control blastomeres	1%	99%
TFP labels control blastomeres	3%	97%
TFP labels reversine blastomeres	6%	94%

Table 3.4 shows the proportion of abnormal cells in each embryo that died or survived according to their position in either the TE or ICM. There were no differences between cells with different labels (χ^2 test; ICM p=0.5, TE p=0.04). A higher level of significance was applied to the TE cells due to the overall low proportion of TE cell death and the effect that clustering of sister blastomeres could have on the overall rate of cell death in each group.

Tables 3.1 to 3.4. Investigating the potential effect of cell labelling on lineage distribution, pattern of division, cell cycle parameters and cell death. In the time-lapse imaging experiments presented in Section 3.3.1 a lineage marker was used to distinguish between the control and reversine-treated blastomeres within each embryo. When embryos were imaged from the 8-cell stage onwards, the lineage marker was Fm4-64. In a subset of experiments the embryos were imaged only during blastocyst cavity expansion, and in these movies the lineage marker was TFP. Although unlikely, it was possible that the lineage marker itself could have an effect on cell behaviour that could then be incorrectly attributed to differences between the control and reversine-treated blastomeres. To minimise the influence of any such effect, in some embryos the control blastomeres were labelled with the lineage marker, and in others the reversine-treated embryos were labelled. This also enabled direct comparisons to be made between the behaviour of labelled and unlabelled blastomeres, and hence detect any unexpected effects due the lineage marker itself. These comparisons are presented above.

major chromosome segregation errors in approximately half of all cells as assessed by high resolution time-lapse imaging (section 2.3.2.3). On that basis it was presumed that when compared to the control clone of blastomeres, reversine treatment had a high probability of inducing chromosome abnormalities in treated blastomeres that would consequently also be inherited by their future progeny. Therefore a comparative approach to analysis was adopted; the reversine-incubated clone would be compared directly with the control clone. However, major chromosome segregation errors were also noted to arise during the time-lapse imaging of the chimeric mosaic embryos, being observed in 4.6 % of all divisions. This finding was in keeping with the previous chapter, where control blastomeres were also observed to have a basal missegregation rate. A comparison of missegregation rates between the control and reversine-treated clones arising during the development of the chimeras revealed that missegregation occurred with similar frequency in both the reversine-treated and control clones (4.0% & 5.0% respectively, χ^2 test; p=0.927, n=921 divisions from 20 embryos). To take account of the major chromosome segregation errors that were observed within the control clone, these blastomeres and their progeny were considered in the same group as the reversine-incubated clone, on the basis that major chromosome missegregation was presumed to be associated with higher rates of aneuploidy than cells undergoing apparently normal mitoses.

Thus for the purposes of terminology control blastomeres with no history of identifiable chromosome segregation errors were classified as the ‘control clone’; and the ‘abnormal clone’ referred to the reversine-treated clone amalgamated with control blastomeres derived directly from an ancestor with a history of major chromosome segregation error that had been noted to occur during the course of time-lapse imaging.

3.3.3 The proportion of reversine-treated blastomeres progressively decreases as blastocyst development proceeds

Lineage trees were assessed for the proportion of reversine-treated blastomeres at the early and expanded blastocyst stages. Chimeras were constructed at the 8-cell stage in a one to one ratio of control to reversine-treated blastomeres, thus at the start the reversine clone constituted 50% of the embryo. The average proportion of the reversine-treated clone

within each embryo was found to be 48.1% at the early blastocyst stage, but decreased to 43.9% by the expanded blastocyst stage (Figure 3.3A). This represented an overall reduction in the reversine-treated clone within the embryo by 12.2%. The depletion was not statistically significant at the early blastocyst stage (binomial test; p=0.37), but became so by the expanded blastocyst stage (binomial test; p=0.002). The depletion was most marked within the ICM cell lineage, with the proportion of reversine-treated blastomeres decreasing to 47.6% at the early blastocyst stage (not significant, binomial test; p=0.36), and then to 39.6% by the expanded blastocyst stage, reaching statistical significance (binomial test; p=0.0009). A smaller but parallel trend occurred within the TE lineage decreasing to 48.7% in early blastocysts (not significant, binomial test; p=0.46) and finally to 45.8% in expanded blastocysts, also reaching statistical significance (binomial test; p=0.02). The overall trend for depletion was in agreement with the findings for whole reversine-treated embryos, presented in section 3.3.1, with the significant depletion occurring during blastocyst cavity expansion, relative to control embryos.

Likewise, evaluating the lineage distribution using the control and abnormal clone classification, the proportion of abnormal clone blastomeres in the embryos decreased significantly between the early and expanded blastocyst stages; decreasing from 53% to 47% respectively (Student's paired t-test; p=0.002, n=20 embryos) (Figure 3.3B). In the TE lineage the proportion of the abnormal clone blastomeres remained stable between the early and expanded blastocyst stages, at 51.3% and 50.3% respectively (Student's paired t-test; p=0.17). Within the ICM lineage the depletion was greater, with the abnormal clone blastomeres decreasing from 55.8% to 44.2%, (Student's paired t-test; p=0.018.).

3.3.2.3 Symmetric and asymmetric divisions

It has been hypothesized that abnormal cells could become eliminated from the future fetal lineage by their preferential allocation to the TE lineage during pre-implantation development (as discussed in the Introduction). Therefore the patterns of cell division were characterised during the fourth (8- to 16-cell) and fifth (16- to 32-cell) rounds of cell cleavage; the fate determining first and second waves of asymmetric divisions respectively (section 1.6.4). During these two cleavages cells can either divide symmetrically giving rise

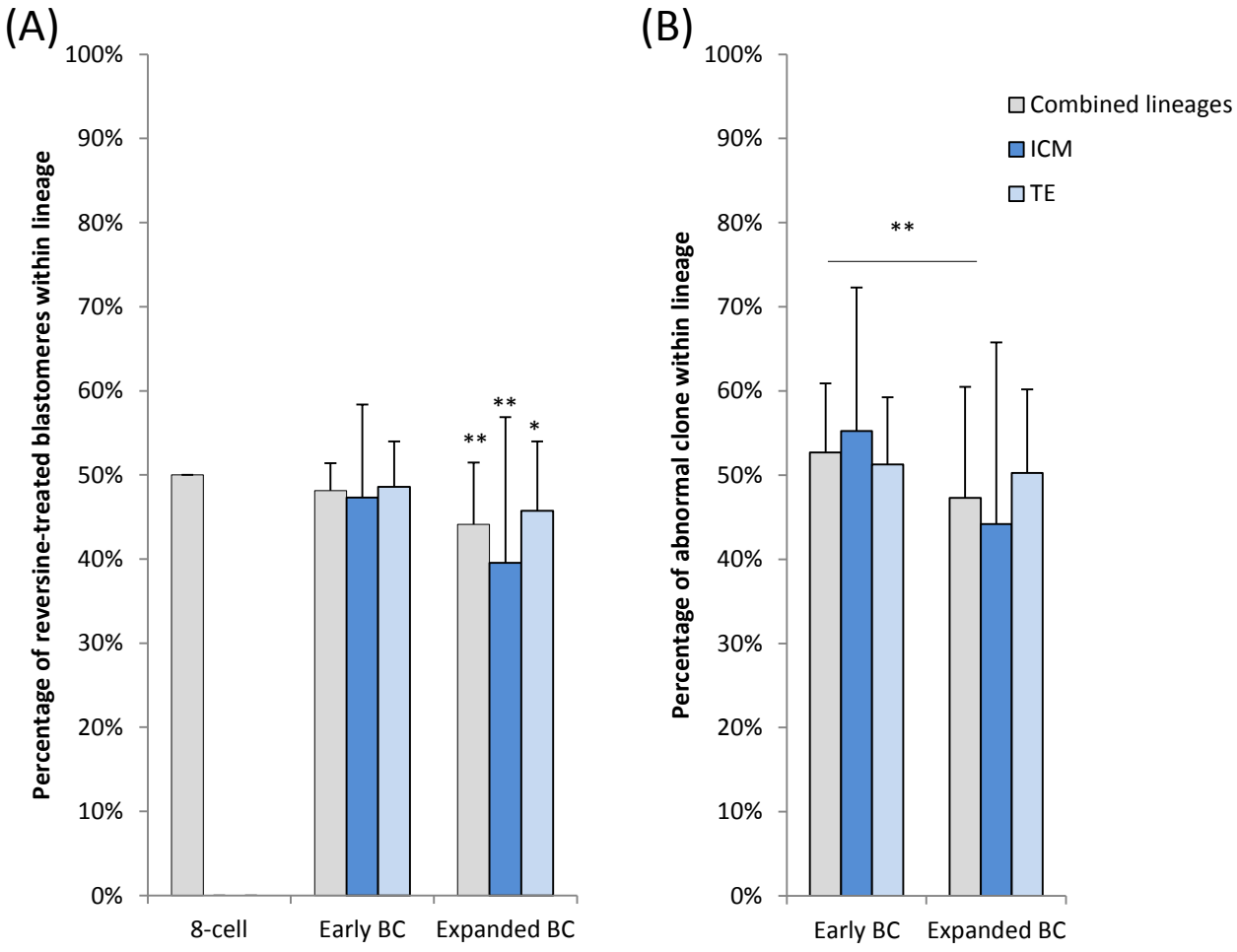

Figure 3.3 Depletion of abnormal blastomeres from chimeric embryos during pre-implantation development. (A) The proportion of reversine-treated blastomeres in the chimeras progressively fell from the 8-cell stage onwards, with a significant reduction by the expanded blastocyst stage, representing an overall reduction in reversine blastomeres by 12.2%. This depletion was statistically significant by the expanded blastocyst stage, and was most marked within the ICM lineage (binomial test). **(B)** Although abnormal divisions arising during development initially increased the proportion of the abnormal clone within the embryo (as expected), there was an overall reduction between the early and expanded blastocyst stage within both the TE and ICM lineages (Student's paired t-test). Error bars = SD, n=20 embryos.

to two outside daughter cells, or asymmetrically giving rise to one outside and one inside daughter cell. The inside cells form the future ICM, while cells that remain on the outside form the future TE, hence any significant differences in pattern of cell division orientation during the fourth and fifth cleavage would result in the differential allocation of the abnormal cells to the one lineage over another.

A total of 361 divisions were assessed from the 20 chimeras. Inside cell divisions during the 16- to 32-cell cleavage were not included in the analysis as these cells were already excluded from a future TE fate. There were no significant differences in the patterns of cell division between the different blastomeres, with symmetric divisions occurring in 60% and 61% of reversine-treated and control blastomeres respectively (χ^2 test; p=0.82). Nor were there any differences when the first wave and second wave divisions were evaluated individually.

Therefore it was concluded that there was no evidence of preferential allocation of aneuploid cells to the TE lineage during the first cell-fate decision. This finding provides evidence against the frequently proposed hypothesis that aneuploid cells are preferentially allocated to the TE lineage during the first fate decision.

3.3.2.3 Evaluation of cell-cycle lengths

The results presented in sections 3.3.1 and 3.3.2.1 demonstrated that the abnormal clones became relatively depleted from the embryo as development progressed to the expanded blastocyst stage. One potential mechanism that could underlie such a finding would be differences in cell-cycle lengths or cell-cycle arrest.

Cell-cycle lengths were measured for all fifth and sixth cleavages at the 16- to 32-cell and 32- to 64-cell stages respectively. From the 20 embryos a total of 280 cell-cycle lengths were measured during the fifth cleavage (151 and 129 in the control and abnormal clones respectively), and 363 during the sixth cleavage (190 and 173 in the control and abnormal clones respectively). The mean cell-cycle lengths were compared between control and abnormal clone blastomeres, matching to cleavage cycle (fifth or sixth) and according to position within the embryo (inside or outside). Overall there were no significant differences

between the control and abnormal clone but with one exception; outside cells undergoing the sixth cleavage (Figure 3.4A). In this case there was a small but highly statistically significant increase in the mean cell-cycle length measured in the abnormal clone of blastomeres, where the cell-cycle lengths was approximately 10% longer than that of the control clone, measuring at 751 and 681 minutes respectively (Student's t-test; $p<<0.001$). Although the differences in other groups did not reach statistical significance it was noted that in all groups the abnormal clone had a longer mean cell-cycle length than their corresponding control clone.

However, the assessment of cell-cycle lengths required the blastomeres to have completed a minimum of two divisions during imaging. By definition, blastomeres that failed to undergo a minimum of two divisions, or whose cell-cycle lengths could not be fully assessed due to completion of the movie before subsequent division (or not) would be excluded from the analysis. Therefore, assessment of the cell-cycle lengths alone would not be sensitive enough to detect differences in more extreme slow cell-cycle lengths or senescent cells. Indeed, reviewing the lineage trees identified examples of blastomeres that had failed to undergo division within the likely expected time frame (Fig. 3.4B). Therefore a system was devised to detect and categorise these cells that would otherwise be excluded from the analysis that was based upon cell-cycle length alone. For each cleavage and lineage, the mean cell-cycle length and standard deviation (SD) was calculated (for example, all blastomeres in the outside lineage during the sixth cleavage / inside fifth cleavage etc). Blastomere cell-cycle lengths were then categorised into one of two groups; either 'standard' or 'slow outliers', based upon a cut-off limit which was set as the sample mean cell-cycle length plus two SDs. Blastomeres were categorised as 'standard' if their cell-cycle length was less than the cut-off limit. In contrast, cells were categorised as 'slow-outliers' if their cell-cycle lengths were greater than the cut-off. In those blastomeres with an un-measurable cell-cycle length (due to completion of the movie, or loss to tracking - see Figure 3.4B), the cell-cycle timing was assessed up until the point at which the movie ended or the cell was lost. Although this was not a measure the cell-cycle length *per se*, with this approach it was still possible to detect some blastomeres which would fit into the 'slow outlier' category. Blastomeres were excluded from categorisation if their cell-cycle length was not measurable but did not exceed the cut-off limit for categorisation as slow outlier, as

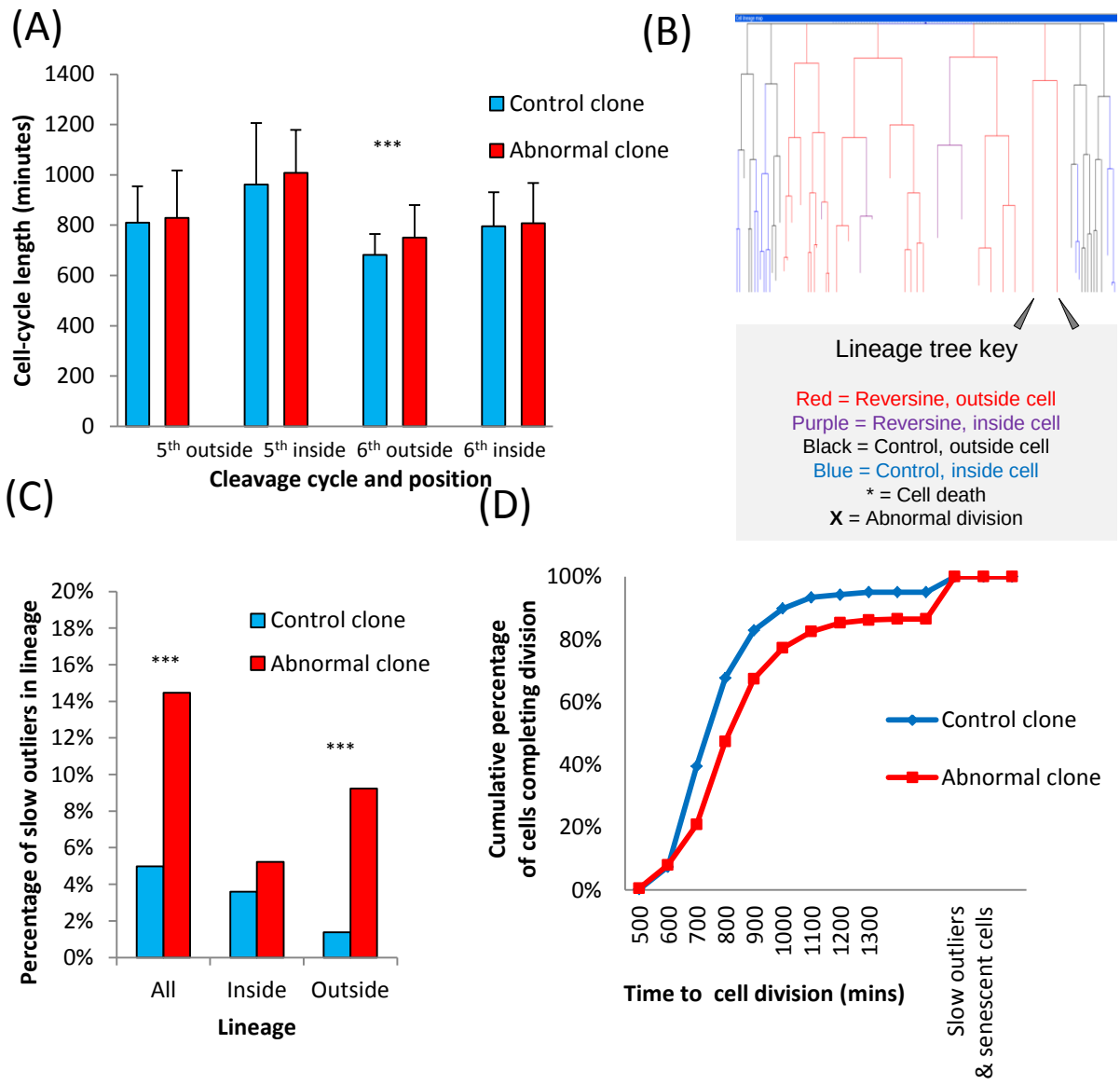

Figure 3.4 Cell-cycle lengths and arrest in chimeric embryos (A) The mean cell-cycle lengths did not differ between control and abnormal clones, with the exception of outside cell lineage where the abnormal clone had significantly longer cell-cycle lengths (Student's t-test; $p<0.0001$) Error bars = SD **(B)** Lineage tree showing an example of two blastomeres classified as 'slow outliers' (grey arrows) due to the very prolonged, but immeasurable cell-cycle length. This finding may represent blastomeres that have undergone transient cell-cycle arrest or senescence; their fate is unknown **(C)** Overall, a greater proportion of abnormal clone blastomeres were slow outliers than controls (χ^2 test; $p=0.0009$), however this effect was only statistically significant in blastomeres of the outer TE lineage (χ^2 test; $p<0.0001$), but not the ICM (χ^2 test; $p=0.21$) **(D)** Cumulative percentage chart showing a graphical representation of the data collated from the mean cell-cycle lengths and slow-outlier classifications. Combining the data together illustrates how the effect of cell-cycle length and / or arrest contributes to progressive depletion of the abnormal clone from the mosaic chimeras; as a group control blastomeres complete their cleavage divisions earlier than abnormal clones.

it was not possible to determine which category they would belong to. The adoption of a cell-cycle length greater than two SDs above the mean as a cut-off for classification was based upon the assumption that the cell-cycle lengths of normal blastomeres were likely to follow a parametric distribution, and thus 2.5% of normal observations would be expected to be 2SDs above the mean. For the purposes of this analysis the absolute cut-off limit and its exact relationship to the data was less important, however this approach enabled differences between clones to be evaluated that would otherwise have been missed.

Using this classification system it was found that a significantly higher proportion blastomeres in the abnormal clone were slow outliers than in the control clone; affecting 13.5% and 5.0% of blastomeres respectively (χ^2 test; $p < 0.0001$) (Figure 3.4C). However, when the inside and outside cell lineages were analysed individually, it was found that this significant effect was confined to the outside cell lineages, affecting 9.2% of the abnormal clone blastomeres, in contrast to just 1.4% of the control clone (χ^2 test, $p<0.0001$). Although the trend was in the same direction within the inside cell lineages, the difference in proportion was small, and not statistically significant; 5.2% and 3.6% in abnormal and control clones respectively (χ^2 test; $p = 0.208$).

When considered together, the trend towards slower cell-cycle lengths combined with the higher proportions of slow outlier cells in the abnormal clone, could potentially account for some of the clonal depletion of abnormal cells from the chimeric embryos. This is represented visually on the cumulative-percentage chart shown in Figure 3.4D.

3.3.2.4 Increased apoptosis occurs in the abnormal clone of blastomeres

In addition to differences in cell-cycle lengths, a further mechanism that may be responsible for the gradual depletion of abnormal blastomeres observed during pre-implantation development could be an increased frequency of cell death. As discussed in the Introduction, apoptosis is frequently observed within the ICM lineage during blastocyst cavity expansion.

In addition to the 20 chimeras that were analysed from the 8-cell stage onwards, a further 14 were included in the analysis of apoptosis to increase the number of ICM cells that could

be included in this analysis. These embryos were labelled with TFP-lineage marker, injected into both blastomeres at the 2-cell stage, and were then used to construct 1:1 reversine – control chimeric embryos (with omission of the FM4-64 labelling procedure).

Time-lapse imaging enabled the recognition of apoptosis by the characteristic morphological features associated with apoptosis; highly condensed chromatin, followed by fragmentation and the formation of apoptotic bodies (Kerr et al., 1972). In some cases the images clearly showed the resulting cellular debris from these apoptotic cells being cleared by the process of efferocytosis; engulfment and ingestion of the cell debris by a neighbouring cell (Figure 3.5A). Apoptosis was observed to occur during blastocyst cavity expansion and usually within the ICM, consistent with the characteristic developmental timing and lineage restriction described during normal development (as described in Chapter I).

From 34 embryos, a total of 634 ICM cells and 1346 TE cells were included in the apoptosis analysis. Apoptosis was frequent within the ICM lineage, occurring in 30.9% of ICM cells overall. However, apoptosis was significantly more frequent in abnormal clone blastomeres, when compared with the control clone; the mean apoptosis rate per embryo was 42% and 20% within the abnormal and control clone blastomeres respectively (Student's paired t-test; p=0.0004). In contrast, apoptosis was rare within the TE lineage, occurring in just 2.0% of TE cells overall. Where apoptosis did occur in TE cells it was significantly more frequent in the abnormal clone; the mean apoptosis rate per embryo was 3.9% and 0.6% in the abnormal and control clone TE blastomeres respectively (Student's paired t-test; p=0.008) (Figure 3.6A).

The higher rate of apoptosis observed within the abnormal clone of blastomeres provided evidence in support of the hypothesis that genetically abnormal cells are eliminated from the future fetal lineage by apoptosis. If this is the case, it would follow that cells with the closest common ancestry would be more likely to die or to survive concomitantly than would be predicted if apoptosis occurred at random or secondary to a non-genetic cause. Indeed, during cell tracking it was noted that sister blastomeres frequently underwent apoptosis (Figure 3.5B). This hypothesis was tested by evaluating the patterns of cell death or survival in blastomere sister pairs; both sister blastomeres both being the direct progeny of one parent blastomere, and thus more likely to share identical genetic constitutions (with

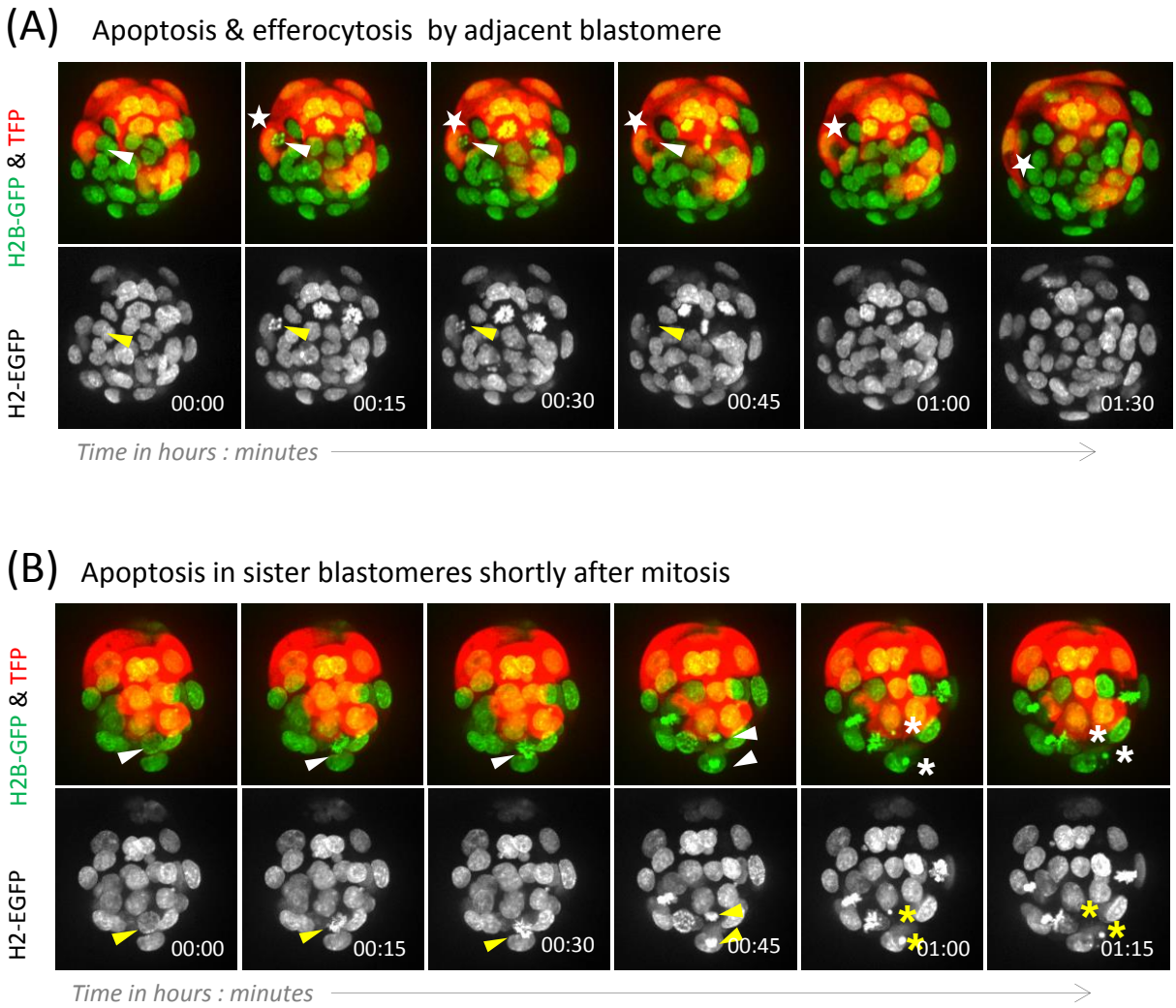

Figure 3.5 Morphology of apoptosis captured during time-lapse imaging. Sequential images from a time-lapse series showing apoptosis in developing blastocysts. The images are 3D projections created from all z-planes. The top panel is a merged image of both channels; in these examples the control clone of blastomeres were labelled with the red lineage marker TFP, and the reversine-treated blastomeres were unlabelled. The lower panel shows only the H2B-GFP (nuclear) images for greater clarity of nuclear morphology. **(A)** Apoptosis followed by immediate efferocytosis; the apoptotic debris is engulfed by a neighbouring blastomere into a cytoplasmic vacuole, the efferosome, where is it gradually cleared. Arrow heads point to cell undergoing apoptosis & stars highlight the efferosome (a cytoplasmic vesicle in an adjacent cell within the apoptotic debris becomes enclosed). **(B)** Still images from a time-lapse sequence to illustrate the characteristic pattern of apoptosis occurring in sister blastomeres immediately after mitosis (arrow heads point to blastomeres about to undergo apoptosis, asterisks to apoptotic bodies).

All images at 40x magnification

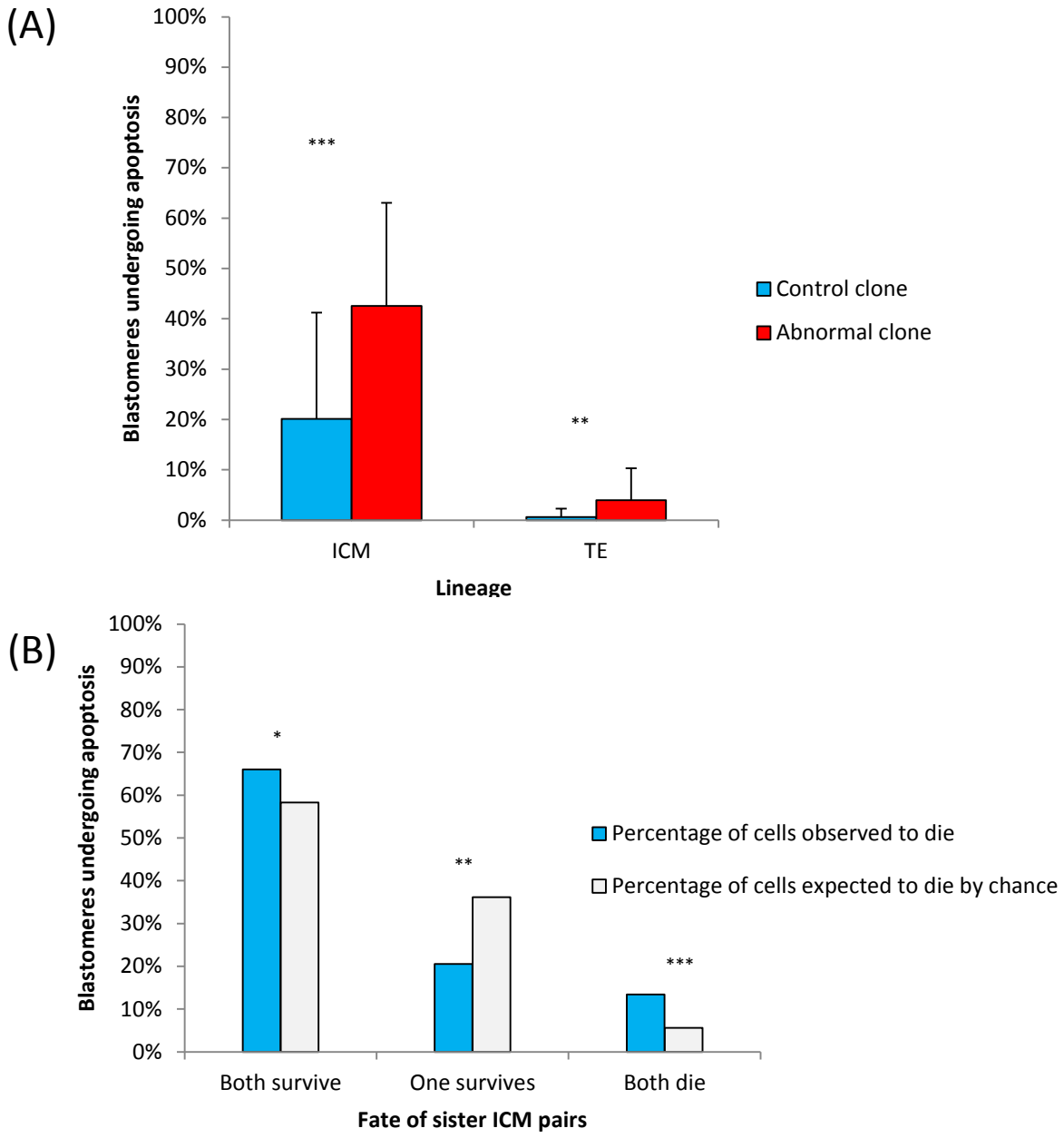

Figure 3.6 Apoptosis rates evaluated by lineage and between sister blastomeres **(A)** Apoptosis occurred more frequently in the abnormal clone and predominated within the ICM lineage. Graph showing the percentage of blastomeres undergoing apoptosis within each lineage (Student's paired t-test; ICM ***p<0.001, TE **p<0.001 & TE). Error bars = SD. **(B)** Sister blastomeres were significantly more likely to undergo apoptosis supporting the hypothesis of an underlying common genetic ancestry between cells that ultimately die (binomial test; * p<0.05, **p<0.01, ***p<0.001). N= 34 embryos

the exception of those few sister pairs where a chromosome segregation error occurred as their common parent cell was dividing). From the 34 embryos there were 321 pairs of sister ICM cells suitable for analysis. Of these, in 13.3% of pairs both sister blastomeres underwent apoptosis. If apoptosis occurred randomly within cells, this would be expected to occur in 5.6% of sister pairs by chance; significantly lower than the rate observed in this study (binomial test; p=0.0014). Conversely, there were more survivors of both sisters in a pair, observed in 66.0% of pairs; significantly more frequent than the 58.2% that would be expected to occur chance alone (binomial test; p=0.045) (Fig 3.6B).

3.3.3 Investigating the fate of tetraploid cells in pre-implantation development

One major hypothesis for elimination of abnormal cells from the future fetus is the preferential allocation to TE lineage proposal, as discussed in the Introduction. This hypothesis has also been used as a potential explanation for how confined placental mosaicism arises (CPM) (Wolstenholme, 1996). The fate of tetraploid cells in diploid–tetraploid chimeric embryos has been cited in support of this hypothesis (Wolstenholme, 1996, Mackay and West, 2005); tetraploid cells remain confined to the placenta with minimal cells present within the fetal tissues (Eakin and Behringer, 2003). The time-lapse imaging studies of reversine-control chimeric mosaics did not find any direct evidence to support this hypothesis, as the patterns of symmetric and asymmetric divisions were identical within both the control and reversine-treated clones (section 3.3.2.2). This led to question of whether the fate of tetraploid cells is unique to tetraploid blastomeres, or were there any shared characteristics with cells containing other chromosomal abnormalities? Previous studies have provided only a snap-shot image of tetraploid-diploid embryo development; thus although it has been shown that lineage biases occur as early as the pre-implantation stage, there is no published data investigating how this happens (Everett and West, 1998, Mackay and West, 2005). Therefore time-lapse imaging was utilized to investigate the development of diploid-tetraploid embryos in greater detail.

3.3.3.1 The pre-implantation development of tetraploid embryos

Initially the pre-implantation development of uniformly tetraploid embryos was assessed. Tetraploid embryos were created by electrofusion at the 2-cell stage and then cultured along with an equivalent group of control embryos until E4.5. In total 30 tetraploid and 32 control embryos were evaluated. There were no significant differences in pre-implantation development rates between the two groups; 30 of 30 (100%) tetraploids underwent successful development (as defined in section 3.3.1), compared to 31 of 32 (96%) control embryos (χ^2 test; p = 0.32). No morphological abnormalities such as fragmentation were detected in the tetraploid embryos.

Tetraploid embryos were then fixed at the expanded blastocyst stage with equivalent control embryos, and immunostaining undertaken for three lineage specific transcription factors: Cdx2 to mark the TE, Nanog to mark the EPI, and Sox17 to mark the PE. In order to directly compare cell numbers between tetraploid and control embryos, the cell counts from analysis of the tetraploid embryos were multiplied by a factor of two. This was necessary to account for the procedure of producing tetraploidy; cell fusion at the 2-cell stage effectively halves the number of cells in the embryo. After correction, tetraploid cells were found to contain an equivalent number of cells as control embryos; tetraploids had an average of 48.9 cells per embryo, compared to 96.7 for controls (n=12 and 23 embryos respectively; Student's t-test; p=0.89) (Figure 3.7A). Further, there were no significant differences in the numbers of cells constituting the TE, EPI and PE lineages, as determined by presence of the lineage specific transcription factors (Student's t-test; Cdx2 p=0.86; Nanog p=0.61, Sox17 p=0.61). In addition, the three lineages were fully segregated into their appropriate positions within the expanded blastocyst (Figure 3.7B). Taken together, these findings suggest that whole tetraploid embryos undergo normal pre-implantation development with respect to the cell number and the establishment and segregation of the first three lineages. These findings were in contrast to the reversine-treated embryos (section 3.3.1), which showed depletion of cells becoming apparent beyond the early blastocyst stage.

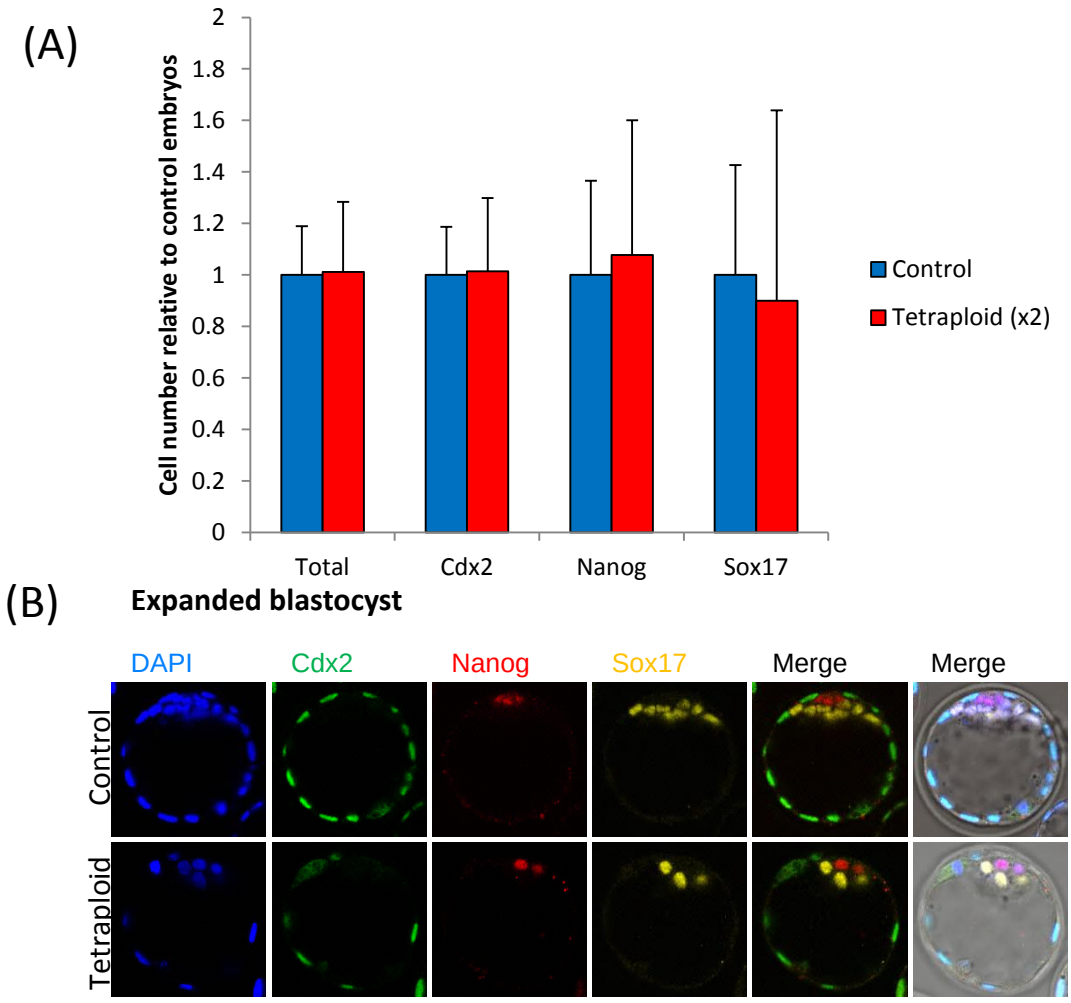

Figure 3.7 Pre-implantation development of tetraploid embryos (A) There were no significant differences in equivalent cell number or transcription factor expression between tetraploid and control embryos at the expanded blastocyst stage (n=12 and 23 embryos respectively, Student's t-test). Error bars = SD **(B)** Immunofluorescence staining for transcription factors showed correct sorting into three distinct lineages in both control and tetraploid embryos: Cdx2 marking the TE, Nanog marking the EPI, and Sox17 marking the PE.

All images at 40x magnification

3.3.3.2 Differential lineage distribution of tetraploid cells in diploid-tetraploid mosaic embryos

In the absence of any identifiable differences between the tetraploid and control embryos, the next step was to evaluate the fate of tetraploid cells within the context of mosaic development; would tetraploid cells behave differently if diploid cells were present within the same embryo? This question was addressed experimentally using time-lapse imaging, and experiments were therefore carried out using H2B-EGFP transgenic embryos to enable nuclear tracking.

The electrofusion protocol was modified in order to generate diploid-tetraploid mosaic embryos; by applying the protocol to 4-cell stage embryos it was possible to generate an intact embryo containing one tetraploid and two diploid cells (Figure 3.8A). Time-lapse imaging was conducted from the late '4'-cell stage (now 3-cell following fusion of the 4-cell embryo) and continued until the mid-blastocyst stage. Cell labelling was not required as the tetraploid blastomere was clearly identifiable by its increased size.

Overall 15 diploid-tetraploid embryos were suitable for analysis. Lineage trees were analysed for the proportion of tetraploid cells contributing to the embryo as a whole, and then to the ICM and TE lineages. At the early blastocyst stage, tetraploid cells were present within the embryo at the expected ratio, comprising 32.8% of the entire embryo (binomial test; $p=0.52$), thus there was no overall depletion of tetraploid cells from the mosaic embryo. However, analysis of the distribution of tetraploid cells within the embryo revealed that they were differentially distributed between the ICM and TE lineages; comprising 16.1% of the ICM and 39.6% of the TE lineages (Student's t-tests; ICM $p=0.0001$; TE $p=0.0014$) (Figure 3.8B). Thus tetraploid cells were enriched within the TE lineage relative to the ICM. A comparison of cell-cycle lengths revealed no significant differences between the tetraploid and diploid cells at either the fourth or fifth cleavage cycles, in keeping with the finding that there was no overall depletion of tetraploid cells from the embryo as a whole (Figure 3.9A).

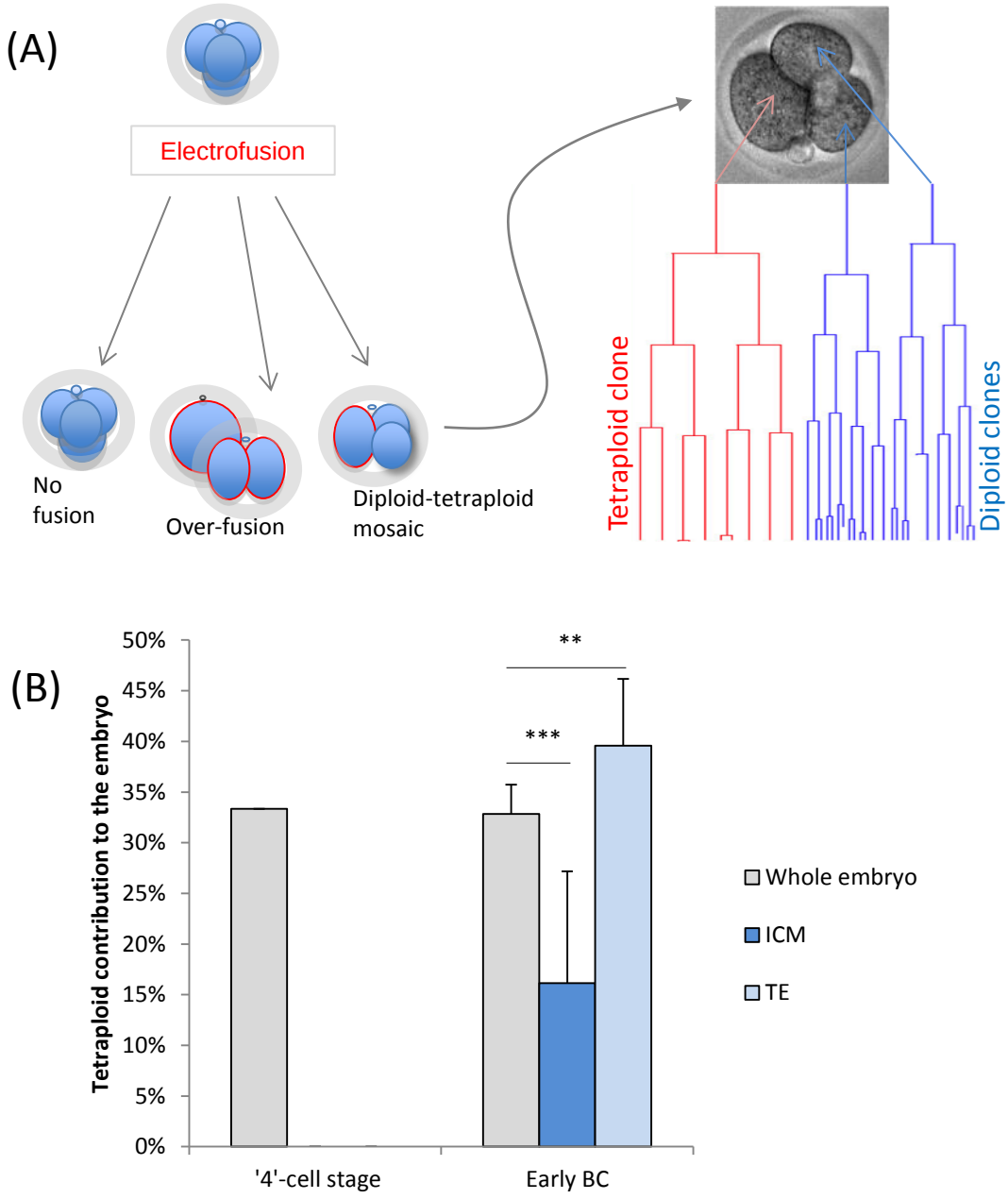

Figure 3.8 Time-lapse imaging of diploid-tetraploid mosaic embryos (A) Experimental overview: diploid-tetraploid mosaics were selected for time-lapse imaging and lineage tree analysis following electrofusion of 4-cell stage embryos. Other embryos that had over-fused or not fused were discarded **(B)** Proportion of tetraploid cells within the embryo at the given developmental stage. Tetraploids were generated at the 4-cell stage (thus becoming 3 cells). By the early blastocyst stage tetraploid cells were significantly enriched within the TE lineage, and conversely depleted from the ICM lineage (Student's t-test; **p<0.001, ***p<0.0001), but with no overall depletion from the embryo as a whole (binomial test, p=0.5) n=15 embryos.

Image at 20x magnification

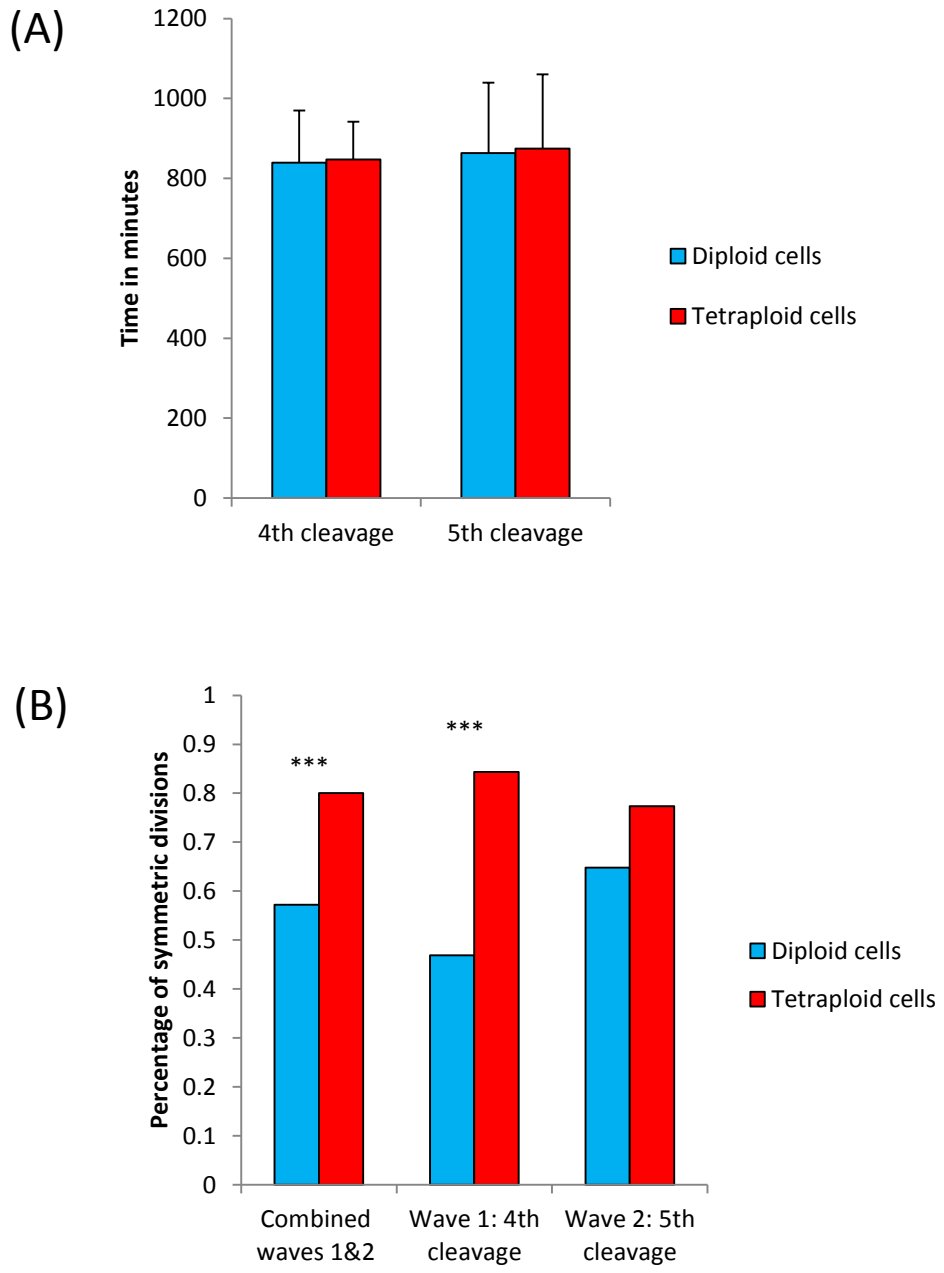

Figure 3.9 Cell-cycle length and patterns of division in diploid-tetraploid mosaic embryos (A) The mean cell-cycle lengths of the tetraploid and diploid clones within the mosaic embryos were identical during both the fourth and fifth cleavage cycles (Student's t-test; p=0.8 and p=0.7 respectively) Error bars = SD **(B)** Overall, a significantly greater proportion of tetraploid cells underwent symmetric divisions when compared to diploid cells., but this effect was predominant during the first wave of symmetric divisions (χ^2 test; ***p<0.0001).

3.3.3.3 Tetraploidy is associated with an increased frequency of symmetric divisions during the first cell-fate decision in diploid-tetraploid mosaics

Next the patterns of symmetric and asymmetric divisions were assessed to determine if the differences in lineage distribution were a result of differences in cell division orientation patterns between diploid and tetraploid blastomeres. In total, 237 outside cell divisions were scored from 15 embryos; of these 152 were in diploid cells and 85 in tetraploid cells. The rate of symmetric divisions was significantly higher in tetraploid cells compared with diploid cells, accounting for 80.0% and 57.2% of tetraploid and diploid divisions respectively (χ^2 test; p=0.0004) (Figure 3.9B). Therefore, it was concluded that the different patterns of cell division occurring during the first cell-fate decision are the major underlying cause for the differential distribution of tetraploid cells between the trophectoderm and ICM lineages.

Interestingly, the differences in patterns of division predominated during the first wave of asymmetric divisions (the fourth cleavage), where 84.3% of tetraploid divisions were symmetric, in contrast to 46.8% of divisions in diploid cells (χ^2 test; p=0.0004). The trend was similar for the second wave of asymmetric divisions (the fifth cleavage) however this difference did not reach statistical significance, with symmetric divisions accounting for 77.3% of tetraploid, and 64.8% of diploid divisions respectively (χ^2 test; p=0.11).

When considered together, these results provide strong support for the hypothesis that tetraploid cells are preferentially allocated to the extra-embryonic lineages during the first cell-fate decision. This would ultimately result in a relative enrichment of the tetraploid clone to the future placenta, together with depletion from the future fetal lineages. The assessment carried out on purely tetraploid embryos showed no differences in proportions of tetraploid cells within and between any of the three blastocyst lineages as compared to control embryos. In addition, there was no evidence of depletion either. Therefore the results obtained from the mosaics suggest that the tetraploid cells behave differently in the presence of diploid cells; but that this difference is confined to lineage segregation differences (manifest through the patterns of cell division), rather than through clonal depletion through cell-cycle effects or apoptosis. Thus it can be concluded that the elimination of tetraploid cells from the future fetal lineage begins through mechanistic

differences during the first cell-fate decision related to orientation of cell-division, and that this mechanism is distinct from the mechanisms occurring in the reversine-treated and chimeric mosaic embryos.

The majority of chromosome abnormalities occurring in human pre-implantation embryos are aneuploid, rather than tetraploid, and are believed to arise as a direct result of chromosome segregation errors that occur during the first few cleavage divisions. Therefore, the reversine-treated embryos and chimeric mosaics are likely to be a better model of human embryo development than the tetraploids. As such, the remainder of this study focussed on the abnormal chromosome segregation model, rather than further characterisation of the effects of tetraploidy.

3.3.4 The post-implantation development of reversine-treated embryos

In section 3.3.1 it was shown that intact reversine-treated embryos can develop into expanded blastocysts and establish the first three lineages; albeit with reduced cell numbers when compared to control embryos. Next the post-implantation development was evaluated. Could these embryos implant successfully and go on to develop into live pups?

To address this question early blastocysts were transferred into recipient foster mothers in two groups; reversine-treated embryos and controls. Embryos were then recovered at E6.5 and E7.5 and assessed for evidence of implantation, embryo viability or resorption sites. A total of 40 reversine-treated and 45 control embryos were transferred, and recovered at the early post-implantation stages, between E6.5 and E7.5 (Table 3.5). Implantation rates were increased in control embryos compared with those incubated in reversine, at 71% and 50% in control and reversine-treated embryos respectively (χ^2 test; $p=0.046$). Moreover, the reversine-treated embryos failed to produce any viable embryos and all implantation sites were resorbing. In striking contrast, every implantation site in the control embryos contained a viable embryo (Fisher's test; $p<0.0001$).

Therefore despite morphologically normal pre-implantation development, reversine-treatment ultimately resulted in complete early post-implantation lethality. These findings are consistent with the mosaic and CIN mouse models discussed in the Introduction.

3.3.5. The post-implantation development of chimeric mosaic embryos

Having established that reversine-treatment was lethal by the early post-implantation stage, the developmental outcome of chimeric mosaic embryos was investigated. Could the presence of normal blastomeres within the embryo rescue the lethal phenotype?

3.3.5.1 Early post-implantation lethality can be rescued by the presence of normal blastomeres

To address this question the transfer experiments were repeated, but this time with chimeric mosaic embryos that contained control blastomeres. Chimeric mosaics containing four reversine-treated and four control blastomeres were constructed at the 8-cell stage, together with controls which consisted of eight control blastomeres, subjected to identical experimental procedures (except that all blastomeres were incubated in DMSO rather than reversine). The experimental embryos were termed '1:1 Rv-C chimeras', and control embryos '1:1 C-C chimeras' to reflect their constitution. These embryos were not subjected to time-lapse imaging during cleavage and therefore it was not possible to identify control cells that had exhibited chromosome segregation errors. Thus for the post-implantation experiments the reversine-treated clones were compared directly with the matched control clones.

Over a series of several experiments a total of 115 1:1 Rv-C chimeras, and 107 1:1 C-C chimeras were transferred into recipients and then recovered at E6.5 or E7.5 (Table 3.6). Implantation rates were equivalent between the two groups, at 64.3% and 53.3% in Rv-C and C-C chimeras respectively (χ^2 test; p=0.094). Every implantation site in 1:1 Rv-C chimeras contained a viable embryo all of which appeared morphologically normal for their developmental stage. Thus the early post-implantation viability of the 1:1 Rv-C chimeras was equivalent to that of the 1:1 C-C controls (Fishers exact test; p=1.0). Therefore the presence of at least 50% of control blastomeres within the embryo was sufficient to completely rescue the early post-implantation lethality that occurred in whole reversine-treated embryos (section 3.3.4).

These chimera transfer experiments were then repeated but this time chimeras were constructed with a lower proportion of control blastomeres: 8-cell stage chimeras were constructed from six reversine-treated and two control blastomeres (3:1 Rv-C chimeras). A total of 53 3:1 Rv-C chimeras were transferred and recovered at E7.5 (Table 3.7). As for the previous sets of transfers, the implantation rates were equivalent, at 47.2% and 53.3% in Rv-C and C-C chimeras respectively (χ^2 test; p=0.47). Viable embryos were recovered within only 44.0% of implantation sites, which was significantly lower than that of controls and 1:1 Rv-C chimeras in which all implantation sites contained viable embryos (Fisher's test; p<0.0001); but significantly greater than in whole reversine-treated embryos in which no viable embryos were recovered (Fisher's test; p<0.0001). Thus, there was partial rescue of early post-implantation embryonic lethality where the chimera comprised of one quarter control blastomeres.

A group of early post-implantation 1:1 Rv-C and 1:1 C-C embryos were evaluated for apoptosis by TUNEL staining. In keeping with the predominantly normal nuclear morphology findings presented in above, there was minimal evidence of apoptosis in either the Rv-C or C-C chimeras (Figure 3.10 inset images). Thus it was concluded that apoptosis is unlikely to play a major role in eliminating abnormal cells at the early post-implantation stage of development.

In a subset of experiments chimeras were constructed using embryos from two different genetic backgrounds; wild-type F1 and H2B-GFP embryos. The purpose of these two different backgrounds was to enable clones to be identified in the post-implantation embryos; cells derived from H2B-GFP blastomeres would be distinguished by the presence of nuclear GFP. 1:1 Rv-C and 1:1 C-C chimeras were transferred to recipients and recovered at E6.5 and E7.5, fixed and then imaged (Figure 3.10). In these experiments, a dominance of the H2B-GFP clone was noted, even in the control embryos which would be expected to contain approximately half H2B-GFP and half F1 cells. This finding was surprising, but may be a reflection of subtle differences between the genetically different backgrounds between the F1 and H2BGFP mice. It is conceivable that H2B-GFP embryos may develop at as slighter quicker rate than F1 embryos, which could account for this predominance. However, in the majority of embryos recovered there was a significant depletion of the reversine-treated clone compared to the controls, although most embryos did retain some clones from the

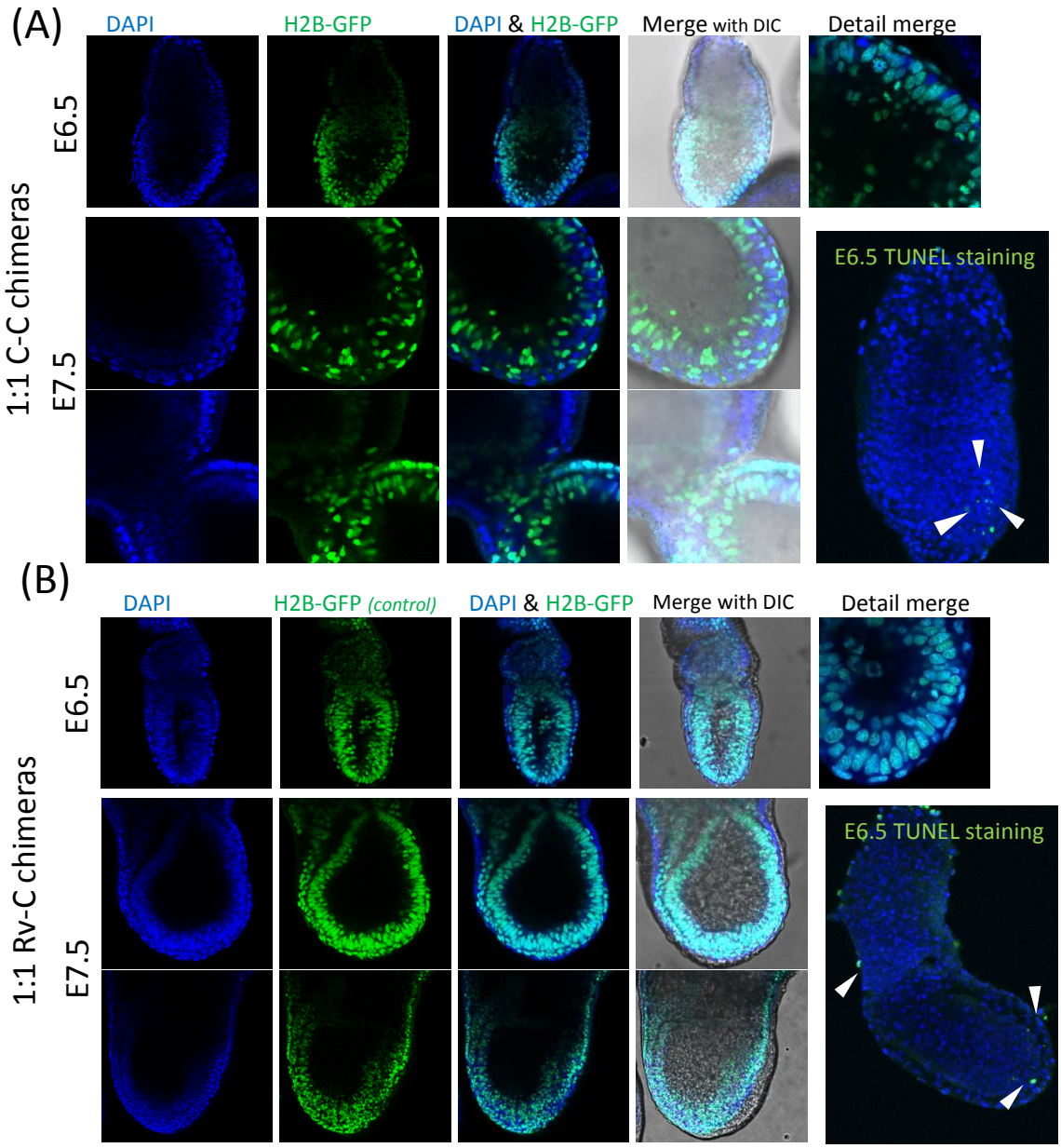

Figure 3.10 Early post-implantation1:1 Rv-C and 1:1 C-C chimeras at E6.5 & E7.5 There were no apparent differences in morphology or developmental stage between control and half mosaic chimeras. **(A)** The majority of control mosaic chimeras comprised of an approximately equal distribution of both F1 and H2B-GFP derived clones, which were well mixed throughout the embryo **(B)** 1:1 Rv-C chimeras were comprised predominantly from the control clone of cells (H2B-GFP) with significant depletion of the reversine treated clone (F1) from the conceptus in the majority of embryos recovered. **Inset images:** representative images of E6.5 chimeras following TUNEL staining. In these embryos both the normal and reversine-treated clone were on an F1 background and so it was not possible to determine the clone of each cell. However, there were no differences in the patterns of TUNEL staining between Rv-C and C-C chimeras with all embryos showing minimal evidence of apoptosis. Projected images are shown with DAPI & TUNEL staining (white arrow heads - FITC).

All images at 20x magnification

treated blastomeres. Although depleted, reversine-treated clones were present throughout the entire conceptus with no evidence of preferential depletion in the embryonic or extra-embryonic lineage, and were well mixed together with the normal clones. There was no evidence of increased apoptosis or necrosis occurring in the treated clones as nuclear morphology appeared equivalent between the reversine-treated and control clones, with no evidence of nuclear debris or cellular remnants. Representative images are shown in Figure 3.10.

Taken together these results demonstrate a critical requirement for a minimum number of control blastomeres for the rescue of the complete embryonic lethality associated with reversine-treatment of pre-implantation stage embryos / blastomeres.

3.3.5.2 Mosaic chimeras have equivalent fetal and post-natal developmental potentials, despite clonal depletion of reversine-treated progeny

The transfer experiments presented above demonstrated that the early post-implantation lethality could be completely rescued provided there were a sufficient number of normal cells present within the embryo. The next step was to determine if this early post-implantation rescue phenotype was also associated with successful on-going development beyond the early post-implantation stage. Would 1:1 Rv-C chimeras be capable of producing viable fetuses and live pups, or did the early post-implantation rescue delay an inevitable lethal phenotype?

To investigate this hypothesis, 1:1 Rv-C chimeras and equivalent controls were transferred into recipient mothers and recovered at E13.5 or allowed to develop to term.

In total 84 1:1 Rv-C and 34 1:1 C-C chimeras were transferred (Table 3.8). Both the control and Rv-C embryos developed to E13.5 or term with equivalent rates; 52.3% and 58.8% of Rv-C and C-C chimeras respectively (χ^2 test; p=0.53). Further, the combined E13.5 recovery and live birth rates were equivalent to early post-implantation viability rates suggesting that successful implantation equated to the complete restoration of developmental potential (χ^2 test; p=0.09) (Table 3.9).

No cases of embryo resorption were identified however in one case a single Rv-C chimera was recovered at E13.5 that looked abnormal, appearing to have arrested at approximately day E9.5. Unfortunately, due to technical problems on the day, a photograph was not taken of this embryo. Due to the small numbers involved, it is not possible to ascertain the significance of this finding. However, it is worth noting that there was also an abnormality detected in the control group; one E13.5 fetus had an unusual morphological appearance with atypical features and an oedematous appearance, although it did appear to be normally grown and was viable at the time of recovery (confirmed by the presence of a beating heart) (Figure 3.11). In all other cases, the Rv-C and C-C chimeras appeared to be normal and of the appropriate size and morphology expected for their gestational stage.

As for the early post-implantation transfers, in some experiments the chimeras were constructed from a mix of wild-type F1 and H2B-GFP embryos in order to evaluate if there was any significant depletion of the reversine-treated clone within the embryo and placenta. In these experiments the reversine-treated clone was on the H2B-GFP background. On recovery of the conceptus at E13.5, whole mount GFP images were taken along with several fetal and placental biopsies (Figures 3.11 & 3.12). In the vast majority of control chimeras both clones were present in both the fetus and placenta; constituting equivalent proportions in both the placenta and fetus as assessed by evaluation of the biopsy results. In contrast, in the 1:1 Rv-C chimeras the reversine-treated H2B-GFP clone was depleted or absent from the majority of conceptuses (only 3 of 9 E13.5 fetuses contained cells derived from the reversine-treated blastomeres). The differences between the control and Rv-C chimeras were statistically significant (Fisher's test; placenta p=0.0019, fetus p=0.0077) (Table 3.10). In those cases where both clones were present within the conceptus, evaluation of the biopsies revealed that both clones were distributed evenly and well mixed with no evidence of clonal pooling or restrictions. There was also no evidence of sequestration or enrichment of the abnormal clone within the placental tissues. In addition, the biopsy results correlated well with the whole mount images.

In the case of Rv-C chimeras, instead of recovery at E13.5 some were allowed to develop to term, in order to determine if viability rates at E13.5 would be consistent with live birth rates. A total of 13 live pups were born confirming that viability at E13.5 was indeed equivalent to viability at term (χ^2 test; p=0.77) (Figure 3.11 & Table 3.9). All pups appeared

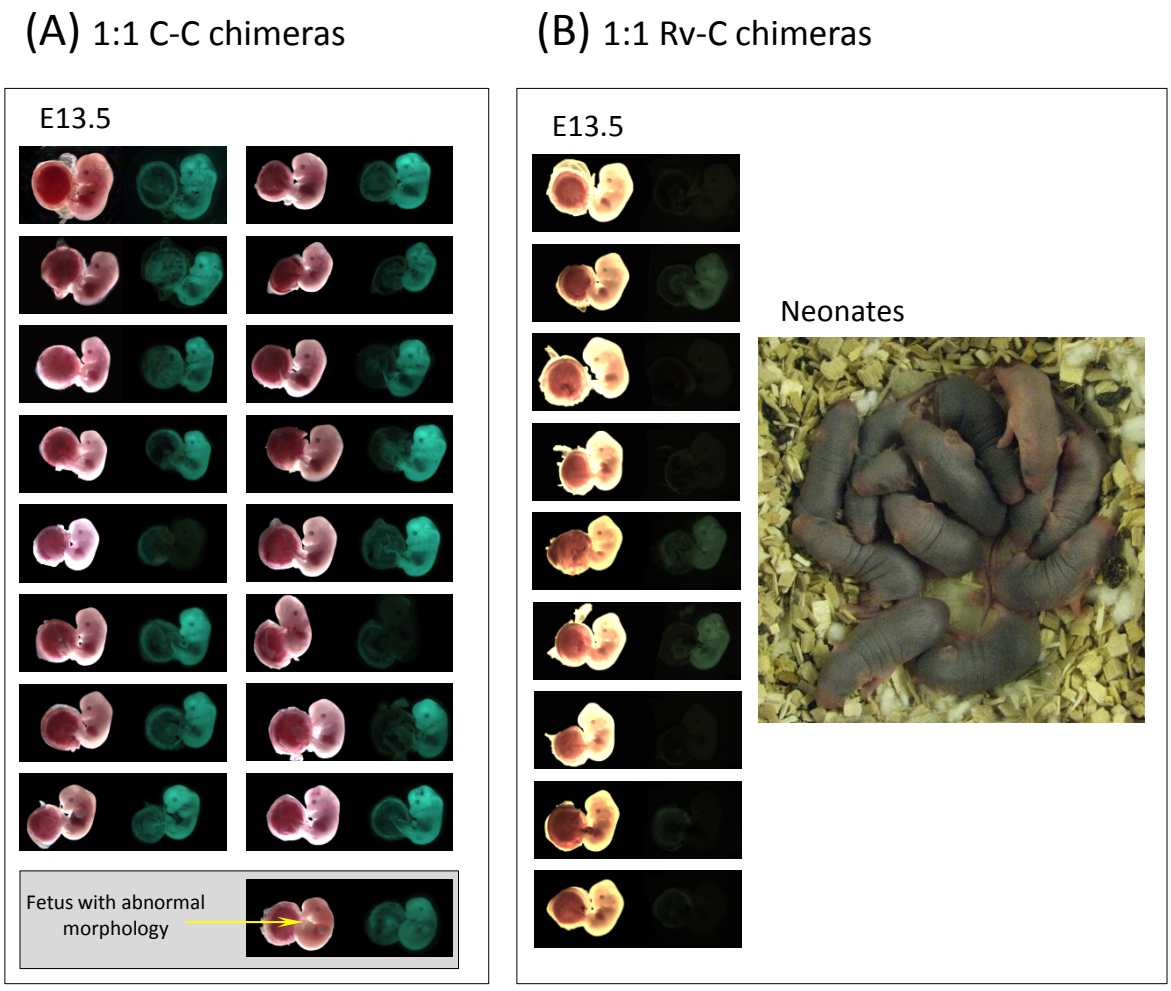

Figure 3.11 Post-implantation development of mosaic chimeras. Post-implantation development was equivalent in 1:1 Rv-C and 1:1 C-C control chimeras. Whole mount images are shown adjacent to fluorescent images taken simultaneously. **(A)** The majority of E13.5 control chimeras contained a significant proportion of both clones (F1 and H2B-GFP) of cells **(B)** In contrast, only a minority of E13.5 1:1 Rv-C chimeras contained any appreciable Rv-treated clones (in this case H2B-GFP), with most containing none or minimal. In the case of Rv-C chimeras, some pregnancies were allowed to continue to term, to determine if the rates of viable of E13.5 pregnancies were equivalent to the rates of live births.
Note – *the E13.5 fetuses were imaged using different microscopes, and hence the difference in the image colours are reflective of the microscope, not differences between the two groups*

In the Rv-C chimeras the normal clone was derived from F1 blastomeres, and reversine-treated clone from H2B-GFP blastomeres.

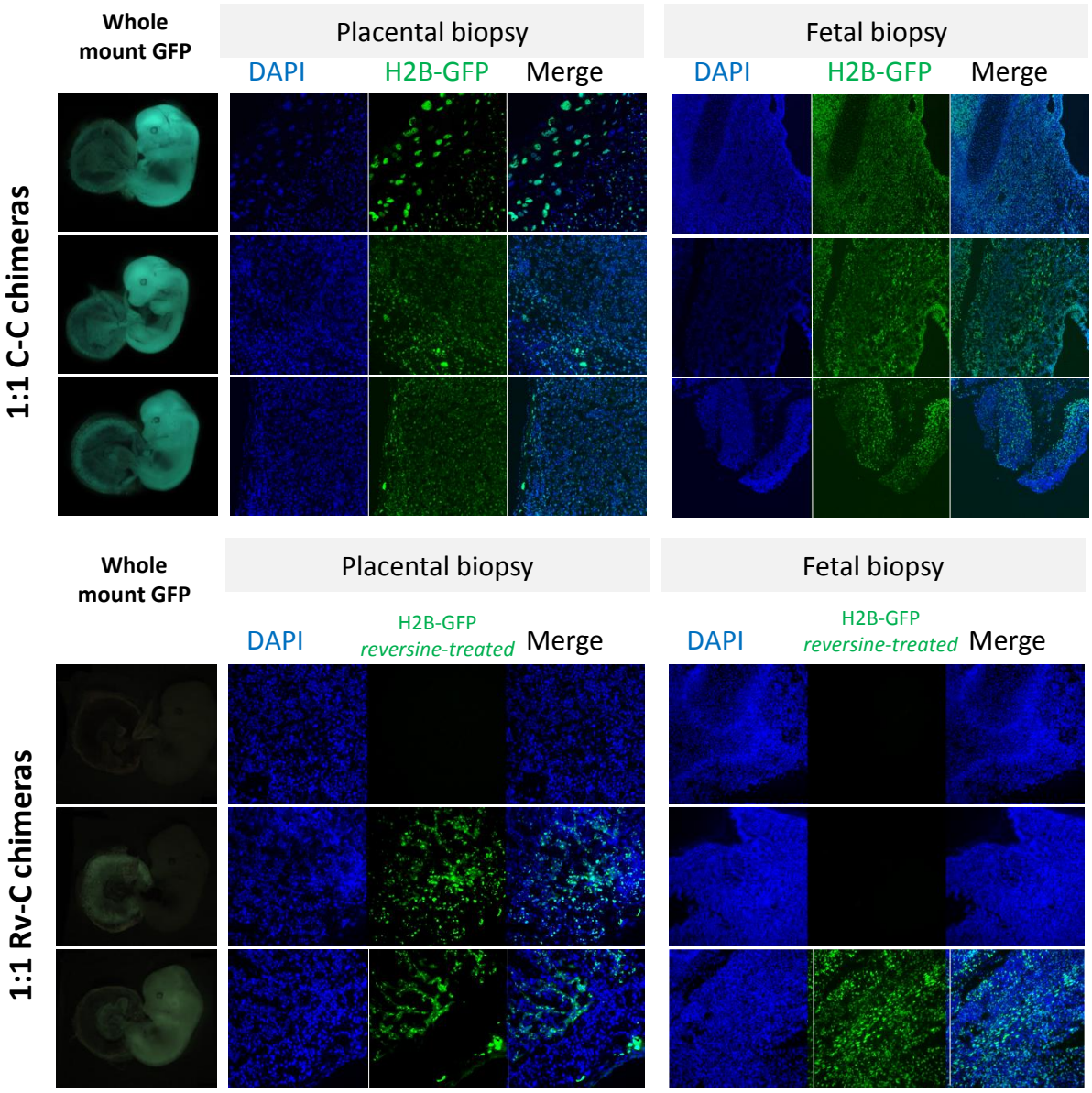

Figure 3.12 Whole mount GFP images with corresponding placental and fetal biopsies of E13.5 chimeras. Several placental and fetal biopsies were taken from each of the E13.5 conceptuses shown in Figure 3.11. Three representative images are shown for both control C-C (top panel) and Rv-C (bottom panel) chimeras. DAPI stained all nuclei from both clones, while H2B-GFP was restricted to the progeny of the four H2B-GFP blastomeres that constituted half of the chimera when constructed at the 8-cell stage (one half of the control blastomeres in C-C chimeras, and Rv-treated blastomeres in Rv-C chimeras). In all cases, where a histone-GFP clone was present, the cells were evenly distributed throughout the tissues. Both placental and fetal biopsy findings were consistent with the whole mount GFP images. These images illustrate that the biopsy results are reflective of the subjective assessment gained from the whole mount images.

In the Rv-C chimeras the control clone was derived from F1 blastomeres.

All images at 10x magnification

Early post-implantation recovery

Table 3.5

Whole embryos	Transferred	Viable	Non-viable
Reversine	40	0	20
Control	45	32	0

Table 3.6

1:1 Chimeras	Transferred	Viable	Non-viable
1:1 Rv-C chimeras	115	74	0
1:1 C-C chimeras	107	57	0

Table 3.7

3:1 Chimeras	Transferred	Viable	Non-viable
3:1 Rv-C chimeras	53	11	14
1:1 C-C chimeras	107	57	0

E13.5 recovery & live pups

Table 3.8

1:1 Chimeras	Transferred	Viable
1:1 Rv-C chimeras	84	44
1:1 C-C chimeras	34	20

Table 3.9

1:1 Rv-C Chimeras	Transferred	Recovered
Early post-implantation	115	74
E13.5	58	31
Live birth	26	13

Table 3.10

	H2B-GFP status:	Present	Absent
Fetus	1:1 Rv-C chimeras	3	6
	1:1 C-C chimeras	15	2
Placenta	1:1 Rv-C chimeras	4	5
	1:1 C-C chimeras	17	0

Tables 3.5 to 3.10. Tables summarising results of transfer experiments. Table 3.5. Peri-implantation recovery of whole reversine-treated embryos and controls (Fishers exact test; $p<0.0001$) **Table 3.6.** Early post-implantation recovery of 1:1 Rv-C chimeras compared with control chimeras (Fisher's exact test; $p=1.0$). **Table 3.7**. Early post-implantation recovery of 3:1 Rv-C chimeras compared with control chimeras (Fishers exact test; $p<0.0001$). **Table 3.8**. Combined E13.5 and live pups born with 1:1 Rv-C chimeras (χ^2 test; $p=0.73$). **Table 3.9.** The proportion of viable early post-implantation embryos recovered was equivalent to E13.5 and live birth rates (χ^2 test; $p=0.68$). **Table 3.10.** Presence of H2B-GFP clone within recovered E13.5 conceptuses.

healthy and well grown (day three mean weight=3.31g, SD=0.26g), and survived with no signs of ill health beyond four months of age. Subjective evaluation of coat fur was undertaken by an independent researcher (Charles-Etienne Dumeau), which also revealed significant depletion of the reversine-treated clone: 7 of 13 mice showed no evidence of the abnormal clone, and only 3 had a major contribution from both clones. Thus in the minority of embryos which contained progeny from reversine-treated clone, there was no evidence of adverse outcome.

Residual clones may represent reversine-treated progeny that did not acquire chromosome abnormalities as a result of reversine-treatment, progeny that self-corrected the error at the cellular level, or cells with abnormal chromosome constitution that remain viable. Indeed, in the previous chapter where the reversine-treated blastomeres were evaluated for aneuploidy either by using FISH or array-based molecular karyotyping, some blastomeres were identified to be euploid. Thus the presence of residual clones within some embryos was not unexpected.

3.3.5.3 1:1 Rv-C chimeras have significantly greater developmental potential than true 'half embryos'

Next an experiment was conducted to compare the developmental potential of 1:1 Rv-C chimeras to that of true 'half embryos', defined as embryos comprised of half the number of control blastomeres with no other cells. Half embryos were generated exactly as for 1:1 C-C chimeras at the 8-cell stage, except that they were only constructed from four rather than eight blastomeres. A total of 122 true half-embryos were transferred into recipient mothers and recovered at E13.5. Recovery yielded 14 embryos (11.5% of those transferred), which was significantly lower than the rate of 53.6% attained from the 1:1 Rv-C chimeras detailed above (χ^2 test, $p<<0.0001$).

Considering all post-implantation results together, it can be concluded that the embryonic lethality of reversine-treated embryos can be completely rescued provided there is a minimum number of control cells present in the embryo, and that development can proceed

even with a significant depletion or complete absence of the reversine-treated clone from the conceptus (Figure 3.13).

3.3.6 Summary of main results

In summary, the results described in this chapter have shown that blastomeres with a history of chromosome abnormalities become progressively depleted from the embryo during development. Depletion became apparent during the expansion of the blastocyst, as abnormal ICM cells underwent apoptosis more frequently, and outer TE cells exhibited more limited proliferation than normal cells. Abnormal embryos (reversine-treated) were able to implant and elicit a maternal decidual reaction, but underwent early post-implantation resorption. In contrast, mosaic embryos that contained a critical number of control blastomeres rescued the early post-implantation lethality. When early post-implantation rescue occurred, it was associated with restoration of full developmental potential.

The time-lapse imaging evaluation of the pre-implantation chimeras revealed that depletion of the abnormal clone begins during pre-implantation development, consequently resulting in fewer progenitors derived from the abnormal clone available to populate the post-implantation tissues. It follows that as development proceeds there will be an on-going reduction in the abnormal clone relative to the control clone as cells proliferate and embryo growth occurs. Additionally it is also possible that cells with residual abnormalities may become depleted further due to poorer proliferation of the abnormal clone or cell-cycle arrest. These findings are consistent with the clonal depletion hypothesis presented in the Introduction. There was no evidence of active segregation of the abnormal clone to the extra-embryonic lineages during pre-implantation development thus providing evidence against this hypothesis.

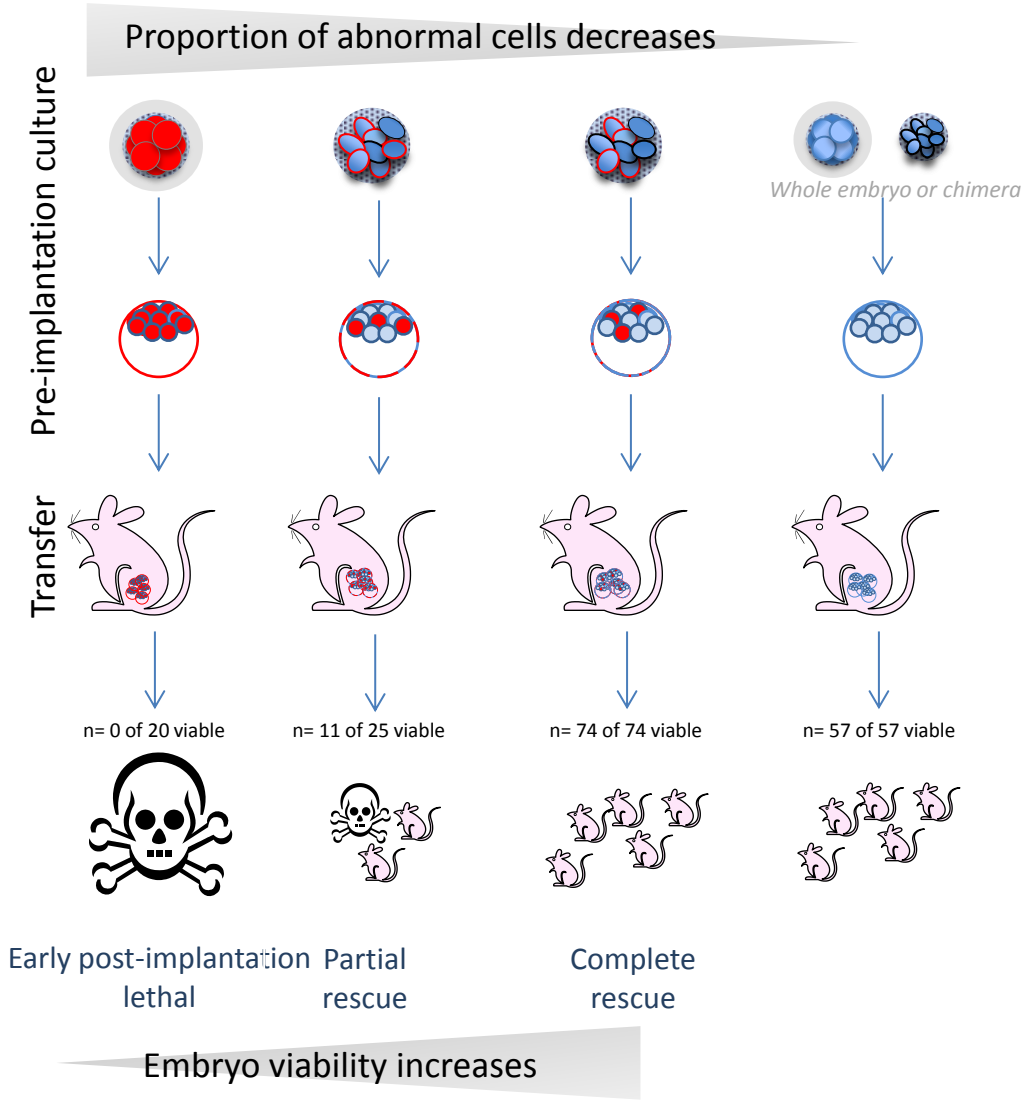

Figure 3.13 Summary of transfer experiments. Reversine-treated embryos were able to form blastocysts at an equivalent rate to controls but all failed to develop further at the early post-implantation stage. Increasing the proportion of control blastomeres partially rescued the lethal phenotype, with complete rescue when 50% was reached. Numbers shown in the figure represent the viability of early post-implantation embryos that had successfully implanted. Early post-implantation rescue resulted in complete rescue of developmental potential, with E13.5 and live birth rates equivalent to viability at the peri-implantation stage (χ^2 test; p=0.68). See Tables 3.5 to 3.10 for detailed summaries of numbers.

In this Figure red represents abnormal clones and blue represents control clones

3.4 RESULTS II DISCUSSION

The aim of the work presented in this chapter was to investigate the fate of abnormal cells within mosaic embryos and to investigate the ultimate fate of the embryo, using the mouse model of chromosome mosaicism developed in the previous chapter.

Abnormal embryos underwent morphologically normal pre-implantation development without evidence of blastomere fragmentation, increased rates of delay or abnormal cavitation. However, within the mosaic embryos abnormal cells were progressively depleted, mediated predominantly through effects on cell-cycle in the TE and increased rates of apoptosis within the ICM. There was no evidence of preferential allocation of abnormal cells to the TE lineage at the first fate decision. Abnormal embryos were unable to develop beyond implantation; however early post-implantation lethality could be completely rescued by increasing the proportion of control cells within the embryo. Viability rates at the early post-implantation stage were equivalent to later fetal and live-birth rates, with no apparent adverse effects on outcome.

3.4.1 The pre-implantation development of mosaic embryos

The first major aim of the experiments presented in this chapter was to investigate the fate of abnormal cells within the developing mosaic embryo. To achieve this goal this study utilized high resolution time-lapse imaging during pre-implantation development, enabling the behaviour and fate of every single cell within each embryo to be evaluated.

Although the experimental procedure did not enable the direct evaluation of the chromosome status in each blastomere, a comparative approach to analysis was adopted, on the basis that blastomeres with high rates of chromosome segregation errors would be expected to exhibit greater rates of chromosome abnormalities than their control counterparts. For this reason, in the few instances in which errors were identified in the control blastomeres, these were included in the same group as reversine-treated clone for the analysis. By using the comparative approach to analysis, it was likely that any small differences in characteristics between normal and abnormal blastomeres would not be detected, unless very large numbers of embryos were subject to analysis. However,

conversely any differences that were detected were more likely to be true differences between the groups.

Despite these limitations, this is the first study of its kind to adopt a live-imaging approach with the aim of determining the fate of abnormal blastomeres in real-time during pre-implantation development. This experimental approach would be difficult to achieve in human embryos as abnormal blastomeres would only be identifiable retrospectively and require a complex and technically challenging labelling regime. Further, a stable, non-toxic nuclear label would be required to enable cell tracking at the single cell level beyond embryo compaction. Here, the use of the transgenic H2B-GFP mouse line provided a bright, and stable nuclear reporter that enabled single cell tracking throughout a prolonged period of imaging; an embryological experimental technique currently exclusive to the mouse.

Thus, this is the first study to directly demonstrate the progressive depletion of abnormal cells from the pre-implantation embryo, and to establish that this occurs through differential mechanisms according to the cell lineage. ICM cells undergo apoptosis more frequently, while TE cells are more likely to exhibit effects on their cell-cycle length. This is also the first study to provide direct evidence that apoptosis within the ICM can occur as a mechanism to eliminate cells with chromosomal abnormalities; a hypothesis frequently proposed that until now has never been tested directly (Hardy, 1997, Pampfer and Donnay, 1999, Fabian et al., 2005). Finally, the novel application of time-lapse imaging enabled the first fate decision to be evaluated directly and found no evidence of preferential allocation of the abnormal cells to the TE lineage. Additional evidence against the preferential allocation hypothesis was gained later when viable conceptions were recovered at E13.5; in the minority of conceptions that contained cells arising from the abnormal clone, there was no evidence of enrichment within the placenta relative to the fetal tissues.

How do these findings fit with other studies and current hypotheses?

Observational studies on human pre-implantation embryos have shown that mosaicism peaks at the cleavage stage and although aneuploid cells are still present in the majority of blastocysts, the proportion of aneuploid cells is lower than at earlier stages of development

(Evsikov and Verlinsky, 1998, Clouston et al., 2002, Coonen et al., 2004, Santos et al., 2010, Johnson et al., 2010, Capalbo et al., 2012). The findings of progressive depletion of abnormal cells during blastocyst expansion observed in this study are therefore in agreement with these observational studies in human embryos.

This study found no direct evidence to support the hypothesis that abnormal cells are preferentially allocated to the TE lineage at the first fate decision. The time-lapse imaging approach offered the unique opportunity to evaluate this hypothesis directly by assessing the patterns of the cell-fate determining symmetric and asymmetric divisions, with no differences identified between the normal and abnormal clones. In addition, there was no significant depletion of the abnormal clone from the ICM lineage when evaluated at the early blastocyst stage, immediately following completion of the first cell-fate decision. These findings were in concordance with the published human studies that have investigated this hypothesis indirectly. Through the comparison of aneuploidy status and rates between the ICM and TE lineages within individual embryos, each of these observational studies found no evidence to support the preferential allocation to the TE lineage hypothesis (Evsikov and Verlinsky, 1998, Magli et al., 2000, Derhaag et al., 2003, Johnson et al., 2010, Northrop et al., 2010).

The preferential allocation of aneuploid cells to the TE lineage has been proposed as an underlying mechanism to explain the occurrence of confined placental mosaicism (see Introduction). However, it is worthwhile considering that rejection of the preferential allocation to the TE hypothesis does not exclude the possibility that CPM may arise as a consequence of events that occur during pre-implantation development. An alternative explanation could arise from the differential fates of aneuploid cells according to their lineage. In this study abnormal cells within the ICM were significantly more likely to undergo apoptosis than those within the TE. Apoptosis results in the complete elimination of that cell, and thus also any future progeny from the embryo. In contrast, abnormal TE cells rarely underwent apoptosis, but instead were more likely to arrest or have prolonged cell cycle lengths. Hence, abnormal TE cells often remained viable, albeit depleted relative to their normal counterparts. If some of these cells continue to proliferate, contributing progeny to the future placenta, it is reasonable to speculate that this could result in CPM in some cases.

As studies in human pre-implantation embryos are limited it is worthwhile reviewing these results in the context of other indirect model systems usually applied for the study of cancer, as discussed in sections 1.4 & 1.5 of the Introduction. Several mouse models of chromosomal instability (CIN) have been developed, either through the knockout of SAC components or key kinetochore proteins, and some have been evaluated at the pre-implantation stage of development (Kalitsis et al., 1998, Kalitsis et al., 2000, Howman et al., 2000, Dobles et al., 2000, Putkey et al., 2002, Wang et al., 2004a, Lightfoot et al., 2006, Iwanaga et al., 2007, Jeganathan et al., 2007). In these embryos the phenotype is most likely to arise as a direct consequence of chromosome abnormalities rather the direct effect of the gene knockdown, as discussed in the Introduction. Evaluation of the pre-implantation embryos found differences between the fates of TE and ICM lineages; blastocysts grown in extended culture *in vitro* showed cell death by apoptosis within the ICM lineage, in contrast to reduced but on-going viability within the TE cells (Mad2 (Dobles et al., 2000), Bub3 (Kalitsis et al., 2000), CenpA (Howman et al., 2000)). These features are strikingly complementary to the findings of this study, and suggest that chromosome abnormalities in ICM cells frequently result in apoptosis and that TE cells may be more tolerant of chromosome abnormalities, or respond by cell-cycle arrest and senescence rather than apoptosis. In addition to knockout mouse models of CIN, studies on cultured cell lines and MEFs also show that chromosome segregation errors and aneuploidies are strongly associated with poor proliferation and in some cases increase rates of apoptosis (Segal and McCoy, 1974, Baker et al., 2004, Burds et al., 2005, Thompson and Compton, 2008, Li et al., 2009). Therefore, the findings presented in this study are entirely consistent with the existing and relevant literature, as both apoptosis and poor proliferation are classic characteristics of chromosome abnormalities in a range of different model systems including mouse embryos and different cell culture lines.

A major finding of potential significance in this study was that whole embryos treated with reversine were able to undergo morphologically normal pre-implantation development to the blastocyst stage, without increased rates of arrest or abnormal morphology such as blastomere fragmentation or failure to cavitate. This result was not unexpected given that the appearance of the CIN mouse model embryos were also found to look normal prior to extended *in vitro* culture after hatching and attachment (Dobles et al., 2000, Kalitsis et al.,

2000, Howman et al., 2000), as were the vast majority of embryos in *Sycp3*$^{-/-}$ mosaic aneuploid blastocysts (Lightfoot et al., 2006). However, the potential significance of this morphologically normal phenotype is worthy of consideration in relation to the human pre-implantation embryo. Human pre-implantation embryos frequently arrest prior to the blastocyst stage, and often exhibit abnormal morphology including blastomere asymmetry and fragmentation. In striking contrast, these characteristics are rare in the mouse embryo, and nor did they occur on induction of chromosome abnormalities in this study or the others previously discussed. The relationship between human embryo morphology and chromosome status has been studied in some detail, and although a relationship does exist it appears to be weak (Wells, 2010). A normal chromosome complement does not always result in normal morphology or developmental potential, and likewise aneuploid embryos frequently undergo apparently normal development (Rubio et al., 2007, Magli et al., 2007, Munne et al., 2007, Eaton et al., 2009, Alfarawati et al., 2011). The finding that the mouse embryo is still able to undergo morphologically normal, unperturbed development, even in the presence of major chromosome abnormalities is thus worthy of consideration, and is suggestive that the high rates of arrest and fragmentation that are common in human embryos may possibly be a result of an additional underlying abnormality in the human embryo, rather than aneuploidy *per se*. Taking this one step further, it is interesting to speculate that although aneuploidy and chromosome abnormalities are detrimental to developmental potential in their own right, the occurrence of aneuploidy could in fact be secondary to an original underlying abnormality, as yet uncharacterised, that in itself is detrimental to future developmental potential, unrelated to aneuploidy.

3.4.2 The fate of tetraploid cells in pre-implantation development

A short series of experiments were conducted on tetraploid and diploid-tetraploid mosaic embryos. The experiments were carried out to determine if the characteristics of aneuploid-diploid and tetraploid- diploid mosaic embryos were comparable.

The results of these experiments showed that tetraploidy had no detrimental effect on pre-implantation development as assessed by morphology, relative cell number, and on the establishment and segregation of the first three lineages. Time-lapse imaging of the diploid-

tetraploid mosaic embryos revealed that in the presence of diploid cells, tetraploid blastomeres undergo more frequent symmetric divisions and are thus preferentially segregated to the TE lineage during the first fate decision. This finding is entirely in keeping with previous studies on fixed diploid-tetraploid chimeras which also showed that by the blastocyst stage tetraploid cells became relatively enriched within the TE lineage and depleted from the ICM lineage (Everett and West, 1996, Everett and West, 1998, Mackay and West, 2005). However, the utilization of time-lapse imaging and cell tracking in this study added to these findings by showing that the underlying mechanism was through the process of increased rates of symmetric divisions. In addition, this was the first study of its kind to assess the development of diploid-tetraploid mosaic embryos, rather than aggregation chimeras, and thus demonstrated that the phenotypes previously described were attributable to tetraploidy and not artefact caused by the generation of aggregation chimeras. It is acknowledged that tetraploid blastomeres are larger than their equivalent diploid counterparts as they are generated through the fusion of two blastomeres together; a difference which could potentially influence the pattern of cell division and thus the phenotype. However this hypothesis has previously been investigated directly in a study that generated large diploid blastomeres through the enucleation of single blastomere in a 2-cell stage embryo followed by electrofusion to create a single large blastomere (Tang et al., 2000). This technique enabled the influence of both ploidy and cell size to be investigated independently in a series of experiments, and it was shown that both increased cell size and tetraploidy are associated with a predominant allocation to the TE lineage independent of each other.

Analysis of whole tetraploid embryos at the blastocyst stage revealed no relative reduction in ICM number compared to control embryos, in contrast to the findings for the reversine-treated embryos. Thus it was considered unlikely that tetraploid cells undergo increased levels of apoptosis within the ICM compared to diploid cells.

The fact that tetraploid cells become restricted to the TE lineage by mid-gestation is already well established (Tarkowski et al., 1977, James et al., 1995, Goto et al., 2002, Viuff et al., 2002), and is widely exploited experimentally in tetraploid complementation experiments (Tam and Rossant, 2003). This characteristic has previously led to proposals that diploid-tetraploid embryos may serve as a representative mouse model for CPM (Wolstenholme,

1996, Mackay and West, 2005) a condition that affects 1-2% of pregnancies undergoing prenatal diagnostic tests for aneuploidy at the end of the first trimester (Ledbetter et al., 1992, Teshima et al., 1992, Hahnemann and Vejerslev, 1997, Stetten et al., 2004). Similarly, it has also been hypothesized that diploid-aneuploid mosaics embryos could be responsible for the development of CPM through the preferential allocation of aneuploid cells to the TE lineage at the first fate decision (Wolstenholme, 1996, Mackay and West, 2005, Robberecht et al., 2009, Mantikou et al., 2012). Comparing the results of diploid-tetraploid with diploid-aneuploid mosaics in this study revealed very different characteristics and fates for the abnormal cells; there was clear experimental evidence of preferential allocation of abnormal cells to the TE in the case of tetraploidy through the increased tendency to undergo symmetric divisions during the first cell-fate decision of pre-implantation development, with no such finding in the diploid-aneuploid model. In addition, given that the most frequent chromosome abnormalities observed in CPM are usually trisomies, and not tetraploidy (Ledbetter et al., 1992, Wolstenholme, 1996) it can be concluded that diploid-tetraploid mosaics are not a good model for CPM. Previous attempts at developing alternative trisomic models for CPM have been hampered by technical challenges, although a few chimeras containing trisomy 3 have been generated that when examined did not show any preferential confinement to the TE, providing further experimental evidence that the classic confined TE fate may be a phenomenon unique to tetraploid cells (Everett et al., 2007).

3.4.3 The peri- and post-implantation fate of diploid-aneuploid mosaic embryos

A major aim of the experiments presented in this study was to investigate the ultimate fate of diploid-aneuploid mosaic embryos. Therefore the post-implantation fates of these embryos were addressed by transferring experimental blastocysts into recipient female mice.

The transfer of whole reversine-treated embryos was universally embryonic lethal at the early post-implantation stage. Embryos underwent implantation at a slightly lower rate than control embryos, as assessed by the frequency of resorption sites identified following transfer. This finding was in line with most other models of pre-implantation mosaicism

secondary to knockout of essential SAC genes, key kinetochore proteins, or *Sycp3*$^{-/-}$ knockout (*Mad2*, (Dobles et al., 2000): *BubR1*, (Wang et al., 2004a); *Bub1* (Jeganathan et al., 2007); *Bub3*,(Kalitsis et al., 2000); *Mad1*, (Iwanaga et al., 2007), *Cenpe*, (Putkey et al., 2002); *Cenpc*, (Kalitsis et al., 1998); *Cenpa*, (Howman et al., 2000), *Sycp3*$^{-/-}$(Lightfoot et al., 2006). These homozygous null knockout mice all shared a universal phenotype of early post-implantation lethality, most likely a direct effect of chromosome missegregations arising secondary to the loss of gene function. The finding that reversine-treated embryos underwent the same fate was particularly interesting in light of the fact that reversine treatment induced a transient inhibition of the SAC during a single cleavage only, and that a functioning SAC was restored on wash-out of the drug. This result therefore offered further support for the hypothesis that the early post-implantation lethal phenotypes observed in the knockout mouse models were a direct result of chromosome segregation errors, and thus only an indirect consequence of the specific gene knockout itself.

In contrast, when the 1:1 Rv-C chimeras were transferred there was complete rescue of the early post-implantation lethality that occurred in the case of reversine-treated embryos alone. Implantation rates and viability were comparable to those in equivalent controls, with no evidence of increased resorption sites following transfer of the Rv-C embryos. At the early post-implantation stages of development, many embryos still contained a small proportion of reversine-treated progeny, but by E13.5 this was not the case in the majority of fetuses and their placenta. There was no evidence of increased apoptosis levels in the early post-implantation embryos, and thus the on-going depletion of the abnormal clone from the embryo may be more likely to be due to a dilutional effect arising as a result of fewer clonal progenitors, with the added possibility of poor proliferation within the abnormal clone.

When the proportion of control blastomeres was decreased and 3:1 Rv-C embryos were transferred, there was partial rescue of embryonic lethality with some embryos surviving and others undergoing resorption. In the case of the 1:1 Rv-C chimeras, a series of experiments were conducted to determine if viability at the early post-implantation stages translated into equivalent viability rates at the late fetal stage and birth, and indeed it was. From these experiments it was concluded that diploid-aneuploid mosaic embryos are likely to be viable provided there are a sufficient number or proportion of normal blastomeres

within the embryo, and that viability at the early post-implantation stage of development was predictive of survival to the fetal stages and live birth.

The finding that mosaic embryos can retain their developmental potential in the presence of a minimum number of normal blastomeres was not unexpected given the highly regulative nature of the mammalian embryo. It is well established in the mouse that in some cases half embryos (embryos containing half the normal number of cells) have the ability to develop into blastocysts and in some cases develop to term to produce apparently healthy offspring, albeit at a significantly lower rate than whole embryos (Tarkowski, 1959, Tsunoda and McLaren, 1983, Morris et al., 2012b). This finding was confirmed in the transfer experiments described above, where 11.5% of true half-embryos were found to be viable at E13.5. In contrast, it has not been possible to generate normal mice from one quarter or one eighth embryos (Tarkowski and Wroblewska, 1967, Rossant, 1976). The limited potential of some half embryos, and inability of quarter and eighth embryos to develop into viable offspring is most likely to be due to the low number of cells present within the embryo. Indeed, at the blastocyst stage half embryos contain fewer cells (as would be expected), but additionally there is a disproportionate decrease in cell number within the ICM lineage when compared to the TE (Papaioannou and Ebert, 1995, Morris et al., 2012b). Likewise, quarter and eighth embryos have been shown to develop into blastocysts with either very small or no ICM at all (trophoblastic vesicles) (Tarkowski and Wroblewska, 1967, Rossant, 1976). One recent study investigated the relationship between cell number and developmental potential of half embryos in greater detail (Morris et al., 2012b). More specifically, the number of EPI cells within the blastocyst (the progenitors of the future fetus) was correlated with the developmental potential and viability of the half embryo. This study found that a minimum of four EPI cells were required for the successful early post-implantation development and beyond. Boosting the number of EPI cells by treating the half embryos with 2i (a combination of two small molecule inhibitors that modulate the Fgf and Wnt signalling pathway) significantly improved the developmental potential of half embryos. In addition, other studies have successfully generated mice from individual blastomeres of 8-, 16- and even 32-cell stage blastomeres by aggregating them with carrier tetraploid cells (Tarkowski et al., 2005, Tarkowski et al., 2010), and although not tested directly it is probable that the

presence of the carrier tetraploid cells did increase the number of EPI cells derived from the single blastomeres, and thus conferring viability to the embryos.

The developmental potential of the 1:1 Rv:C embryos was equivalent to the 1:1 C:C controls, and thus significantly greater than half embryos comprising of a reduced number of cells, confirmed both in the experiments described above and in keeping with the literature (Tarkowski, 1959, Tsunoda and McLaren, 1983, Morris et al., 2012b). These results suggest that the presence of abnormal cells within the embryo may serve to improve embryo viability (compared to normal embryos with a reduced cell number) potentially by boosting the number of normal EPI cells within the ICM to the critical number required for on-going successful development. Thus abnormal cells could be considered as carrier cells whose presence increase the developmental potential of the normal cells within the embryo. Ultimately however, the developmental potential of each individual embryo is likely to rely upon the generation of inside cells through asymmetric divisions during the first cell-fate decision, followed by the allocation to the EPI lineage. Time-lapse imaging analysis of the mosaic model showed that there was no bias towards asymmetric divisions according to chromosome status. Thus the partial rescue of peri-embryonic lethality phenotype in 3:1 Rv:C chimeras, where some but not of all the embryos were viable is likely to be related to the specific developmental history of that embryo. For example, if the normal blastomere clone only underwent symmetric divisions then there would an insufficient number of normal EPI cells within the embryo for on-going development; likewise if normal blastomeres underwent asymmetric divisions and did not undergo apoptosis, the critical number of normal EPI cells would be reached resulting in a viable embryo with on-going developmental potential.

The hypothesis for a threshold proportion or number of normal blastomeres required for viability has been considered in the context of human pre-implantation development on many occasions (Evsikov and Verlinsky, 1998, Frumkin et al., 2008, Lavon et al., 2008, Barbash-Hazan et al., 2009, Mantikou et al., 2012). Although no such study to directly investigate this hypothesis has ever been, or is likely to be conducted on human embryos due to practical and ethical limitations, there is some indirect evidence that this may be the case; live births have been reported from human embryos that have lost up to half of their blastomeres following cryopreservation, albeit infrequently (Guerif et al., 2002). Further,

although there is no evidence to support this hypothesis, it is interesting to speculate if the role of carrier cells in maximising embryo viability may be an underlying reason why apoptosis rarely occurs before the blastocyst stage during pre-implantation development.

3.4.4 Limitations of the mouse model

The general suitability of the mouse model for this study was discussed in detail in section 2.4.4 of the previous chapter. However this topic warrants a brief further discussion in context of the results presented in this chapter.

Until an additional model of mosaicism is developed the findings of this study should be viewed with the caveat that the phenotype may be secondary to the treatment with reversine, rather due to chromosome errors *per se*. Reversine is a 2,6-disubstituted purine, and a small molecule inhibitor of the key SAC protein Mps1, an effect that was utilized in this study to induce chromosome segregation errors (Santaguida et al., 2010). However, additional effects of reversine, unrelated to Mps1 inhibition have been characterised. Reversine was originally described in the context of myoblasts, where prolonged incubation in 5μM of reversine induced dedifferentiation of C2C12 myoblasts into multipotent progenitor cells (Chen et al., 2004). Subsequently, the same group published a similar study showing the effects of reversine on myoblasts at a concentration as low as 0.02μM, potentially mediated through its effects on non-muscle Myosin II (NMMII), MEK1 and phosphatidyl-inositol 3-kinase (PI3K) (Chen et al., 2007). Reversine has also been shown to inhibit Aurora B, however only at much higher concentrations than required for Mps1 inhibition (5μM, ten times the concentration used in this study) (Santaguida et al., 2010). This same study also demonstrated that reversine did not inhibit MEK1, NMMII or PIK3 during mitosis and concluded that chromosome segregation errors were secondary to Mps1 inhibition at low concentrations of the drug. Although it is clear that treatment with reversine has the potential to exert additional indirect effects, steps were taken in this study to minimise this possibility by using the lowest effective concentration required for Mps1 inhibition (0.5μM) and for the shortest possible duration to cover the period of mitosis. The immediate reversibility of the drug on washout from the culture media was advantageous in minimising the potential for unwanted effects.

In context of the critical cell number threshold hypothesis it is of worth noting that the mouse embryo is somewhat different than other mammalian embryos. In the rabbit, cow and sheep it is possible to generate live animals from single blastomeres at the 4- and 8- cell stage (Moore et al., 1968, Willadsen, 1981, Willadsen and Polge, 1981). In contrast, in the mouse only single blastomeres from the 2-cell stage have the potential to develop into a normal animal, and not 4- or 8- cell stage onwards in the absence of carrier cells (Tarkowski, 1959, Tarkowski and Wroblewska, 1967, Rossant, 1976, Tsunoda and McLaren, 1983). A key difference between the mouse and these other mammalian embryos is the timing of implantation; mice embryos attach and implant approximately 24 hours following blastocyst formation, in contrast to rabbits which implant at day six (Fischer et al., 2012), and cattle (including sheep and cow) which attach two to three weeks following blastocyst formation (Spencer et al., 2004, Oron and Ivanova, 2012). Although differences between each mammalian species are complex, it is worthwhile noting that a major difference between the mouse and these other species is that the number of cells within the blastocyst at the time of normal implantation is considerably lower. It is interesting to speculate whether human embryos might share more similarities with the non-murine embryo given that the human embryo implants at around day seven onwards. If so, it may be that the threshold number of cells required for viability in human embryos could be even lower than that in the mouse.

Although the limitations of this model are acknowledged, the results of the experiments presented in this chapter are nonetheless important, as this is the first study of its kind to attempt to directly address the developmental fate of mosaic embryos in mammalian development. The results were in keeping with both observational studies in human embryos, and also with fate of aneuploid cells in other systems.

If the results of these experiments are directly relevant to the human IVF embryo, several points merit discussion. The finding that embryos maintained normal morphology and were able to develop into blastocysts despite undergoing chromosome segregation errors raises the question of whether aneuploidy in human embryos is a secondary effect of a different underlying abnormality, rather than the primary cause of a poor developmental outcome. If this is indeed the case, this may require a re-evaluation of the significance of aneuploidy in the context of human IVF embryos; although it is likely that high levels of aneuploidy will be

associated with poor clinical outcome. This hypothesis merits further research, and most likely in the human embryo in the first instance. In addition, the rescue of early post-implantation lethality by the presence of normal blastomeres within the embryo demonstrates that some mosaic embryos do have the potential to develop into on-going viable pregnancies. Further, if it is so that the presence of abnormal cells may maximise the developmental potential of mosaic embryos by acting as carrier cells, this finding could provide an additional explanation as to why cleavage stage embryo biopsy for PGS can in some cases have a detrimental impact upon IVF outcomes. When considered together with the finding that abnormal cells become depleted during blastocyst cavity expansion, and not earlier, the results of this study provide further support for the more recent approaches to PGS; that is a shift away from cleavage stage biopsy to TE blastocyst biopsy. Theoretically this approach offers several advantages over cleavage stage biopsy. By definition, TE biopsy pre-selects embryos that have successfully developed to the blastocyst stage. Additionally it allows for several cells to be removed without significantly altering the constitution of the underlying embryo. In addition, the depletion of the abnormal cells by the blastocyst stage relative to cleavage stage biopsy minimises the potential influence of mosaicism. Although TE biopsy does not evaluate progenitors of the future fetal lineage, the results of this study together with observational data in human embryos, have not demonstrated any evidence that abnormal cells are preferentially allocated to the TE lineage. However until large, well-conducted clinical trials are undertaken whether these theoretical advantages are borne out in clinical practice, or will improve IVF outcomes is not known.

The results presented in this chapter have provided the first direct evidence that blastomeres with chromosome abnormalities can be eliminated or depleted from a mosaic embryo as development proceeds, thus supporting the clonal normalisation hypothesis presented in the Introduction. The underlying mechanisms responsible for the elimination or depletion of these abnormal cells are the subject of investigation in the following chapter.

INVESTIGATING THE MECHANISMS UNDERLYING THE ELIMINATION OF BLASTOMERES WITH CHROMOSOMAL ABNORMALITIES

4.1 INTRODUCTION TO RESULTS III

The results in the previous chapter established that the acquisition of acute chromosome segregation errors during early pre-implantation development was associated with the depletion or elimination of the abnormal clone of cells from the embryo in the majority of cases. The primary aim of this chapter was to investigate the underlying mechanisms potentially responsible for the elimination or depletion of these cells. The experiments were conducted in pre-implantation embryos, because although the majority of depletion occurred at the peri- and early post-implantation stages of development, these embryos are not readily accessible for study.

As discussed in the Introduction, aneuploidy and the consequences of chromosome segregation errors are most widely studied in the context of cancer research. Recent work has shown that both acutely arising and chronic aneuploidies can adversely affect cellular physiology and result in poor proliferation, cell cycle arrest, senescence and apoptosis (Torres et al., 2007, Williams et al., 2008, Thompson and Compton, 2008, Li et al., 2009, Li et al., 2010, Thompson and Compton, 2010, Pfau and Amon, 2012).

Although these studies were not conducted in pre-implantation embryos, it is reasonable to speculate that the adverse effects on cellular physiology might also occur in embryos affected by chromosome missegregation and aneuploidy. Indeed, the results presented in the previous chapter demonstrated similar outcomes of increased levels of apoptosis and poor proliferation in cells following acute chromosome missegregation.

A recent body of work undertaken on yeast cells and MEFs harbouring chronic aneuploidies described of a set of shared phenotypes described as the ‘aneuploidy stress response’, characterised by defects in cell growth and altered metabolism (Torres et al., 2007, Williams et al., 2008, Torres et al., 2010). The increased energy and metabolic demands characteristic of the aneuploidy stress response may result in the production of elevated levels of reactive

oxygen species (ROS) which may activate the p53 pathway resulting in poor proliferation, cell-cycle arrest and apoptosis (Li et al., 2010).

In the pre-implantation embryo the 'quiet embryo hypothesis' proposes that viable embryos have a lower metabolism than those which arrest (and therefore more likely to be abnormal) based on data from metabolic experiments undertaken in human and mouse embryos (Leese, 2002). This hypothesis speculates that less viable embryos consume greater quantities of nutrients resulting from molecular or cellular damage, and have higher energy requirements due to additional cellular processes required for repair, compensation or apoptosis (Leese et al., 2008). It is possible that this may be applicable to embryos with high rates of aneuploidy, similar to the 'aneuploidy stress response' described above.

In addition to potential metabolic consequences of aneuploidy, it is also possible that the reduced viability of acutely arising aneuploid clones may be a direct result of the effects of acute chromosome missegregation itself; an effect mediated through double-stranded DNA (dsDNA) damage. Several recent publications have shown a link between whole chromosome missegregation and dsDNA breaks, although the proposed mechanisms underlying the DNA damage differ between studies (Quignon et al., 2007, Dalton et al., 2007, Guerrero et al., 2010, Janssen et al., 2011, Crasta et al., 2012). Both prolonged mitoses and abnormal kinetochore-microtubule attachments at the mitotic spindle (so-called merotelic chromosome attachments) have been associated with the acquisition of dsDNA breaks during cell division (Quignon et al., 2007, Dalton et al., 2007, Guerrero et al., 2010), although neither mechanism is likely to occur as a consequence of bypass of the SAC. However, two recent studies have identified additional mechanisms underlying the acquisition of dsDNA damage which may be of direct relevance to acutely arising segregation errors secondary to abrogation of the SAC (Janssen et al., 2011, Crasta et al., 2012). Jannsen *et al*. induced chromosome segregation errors in several mammalian cell culture lines and found that daughter cells exhibited increased levels of dsDNA damage, acquired during cytokinesis as a consequence of cleavage furrow-generated forces. In a similar study Crasta *et al.* showed that whole chromosome segregation errors were also associated with dsDNA damage (Crasta et al., 2012). However in this study the damage was confined to the resulting micronuclei and not the primary nucleus of the cell, arising as a consequence of defective and asynchronous replication of the chromatin trapped within the

micronucleus. Despite their differences, both studies also identified an increased rate of structural chromosome aberrations in addition to the experimentally-induced whole chromosome aneuploidy. These structural aberrations were speculated to arise secondary to repair of the dsDNA breaks that occurred during chromosome missegregation through incorrect re-ligation of broken chromosomes (Janssen et al., 2011, Crasta et al., 2012). *Crasta et al.* proposed that their findings may account for the recently described phenomenon of chromothripsis, whereby a cellular event results in the fragmentation of a single chromosome that is then reassembled, resulting in extensive intra-chromosomal rearrangements (Stephens et al., 2011).

This recent link between acutely arising whole chromosome aneuploidy and the acquisition of structural chromosomal rearrangements is remarkable. By acquiring DNA breaks as a consequence of missegregation the damaged chromosomes may become reincorporated together, in some cases resulting in extensive chromosome rearrangements. These finding are of particular significance in the context of cancer biology, as this may be a mechanism by which tumorigenic genetic mutations are acquired. Could this phenomenon also be relevant if viewed in context of the human pre-implantation embryo? The recent application of high resolution single-cell array-based karyotyping techniques in blastomeres suggests that it might; in addition to whole chromosome aneuploidy, structural chromosome aberrations are now being reported - abnormalities that may previously have gone undetected due to the technical limitations of FISH (Vanneste et al., 2009, Johnson et al., 2010, Rabinowitz et al., 2012). Therefore a major aim of this chapter was to investigate whether chromosome segregation errors arising during pre-implantation development were associated with significant DNA damage.

DNA damage results in the activation of the DNA damage response (DDR), an intricate network of pathways that orchestrate the cellular response in order to protect genomic integrity. Owing to its complexity, a detailed overview of the DDR pathway and its components is not within the remit of this study, and it has been the subject of a number of recent reviews (Bartek and Lukas, 2007, Jackson and Bartek, 2009, Bekker-Jensen and Mailand, 2010, Ciccia and Elledge, 2010, Thompson, 2012). In brief, dsDNA breaks elicit the localisation of DDR factors to the site of damage and trigger a signalling cascade to activate checkpoints to arrest the cell-cycle while the DNA is repaired. The degree of damage

determines the ultimate outcome; if the DNA can be repaired successfully the cell can progress to the next cell-cycle following transient cell-cycle arrest, however if the damage is severe and cannot be repaired, chronic DDR signalling triggers either cell death by apoptosis or cellular senescence (a state of permanent cell-cycle arrest). Indeed, the results in the previous chapter found that both apoptosis and prolonged cell-cycle lengths occurred more frequently in blastomeres with a history of chromosome missegregation during pre-implantation development. Thus it is plausible that underlying DNA damage could be responsible for the phenotype; a hypothesis that was tested and is reported in this thesis chapter.

For this study it was necessary to detect the presence of dsDNA breaks in blastomeres and confirm activation of the DDR pathway. The presence of a single dsDNA break results in the instantaneous activation of the DDR pathway resulting in immediate chromatin modifications flanking the site of damage, together with rapid accumulation of DDR proteins resulting in the formation of so-called ionizing radiation-induced foci (IRIF). Such foci can be detected by immunofluorescence (IF) enabling the presence of dsDNA damage to be readily identified and quantified. The phosphorylation of the histone H2A variant X at serine residue 139 (known as γH2AX) is the first event in the DDR pathway hierarchy (Bartek and Lukas, 2007). The γH2AX foci provide a high-affinity platform for the mediator of DNA damage-checkpoint protein 1 (MDC1), forming MDC1 foci. MDC1 foci orchestrate the recruitment of all other downstream IRIF-associated factors to the site of damaged chromatin. Other recruited factors that form localised foci include the MRN complex (Mre-11-Rad50-Nbs1), 53BP1 (tumour protein p53 binding protein 1), RNF8 (ring finger protein 8) and BRCA1 (breast cancer 1) amongst others (Bartek and Lukas, 2007). Therefore multiple IRIF-forming proteins are potential candidates suitable for the detection of dsDNA damage. Further evidence for activation of the DDR pathway can be acquired by confirming the activation of cell-cycle arrest; a main purpose of the DDR is the activation of cell-cycle arrest via the activation of checkpoint kinases (Jackson and Bartek, 2009).

Overall, it is likely that a variety of different mechanisms collectively contribute to the depletion of the abnormal clone of cells from the developing embryo. The various mechanisms proposed are summarised in Figure 4.1**.** The major aim of this chapter was to investigate the potential role of these mechanisms in the fate of the aneuploid cell in the

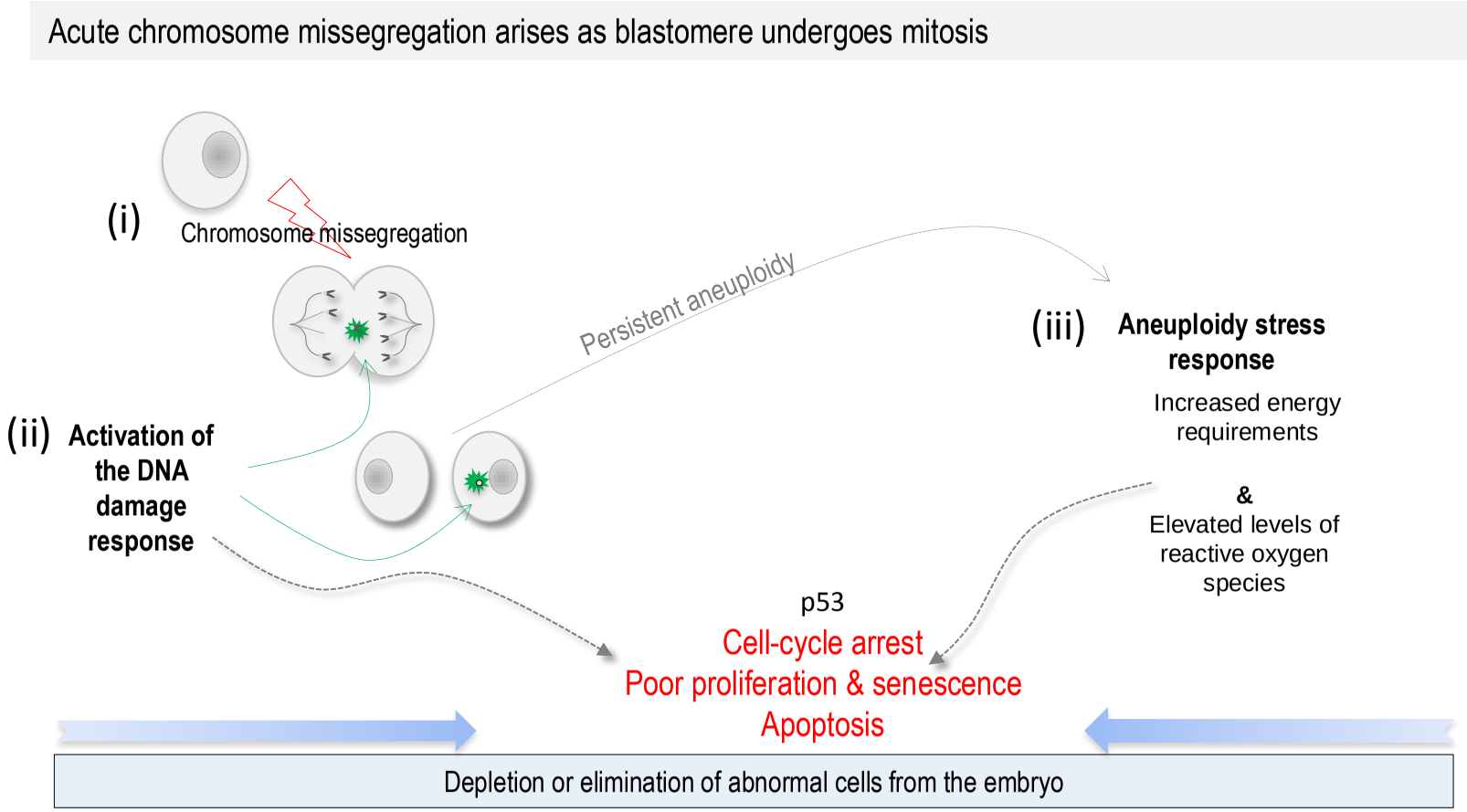

Figure 4.1. Potential mechanisms to account for the depletion of abnormal clones from the developing embryo. **(i)** On mitosis, acute chromosome missegregation may result in aneuploidy in daughter cells and in some cases the formation of a whole-chromosome containing micronucleus. **(ii)** Whole chromosome missegregation has been associated with the acquisition of double-stranded DNA damage through different mechanisms (✸ see section 4.1) which may activate the DNA damage response (DDR). The DDR can result in cell-cycle arrest, senescence or apoptosis, depending upon the degree of damage and cellular response, mediated through the p53 pathway. **(iii)** Cells which acquire persistent aneuploidy secondary to chromosome missegregation may also exhibit characteristics of the aneuploidy stress response, such as increased energy requirements and elevated reactive oxygen species. These effects may accumulate during on-going development and ultimately result in poor proliferation, cell cycle arrest and in some cases apoptosis. These effects may be mediated through DNA damage-independent activation of the p53 pathway (see section 4.4).

pre-implantation embryo. Additionally, a series of experiments investigating other potential causes of apoptosis within the ICM is presented, given that apoptosis was found to occur in 20% of control ICM blastomeres in the previous chapter.

4.2 MATERIALS AND METHODS

4.2.1 Pre-implantation embryo collection, culture & treatment with reversine

As described in the previous chapter.

4.2.2 Evaluation of oxidative stress using CellROX ® Deep Red reagent

CellROX® Deep Red (Invitrogen) reagent was used to compare levels of ROS between different groups of embryos. For each experiment CellROX was used from a fresh unopened vial and care taken to minimise its exposure to light or air to prevent any potential oxidation prior to the experiment. When comparing groups of embryos, each group was processed simultaneously and expediently to minimise the influence of any potential environmental factors. CellROX was used at a working concentration of 5μM diluted in M2 medium. Embryos were washed through three drops of CellROX and incubated in a final drop for 30 minutes at 37^{o}C for 30 minutes, in the dark. Embryos were then washed through fresh drops of M2 media and placed into a glass-bottomed dish (Matek) and imaged immediately using an Olympus FV1000 inverted confocal microscope. Embryos were imaged for Deep Red fluorescence (peak emission/excitation wavelengths 640/655 nm respectively) in groups in a single plane with a 20x air objective. Fluorescent intensity measurements for each embryo were evaluated using FIJI software.

Positive control embryos were incubated in 100μM hydrogen peroxide (H_2O_2) (Sigma) diluted in M2 for one hour and then washed through M2 drops immediately prior to incubation in CellROX.

4.2.3 Culture in low-energy KSOM

For the low-energy KSOM experiments a modified KSOM media was prepared. The constituents are presented in Table 4.1, alongside the standard control KSOM recipe. For cell counting, embryos were fixed in 4% PFA, stained with DAPI and imaged on a Leica SP5 inverted confocal microscope. Images were analysed for cell numbers using FIJI software.

4.2.4 Immunocytochemistry, TUNEL staining & confocal imaging

Immunocytochemistry and TUNEL staining was carried out as described in section 3.2 of the previous chapter. Mouse embryonic fibroblasts (MEFs) for antibody testing were obtained ready in culture from Dr Krzysztof Wicher.

In this chapter the primary antibodies used together with their dilutions were as follows: γH2AX mouse monoclonal 1:250 (Millipore), 53Bp1 rabbit polyclonal 1:500 (Novus Biologicals), Mdc1 rabbit polyclonal 1:1000 (custom antibody, a gift from Steve Jackson's laboratory, Gurdon Institute), H4K20me2 rabbit polyclonal 1:250 (gift from Steve Jackson's lab), β-tubulin 1:250 (a gift from Krzysztof Wicher), mouse monoclonal Cdx2 1:200 (BioGenex), rabbit polyclonal activated caspase-3 1:200 (Millipore). All secondary antibodies were AlexaFluor Dye conjugates (Invitrogen) and used at a concentration of 1:500.

Confocal images were captured using a Leica SP5 confocal microscope through a 40x oil objective into LAS AF software. Where DDR foci were to be quantified all imaging was undertaken during the same confocal session using identical imaging parameters in the same z-plane. Foci analysis was undertaken using a custom-designed plugin in FIJI.

4.2.5 Induction of DNA damage with ionizing radiation (IR)

Irradiation induced DNA damage was performed with a Faxitron X-ray machine (Faxitron X-ray Corporation) as per the manufacturer's instruction. Embryos or cells were fixed in 4% PFA two hours following ionizing radiation (IR) unless otherwise stated.

4.2.6 Time-lapse imaging and analysis

Time-lapse movies were generated using a spinning disk confocal microscopy system (Axiovert Observer Z1, Carl Zeiss, Inc.) as described in the previous chapter. For these movies embryos were imaged using a 20x air objective, in 20 Z-planes at 3μM increments, in GFP and brightfield channels every 15 minutes for 24 hours. Movies were analysed using SimiBiocell software.

4.2.7 Drug treatment to inhibit apoptosis

To inhibit apoptosis embryos were incubated in 200μM of the pan-caspase inhibitor ZVAD (R&D systems) dissolved in KSOM. Once ZVAD treatment was initiated, every subsequent step of the experiments were conducted in the presence of ZVAD until the point at which the embryos were fixed in PFA. ZVAD was reconstituted in DMSO, and all control embryos were incubated in an equivalent concentration of DMSO (0.01%).

4.2.8 Statistical analysis

Statistical analysis was carried out as described in the Results I and Results II as appropriate. Calculations were carried out in GraphPad or Microsoft Excel software.

	Standard KSOM	Low-energy KSOM
NaCl	95	95
KCl	2.5	2.5
KH_2PO_4	0.35	0.35
$MgSO_4$-$7H_2O$	0.2	0.2
Na lactate	10	10
$NaHCO_3$	25	25
$CaCl_2$-$2H_2O$	1.71	1.71
D-Glucose	55	20
Na pyruvate	0.2	0.2
EDTA	0.01	0.01
L-Glutamine	1	-
BSA	1.0g/L	1.0g/L
EAA	*at* 1x *conc.*	-
NEAA	*at* 1x *conc.*	-

Table 4.1 The chemical composition of standard (control) and low-energy KSOM media. Concentrations are given in mM unless otherwise stated. All components were acquired from Sigma, with the exception of EAA and NEAA which were acquired from Invitrogen.

4.3 RESULTS III

The main aim of the work presented in this chapter was to investigate the potential mechanisms underlying the depletion or elimination of chromosomally abnormal cells during embryo development. Unless otherwise stated, whole embryos treated with reversine during the 4- to 8- cell stage were used as a model for chromosome missegregation and were compared directly to equivalent whole control embryos.

4.3.1 Oxidative stress levels are equivalent between control and reversine-treated embryos during pre-implantation development

Cells with both chronic and acutely arising aneuploidies have been shown to exhibit elevated levels of oxidative stress in comparison to euploid cells, and this has been proposed as a mechanism underlying the reduced cellular fitness of aneuploid cells (Li et al. 2010). To investigate if this could also be the case in pre-implantation oxidative stress levels were evaluated in blastocysts by using CellROX® Deep Red reagent (Invitrogen) to evaluate ROS levels. CellROX is a cell-permeable fluorogenic probe designed to assay ROS in live cells. It is non-fluorescent while in the reduced state and becomes brightly fluorescent upon oxidation. The resulting fluorescence can be detected using microscopy, quantified, and used to compare the relative levels of ROS between different cells or embryos. The reagent and protocol were first tested in two groups of early blastocysts; controls and embryos treated with H_2O_2. Embryos were cultured in CellROX or DMSO (vehicle) followed by immediate imaging. Deep Red signal was clearly detectable in all CellROX-treated embryos with stronger signal intensity in embryos incubated in H_2O_2, with no discernible signal detected in any embryos incubated in DMSO rather than CellROX, even after adjustment of imaging parameters to maximise signal detection (Figure 4.2A). With the protocol optimised, ROS levels were then compared between control and reversine-treated embryos.

First embryos were assessed at the early blastocyst stage. ROS levels were assayed by evaluating fluorescent-signal intensity in three groups of embryos all treated simultaneously: controls, reversine-treated embryos, and embryos treated with H_2O_2 as a positive control. There were no significant differences in signal intensity, and thus

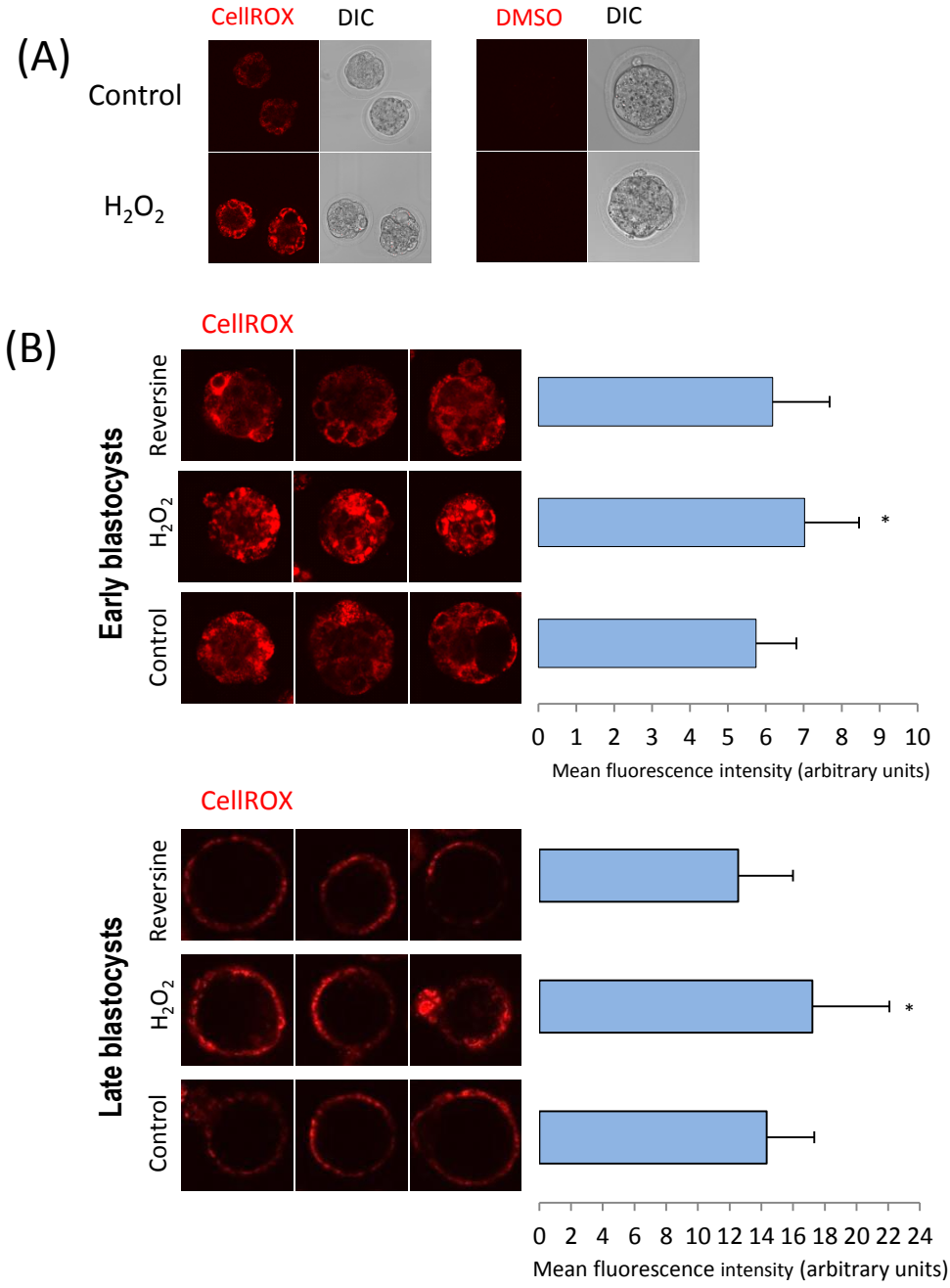

Figure 4.2 Evaluating reactive oxygen species (ROS) levels using CellROX dye in embryos (A) Testing CellROX® Deep Red in early blastocysts. Control and H_2O_2-treated embryos were incubated in CellROX or DMSO and imaged using identical parameters. Minimal signal was detected in DMSO controls. In contrast, signal was detectable in control embryos and bright in H_2O_2 positive controls **(B)** Evaluation of ROS levels in early and late blastocysts using CellROX. Representative images of example embryos in each group are shown in the panels, alongside the graphical representation of combined mean intensity levels for all embryos in each group. Error bars = SD. At both developmental stages there were no significant differences ROS levels between control and reversine-treated embryos (Student's t-test *$p<0.05$ for early and late blastocysts respectively; positive H_2O_2 controls were compared directly to control embryos).

All images at 20x magnification

measurable ROS levels, between control and reversine-treated embryos (Student's t-test, p=0.41, n= 14 control and 10 reversine-treated embryos respectively) (Figure 4.2B). As expected ROS levels were significantly higher in embryos treated with H_2O_2 compared to control embryos (Student's t-test; p=0.02, n=9 embryos). Thus there was no evidence of increased oxidative stress in reversine-treated embryos at the early blastocyst stage.

These experiments were then repeated at the expanded blastocyst stage (E4.5), by which time differences in cell numbers between reversine-treated and control embryos were already apparent (Results II). Similarly to the early blastocyst stage there were no significant differences in signal intensity, and thus measurable ROS levels, between control and reversine-treated embryos (Student's t-test; p=0.18, n= 12 control and 13 reversine-treated embryos respectively). The H_2O_2 positive control embryos showed significantly higher signal intensity than control embryos, as expected (Student's t-test; p=0.04 n=15) (Figure 4.2B).

Thus, using CellROX as an assay, there were no detectable differences in oxidative stress levels between control and reversine-treated embryos at the early and late blastocyst stages of development.

4.3.2 Pre-implantation development of reversine-treated embryos is more sensitive to adverse culture conditions

Studies in aneuploid MEFs and budding yeast cells have demonstrated altered metabolic properties relative to euploid controls such as increased energy consumption and perturbations in amino acid metabolism (Torres et al., 2007, Williams et al., 2008).

Detailed functional study of metabolism in pre-implantation embryos is technically challenging without specialist equipment. Experimental techniques used in cultured cell lines may not be suitable or require specialist adaptation due to the small number of cells within the embryo. Therefore, the potential differences in energy metabolism between embryos were investigated indirectly by comparing the development of embryos cultured in different culture media. The optimal culture media composition for mouse pre-implantation development has evolved over many years since the first embryos were cultured by Whitten in the mid-1950s (Whitten, 1956). Currently KSOM media supplemented with amino acids

(AA) is considered to be suitable for the culture of most, if not all mouse pre-implantation embryos (Nagy et al., 2003). Accordingly, all embryos in this thesis were cultured in this standard KSOM medium (see Table 4.1), and for the purposes of this experiment will be referred to as standard KSOM.

To determine if reversine-treated embryos had greater energy demands than controls, a modified low-energy KSOM was devised. The constituents of the low-energy KSOM were identical to standard KSOM with the following exceptions: the glucose concentration was lower at 20mM compared to 55mM in control KSOM, and there was also no supplementation with L-glutamine, essential or non-essential amino acids (EAA or NEAA). The composition of both KSOM formulations is summarised in Table 4.1. Groups of control and reversine-treated embryos were cultured in either standard or low energy KSOM from the early 8-cell stage onwards. Embryos were then fixed at the early and expanded blastocyst stage and cell number evaluated following confocal imaging. The potential effect of the low-energy KSOM on embryo development was evaluated by comparing the mean cell number in embryos cultured in low energy KSOM, given as a relative proportion to the cell number in their matched controls that had been cultured in standard KSOM ($^{\text{cell number in low-energy KSOM}}/_{\text{cell number in standard KSOM}}$).

When assessed at the early blastocyst stage there were no significant differences in cell number between standard KSOM and low-energy KSOM-cultured embryos in either DMSO-treated control or reversine-treated embryo groups (Student's t-tests: Control embryos $^{\text{low energy}}/_{\text{standard KSOM}}$ =1.03, p=0.11, n= 12 embryos in each group; reversine-incubated embryos $^{\text{low energy}}/_{\text{standard KSOM}}$ =0.95, p=0.46, n=13 and 14 embryos respectively) (Figure 4.3A).

However, when evaluated at the expanded blastocyst stage, there was a significant decrease by 14% in total cell number in reversine-treated embryos incubated in low-energy KSOM, relative to standard KSOM (Student's t-test; p=0.0097, n=19 and 20 embryos in standard KSOM and low-energy KSOM groups respectively) (Figure 4.3B). Within the TE lineage the relative depletion was 8% and not statistically significant (p=0.21). However within the ICM the depletion was greater with 27% depletion, which was highly significant (p=0.002). In contrast, this effect did not occur in the DMSO-treated control embryos. Control embryos incubated in low-energy KSOM did not show any significant depletion in

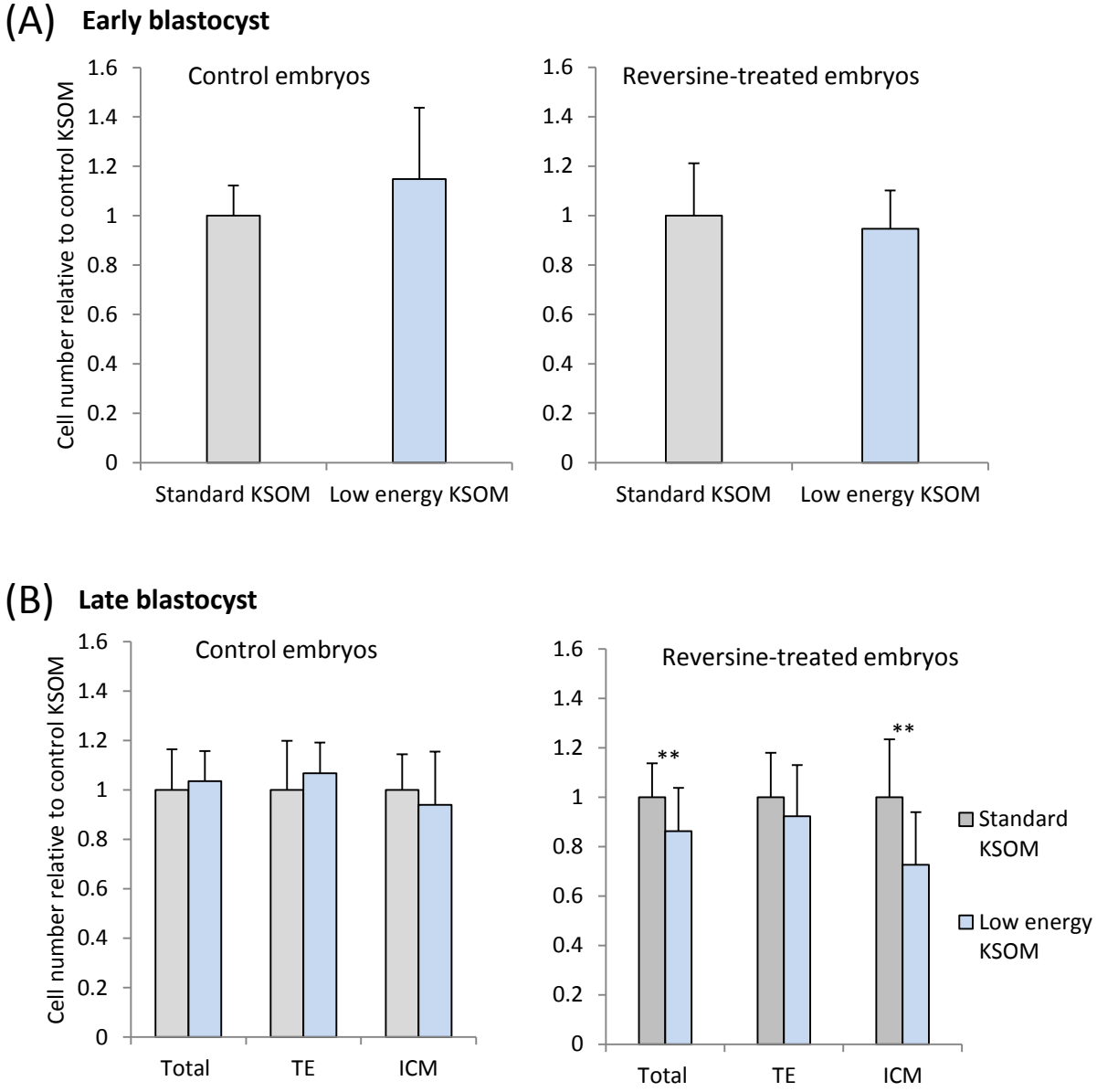

Figure 4.3 Effect of composition of culture media on cell number in developing embryos. Embryos were cultured in standard KSOM media, or modified low energy KSOM (see main text for further details). DMSO-treated control and reversine-treated embryos were assessed for cell number at early and late blastocyst stage. Error bars=SD **(A)** At the early blastocyst stage there were no significant differences in cell numbers between control and low energy KSOM cultured embryos in both control and reversine-treated embryos (Student's t-test; p=n/s). **(B)** At the late blastocyst stage, DMSO-treated control embryos had equivalent cell numbers in both culture media (Student's t-test; p=n/s), however in the reversine-treated embryos the total number of cells in embryos cultured in low energy KSOM relative to control KSOM dropped significantly by 14%. Cell numbers were depleted in both the TE and ICM lineages, but the depletion was only significant in the ICM with a 28% depletion relative to control KSOM (**p<0.01).

total cell number, or individual lineages when compared to embryos cultured in standard KSOM (Student's t-test; relative cell numbers 1.03 (p=0.44), 1.06 (p=0.30) and 0.93 (p=0.20) in combined, TE and ICM lineages respectively, n = 20 embryos in each group) (Figure 4.3B).

Therefore, the pre-implantation development of reversine-treated embryos beyond the early blastocyst stage was compromised in culture media containing fewer energy resources. These results suggest that the metabolic requirements of these embryos may differ from controls, and that they may have increased energy consumption secondary to the effects of chromosome missegregation.

4.3.3 Evaluating the DNA damage hypothesis

As discussed in section 4.1 several recent studies have demonstrated that acute chromosome missegregation can result in double-stranded DNA (dsDNA) breaks which may affect the ultimate fate of the cell. Therefore the next experimental aim was to investigate this hypothesis in the context of pre-implantation development - does acute chromosome missegregation in blastomeres result in dsDNA damage?

To investigate this hypothesis the first experimental strategy was to detect and quantify dsDNA damage in blastomeres, and compare levels between control and reversine-treated embryos. A well-established technique for identifying DNA damage in individual cells is the detection by IF of DDR markers that form localised foci (IRIF) at the site of damage (section 4.1).

The DDR markers γH2AX and 53Bp1 were selected for the evaluation and quantification of dsDNA damage in the embryos. Numerous DDR factors form localized foci and were therefore potentially suitable, however γH2AX and 53Bp1 were selected due to the effectiveness and availability of antibodies required for IF studies, and are widely used in DDR studies. Initially pilot experiments were conducted to check the antibodies in the mouse pre-implantation embryo.

4.3.3.1 The atypical distribution of DDR foci throughout pre-implantation development

The pilot studies revealed unexpected results with both γH2AX and 53Bp1 exhibiting surprisingly high basal levels in control embryos (pilot images not shown - see following section). Before further experiments were conducted the IF protocol was repeated in MEF cells to determine if these unexpected findings were arising secondary to antibody or IF-induced artefact. Both control and ionizing radiation-treated (to induce DNA damage) MEF cells were stained for γH2AX, 53Bp1 or Mdc1 (an additional DDR factor used in later experiments). All three factors exhibited their characteristic staining patterns in both control and IR-treated MEF cells; minimal γH2AX in control MEF cells with multiple IRIF following IR treatment (Figure 4.4A), and both 53Bp1 and Mdc1 demonstrating diffuse nuclear staining in control MEFs followed by the formation of multiple IRIF following IR-induced DNA damage (Figure 4.4B & 4.4C respectively). Accordingly it was concluded that the antibodies were effective and that a systematic study of the distribution of these factors in the pre-implantation embryo was necessary prior to further investigation of the DNA damage hypothesis.

Therefore a systematic characterisation of γH2AX and 53Bp1 was undertaken throughout pre-implantation development to establish the baseline IF staining patterns in control untreated embryos in the absence of induced DNA damage. At least five embryos were evaluated for each factor at the different stages of development. There was minimal variation in IF staining patterns between different embryos and representative images are shown in Figures 4.5 and 4.6.

γH2AX was detected at high levels throughout pre-implantation development, with the exception of the 2-cell stage where minimal levels were detected. Further, where γH2AX was present the pattern had the classic appearance of bright foci characteristic of DNA damage, in addition to smaller clusters of background foci (Figure 4.5). The staining pattern of 53Bp1 was also unexpected. 53Bp1 characteristically displays a predominantly nuclear location (although it can also be cytoplasmic in some cells) and is recruited to the sites of dsDNA damage forming foci co-localising directly or in close proximity to the γH2AX foci (UniProtKB Database). However, in control embryos the expression of nuclear 53Bp1 was minimal until the 8-cell stage when the nuclear expression became more enriched relative to the cytoplasm and from then onwards remained predominantly nuclear in all cells of the

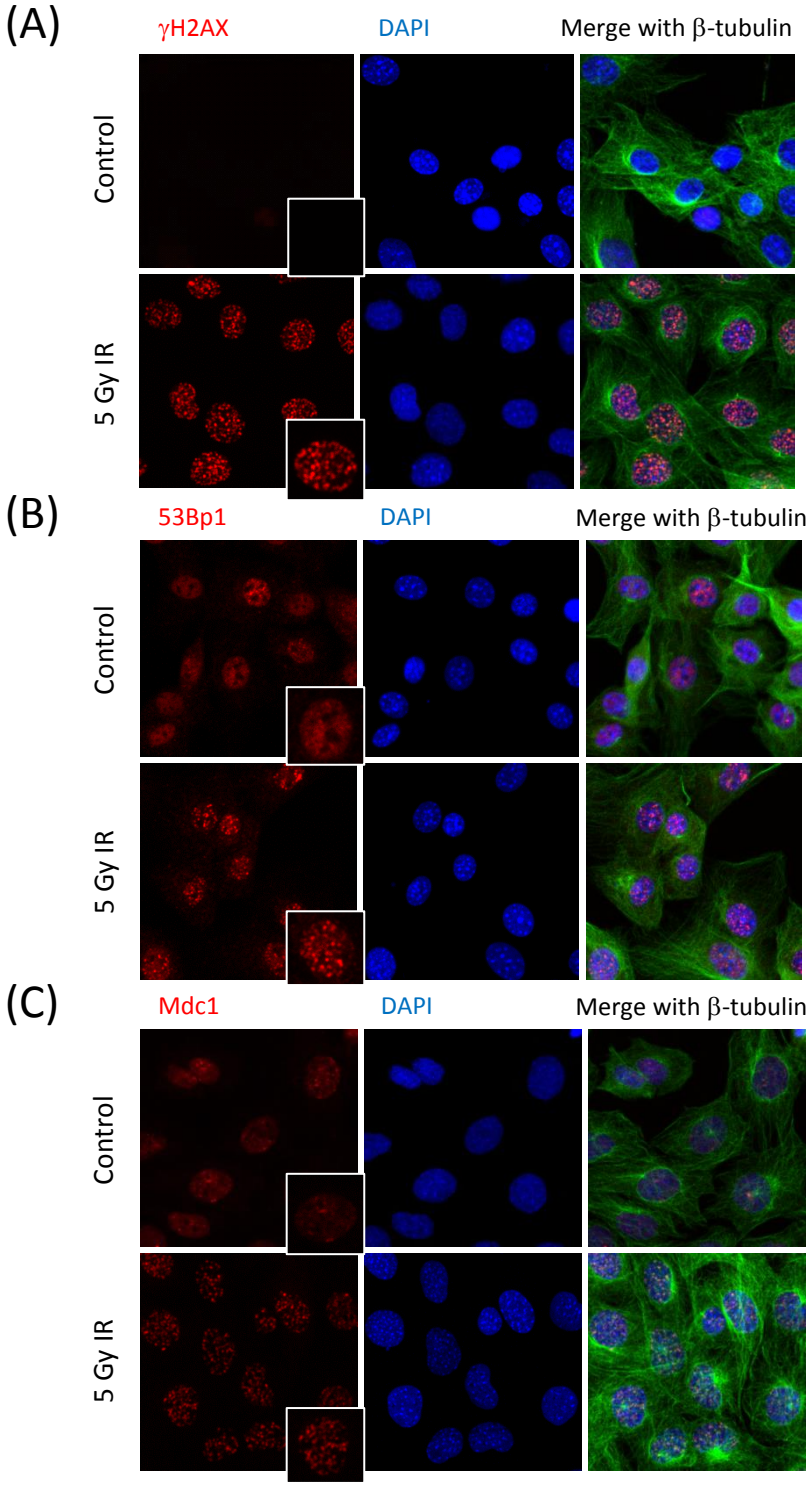

Figure 4.4 IF staining for the DNA damage response (DDR) factors γH2AX, 53Bp1 and Mdc1 in MEF cells Both control and MEF cells treated with 5 Gray irradiation (5Gy IR) are shown, demonstrating the classic distribution and response following IR-induced DNA damage **(A)** γH2AX IF with minimal signal in control MEF cells and multiple nuclear foci following IR **(B)** 53Bp1 showing diffuse nuclear staining with minimal nuclear foci in controls, and multiple nuclear foci following IR **(C)** Mdc1 with diffuse nuclear staining and minimal nuclear foci in controls and multiple nuclear foci following IR.

Inset images at the lower right corner show single representative nuclei close-up
All images at 20x magnification

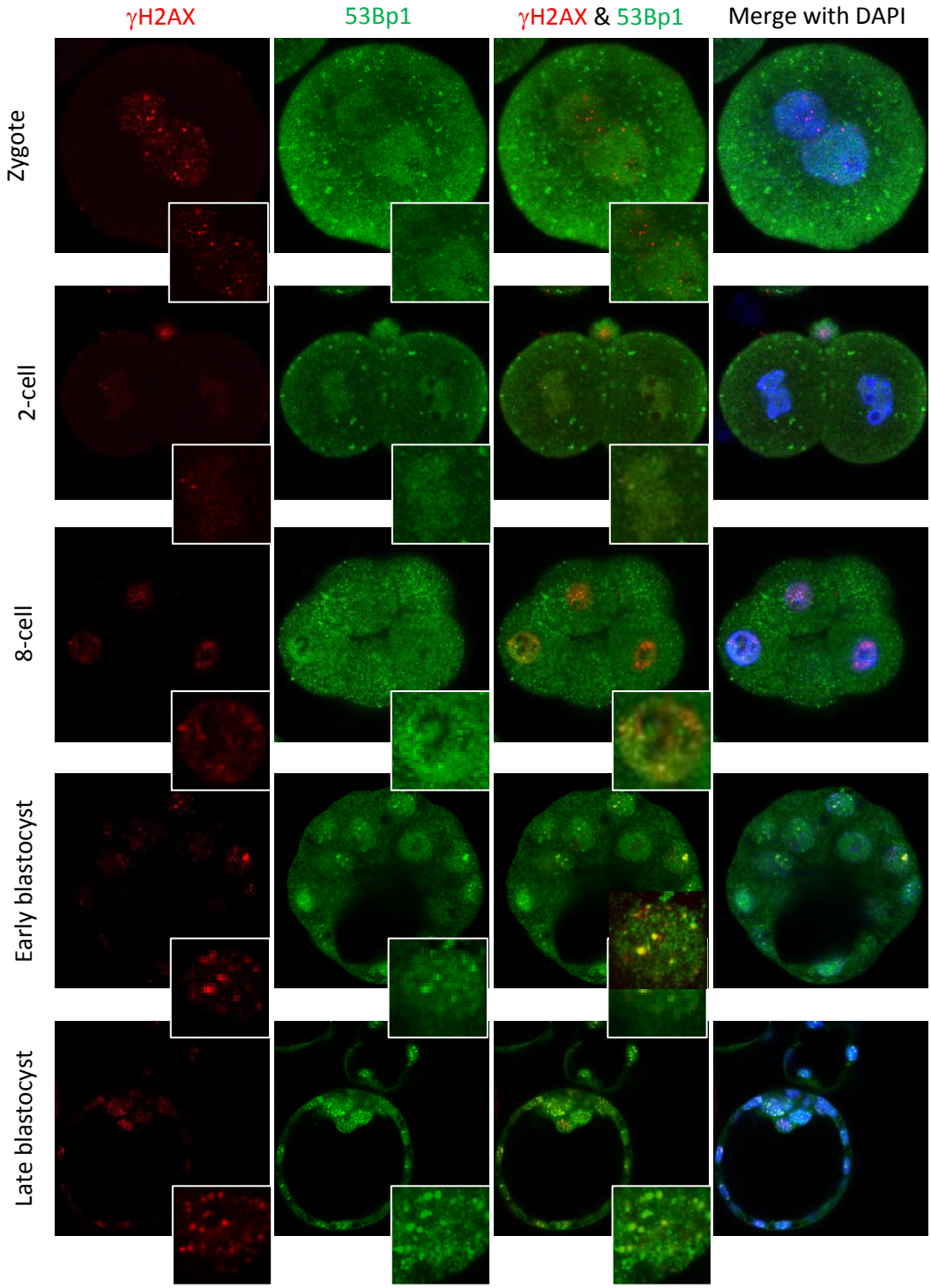

Figure 4.5 γH2AX and 53Bp1 in control embryos during pre-implantation development. Representative images taken in a single plane are shown. Basal levels of γH2AX were high throughout pre-implantation development with the exception of the 2-cell stage. 53Bp1 became enriched within the nucleus from the 8-cell stage and from then onwards was co-localised with or in close proximity to foci of γH2AX.
Inset images at the lower right corner show single representative nuclei close-up

All images at 40x magnification

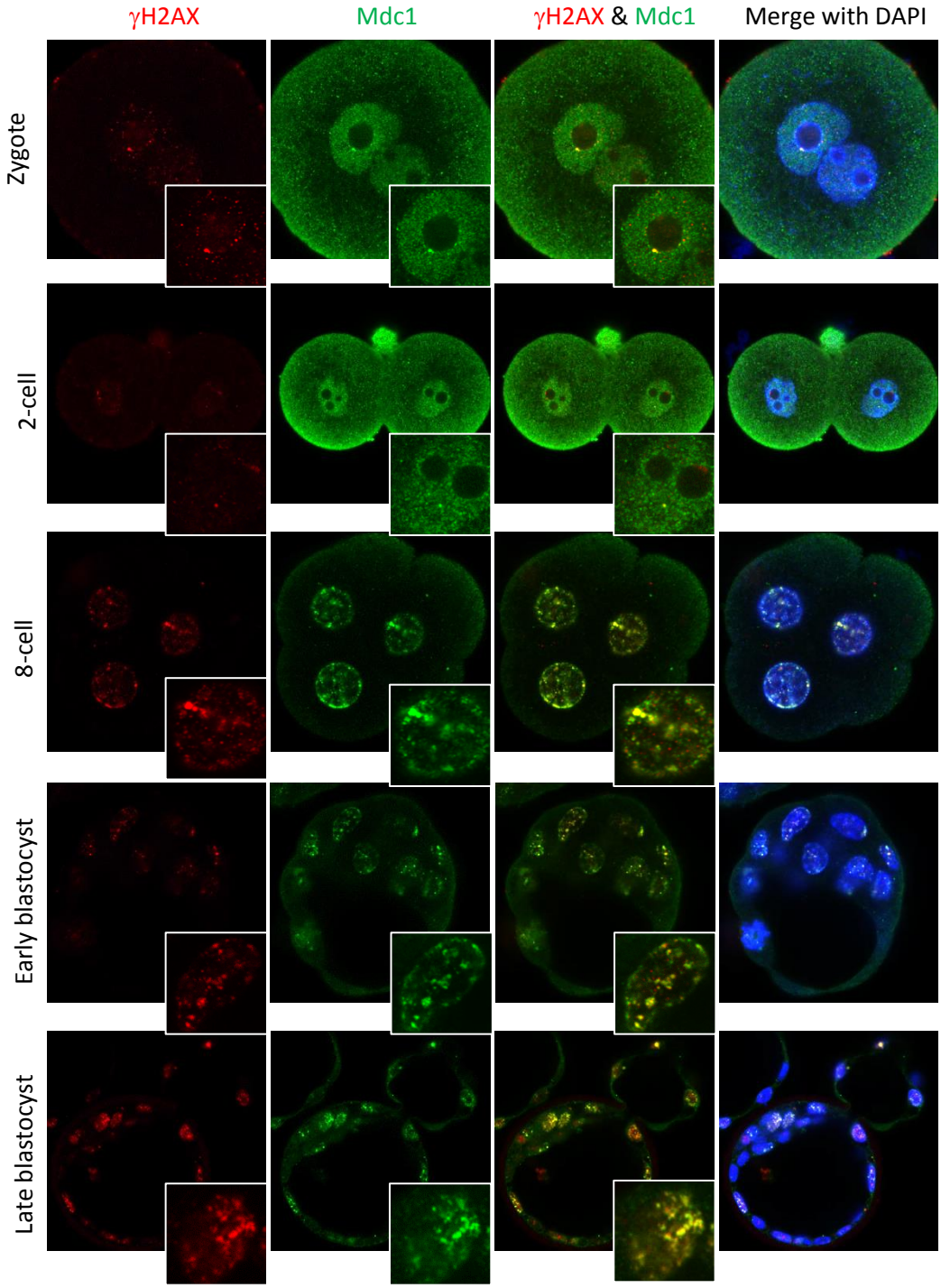

Figure 4.6 γH2AX and Mdc1 in control embryos during pre-implantation development. Representative images taken in a single plane are shown. Basal levels of γH2AX were high throughout pre-implantation development with the exception of the 2-cell stage. Mdc1 was enriched within the nucleus throughout pre-implantation development and foci co-localised with the foci of γH2AX.
Inset images at the lower right corner show single representative nuclei close-up

All images at 40x magnification

embryo (Figure 4.5). 53Bp1 foci were not identified prior to the 8-cell stage; this was unexpected given the presence of γH2AX foci with which 53Bp1 usually localises. By the blastocyst stage, 53Bp1 foci were more widespread and co-localising with or in close proximity to the γH2AX foci, as would be expected, in the majority of cells within the embryos (Figure 4.5).

In view of the unexpected distribution patterns of γH2AX and 53Bp1 the distribution of a third key DDR protein was characterised; mediator of DNA-damage checkpoint protein 1 (Mdc1). Mdc1 is a nuclear protein that re-localizes to bind to γH2AX in response to dsDNA damage and thus forms discrete nuclear foci with complete co-localisation to γH2AX foci (UniProtKB Database). A minimum of five embryos were evaluated at each stage, and there was minimal variation in the IF staining between different embryos. Representative images are shown in Figure 4.6. In contrast to 53Bp1, the distribution of Mdc1 was complementary to the patterns of γH2AX staining throughout all stages of pre-implantation development examined, and displayed the expected pattern of co-localisation with γH2AX.

Therefore these experiments revealed an unexpected, atypical distribution pattern for γH2AX, 53Bp1 and Mdc1 and consequently raised further questions. Did the presence of DDR foci reflect *de novo* intrinsic DNA breaks, or were they secondary to an alternative, non-damage related biological process unique to pre-implantation development? By the blastocyst stage, 53Bp1 foci co-localized at or near γH2AX foci, as would occur secondary to activation of the DDR, however this did not occur prior to the 8-cell stage. What could account for the absence of 53Bp1 and the uncoupling from γH2AX at earlier stages of development?

The absence of detectable nuclear positive 53Bp1 foci at early stages of embryo development could be due to the absence of activation of the DDR pathway, with γH2AX and Mdc1 foci a consequence of a non-DDR pathway related process. Alternatively, it was hypothesized that the absence could be secondary to developmental stage-specific epigenetic modifications. The nuclear localisation and recruitment of 53Bp1 to sites of DNA damage requires the dimethylation (me2) of Histone 4 (H4) at lysine (K) residue 20 (H4K20) (Botuyan et al., 2006). Therefore, the H4K20me2 status was characterised in the pre-implantation embryo using IF. Both H4K20me2 and 53Bp1 antibodies were raised in the

same host animal (rabbit) and consequently it was not possible to undertake simultaneous IF studies for both proteins within the same embryo. However, when H4K20me2 status was evaluated in isolation it was found to correlate exactly with 53Bp1 distribution characterised above; significant dimethylation of H4K20 only occurred from the 8-cell stage onwards (Figure 4.7). Thus the initial absence of 53Bp1 co-localisation at or near γH2AX foci is most likely due to the developmental absence of dimethylation at H4K20, rather than a stage-specific uncoupling from the DDR pathway.

Determining the underlying causes of the high basal levels of γH2AX, Mdc1 and (from the 8-cell stage) 53Bp1 foci in the embryo was more challenging. In the first instance a further review of the literature was undertaken to determine if any other studies had characterised or investigated the distribution of these DDR factors, or the DNA damage response itself in the pre-implantation mouse embryo either directly, or indirectly. The literature search identified very few directly relevant studies, and overall the findings were highly variable with a range of different γH2AX staining patterns described, with minimal or no characterisation of 53Bp1 or Mdc1 (Yukawa et al., 2007, Adiga et al., 2007, Ziegler-Birling et al., 2009, Mu et al., 2011, Marangos and Carroll, 2012). In addition, several of these studies proposed that the DNA damage response may be limited or atypical in the mouse oocyte and early pre-implantation embryo however comprehensive, systematic evaluations of the DDR in the pre-implantation embryo were lacking.

The cellular response to DNA damage is a highly complex process involving a myriad of proteins and processes with multiple protein interactions, different pathways, and functional redundancy, ultimately ensuring the efficient and faithful repair of the damaged genome (Thompson, 2012). Thus investigating the potential cause of the high basal levels of DDR foci would be complex and was considered out of the scope of this study. However, to exclude the possibility that activation of the DDR pathway was induced by adverse culture conditions or superovulation E3.5 blastocysts were recovered following natural mating and were immediately fixed and evaluated by IF for γH2AX and Mdc1; subjective evaluation revealed equivalent findings to embryos attained following superovulation and *in vitro* culture.

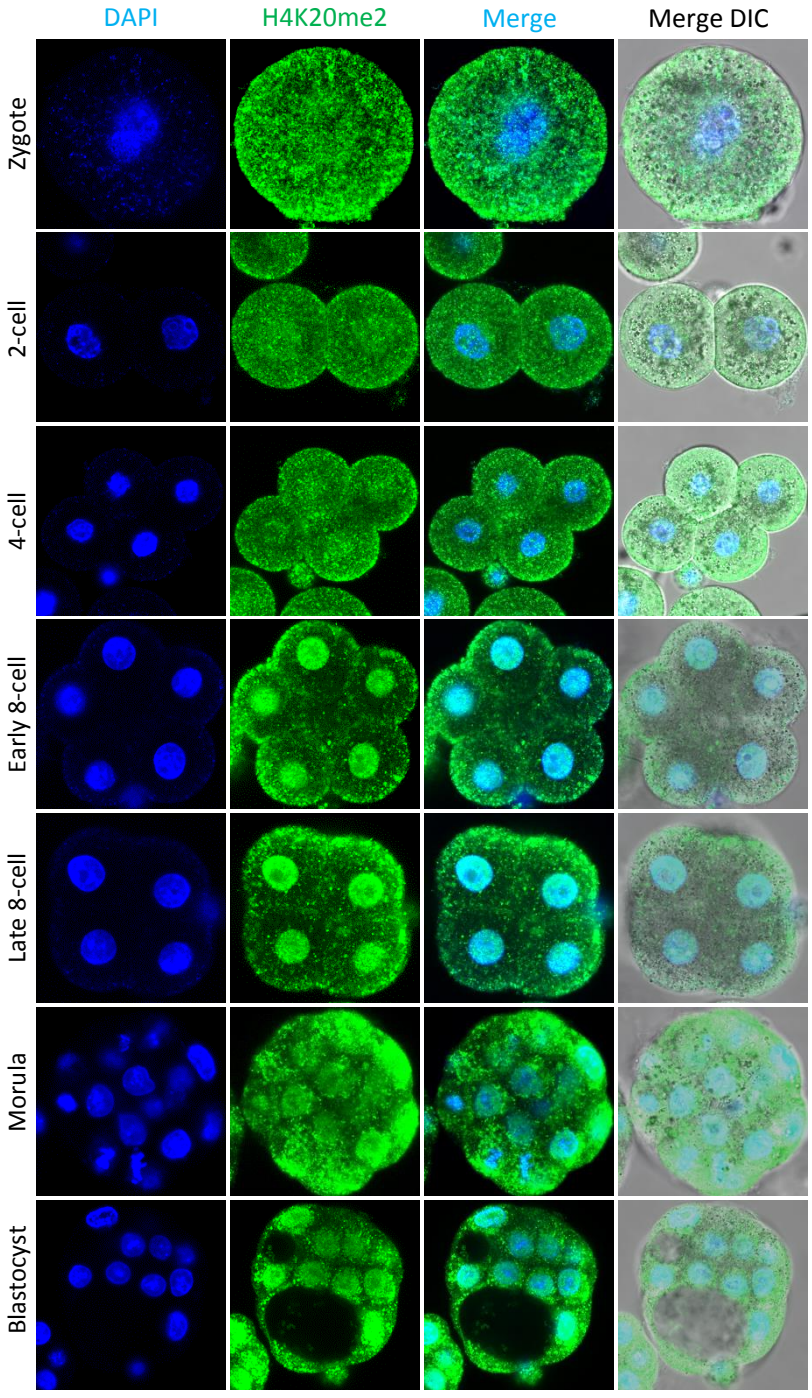

Figure 4.7 H4K20me2 profile in pre-implantation embryos. Representative IF images of embryos stained with antibodies against H4K20me2 throughout different stages of pre-implantation development. Minimal nuclear H4K20me2 was detected in the embryos prior to the 8-cell stage. From the 8-cell stage onwards H4K20me2 was clearly present in all nuclei of all embryos. This developmental profile correlated with the nuclear localisation of 53BP1 (see figure 4.5).

All images at 40x magnification

The primary goal of this study was to investigate the hypothesis that acutely arising chromosome missegregation errors may cause DNA damage that may determine the ultimate fate of the abnormal cells. In light of the unexpected findings presented above, the direct comparison of foci levels between the two groups may not be a reliable measure of DNA damage in the pre-implantation embryo. On that account before investigating this hypothesis further, a series of experiments were conducted to determine the response of the embryo to externally induced DNA damage.

4.3.3.2 Externally induced DNA damage elicits a dose-dependent increase in DDR foci throughout pre-implantation development

Pre-implantation embryos at different developmental stages were treated with 5 or 10 Gray (Gy) of IR to induce DNA damage. Two hours later they were fixed together with an equivalent control group, and were used for IF evaluation of γH2AX with Mdc1 or 53Bp1. Confocal images were captured and evaluated for evidence of an increase in DDR foci in response to IR-induced DNA damage. At least five embryos were included in each experimental and control group.

Assessment of DDR foci images confirmed an increase in γH2AX and Mdc1 foci in response to IR at all stages of pre-implantation embryo development (Figure 4.8). The density of foci increased as IR exposure increased from 0 to 5 and 10Gy. An identical pattern was also found for the embryos assessed for γH2AX and 53Bp1, with the exception of the embryos prior to the 8-cell stage, where no 53Bp1 foci were identified, and minimal in the 8-cell stage itself (Figure 4.8). As discussed previously, this is likely to be due to the stage-specific variation in the methylation status of H4K20.

Therefore, despite the high basal levels of foci in control embryos an increase in response to DNA damage did occur, and it was concluded that the evaluation of foci levels could be used to compare levels of DNA damage in the subsequent experiments after the induction of chromosome missegregation using reversine treatment.

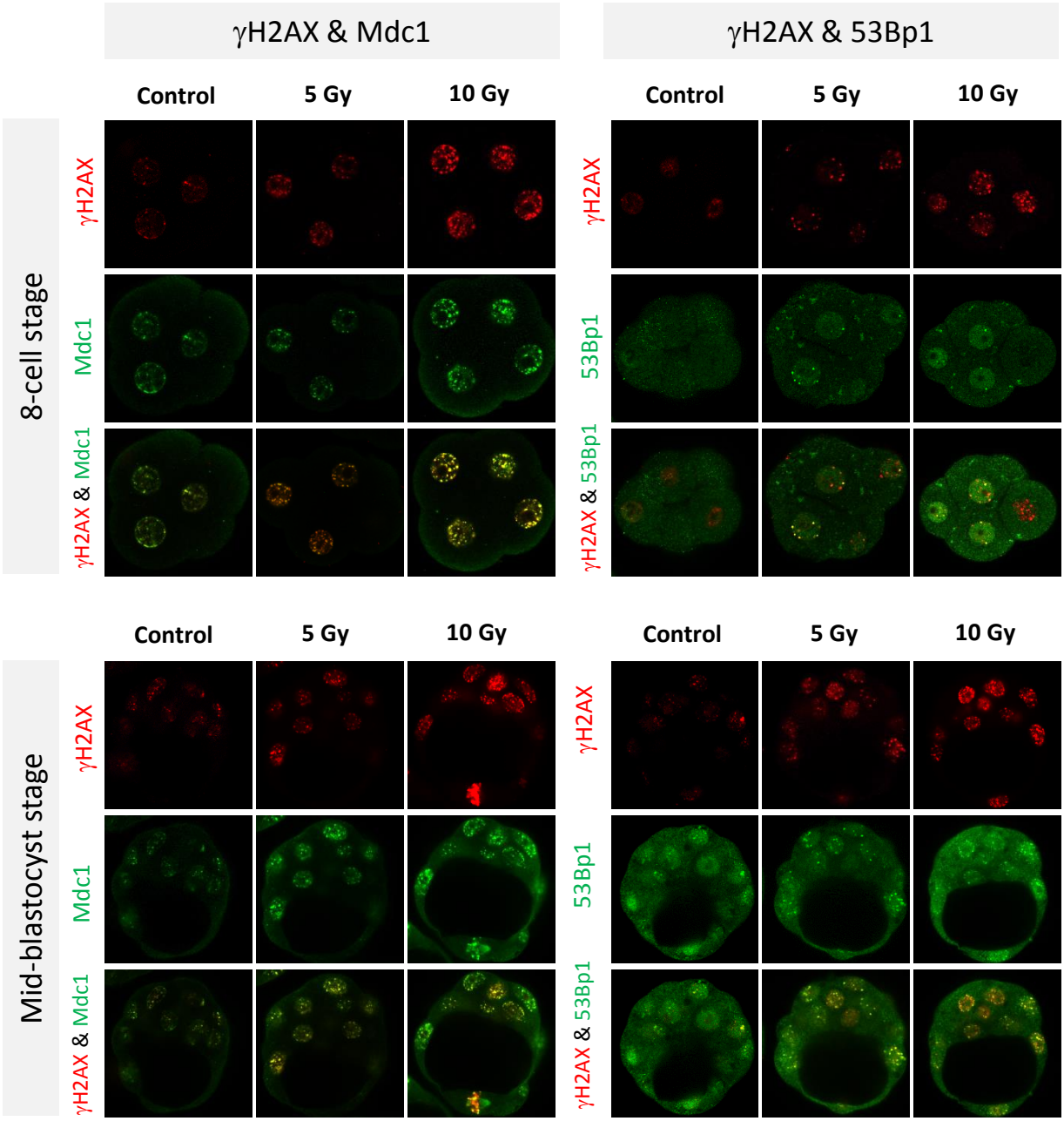

Figure 4.8 Ionising radiation (IR)-induced DNA damage elicits an increase in IRIF in the pre-implantation embryo. Embryos were subjected to 5 or 10Gy of IR to induce DNA damage and IRIF (DDR factor recruitment) were evaluated. Representative images for the 8-cell stage and mid-blastocyst stage are shown although all stages were evaluated. γH2AX and Mdc1 foci levels increased with greater exposure to IR throughout all stages of development. The effect for 53Bp1 was less striking prior to the blastocyst stage and no 53Bp1 foci were induced prior to the 8-cell stage.

All images at 40x magnification

4.3.3.3 Optimisation of DDR foci analysis in the pre-implantation embryo

The image capture and quantification of DDR foci in mouse pre-implantation embryos posed challenges not usually encountered when evaluating cells in culture necessitating optimisation of imaging conditions and data analysis approaches.

The mouse embryo is a three-dimensional structure that requires imaging in multiple z-planes in order to capture every nucleus and cell. When imaging parameters are kept constant the intensity and quality of the captured signal can vary enormously between the top and bottom z-position secondary to the 3D structure and in some cases photobleaching; an effect especially pronounced from the blastocyst stage onwards. Imaging of DDR foci in the pre-implantation embryo was found to be exquisitely sensitive to variations in signal detection acquired from different z-planes and even different positions within the imaging dish. In addition, multiple averaging images were necessary to reduce the signal noise to a threshold acceptable for foci analysis, thus increasing the potential problem of photobleaching.

To ensure that the quantification of foci between different groups of embryos was directly comparable a stringent imaging protocol was developed. Embryo groups that were to be compared directly were imaged on the same day during the same session with identical imaging parameters. Images were captured along the same z-plane in a maximum of two different planes, rather than capturing all cells within the embryo, thus minimising the effects of photobleaching and the 3D structure. Even with this stringent imaging protocol the subjective quantification of foci was not possible. Therefore a software plugin for FIJI was developed to enable the objective and reproducible quantification of foci to be undertaken (Figure 4.9). The plugin was designed in collaboration with Dr Richard Butler (Gurdon Institute Imaging Facility). Mdc1 foci were evaluated as these IF images contained the least background noise, and the foci directly co-localized with those of γH2AX.

4.3.3.4 Comparing DDR foci between control and reversine-treated blastomeres

The DNA damage hypothesis could now be investigated by comparing foci levels between control and reversine-treated blastomeres/embryos. Nuclear Mdc1 foci were evaluated at

Original images

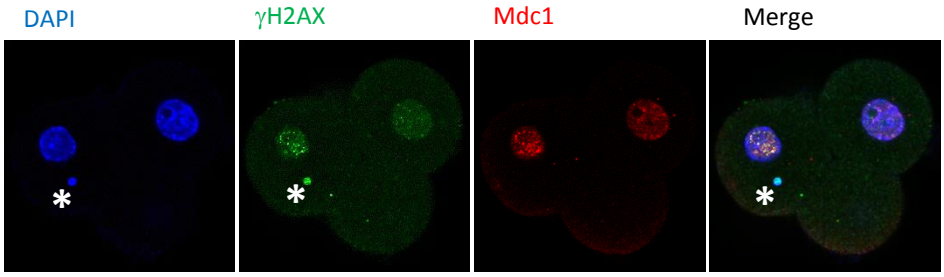

Image processing & analysis in FIJI

(1). Select nucleus in desired channel (MDC1) as ROI

(2). Standardised image processing algorithm

(3). Standardised object analysis & foci count read-out

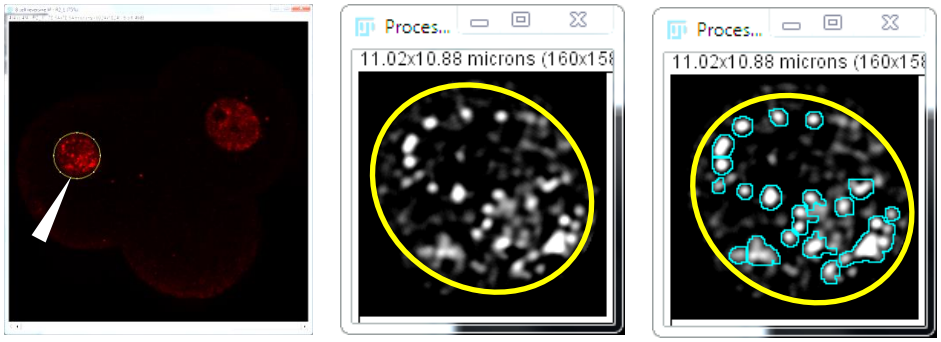

Figure 4.9 Objective standardised quantification of DNA damage foci using FIJI software. Original image files were opened in FIJI in separate channels. The figure shows a representative image of an embryo containing two nuclei within a single plane, together with a single micronucleus (shown by an asterisk).To evaluate the foci within a nucleus, the nucleus was first selected as a region of interest (ROI) within the desired channel ***(1).*** Mdc1 images had the least background fluorescence and were therefore selected for foci analysis. A plugin was run which executed a standardised image processing algorithm ***(2)*** followed by a standardised object analysis with a foci count read out ***(3).*** Although the algorithm did on occasions merge foci that were considered separate on subjective evaluation, as every nucleus was subjected to identical image processing and analysis the results were thus comparable between different groups of embryos.

All images at 40x magnification

the 8-cell stage; this was to detect newly arising DNA damage occurring as a consequence of acute chromosome missegregation secondary to reversine treatment during the preceding cleavage. There were no significant differences in nuclear Mdc1 foci between control and reversine-treated embryos, with control embryos containing a mean of 10.2 foci per nucleus in each embryo, compared to 9.6 in reversine-treated embryos (Student's t-test; p=0.21, n= 84 and 55 control and reversine-treated blastomeres respectively) (Figure 4.10A). Therefore, there was no evidence of increased nuclear DNA damage arising secondary to acute chromosome missegregation. A group of embryos were also evaluated at the mid-blastocyst stage to determine if DNA damage accumulated as the embryo developed. Elevated levels of ROS species can cause DNA damage, usually single stranded (which would not be detectable as foci), however if breaks occur in close proximity then dsDNA damage can also arise. However, there were also no significant differences in foci levels between control and reversine-treated blastocysts with a mean of 6.6 and 5.9 foci per nucleus respectively (Student's t test; p=0.43, n=119 control and 83 reversine blastomeres)(Figure 4.10A.).

Next micronuclei were evaluated as previous studies have demonstrated DNA damage within the resulting micronuclei (Crasta et al., 2012). Micronuclei were found to exhibit a strikingly different pattern of expression of DDR factors when compared to the main nucleus. Within the main nuclei γH2AX and Mdc1 were consistently co-localised. In contrast, Mdc1 was present in only 2 of 22 micronuclei assessed (9%) with the majority consisting of γH2AX alone (15 of 22; 68%). There were no cases of Mdc1 alone in the absence of γH2AX. Finally some micronuclei did not stain for either γH2AX or Mdc1 (5 of 22; 23%) (Figure 4.10B). However, the absence of Mdc1 in micronuclei did not exclude the possibility of underlying DNA damage; it has previously been shown that DDR factors are not consistently recruited to micronuclei (Terradas et al., 2010). Therefore, for micronuclei γH2AX was evaluated to compare levels of DNA damage between the main and micronucleus within the same cell. However, due to the small size and compacted nature of the chromatin within the micronucleus it was not possible to compare number of foci *per se*; therefore an alternative strategy was applied, comparing the overall intensity of γH2AX within the main or micronucleus, normalised against the respective DAPI signal intensities. Using this approach the mean γH2AX levels in the main nuclei were found to be identical to those within the

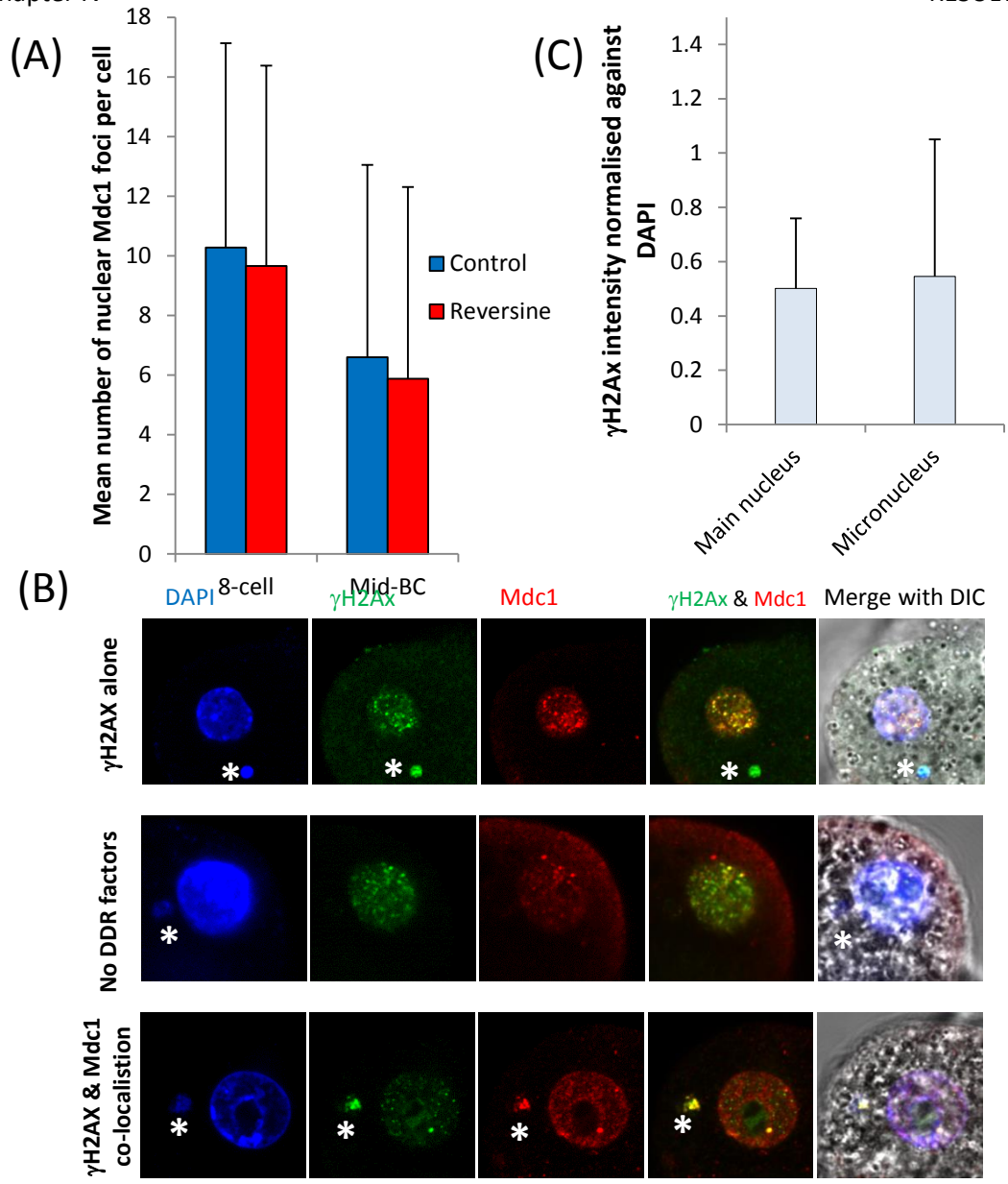

Figure 4.10 Evaluation of reversine-treated embryos for evidence of DNA damage arising secondary to chromosome missegregation (A) Blastomeres were evaluated for levels of dsDNA damage in their nuclei by quantification of the Mdc1 foci. There were no differences between control and reversine-treated embryos at the 8-cell or blastocyst stage (Student's t-test; p = n/s). Error bars=SD. **(B)** Localisation of DDR factors within micronuclei showed a variable pattern. In 68% of micronuclei there was no detectable Mdc1. 23% of micronuclei did not stain for either γH2AX or Mdc1 and only 9% showed co-localisation of both γH2AX and Mdc1. In contrast, in the main nuclei there were relatively high basal levels of γH2AX, and Mdc1always co-localised with γH2AX foci. **(C)** Micronuclei resulting from reversine-treatment were evaluated for evidence of dsDNA damage by comparing γH2AX staining intensity between the main and micronucleus, normalised against the DAPI signal. Levels between paired principle and micronuclei (denoted by asterisks) were equivalent and thus there was no evidence of increased DNA damage within micronuclei (Student's paired t-test; p=n/s). Error bars = SD.

All images at 40x magnification

micronuclei (Student's paired t-test; intensity ratio 0.50 and 0.54 in main and micronuclei respectively, n=22, p=0.66 – Figure 4.10C).

Thus it was concluded that there was no evidence of DNA damage in the micronuclei of pre-implantation mouse embryos.

4.3.3.5 Evaluating for checkpoint activation in reversine-treated blastomeres

Evaluation of DDR foci did not reveal any direct evidence to support the DNA damage hypothesis. However, due to the high basal levels of DDR foci in the embryo it is possible that small increases in DNA damage may be missed. A major function of the DNA damage response is to arrest the cell-cycle, preventing cell division in the presence of a damaged genome (Jackson and Bartek, 2009). Therefore, time-lapse imaging parameters of cell-cycle lengths could be used as an indirect marker for activation of the cell-cycle checkpoints, and is a technique readily applicable to the pre-implantation embryo.

It was first necessary to confirm that DNA damage occurring at the 8-cell stage would result in cell-cycle arrest. Therefore 8-cell stage embryos were treated with 2Gy or 5Gy IR to induce DNA damage and underwent time-lapse imaging with control embryos to determine the length of time to the next division. Blastomeres treated with 2 or 5Gy of IR had a significant delay in the onset of their next division, occurring an average of 392 and 383 minutes later than controls respectively (Student's t-test; $p<0.0001$, n=10 embryos in each group) (Figure 4.11A). Thus it was concluded that acutely arising DNA damage at the 8-cell stage results in significant cell-cycle arrest that is detectable by time-lapse imaging.

Therefore the data generated from the time-lapse imaging undertaken on the reversine-control chimeric embryos presented in the previous chapter was re-evaluated to assess for any differences in cell-cycle timing occurring immediately after chromosome missegregation was induced. If significant DNA damage had occurred then an increase in the 8- to 16-cell cell-cycle length would be expected in the clone of blastomeres that had been treated by reversine. However, a direct measure of the 8- to 16- cell-cycle length was not possible as time-lapse imaging could only be commenced after the reversine-treatment had been completed. An alternative strategy was therefore required. Each chimeric mosaic embryo was comprised of four control and four reversine-treated blastomeres. The order of cell

(A)

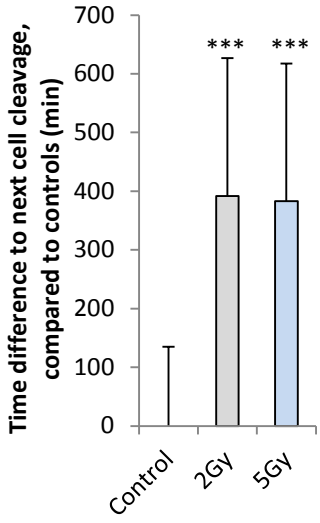

(B)

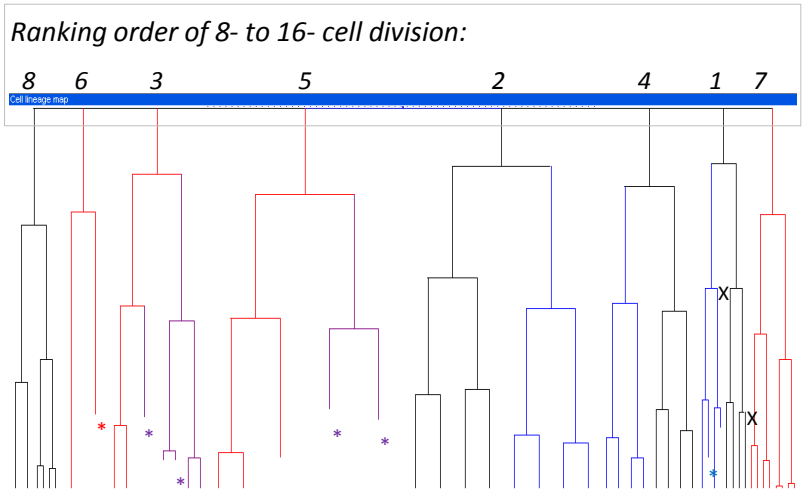

Rank	1	2	3	4	5	6	7	8
Control blastomeres	10	12	8	9	8	8	14	11
Reversine blastomeres	10	8	12	11	12	12	6	7

n=158 blastomeres from 20 embryos

χ^2 test p=0.4

Figure 4.11 Evaluation of cell-cycle response to DNA damage at the 8-cell stage. **(A)** Cell-cycle lengths were significantly prolonged in response to 2 or 5 Gy IR at the 8-cell stage, thus confirming that DNA damage at the 8-cell stage results in activation of cell-cycle checkpoints (Student's t-test, ***p<0.0001 compared to controls). Error bars=SD. **(B)** Representative lineage tree of a chimeric embryo comprising of four control (black branches) and four reversine-treated (red branches) blastomeres at the 8-cell stage. To determine if reversine-treated blastomeres exhibited signs of cell-cycle delay at the 8-cell stage, the sequence of division from the 8- to 16-cell stage was ranked in order and related to cell origin (reversine or control blastomere). In total, 20 chimeric embryos were evaluated and there were no significant differences in order of division between control and reversine-treated blastomeres. Thus there was no evidence of delay to the 8- to 16- cell cleavage in the reversine-treated blastomeres compared to controls.

division was ranked from first through to last for each embryo, and related to cell history (control or reversine). If there were no differences in the cell-cycle lengths between the groups, then the ranking order between the two groups would also be equivalent. Conversely, if reversine-treated blastomeres underwent a significant cell-cycle arrest secondary to DNA damage, then their distribution would be skewed towards the lower ranks. All 20 chimeric embryos were evaluated and there were no significant differences in order of cell division between reversine or control blastomeres (χ^2 test; p=0.38). Therefore it was concluded that there was no evidence of cell-cycle delay or checkpoint activation occurring at the 8- to 16-cell cleavage (Figure 4.11B).

Considering all experiments together it was therefore concluded that there was no evidence to support the hypothesis that acutely arising chromosome missegregations resulted in DNA damage in the pre-implantation embryo.

4.3.4 Investigating additional potential causes for apoptosis within the ICM

The results presented in the previous chapter demonstrated that ICM clones with a history of chromosome missegregation were significantly more likely to undergo apoptosis compared to control blastomeres. However, apoptosis was not exclusively limited to the abnormal clone of cells as 20% of the control clone was also eliminated by apoptosis in the ICM. It is not known if these control cells were also abnormal and thus reflective of the basal level of aneuploidy within the mouse embryo. Indeed, when control embryos were evaluated by FISH in Chapter II, 17% of blastomeres were classified as aneuploid, and thus this hypothesis is plausible. However, other hypotheses have been proposed to account for apoptosis within ICM lineage and it is possible that more than one mechanism may underlie this phenomenon (Hardy, 1997, Pampfer and Donnay, 1999, Fabian et al., 2005). One hypothesis is that apoptosis within the ICM is a mechanism through which misplaced cells with TE potential are eliminated. It has also been speculated that abnormal cells are eliminated by apoptosis; in non-developmental settings a major cause of apoptosis is the elimination of cells containing significant DNA damage that is too severe to be repaired by the cell (Jackson and Bartek, 2009). Thus it is possible that ICM apoptosis may be arising secondary to DNA damage, to eliminate genetically abnormal cells from the future fetal

lineage. A series of experiments were designed to investigate these hypotheses in greater detail.

These experiments necessitated the ability to inhibit apoptosis. First it was confirmed that the pan-caspase inhibitor ZVAD was effective at inhibiting apoptosis in the mouse blastocyst. Embryos were cultured in KSOM containing 200μM ZVAD during blastocyst cavity expansion. Equivalent controls were incubated in DMSO (vehicle) alone. Blastocysts were then exposed to 10Gy of IR to induce widespread apoptosis. 28 hours later embryos were fixed and IF was undertaken to detect activated caspase-3, a key enzyme central for the execution of apoptosis. Control embryos showed extensive staining for activated caspase-3 following IR treatment, thus confirming initiation of the apoptosis pathway. In contrast, in embryos incubated in ZVAD minimal or no activated caspase-3 was detected following IR treatment (Figure 4.12A). Finally, a group of untreated control embryos incubated in ZVAD also showed minimal caspase-3 activation, with otherwise normal morphology confirming that incubation in ZVAD did not inhibit normal blastocyst maturation.

To exclude the possibility of caspase-independent cell death in normally cultured blastocysts, the morphology of the ICM population was evaluated in a group of control and ZVAD-incubated blastocysts. In a subset of embryos TUNEL staining was undertaken to evaluate for the presence of programmed cell death. Apoptosis was identified by the presence of apoptotic bodies in 90% of control blastocysts (27 of 30), significantly more than the 3% identified in ZVAD-incubated blastocysts (1 of 31) (Fisher's test; $p<0.001$) (Figure 4.12B). Likewise, the majority of control embryos were positive for TUNEL staining which did not occur in the ZVAD-incubated embryos (Figure 4.12C). Thus it was concluded that ZVAD is a potent inhibitor of cell death within the blastocyst and could be used as an effective inhibitor of apoptosis in the subsequent experiments.

In the first instance, an experiment designed to test the hypothesis that ICM apoptosis eliminates aneuploid cells in wild-type untreated embryos (i.e. in the absence of induced chromosome missegregation) is currently underway in collaboration with Dr Thierry Voet. Individual ICM cells from E4.5 blastocysts have been collected for single cell array-based molecular karyotyping (as described in Chapter II) in two groups; control embryos and

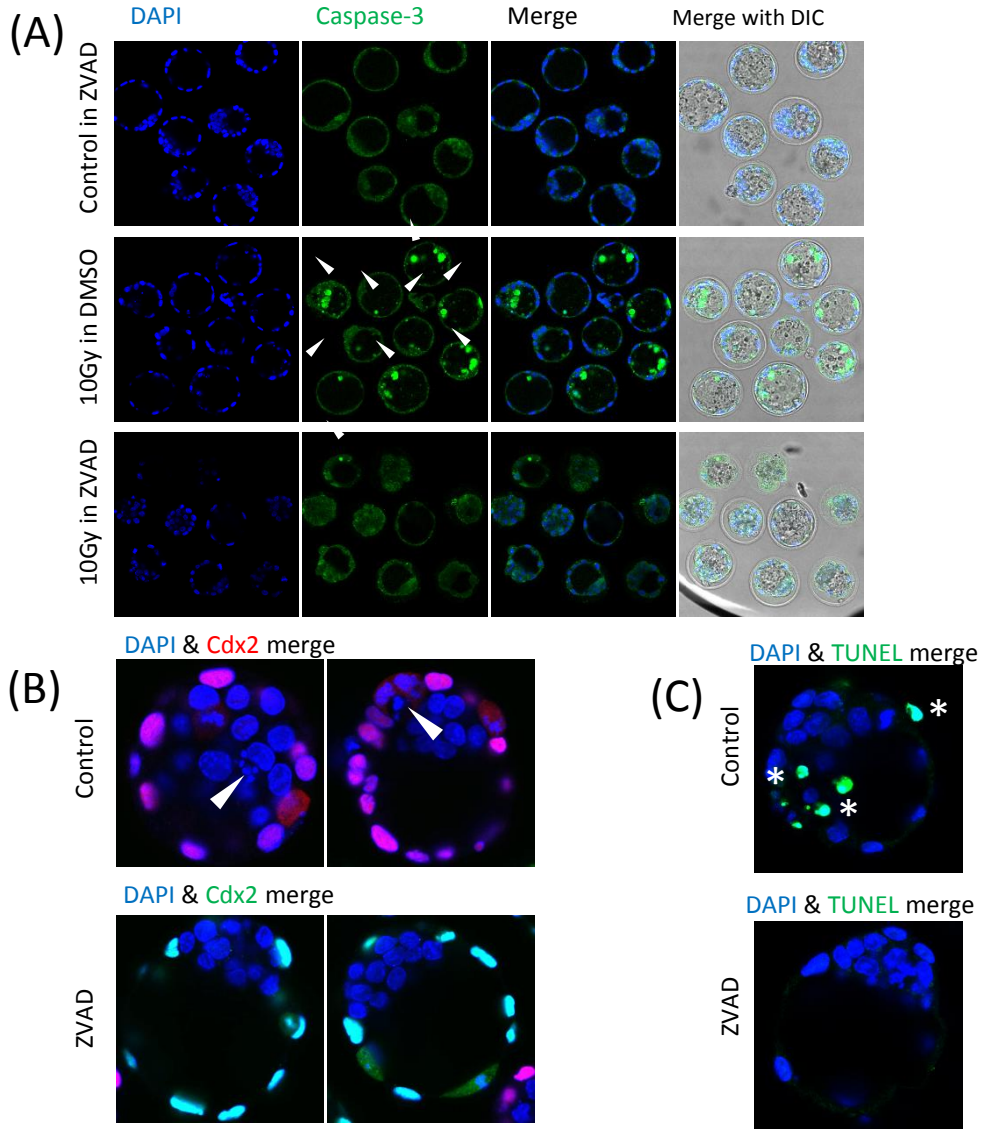

Evidence of apoptosis within ICM

	Apoptosis	No apoptosis
Control embryos	27	3
ZVAD embryos	1	31

p<0.001

Figure 4.12 Incubating blastocysts in 200μM ZVAD inhibits apoptosis (A) Incubation in ZVAD during blastocyst cavity expansion did not have any apparent adverse effects on control embryos as assessed by morphology. Exposing blastocysts to 10Gy IR induced extensive activation of caspase-3 (white arrow heads); an effect which was significantly inhibited by the presence of ZVAD. **(B & C)** Most control untreated blastocysts showed evidence of apoptosis occurring within the ICM as assessed by morphology (white arrow heads in B) and TUNEL staining (asterisks in C). In contrast embryos incubated in ZVAD rarely exhibited any signs of apoptosis or cell death within the ICM ***p<0.001 Fisher's test). Representative images of control and ZVAD-incubated embryos are shown.

All images at 40x magnification

embryos that have been incubated in ZVAD to inhibit apoptosis. The rates of aneuploidy between the two groups will be compared to determine if there are higher rates of aneuploidy in embryos that cannot undergo apoptosis. At the time of writing (May 2013), the results are still pending.

Next the hypothesis that apoptosis eliminates ICM cells with increased levels of DNA damage was investigated. Both control and apoptosis-inhibited blastocysts were cultured to E4.5 and then fixed. Simultaneous IF for Mdc1 and Cdx2 was undertaken; Mdc1 for quantification of DDR foci and Cdx2 to distinguish between the TE and ICM. In total 184 control and 237 apoptosis-inhibited ICM cells were evaluated. The mean number of Mdc1 foci per cell in control ICM cells was 2.25 compared to 3.14 in apoptosis-inhibited ICM cells, a small but highly significant difference (Student's t-test; p=0.006). When TE cells were evaluated within the same group of embryos there were no differences between the control and apoptosis-inhibited group; control TE cells contained a mean of 11.1 foci per cell, compared with 10.9 in the apoptosis-inhibited blastocysts (Student's t-test; p=0.80, n=181 control and 161 apoptosis-inhibited cells respectively) (Figure 4.13A). Therefore it was considered unlikely that the increase in Mdc1 foci were an artefact secondary to ZVAD. However, although there was a highly significant difference in the foci number between the control and apoptosis-inhibited ICM cells, the biological significance of a difference of less than one (0.89) was questionable. Therefore the distribution of the ICM foci for each group of embryos was plotted on a frequency (percentage) distribution graph, and the two distributions compared (Figure 4.13B). This was to determine if the distribution of the apoptosis-inhibited foci was bimodal, comprising of a second small sub-population of cells with very high levels of foci, which could represent a subset of cells that would have been otherwise eliminated through apoptosis due to high levels of DNA damage. Such a distribution could reconcile the finding of the small but highly significant statistical differences between the mean numbers of foci in each group. Both groups were found to have similarly-shaped positively skewed distribution, with no evidence of a bimodal pattern in the apoptosis-inhibited group or threshold level above which point apoptosis occurred (Figure 4.13B). Therefore it was concluded that there was minimal evidence to suggest that DNA damage is a major cause of apoptosis within the ICM lineage during the development of apparently normal embryos.

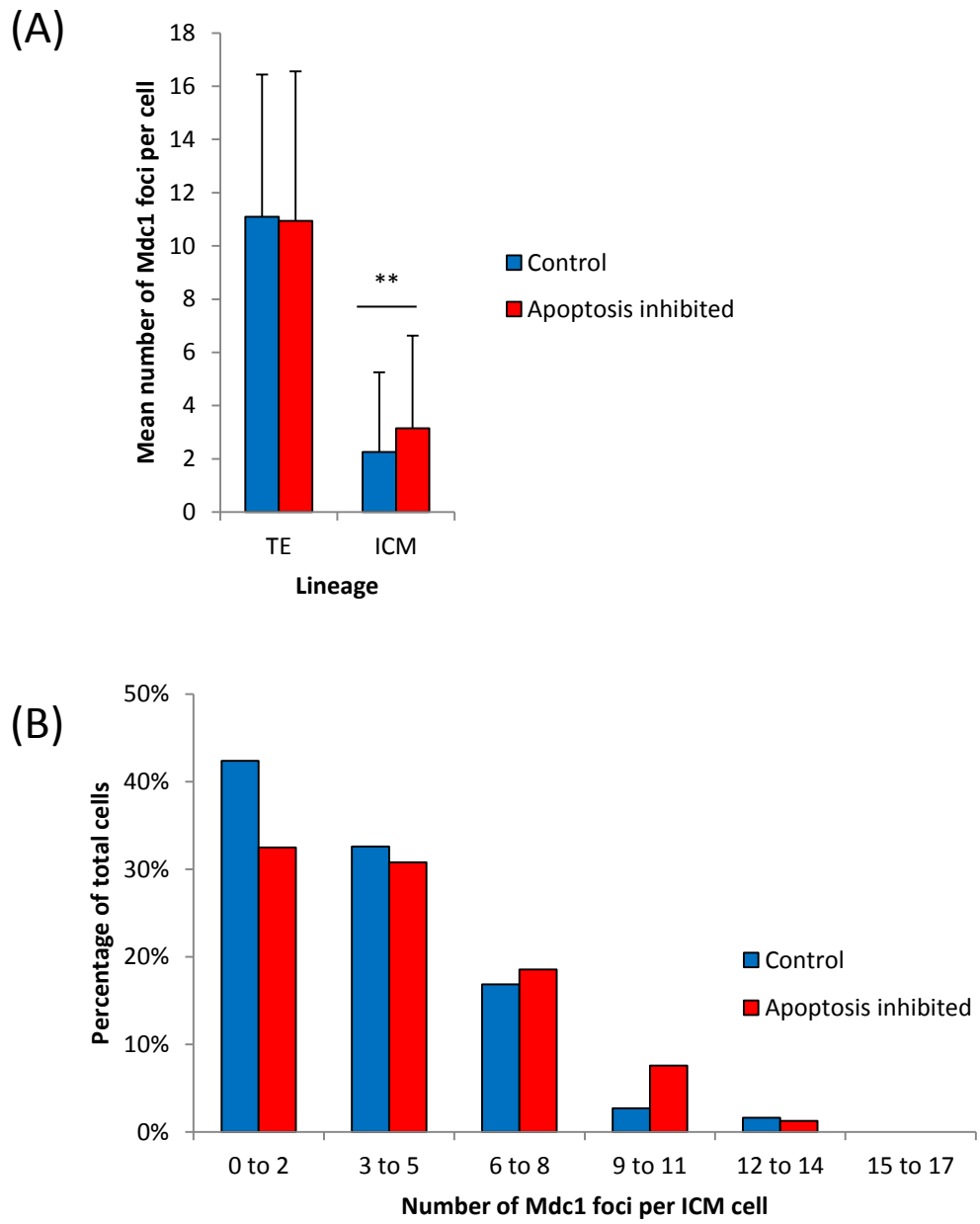

Figure 4.13 Comparison of MDC1 foci between control blastomeres and blastomeres incubated in ZVAD apoptosis inhibitor. Evaluation of MDC1 foci was undertaken as a comparative marker of DNA damage between the control and apoptosis-inhibited blastocysts **(A)** Mdc1 foci levels were identical between the two groups within the TE lineage. In contrast within the ICM there was a small but highly significant increase in mean number of foci within the cells from the apoptosis-inhibited blastocysts compared to controls (Student's t-test;** $p<0.01$) (Error bars =SD)**(B)** Percentage distribution graphs comparing Mdc1 foci within the ICM lineage of control and apoptosis-inhibited blastocysts. Both distributions were similar in shape, with no evidence of a bimodal distribution for the apoptosis-inhibited population. Thus there was no evidence of a threshold level of DNA damage triggering apoptosis within ICM blastomeres.

While embryos were evaluated for evidence of DNA damage in the previous set of experiments, it was observed that cells expressing the TE-specific transcription factor Cdx2 were occasionally present within the ICM population. It has previously been hypothesized that apoptosis within the ICM is a mechanism through which misplaced cells with TE potential are eliminated (Hardy, 1997, Pampfer and Donnay, 1999, Fabian et al., 2005). Therefore these images were re-evaluated for evidence Cdx2-positive cells malpositioned within the ICM population. Cells were classified as malpositioned only if they were clearly present within the ICM population and completely surrounded by other ICM cells. Of a total of 62 embryos assessed two contained malpositioned Cdx2-positive cells within their ICM, one of which was in the control group and the other within the apoptosis group (Fisher's test; p=1.0) (Figure 4.14). Thus although the occurrence of Cdx2-expressing cells within the ICM was infrequent, there was no evidence to support the hypothesis that apoptosis eliminates cells with TE-potential (as defined by expression of Cdx2) from the ICM.

4.3.5 Summary of main results

In summary, the results presented in this chapter demonstrated that pre-implantation embryos treated with reversine to induce chromosome missegregation exhibit compromised pre-implantation development when cultured in conditions with limited energy resources, suggesting that these embryos may have higher metabolic demands compared to controls, in keeping with studies undertaken on aneuploid MEFs (Williams et al., 2008, Li et al., 2010). No evidence of DNA breaks was detected following acute chromosome missegregation in blastomeres following reversine treatment. Consequently the DNA damage hypothesis proposed in section 4.1 was considered unlikely to contribute the elimination of chromosomally abnormal cells from the embryo. However, investigation of this hypothesis revealed high basal levels of nuclear DDR foci in the pre-implantation embryo. Micronuclei that arose as a result of chromosome missegregation (induced by reversine) were found to be deficient in the recruitment of the DDR factor Mdc1 to sites of γH2AX. Although the role of the high basal levels of nuclear DDR factors was not established, it is speculated that the deficiency within the micronuclei could potentially be detrimental to the cell and thus contribution to its removal.

Cdx2 Correctly positioned and restricted to outside cells

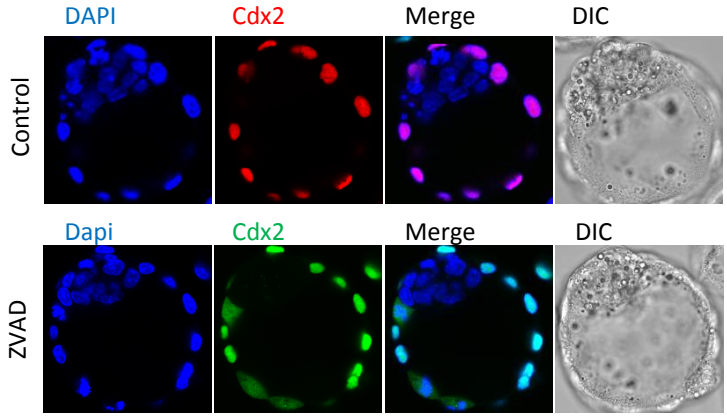

Cdx2 Malpositioned within the ICM population

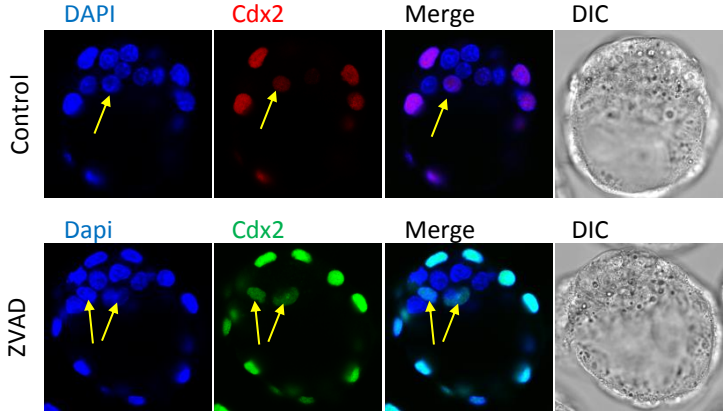

	Cdx2 within ICM	Cdx2 restricted to outside lineage
Control embryos	1	29
ZVAD embryos	1	31

Fisher's test p=1.0

Figure 4.14 Cdx2-positive cells within the ICM are infrequent and not a significant cause of apoptosis. Embryos were evaluated for the presence of malpositioned cells with TE-potential within the ICM, as defined by the presence Cdx2-positive cells surrounded by ICM. The majority of Cdx2-positive cells were correctly positioned within the TE lineage in both the control and apoptosis-inhibited (ZVAD) blastocysts, and there were no significant differences between the two groups.

All images at 40x magnification

4.4 RESULTS III DISCUSSION

The major aim of the work described in this chapter was to explore potential mechanisms that may account for how clones derived from blastomeres with a history of chromosome segregation errors become depleted from the developing embryo.

4.4.1 Investigating ROS levels and the effect of adverse culture conditions

ROS levels were evaluated at early and late blastocyst stages using the CellROX assay. There was no evidence of elevated ROS levels in reversine-treated embryos compared to their equivalent controls at either stage of development. There are two possibilities to account for this finding; either that ROS levels were indeed unchanged in reversine-treated embryos at the time of evaluation, or because the assay was insufficiently sensitive to detect small, yet potentially significant, differences between the two groups. Positive control embryos incubated in H_2O_2 did show elevated levels of ROS, confirming that the assay could detect differences in oxidation status. However, while the results of this study showed no detectable elevation in ROS levels in reversine-treated embryos, the hypothesis was not ruled out due to the possibility of small but undetectable differences in ROS levels, or that ROS levels become significantly elevated at later developmental stages.

It was also hypothesized that embryos harbouring aneuploidies secondary to acute chromosome segregation errors may share features of the 'aneuploidy stress response' and altered metabolic properties previously characterised in aneuploid yeast and MEF cells (Torres et al., 2007, Williams et al., 2008). An indirect approach was adopted to investigate this hypothesis. Would adverse culture conditions (with depleted energy resources) affect aneuploid embryos to a greater extent than control embryos? Between the mid and expanded blastocyst stage, the development of reversine-treated embryos cultured in low-energy KSOM was found to be compromised relative (as determined by total cell number) to those cultured in standard KSOM; an effect that did not occur in the control embryos. This suggests that there may be increased metabolic demands in embryos with aneuploidy, which could contribute to the depletion of the abnormal clone from the developing embryo.

This effect became apparent at the expanded blastocyst stage, with no differences detected earlier. It was not known if this timing was reflective of the increased energy demands associated with blastocyst formation, or a cumulative detrimental effect that became apparent only after several cell cycles. In the study evaluating aneuploid MEF cell lines, proliferation defects were only detectable after two days in culture and overall glucose consumption was measured after nine days (Williams et al., 2008). The developmental time-frame in these experiments necessitated mid-blastocyst stage embryos to be evaluated just one day after the induction of chromosome segregation errors, and at a maximum of two and a half days in the case of late-blastocysts. Thus it is possible that the impact of the adverse culture conditions was only just becoming apparent at the late blastocyst stage. An aneuploidy stress -like response may become more significant as the embryo undergoes implantation, the time at which the epiblast experiences a rapid burst of proliferation (Snow, 1977). Interestingly, the difference was also noted during the time at which the metabolic demands of the pre-implantation embryo are known to increase dramatically for two reasons: the Na^+/K^+ ATPase-mediated transport of Na^+ ions by TE cells required for blastocoel formation, and the onset of embryo growth requiring protein synthesis (Leese et al., 2008).

A link between pre-implantation embryo metabolic activity and viability is well established, and has driven a search for metabolic biomarkers with the aim of improving the success of IVF. One study directly examined the association between amino acid metabolism and aneuploidy in human embryos (Picton et al., 2010). This study demonstrated significant differences in amino acid turnover between uniformly euploid and uniformly aneuploid embryos (as defined by FISH), but not in mosaic embryos. Given the high prevalence of aneuploidy in human embryos, the lack of publications directly comparing the metabolic profiles between euploid and aneuploid embryos is surprising. Perhaps this may reflect the minimal impact of aneuploidy on metabolism during the pre-implantation stages of development.

4.4.2 Investigating the DNA damage hypothesis

Investigation of the DNA damage hypothesis was not straightforward and required further evaluation of the DDR in the pre-implantation embryo before the original hypothesis could be addressed.

The extensive basal γH2AX foci detected in the pre-implantation embryo, together with the absence of nuclear 53Bp1 prior to the 8-cell stage, was unexpected. It was hypothesized that the absence of 53Bp1 might be due to the inadequate global methylation status of H4K20 as 53Bp1 recruitment to chromatin sites of dsDNA damage requires the dimethylation H4K20 (Botuyan et al., 2006). Indeed, evaluation of H4K20me2 status revealed that H4K20 was dimethylated only from the 8-cell stage onwards, consistent with this hypothesis. Beyond the 8-cell stage the distribution of 53Bp1 was consistent with γH2AX, as would be expected if the foci were a result of the activation of the DDR pathway. Moreover, the distribution of an additional DDR factor, Mdc1, characterised for the first time in this study, was also found to show co-localisation with γH2AX at all stages. These findings suggest that a basal constitutive activation of the DDR pathway occurs during apparently normal pre-implantation development in the cultured mouse embryo.

Evaluation of the literature revealed a paucity of systematic characterisations of the DDR in pre-implantation embryos. However, one study identified was of particular relevance because it specifically characterised the distribution of 53Bp1 and γH2AX throughout the pre-implantation mouse embryo in the absence of induced DNA damage (Ziegler-Birling et al., 2009). For γH2AX this study revealed comparable, but not identical, findings to the results presented in this thesis. Similarly high basal levels of γH2AX were described throughout all pre-implantation stages, likewise with the exception of the 2-cell stage where it was also shown that basal levels were minimal. Based upon the assessment of the H2AX levels (in the absence of phosphorylation) the authors concluded that the 2-cell stage-specific reduction in γH2AX was not secondary to reduction in the actual level of H2AX itself. The findings for 53Bp1 distribution were somewhat different than this thesis (Ziegler-Birling et al., 2009). In that study 53Bp1 was determined to be nuclear from the 2-cell stage with enrichment occurring from the 8-cell stage. From the morula stage and blastocyst stage, 53Bp1 was identified only in the cytoplasm of the outer cells with complete exclusion from the inner cell population; a small minority of outer cells showed some nuclear 53Bp1

localisation. Further, there was minimal co-localisation of 53Bp1 with γH2AX foci. The differences between this published study and the work presented in this theses are likely secondary to experimental variations. In the published study embryos were recovered fresh from natural matings, in contrast to this thesis where embryos were obtained following super-ovulation, and cultured *in vitro* from the 2-cell stage (with the exception of zygotes which were recovered fresh). Although it is possible that super-ovulation and *in vitro* culture may affect the distribution of γH2AX and 53Bp1 this was deemed unlikely based upon pilot studies conducted during the course of this thesis; E3.5 blastocysts obtained following natural matings and *in vivo* culture were evaluated and appeared identical to the findings in the superovulated, *in vitro* cultured embryos. It is most likely that the source of most differences between the two findings lie in the imaging techniques, and for 53Bp1 the IF protocol. For the purposes of this study it was essential to optimise a stringent imaging regime that would later be used for quantitative analysis of DDR foci. As discussed in section 4.3.3.3, during optimisation it was noted that the images were exquisitely sensitive to imaging conditions. Attempts to image throughout the entire 3D structure of the embryo were abandoned in favour of fewer, higher quality single planes, due to vast differences in images acquired from the same embryo between the upper and lower-most z-plane. In addition, to capture images of reasonable quality for the detection of well-defined foci, the application of averaging function was essential. Imaging for 53Bp1 was particularly demanding due to high levels of background noise; frame averages of 16 times were required to generate images of sufficient quality to clearly demarcate foci from background signal noise. Precise imaging details were not given in the published paper, however in all cases the images are presented as projections of serial z-stacks (Ziegler-Birling et al., 2009). However, despite some differences in overall findings both the published study and this thesis found the basal γH2AX levels remarkable. Zeigler-Birling *et al.* speculated that their findings may be unrelated to DNA damage and instead be reflective of the genome-wide chromatin remodelling that occurs during the epigenetic reprogramming characteristic of pre-implantation development. This hypothesis is plausible and indeed the differences in DDR foci between ICM and TE lineages in this thesis from the blastocyst stage onwards were notable (as assessed by Mdc1 foci in the TE and ICM in section 4.3.4). Non DNA damage-related populations of small γH2AX foci have previously been described in cultured

mammalian cell lines (McManus and Hendzel, 2005). Their exact function remains speculative but is considered to be distinct from DNA damage due to the absence of other associated DDR factors. However, the detailed imaging protocol in this thesis revealed that the majority of larger γH2AX foci in mouse blastomeres were associated with both Mdc1 foci, and with 53Bp1 foci beyond the 8-cell stage (with the earlier absence due to the stage-specific methylation status of H4K20). Therefore the co-localisation of γH2AX with both 53Bp1 and Mdc1 is highly suggestive of constitutive activation of the DDR pathway in the pre-implantation embryo, in the absence of externally induced DNA damage. However, whether this is a response to endogenously arising dsDNA damage or an alternative unknown trigger remains unclear. That the pre-implantation embryo genome may naturally be in a state of constant damage and repair seems unlikely. Unfortunately, a detailed investigation into these interesting findings was beyond the scope of this study.

Despite these unexpected findings, a series of experiments exposing embryos to different doses of IR to induce dsDNA damage did confirm that embryos underwent the expected response of an increase in DDR foci and cell-cycle delay/ checkpoint activation. Therefore the DNA-damage hypothesis could be investigated.

The experiments described in this chapter found no evidence to suggest that acute chromosome segregation errors occurring in pre-implantation blastomeres resulted in DNA damage, either as a consequence of cleavage furrow-generated forces during cytokinesis (Janssen et al., 2011) or through defective replication and repair within the micronuclei (Crasta et al., 2012). It is possible that the high levels of DDR foci found within the pre-implantation embryo may have masked small increases in DDR foci arising secondary to chromosome missegregation with the resolution of the imaging assay insufficiently sensitive to detect the difference. To exclude this possibility the effect on the cell-cycle was also evaluated, as dsDNA breaks result in activation of checkpoint kinases causing transient cell-cycle arrest (Jackson and Bartek, 2009). Re-evaluation of the time-lapse imaging movies presented in the preceding chapter revealed no evidence of transient cell-cycle arrest in reversine-treated blastomeres at the 16- to 32 cell division (the first division following the induction of chromosome missegregation), compared to control blastomeres in chimeric embryos.

Thus there was no evidence of DNA damage arising as a consequence of chromosome missegregation errors in the pre-implantation embryo. Although these findings were in contrast to several studies in other model systems, as discussed in section 4.1, other studies have also failed to demonstrate the occurrence of DNA damage in association with chromosome missegregation (Burds et al., 2005, Thompson and Compton, 2010, Li et al., 2010). In colorectal cancer HCT116 cells chromosome missegregation resulted in a p53-mediated limitation of proliferation without any accompanying increase in γH2AX foci (Thompson and Compton, 2010). Likewise, Li *et al.* also demonstrated a p53-mediated response to aneuploidy in SAC-inactivated MEF cells, resulting in poor proliferation and apoptotic cell death with no evidence of elevated γH2AX foci (Li et al., 2010). Interestingly, this study also found elevated levels of ROS and increased glucose consumption similar to the findings in the chronic aneuploidy studies previously discussed (Torres et al., 2007, Williams et al., 2008). Finally, MEF cells derived from *Mad2*$^{-/-}$*p53*$^{-/-}$ embryos also showed no increase in γH2AX levels despite high levels of chromosome missegregation (Burds et al., 2005). Therefore it is likely that different cell types respond to acute chromosome missegregation in different ways, with some more susceptible to DNA breakage than others. In those cells which do not accumulate DNA damage it is likely that other physiological responses contribute to the poor proliferation or elimination of aneuploid cells. Notably in these three studies that did not find any evidence of DNA damage, all demonstrated an important role for p53 in inhibiting the proliferation of aneuploid cells (Burds et al., 2005, Thompson and Compton, 2010, Li et al., 2010). The study by Burds *et al.* was of particular interest, as it showed that the early embryonic lethality in *Mad2*$^{-/-}$ embryos could be postponed by the additional deletion of *p53* (Burds et al., 2005). As discussed previously in the Introduction chapter, it is most likely that the embryonic lethal phenotype is a direct consequence of aneuploidy arising due to SAC deficiency secondary to the absence of Mad2. It would be interesting to determine if the outcome of reversine-treated embryos would be any different if carried out on a *p53* null genetic background.

When micronuclei induced by reversine-treatment were specifically assessed for DDR factors it was noted that Mdc1 only co-localised with γH2AX in 9% of cases, in stark contrast to the consistent co-localisation found within the main nuclei of both treated and control blastomeres. The deficient recruitment of DDR factors to DNA damage within micronuclei

has previously been described in cell culture studies and it has been proposed that this is a consequence of defective nucleo-cytoplasmic transport of DDR factors through the micronuclear envelope (Terradas et al., 2010, Terradas et al., 2012, Crasta et al., 2012). If micronuclei contain damaged chromatin this phenomenon could have a significant detrimental impact upon the genetic constitution of the cell as a result of ineffective DNA repair (Terradas et al., 2010, Terradas et al., 2012). Although there was no evidence of acutely arising DNA damage in micronuclei in this study, it is still possible that the lack of recruitment of Mdc1 to sites of γH2AX may have a detrimental effect on the cell. This may be of particular relevance for cells that missegregate their chromosomes but do not become aneuploid, for example when a lagging chromosome segregates to the correct daughter cell but becomes encapsulated in a micronucleus and remains as a separate entity from the main nucleus. However, until the role of the high basal levels of DDR factors in the pre-implantation embryo is established, it is not possible to determine exactly what that effect may be.

4.4.3 Investigating additional potential causes of apoptosis within the ICM

In the previous chapter it was shown that cells undergoing apoptosis within the ICM were significantly more likely to arise from the clone with a previous history of chromosome missegregation. However, 20% of the control ICM cells also underwent apoptosis. The occurrence of apoptosis within the ICM during blastocyst cavity expansion is well documented (Copp, 1978, Hardy et al., 1989). Although environmental factors such as *in vitro* culture and hyperglycaemia can increase the rates of apoptosis, it also occurs during *in vivo* development (Pampfer and Donnay, 1999).

It is possible that cells within the control clone may also have harboured aneuploidies which were then eliminated by apoptosis. This hypothesis is currently under investigation in collaboration with Dr Thierry Voet and the results are awaited (May 2013).

However, other hypotheses unrelated to aneuploidy have also been proposed to account for this phenomenon and these were investigated in a series of experiments.

Having developed an assay to evaluate DDR foci levels in pre-implantation embryos this assay was applied in order to determine if DNA damage could be a significant cause of ICM apoptosis *in vitro* cultured mouse embryos. There was a small but highly significant difference in the mean number of Mdc1 foci within the ICM of embryos cultured in the presence of an apoptosis inhibitor. Within the TE lineage the foci levels were comparable with controls. Evaluating the distribution of the number of foci per ICM cell within that apoptosis-inhibited group did not reveal a subpopulation of cells containing high levels of Mdc1 foci above which were not present within the control group; a finding which may have been expected if there was a threshold of damage above which cells underwent apoptosis. It was thus concluded that dsDNA damage itself is unlikely to be the major cause of ICM apoptosis, although it may be responsible for some limited instances.

During these experiments it was also noted that a minority of embryos contained ICM cells expressing Cdx2 protein, a TE-specific transcription factor. If apoptosis was a means by which embryos eliminated ICM cells that retained the potential to differentiate into TE it was figured that apoptosis-inhibited embryos may harbour greater numbers of Cdx2-positive ICM cells than controls. This was not found to be the case. This finding was in contrast to a previous study that investigated this hypothesis using a different experimental approach (Pierce et al., 1989). Two different strains of murine embryonal carcinoma cells with differing TE-potentials were injected into the cavity of giant blastocysts (created by aggregating several embryos together), thus exposing the cells to blastocoel fluid. Injected cells derived from the clone with TE potential were significantly more likely to undergo apoptosis within the cavity than those without TE potential. However the relevance of these findings to the developing embryos is questionable due to the unphysiological experimental system used to investigate the hypothesis. It is possible that the experimental design of the study presented in this thesis was unable to detect all ICM cells with TE-potential, as it could be that some retain TE-potential without expressing Cdx2 or other TE-specific transcription factors.

The work presented in the previous chapter represents the first study to demonstrate that apoptosis has a direct role in the elimination of aneuploid cells from the ICM lineage of the mammalian blastocyst. Whether aneuploidy accounts for the majority of ICM apoptosis that is observed during unperturbed development remains to be determined. In the

absence of strong experimental evidence in support of other hypotheses accounting for ICM apoptosis in control blastocysts, the results of the ICM array-based karyotyping experiments conducted in control and apoptosis-inhibited ICM will be most enlightening.

CONCLUDING REMARKS

The major aim of this thesis was to develop a mouse model for acutely arising diploid-aneuploid chromosome mosaicism in the pre-implantation embryo. This model was then to be used to investigate the fate of abnormal cells within the developing embryo, and to determine the ultimate developmental potential of mosaic embryos**.**

The work described in Results I characterised the development of a mouse model for acutely arising diploid-aneuploid chromosome mosaicism in the pre-implantation embryo. This is the first mouse model of its kind to be developed and offered a unique opportunity to probe the fate of abnormal cells and mosaic embryos during development. Research on human pre-implantation embryos is constrained by practical and ethical limitations, and there is a dearth of alternative models suitable for research. Given that *in-vitro* fertilization (IVF) is now a routine treatment option for sub-fertility, there is a pressing need for the development of relevant animal models. Moreover, using animal models bypasses the majority of ethical issues associated with human research; opening up the range of experiments that are possible. Additionally, the mouse offers unique advantages due to its relatively low research costs, the availability of large numbers of embryos, and the potential for genetic manipulation; characteristics that were exploited during this thesis.

The work presented in Results Chapter II utilized this mouse model to explore the fate of chromosomally abnormal cells in mosaic embryos. Time-lapse imaging revealed that abnormal cells were progressively depleted from the pre-implantation embryo during blastocyst maturation. Moreover, it was directly demonstrated that inner cell mass (ICM) cells with chromosome abnormalities exhibited higher rates of apoptosis than controls, and that abnormal cells within the trophectoderm (TE) lineage were more likely to exhibit prolonged cell-cycle lengths or arrest. This study provides the first direct evidence that ICM cells containing chromosome abnormalities are subject to higher rates of apoptosis during pre-implantation development. The potential role of apoptosis in eliminating cells with chromosome abnormalities has frequently been speculated upon, but until now has never been demonstrated (Hardy, 1997, Pampfer and Donnay, 1999, Fabian et al., 2005). Taken together, these findings provide direct evidence for the clonal normalisation hypothesis

(section 1.3.4.3 and Figure 1.4), whereby the euploid clone of cells has an advantage over the abnormal clone ultimately resulting in depletion of the abnormal clones from the developing embryo. The depletion of abnormal clones from the embryos emerged during the maturation of the blastocyst; however the majority of depletion occurred following implantation. These results suggest that the early pre-implantation embryo is relatively tolerant of chromosome abnormalities and that regulation occurs pre-dominantly at or after implantation. The post-implantation studies confirmed on-going depletion of abnormal clones as development proceeded.

The unique application of time-lapse imaging technology also demonstrated directly that there was no evidence to support the hypothesis that aneuploid cells are preferentially allocated to the TE-lineage during pre-implantation development (section 1.3.4.3 and Figure 1.4); a finding that added support to previous observational studies in the human embryos that had provided indirect evidence against this hypothesis (Evsikov and Verlinsky, 1998, Magli et al., 2000, Derhaag et al., 2003, Johnson et al., 2010, Northrop et al., 2010). In addition, the time-lapse imaging experiments evaluating the development of diploid-tetraploid mosaic embryos demonstrated that tetraploid cells behave altogether differently from aneuploid cells; tetraploid cells were preferentially allocated to the TE lineage through the increased frequency of symmetric divisions at the time of the first cell-fate decision in cleavage stage embryos. The fate of tetraploid cells in diploid-tetraploid mosaic embryos has been cited as evidence for the development of confined placental mosaicism (CPM) (Mackay and West, 2005). Given that the cells in CPM are aneuploid rather than tetraploid, the findings of this study demonstrate conclusively that diploid-tetraploid mosaicism is not a suitable model for CPM. Moreover, if next generation pre-implantation genetic screening (PGS) approaches are to focus on blastocyst (and hence TE) biopsy, this study adds further evidence that the chromosome status of the TE cell is representative of the ICM lineage.

A key finding in Results II was the rescue of embryonic lethality by the presence of control blastomeres within the pre-implantation embryo, with the effectiveness of rescue determined by the number of control blastomeres present. Based on these results it was hypothesized that the presence of chromosomally abnormal cells may act as ‘carrier cells’ that actually serve to maximise the developmental potential of the mosaic embryo by increasing the likelihood that the epiblast population attains the critical number of euploid

cells required for on-going development. It is speculated that this finding may be of clinical significance when viewed in the context of embryo biopsy and PGS, and potentially an underlying cause of why cleavage stage embryo biopsy was found to detrimental to IVF success rates in couples with a poor prognosis for IVF (Twisk et al., 2006, Mastenbroek et al., 2007). This finding also adds additional support for the current sea-change away from biopsy at the cleavage stage towards blastocyst biopsy, when removal of cells has less impact on the overall constitution of the embryo.

Results III focused on identifying the potential mechanisms underlying the elimination of the chromosomally abnormal cells from the developing embryo. No such study has previously been undertaken in the pre-implantation embryo. Therefore hypotheses were proposed based upon a review of published literature investigating aneuploidy in the context of cancer, and focussed on the potential role of an 'aneuploidy stress response' or the possibility of acutely arising double-stranded DNA (dsDNA) damage following chromosome missegregation (section 4.1 & Figure 4.1). This study found no evidence of activation of the DNA damage response (DDR) following chromosome missegregation in embryos and thus this hypothesis was rejected. However, during investigation of the DNA damage hypothesis it was found that there was a degree of basal activity of the DDR pathway in the pre-implantation embryo in the absence of externally arising DNA damage. This finding was unexpected and it remains unknown if this activation was related to underlying DNA damage or an alternative, as yet undermined, reason.

A detailed study of the aneuploidy stress response was constrained by the limited developmental time-frame and the small number of cells in pre-implantation embryo. However this study revealed that embryos harbouring increased levels of aneuploidy (induced by reversine treatment) fared less well than control embryos, when cultured in media with fewer energy sources, as determined by a small but significant depletion in their cell number during blastocyst cavity expansion. This suggests that aneuploidy arising during pre-implantation development may result in increased metabolic demands, similar to the characteristics of the aneuploidy stress response. If so, it is likely that these effects may accumulate over time and manifest as poor proliferation. Implantation is associated with a burst of cellular proliferation and thus increased energy requirements. This study found that the embryonic lethality associated with reversine treatment (and thus aneuploidy) occurred

at the peri- / early post-implantation stage of development; notably coinciding with the time of rapid proliferation and growth in the embryo. Thus it is possible that the impact of the metabolic consequences of aneuploidy is minimal during pre-implantation development, and perhaps explains why a firm link between aneuploidy and metabolic imbalances has never been established in the human embryo. Recently, significant progress has been achieved in establishing *in vitro* culture systems and consequently improving accessibility to embryos at the time of implantation (Morris et al., 2012a). In the future the application of such *in vitro* culture systems may provide the opportunity to investigate this hypothesis in greater detail.

Overall the development of a novel mouse model for pre-implantation diploid-aneuploid mosaicism in this thesis has enabled valuable insights to be gained for the first time into the developmental outcomes and consequences of mosaicism. Such studies would not be possible in the human embryo, and to date have not been conducted in other mammalian embryos. The direct findings of this thesis are in keeping with indirect observational evidence gained from studies in human embryos, most notably that aneuploid cells become depleted from the embryo as development progresses from the cleavage to blastocyst stage (Evsikov and Verlinsky, 1998, Clouston et al., 2002, Coonen et al., 2004, Santos et al., 2010, Johnson et al., 2010, Capalbo et al., 2012), that aneuploid cells are not preferentially allocated to the TE lineage (Evsikov and Verlinsky, 1998, Magli et al., 2000, Derhaag et al., 2003, Johnson et al., 2010, Northrop et al., 2010) and that the diploid-aneuploid mosaic embryos can be associated with full developmental potential (Vanneste et al., 2009, Mertzanidou et al., 2013). In addition, the findings in this study were also consistent with those in mouse embryo models of chromosomal instability (CIN) (Kalitsis et al., 1998, Howman et al., 2000, Kalitsis et al., 2000, Dobles et al., 2000, Putkey et al., 2002, Wang et al., 2004a, Lightfoot et al., 2006, Jeganathan et al., 2007, Iwanaga et al., 2007), and shared characteristic features associated with aneuploidy in cultured cells lines including poor proliferation and apoptosis (Thompson and Compton, 2010, Li et al., 2010).

However, a notable key difference between the mouse and human embryos was the finding that the induction of aneuploidy in the mouse embryo did not result in increased rates of arrested development or abnormal morphology such as fragmentation and irregular blastomere size; features typically associated human embryo development. One recent

publication utilized time-lapse imaging to study the developmental characteristics of human embryos from the zygote to the 4-cell stage (Chavez et al., 2012). This study reported high levels of cellular fragmentation, often arising during interphase, amongst embryos that were found to be aneuploid when evaluated at the 4-cell stage. Many of these fragments contained chromatin. Cellular fragments exhibited a range of different dynamics as development proceeded; some remained as fragments, some re-adsorbed into their blastomere of origin, while others fused with neighbouring blastomeres. Based upon these findings, the authors proposed that fragmentation may occur as a response to acutely arising aneuploidy in the human embryo and speculated that this phenomenon could be a survival mechanism. In brief, their hypothesis proposed that the embryo responds to misaligned or lagging chromosomes that arise during mitosis by encapsulating the chromosome within a micronucleus that then forms a cellular fragment. The cellular fragment may resorb during interphase and thus restore the ploidy status of the blastomere back to normal. If resorption does not occur or if the fragment fuses with the wrong blastomere the result will be the generation of complex aneuploidies and compromised development (Chavez et al., 2012). However, cellular fragmentation is not a typical response to acutely arising aneuploidy secondary to lagging chromosomes or abrogation of the spindle assembly checkpoint (SAC) in a range of human or mouse cell culture lines. Likewise, the pre-implantation mouse embryos studied in this thesis did not exhibit fragmentation following the induction of high levels of chromosome missegregation, consistent with the mouse models of CIN (Kalitsis et al., 1998, Howman et al., 2000, Kalitsis et al., 2000, Dobles et al., 2000, Putkey et al., 2002, Wang et al., 2004a, Lightfoot et al., 2006, Jeganathan et al., 2007, Iwanaga et al., 2007). Consequently, until more direct experimental evidence is presented, the hypothesis proposed above remains speculative (Chavez et al., 2012). An alternative hypothesis may be that aneuploidy arises as an indirect consequence of a yet uncharacterized aberration in the human embryo that itself could be responsible for high rates of embryo arrest and blastomere fragmentation that ultimately contributes to the poor success rate of IVF.

Thus while the mouse model developed in this thesis has provided new and valuable insights into the developmental fate of diploid-aneuploid mosaic embryos, there is still a clear necessity for additional models to be developed in order to dissect the underlying

causes for responsible for aneuploidy, fragmentation and embryo arrest. More research on non-murine mammalian embryos that share greater similarities with the human, such as the cow or non-human primates, may be further enlightening. Given that IVF treatment is now increasingly offered as routine treatment option for couples experiencing subfertility throughout the world, the need for such research is even greater now than ever before.

BIBLIOGRAPHY

ABRIEU, A., MAGNAGHI-JAULIN, L., KAHANA, J. A., PETER, M., CASTRO, A., VIGNERON, S., LORCA, T., CLEVELAND, D. W. & LABBE, J. C. 2001. Mps1 is a kinetochore-associated kinase essential for the vertebrate mitotic checkpoint. *Cell,* 106**,** 83-93.

ADIGA, S. K., TOYOSHIMA, M., SHIMURA, T., TAKEDA, J., UEMATSU, N. & NIWA, O. 2007. Delayed and stage specific phosphorylation of H2AX during preimplantation development of gamma-irradiated mouse embryos. *Reproduction,* 133**,** 415-22.

AIKEN, C. E., SWOBODA, P. P., SKEPPER, J. N. & JOHNSON, M. H. 2004. The direct measurement of embryogenic volume and nucleo-cytoplasmic ratio during mouse pre-implantation development. *Reproduction,* 128**,** 527-35.

ALFARAWATI, S., FRAGOULI, E., COLLS, P., STEVENS, J., GUTIERREZ-MATEO, C., SCHOOLCRAFT, W. B., KATZ-JAFFE, M. G. & WELLS, D. 2011. The relationship between blastocyst morphology, chromosomal abnormality, and embryo gender. *Fertil Steril,* 95**,** 520-4.

AMBARTSUMYAM, G. & CLARKE, A. T. 2008. Aneuploidy & early human embryo development. *Human Molecular Genetics,* 17**,** R10-16.

ANGELL, R. R., AITKEN, R. J., VAN LOOK, P. F., LUMSDEN, M. A. & TEMPLETON, A. A. 1983. Chromosome abnormalities in human embryos after in vitro fertilization. *Nature,* 303**,** 336-8.

ANGELL, R. R., SUMNER, A. T., WEST, J. D., THATCHER, S. S., GLASIER, A. F. & BAIRD, D. T. 1987. Post-fertilization polyploidy in human preimplantation embryos fertilized in-vitro. *Hum Reprod,* 2**,** 721-7.

BAART, E. B., MARTINI, E., EIJKEMANS, M. J., VAN OPSTAL, D., BECKERS, N. G., VERHOEFF, A., MACKLON, N. S. & FAUSER, B. C. 2007a. Milder ovarian stimulation for in-vitro fertilization reduces aneuploidy in the human preimplantation embryo: a randomized controlled trial. *Hum Reprod,* 22**,** 980-8.

BAART, E. B., MARTINI, E., VAN DEN BERG, I., MACKLON, N. S., GALJAARD, R. J., FAUSER, B. C. & VAN OPSTAL, D. 2006. Preimplantation genetic screening reveals a high incidence of aneuploidy and mosaicism in embryos from young women undergoing IVF. *Hum Reprod,* 21**,** 223-33.

BAART, E. B., VAN DEN BERG, I., MARTINI, E., EUSSEN, H. J., FAUSER, B. C. & VAN OPSTAL, D. 2007b. FISH analysis of 15 chromosomes in human day 4 and 5 preimplantation embryos: the added value of extended aneuploidy detection. *Prenat Diagn,* 27**,** 55-63.

BACHVAROVA, R. & DE LEON, V. 1980. Polyadenylated RNA of mouse ova and loss of maternal RNA in early development. *Dev Biol,* 74**,** 1-8.

BAKER, D. J., JEGANATHAN, K. B., CAMERON, J. D., THOMPSON, M., JUNEJA, S., KOPECKA, A., KUMAR, R., JENKINS, R. B., DE GROEN, P. C., ROCHE, P. & VAN DEURSEN, J. M. 2004. BubR1 insufficiency causes early onset of aging-associated phenotypes and infertility in mice. *Nat Genet,* 36**,** 744-9.

BARBASH-HAZAN, S., FRUMKIN, T., MALCOV, M., YARON, Y., COHEN, T., AZEM, F., AMIT, A. & BEN-YOSEF, D. 2009. Preimplantation aneuploid embryos undergo self-correction in correlation with their developmental potential. *Fertil Steril,* 92**,** 890-6.

BARTEK, J. & LUKAS, J. 2007. DNA damage checkpoints: from initiation to recovery or adaptation. *Curr Opin Cell Biol,* 19**,** 238-45.

BEAN, C. J., HASSOLD, T. J., JUDIS, L. & HUNT, P. A. 2002. Fertilization in vitro increases non-disjunction during early cleavage divisions in a mouse model system. *Hum Reprod,* 17**,** 2362-7.

BEKKER-JENSEN, S. & MAILAND, N. 2010. Assembly and function of DNA double-strand break repair foci in mammalian cells. *DNA Repair (Amst),* 9**,** 1219-28.

BIANCOTTI, J. C., NARWANI, K., BUEHLER, N., MANDEFRO, B., GOLAN-LEV, T., YANUKA, O., CLARK, A., HILL, D., BENVENISTY, N. & LAVON, N. 2010. Human embryonic stem cells as models for aneuploid chromosomal syndromes. *Stem Cells,* 28**,** 1530-40.

BISCHOFF, M., D.E., P. & ZERNICKA-GOETZ, M. 2008. Formation of the embryonic-abembryonic axis of the mouse blastocyst: relationships between orientation of early cleavage divisions and pattern of symmetric/asymmetric divisions. *Development,* 135**,** 953-62.

BOISO, I., VEIGA, A. & EDWARDS, R. G. 2002. Fundamentals of human embryonic growth in vitro and the selection of high-quality embryos for transfer. *Reprod Biomed Online,* 5**,** 328-50.

BOND, D. & CHANDLEY, A. 1983. *Aneuploidy,* Oxford, Oxford University Press.

BOTUYAN, M. V., LEE, J., WARD, I. M., KIM, J. E., THOMPSON, J. R., CHEN, J. & MER, G. 2006. Structural basis for the methylation state-specific recognition of histone H4-K20 by 53BP1 and Crb2 in DNA repair. *Cell,* 127**,** 1361-73.

BRAUDE, P., BOLTON, V. & MOORE, S. 1988. Human gene expression first occurs between the four- and eight-cell stages of preimplantation development. *Nature,* 332**,** 459-61.

BRAUDE, P., PELHAM, H., FLACH, G. & LOBATTO, R. 1979. Post-transcriptional control in the early mouse embryo. *Nature,* 282**,** 102-5.

BRISON, D. R. & SCHULTZ, R. M. 1997. Apoptosis during mouse blastocyst formation: evidence for a role for survival factors including transforming growth factor alpha. *Biol Reprod,* 56**,** 1088-96.

BRUNET-SIMON, A., HENRION, G., RENARD, J. P. & DURANTHON, V. 2001. Onset of zygotic transcription and maternal transcript legacy in the rabbit embryo. *Mol Reprod Dev,* 58**,** 127-36.

BURDS, A. A., LUTUM, A. S. & SORGER, P. K. 2005. Generating chromosome instability through the simultaneous deletion of Mad2 and p53. *Proc Natl Acad Sci U S A,* 102**,** 11296-301.

CANMAN, J. C., SALMON, E. D. & FANG, G. 2002. Inducing precocious anaphase in cultured mammalian cells. *Cell Motil Cytoskeleton,* 52**,** 61-5.

CAPALBO, A., BONO, S., SPIZZICHINO, L., BIRICIK, A., BALDI, M., COLAMARIA, S., UBALDI, F. M., RIENZI, L. & FIORENTINO, F. 2012. Sequential comprehensive chromosome analysis on polar bodies, blastomeres and trophoblast: insights into female meiotic errors and chromosomal segregation in the preimplantation window of embryo development. *Hum Reprod*.

CHAVEZ, S. L., LOEWKE, K. E., HAN, J., MOUSSAVI, F., COLLS, P., MUNNE, S., BEHR, B. & REIJO PERA, R. A. 2012. Dynamic blastomere behaviour reflects human embryo ploidy by the four-cell stage. *Nat Commun,* 3**,** 1251.

CHEESEMAN, I. M. & DESAI, A. 2008. Molecular architecture of the kinetochore-microtubule interface. *Nat Rev Mol Cell Biol,* 9**,** 33-46.

CHEN, S., TAKANASHI, S., ZHANG, Q., XIONG, W., ZHU, S., PETERS, E. C., DING, S. & SCHULTZ, P. G. 2007. Reversine increases the plasticity of lineage-committed mammalian cells. *Proc Natl Acad Sci U S A,* 104**,** 10482-7.

CHEN, S., ZHANG, Q., WU, X., SCHULTZ, P. G. & DING, S. 2004. Dedifferentiation of lineage-committed cells by a small molecule. *J Am Chem Soc,* 126**,** 410-1.

CICCIA, A. & ELLEDGE, S. J. 2010. The DNA damage response: making it safe to play with knives. *Mol Cell,* 40**,** 179-204.

CIFERRI, C., MUSACCHIO, A. & PETROVIC, A. 2007. The Ndc80 complex: hub of kinetochore activity. *FEBS Lett,* 581**,** 2862-9.

CIMINI, D., HOWELL, B., MADDOX, P., KHODJAKOV, A., DEGRASSI, F. & SALMON, E. D. 2001. Merotelic kinetochore orientation is a major mechanism of aneuploidy in mitotic mammalian tissue cells. *J Cell Biol,* 153**,** 517-27.

CLOUSTON, H. J., FENWICK, J., WEBB, A. L., HERBERT, M., MURDOCH, A. & WOLSTENHOLME, J. 1997. Detection of mosaic and non-mosaic chromosome abnormalities in 6- to 8-day old human blastocysts. *Hum Genet,* 101**,** 30-6.

CLOUSTON, H. J., HERBERT, M., FENWICK, J., MURDOCH, A. P. & WOLSTENHOLME, J. 2002. Cytogenetic analysis of human blastocysts. *Prenat Diagn,* 22**,** 1143-52.

COCKBURN, K. & ROSSANT, J. 2010. Making the blastocyst: lessons from the mouse. *J Clin Invest,* 120**,** 995-1003.

COHEN, J., WELLS, D. & MUNNE, S. 2007. Removal of 2 cells from cleavage stage embryos is likely to reduce the efficacy of chromosomal tests that are used to enhance implantation rates. *Fertil Steril,* 87**,** 496-503.

CONLIN, L. K., THIEL, B. D., BONNEMANN, C. G., MEDNE, L., ERNST, L. M., ZACKAI, E. H., DEARDORFF, M. A., KRANTZ, I. D., HAKONARSON, H. & SPINNER, N. B. 2010. Mechanisms of mosaicism, chimerism and uniparental disomy identified by single nucleotide polymorphism array analysis. *Hum Mol Genet,* 19**,** 1263-75.

COONEN, E., DERHAAG, J. G., DUMOULIN, J. C., VAN WISSEN, L. C., BRAS, M., JANSSEN, M., EVERS, J. L. & GERAEDTS, J. P. 2004. Anaphase lagging mainly explains chromosomal mosaicism in human preimplantation embryos. *Hum Reprod,* 19**,** 316-24.

COPP, A. J. 1978. Interaction between inner cell mass and trophectoderm of the mouse blastocyst. I. A study of cellular proliferation. *J Embryol Exp Morphol,* 48**,** 109-25.

CRASTA, K., GANEM, N. J., DAGHER, R., LANTERMANN, A. B., IVANOVA, E. V., PAN, Y., NEZI, L., PROTOPOPOV, A., CHOWDHURY, D. & PELLMAN, D. 2012. DNA breaks and chromosome pulverization from errors in mitosis. *Nature,* 482**,** 53-8.

CRUZ, M., GADEA, B., GARRIDO, N., PEDERSEN, K. S., MARTINEZ, M., PEREZ-CANO, I., MUNOZ, M. & MESEGUER, M. 2011. Embryo quality, blastocyst and ongoing pregnancy rates in oocyte donation patients whose embryos were monitored by time-lapse imaging. *J Assist Reprod Genet,* 28**,** 569-73.

CUI, X. S., SHEN, X. H. & KIM, N. H. 2007. Dicer1 expression in preimplantation mouse embryos: Involvement of Oct3/4 transcription at the blastocyst stage. *Biochem Biophys Res Commun,* 352**,** 231-6.

CURLEJ, J., BULLA, J. & CHRENEK, P. 2010. Occurrence of chromosomal aneuploidy in rabbit oocytes and embryos at different developmental stages. *Zygote,* 18**,** 203-7.

DALTON, W. B., NANDAN, M. O., MOORE, R. T. & YANG, V. W. 2007. Human cancer cells commonly acquire DNA damage during mitotic arrest. *Cancer Res,* 67**,** 11487-92.

DAPHNIS, D. D., DELHANTY, J. D., JERKOVIC, S., GEYER, J., CRAFT, I. & HARPER, J. C. 2005. Detailed FISH analysis of day 5 human embryos reveals the mechanisms leading to mosaic aneuploidy. *Hum Reprod,* 20**,** 129-37.

DE BOER, K. A., CATT, J. W., JANSEN, R. P., LEIGH, D. & MCARTHUR, S. 2004. Moving to blastocyst biopsy for preimplantation genetic diagnosis and single embryo transfer at Sydney IVF. *Fertil Steril,* 82**,** 295-8.

DE VOS, A., STAESSEN, C., DE RYCKE, M., VERPOEST, W., HAENTJENS, P., DEVROEY, P., LIEBAERS, I. & VAN DE VELDE, H. 2009. Impact of cleavage-stage embryo biopsy in view of PGD on human blastocyst implantation: a prospective cohort of single embryo transfers. *Hum Reprod,* 24**,** 2988-96.

DELHANTY, J. & HANDYSIDE, A. 1995. The origin of genetic defects in the human and their detection in the preimplantation embryo. *Human Reproduction Update,* 1**,** 201-215.

DELHANTY, J. D., GRIFFIN, D. K., HANDYSIDE, A. H., HARPER, J., ATKINSON, G. H., PIETERS, M. H. & WINSTON, R. M. 1993. Detection of aneuploidy and chromosomal mosaicism in human embryos during preimplantation sex determination by fluorescent in situ hybridisation, (FISH). *Hum Mol Genet,* 2**,** 1183-5.

DERHAAG, J. G., COONEN, E., BRAS, M., BERGERS JANSSEN, J. M., IGNOUL-VANVUCHELEN, R., GERAEDTS, J. P., EVERS, J. L. & DUMOULIN, J. C. 2003. Chromosomally abnormal cells are not selected for the extra-embryonic compartment of the human preimplantation embryo at the blastocyst stage. *Hum Reprod,* 18**,** 2565-74.

DEVLIN, L. & MORRISON, P. 2004. Mosaic Down's sydrome prevalence in a complete population study. *Archives of Disease in Childhood,* 89**,** 1177-1178.

DOBLES, M., LIBERAL, V., SCOTT, M. L., BENEZRA, R. & SORGER, P. K. 2000. Chromosome missegregation and apoptosis in mice lacking the mitotic checkpoint protein Mad2. *Cell,* 101**,** 635-45.

DONOSO P, S. C., FAUSER BC, DEVROEY P 2007. Current value of preimplantation genetic aneuploidy screening in IVF. *Human Reproduction Update,* 13**,** 15 - 25.

DYCE, J., GEORGE, M., GOODALL, H. & FLEMING, T. P. 1987. Do trophectoderm and inner cell mass cells in the mouse blastocyst maintain discrete lineages? *Development,* 100**,** 685-98.

EAKIN, G. S. & BEHRINGER, R. R. 2003. Tetraploid development in the mouse. *Dev Dyn,* 228**,** 751-66.

EATON, J. L., HACKER, M. R., HARRIS, D., THORNTON, K. L. & PENZIAS, A. S. 2009. Assessment of day-3 morphology and euploidy for individual chromosomes in embryos that develop to the blastocyst stage. *Fertil Steril,* 91**,** 2432-6.

EGGAN, K., RODE, A., JENTSCH, I., SAMUEL, C., HENNEK, T., TINTRUP, H., ZEVNIK, B., ERWIN, J., LORING, J., JACKSON-GRUSBY, L., SPEICHER, M. R., KUEHN, R. & JAENISCH, R. 2002. Male and female mice derived from the same embryonic stem cell clone by tetraploid embryo complementation. *Nat Biotechnol,* 20**,** 455-9.

ELAIMI, A., GARDNER, K., KISTNAREDDY, K. & HARPER, J. 2012. The effect of GM-CSF on development and aneuploidy in murine blastocysts. *Hum Reprod,* 27**,** 1590-5.

EVERETT, C., KEIGHREN, M., FLOCKHART, J. & WEST, J. 2007. Evaluation of triploid<-->diploid and trisomy-3<-->diploid mouse chimeras as models for investigating how lineage restriction occurs in confined placental mosaicism. *Reproduction,* 134**,** 799-809.

EVERETT, C. A. & WEST, J. D. 1996. The influence of ploidy on the distribution of cells in chimaeric mouse blastocysts. *Zygote,* 4**,** 59-66.

EVERETT, C. A. & WEST, J. D. 1998. Evidence for selection against tetraploid cells in tetraploid<-->diploid mouse chimaeras before the late blastocyst stage. *Genetic Research,* 72**,** 225-228.

EVSIKOV, S. & VERLINSKY, Y. 1998. Mosaicism in the inner cell mass of human blastocysts. *Hum Reprod,* 13**,** 3151-5.

FABIAN, D., KOPPEL, J. & MADDOX-HYTTEL, P. 2005. Apoptotic processes during mammalian preimplantation development. *Theriogenology,* 64**,** 221-31.

FANG, X. & ZHANG, P. 2011. Aneuploidy and tumorigenesis. *Semin Cell Dev Biol,* 22**,** 595-601.

FAUSER, B. C. 2008. Preimplantation genetic screening: the end of an affair? *Hum Reprod,* 23**,** 2622-5.

FENECH, M. 2007. Cytokinesis-block micronucleus cytome assay. *Nat Protoc,* 2**,** 1084-104.

FISCH, J. D., RODRIGUEZ, H., ROSS, R., OVERBY, G. & SHER, G. 2001. The Graduated Embryo Score (GES) predicts blastocyst formation and pregnancy rate from cleavage-stage embryos. *Hum Reprod,* 16**,** 1970-5.

FISCHER, B., CHAVATTE-PALMER, P., VIEBAHN, C., NAVARRETE SANTOS, A. & DURANTHON, V. 2012. Rabbit as a reproductive model for human health. *Reproduction,* 144**,** 1-10.

FOIJER, F., DRAVIAM, V. M. & SORGER, P. K. 2008. Studying chromosome instability in the mouse. *Biochim Biophys Acta,* 1786**,** 73-82.

FORMAN, E. J., TAO, X., FERRY, K. M., TAYLOR, D., TREFF, N. R. & SCOTT, R. T., JR. 2012. Single embryo transfer with comprehensive chromosome screening results in improved ongoing pregnancy rates and decreased miscarriage rates. *Hum Reprod,* 27**,** 1217-22.

FRAGOULI, E., ALFARAWATI, S., DAPHNIS, D. D., GOODALL, N. N., MANIA, A., GRIFFITHS, T., GORDON, A. & WELLS, D. 2010. Cytogenetic analysis of human blastocysts with the use of FISH, CGH and aCGH: scientific data and technical evaluation. *Hum Reprod,* 26**,** 480-90.

FRAGOULI, E., LENZI, M., ROSS, R., KATZ-JAFFE, M., SCHOOLCRAFT, W. B. & WELLS, D. 2008. Comprehensive molecular cytogenetic analysis of the human blastocyst stage. *Hum Reprod,* 23**,** 2596-608.

FRITZ, B., HALLERMANN, C., OLERT, J., FUCHS, B., BRUNS, M., ASLAN, M., SCHMIDT, S., COERDT, W., MUNTEFERING, H. & REHDER, H. 2001. Cytogenetic analyses of culture failures by comparative genomic hybridisation (CGH)-Re-evaluation of chromosome aberration rates in early spontaneous abortions. *Eur J Hum Genet,* 9**,** 539-47.

FRUMKIN, T., MALCOV, M., YARON, Y. & BEN-YOSEF, D. 2008. Elucidating the origin of chromosomal aberrations in IVF embryos by preimplantation genetic analysis. *Mol Cell Endocrinol,* 282**,** 112-9.

GANEM, N. J. & PELLMAN, D. 2012. Linking abnormal mitosis to the acquisition of DNA damage. *J Cell Biol,* 199**,** 871-81.

GARDNER, R. L. 1997. The early blastocyst is bilaterally symmetrical and its axis of symmetry is aligned with the animal-vegetal axis of the zygote in the mouse. *Development,* 124**,** 289-301.

GARDNER, R. L. 2001. Specification of embryonic axes begins before cleavage in normal mouse development. *Development,* 128**,** 839-47.

GARSIDE, W. & HILLMAN, N. 1985. A method for karyotyping mouse blastocyst embryos developing from in vivo and in vitro fertilized eggs. *Experientia,* 41**,** 1183-4.

GIANAROLI, L., MAGLI, M. C., FERRARETTI, A. P. & MUNNE, S. 1999. Preimplantation diagnosis for aneuploidies in patients undergoing in vitro fertilization with a poor prognosis: identification of the categories for which it should be proposed. *Fertil Steril,* 72**,** 837-44.

GIUNTA, S., BELOTSERKOVSKAYA, R. & JACKSON, S. P. 2010. DNA damage signaling in response to double-strand breaks during mitosis. *J Cell Biol,* 190**,** 197-207.

GIUNTA, S. & JACKSON, S. P. 2011. Give me a break, but not in mitosis: the mitotic DNA damage response marks DNA double-strand breaks with early signaling events. *Cell Cycle,* 10**,** 1215-21.

GLEICHER, N. & BARAD, D. H. 2012. A review of, and commentary on, the ongoing second clinical introduction of preimplantation genetic screening (PGS) to routine IVF practice. *J Assist Reprod Genet,* 29**,** 1159-66.

GLEICHER, N., WEGHOFER, A. & BARAD, D. 2008. Preimplantation genetic screening: "established" and ready for prime time? *Fertil Steril,* 89**,** 780-8.

GLENISTER, P. H., WOOD, M. J., KIRBY, C. & WHITTINGHAM, D. G. 1987. Incidence of chromosome anomalies in first-cleavage mouse embryos obtained from frozen-thawed oocytes fertilized in vitro. *Gamete Res,* 16**,** 205-16.

GOOSSENS, V., DE RYCKE, M., DE VOS, A., STAESSEN, C., MICHIELS, A., VERPOEST, W., VAN STEIRTEGHEM, A., BERTRAND, C., LIEBAERS, I., DEVROEY, P. & SERMON, K. 2008. Diagnostic efficiency, embryonic development and clinical outcome after the biopsy of one or two blastomeres for preimplantation genetic diagnosis. *Hum Reprod,* 23**,** 481-92.

GORBSKY, G. J., CHEN, R. H. & MURRAY, A. W. 1998. Microinjection of antibody to Mad2 protein into mammalian cells in mitosis induces premature anaphase. *J Cell Biol,* 141**,** 1193-205.

GOTO, Y., MATSUI, J. & TAKAGI, N. 2002. Developmental potential of mouse tetraploid cells in diploid <--> tetraploid chimeric embryos. *Int J Dev Biol,* 46**,** 741-5.

GOTTESFELD, J. M. & FORBES, D. J. 1997. Mitotic repression of the transcriptional machinery. *Trends Biochem Sci,* 22**,** 197-202.

GUERIF, F., BIDAULT, R., CADORET, V., COUET, M. L., LANSAC, J. & ROYERE, D. 2002. Parameters guiding selection of best embryos for transfer after cryopreservation: a reappraisal. *Hum Reprod,* 17**,** 1321-6.

GUERRERO, A. A., MARTINEZ, A. C. & VAN WELY, K. H. 2010. Merotelic attachments and non-homologous end joining are the basis of chromosomal instability. *Cell Div,* 5**,** 13.

GUTIERREZ-MATEO, C., BENET, J., STARKE, H., OLIVER-BONET, M., MUNNE, S., LIEHR, T. & NAVARRO, J. 2005. Karyotyping of human oocytes by cenM-FISH, a new 24-colour centromere-specific technique. *Hum Reprod,* 20**,** 3395-401.

HADJANTONAKIS, A. K. & PAPAIOANNOU, V. E. 2004. Dynamic in vivo imaging and cell tracking using a histone fluorescent protein in mice. *BMC Biotechnology,* 4**,** 33.

HAHNEMANN, J. M. & VEJERSLEV, L. O. 1997. Accuracy of cytogenetic findings on chorionic villus sampling (CVS)--diagnostic consequences of CVS mosaicism and non-mosaic discrepancy in centres contributing to EUCROMIC 1986-1992. *Prenat Diagn,* 17**,** 801-20.

HAMATANI, T., KO, M., YAMADA, M., KUJI, N., MIZUSAWA, Y., SHOJI, M., HADA, T., ASADA, H., MARUYAMA, T. & YOSHIMURA, Y. 2006. Global gene expression profiling of preimplantation embryos. *Hum Cell,* 19**,** 98-117.

HANDYSIDE, A. H., KONTOGIANNI, E. H., HARDY, K. & WINSTON, R. M. 1990. Pregnancies from biopsied human preimplantation embryos sexed by Y-specific DNA amplification. *Nature,* 344**,** 768-70.

HANSTEEN, I. L., VARSLOT, K., STEEN-JOHNSEN, J. & LANGARD, S. 1982. Cytogenetic screening of a new-born population. *Clin Genet,* 21**,** 309-14.

HARDWICK, K. G. & SHAH, J. V. 2010. Spindle checkpoint silencing: ensuring rapid and concerted anaphase onset. *F1000 Biol Rep,* 2**,** 55.

HARDY, K. 1997. Cell death in the mammalian blastocyst. *Mol Hum Reprod,* 3**,** 919-25.

HARDY, K., HANDYSIDE, A. H. & WINSTON, R. M. 1989. The human blastocyst: cell number, death and allocation during late preimplantation development in vitro. *Development,* 107**,** 597-604.

HARPER, J., COONEN, E., DE RYCKE, M., FIORENTINO, F., GERAEDTS, J., GOOSSENS, V., HARTON, G., MOUTOU, C., PEHLIVAN BUDAK, T., RENWICK, P., SENGUPTA, S., TRAEGER-SYNODINOS, J. & VESELA, K. 2010. What next for preimplantation genetic screening (PGS)? A position statement from the ESHRE PGD Consortium Steering Committee. *Hum Reprod,* 25**,** 821-3.

HARPER, J., SERMON, K., GERAEDTS, J., VESELA, K., HARTON, G., THORNHILL, A., PEHLIVAN, T., FIORENTINO, F., SENGUPTA, S., DE DIE-SMULDERS, C., MAGLI, C., MOUTOU, C. & WILTON, L. 2008. What next for preimplantation genetic screening? *Hum Reprod,* 23**,** 478-80.

HARPER, J. C., COONEN, E., HANDYSIDE, A. H., WINSTON, R. M., HOPMAN, A. H. & DELHANTY, J. D. 1995. Mosaicism of autosomes and sex chromosomes in morphologically normal, monospermic preimplantation human embryos. *Prenat Diagn,* 15**,** 41-9.

HARPER, J. C. & HARTON, G. 2010. The use of arrays in preimplantation genetic diagnosis and screening. *Fertil Steril,* 94**,** 1173-7.

HARRISON, R. H., KUO, H. C., SCRIVEN, P. N., HANDYSIDE, A. H. & OGILVIE, C. M. 2000. Lack of cell cycle checkpoints in human cleavage stage embryos revealed by a clonal pattern of chromosomal mosaicism analysed by sequential multicolour FISH. *Zygote,* 8**,** 217-24.

HASHIMOTO, S., KATO, N., SAEKI, K. & MORIMOTO, Y. 2012. Selection of high-potential embryos by culture in poly(dimethylsiloxane) microwells and time-lapse imaging. *Fertil Steril,* 97**,** 332-7.

HASSOLD, T. 1982. Mosaic trisomies in human spontaneous abortions. *Hum Genet,* 61**,** 31-5.

HASSOLD, T., CHEN, N., FUNKHOUSER, J., JOOSS, T., MANUEL, B., MATSUURA, J., MATSUYAMA, A., WILSON, C., YAMANE, J. A. & JACOBS, P. A. 1980. A cytogenetic study of 1000 spontaneous abortions. *Ann Hum Genet,* 44**,** 151-78.

HENS, K., DONDORP, W. & DE WERT, G. 2012. Embryos without secrets: An expert panel study on comprehensive embryo testing and the responsibility of the clinician. *Eur J Med Genet*.

HERSKOWITZ, I. 1987. Functional inactivation of genes by dominant negative mutations. *Nature,* 329**,** 219-22.

HERTIG, A. T., ROCK, J. & ADAMS, E. C. 1956. A description of 34 human ova within the first 17 days of development. *Am J Anat,* 98**,** 435-93.

HEWITT, L., TIGHE, A., SANTAGUIDA, S., WHITE, A. M., JONES, C. D., MUSACCHIO, A., GREEN, S. & TAYLOR, S. S. 2010. Sustained Mps1 activity is required in mitosis to recruit O-Mad2 to the Mad1-C-Mad2 core complex. *J Cell Biol,* 190**,** 25-34.

HILLMAN, N., SHERMAN, M. I. & GRAHAM, C. 1972. The effect of spatial arrangement on cell determination during mouse development. *J Embryol Exp Morphol,* 28**,** 263-78.

HOLLAND, A. J. & CLEVELAND, D. W. 2009. Boveri revisited: chromosomal instability, aneuploidy and tumorigenesis. *Nat Rev Mol Cell Biol,* 10**,** 478-87.

HOOK, E. B. 1977. Exclusion of chromosomal mosaicism: tables of 90%, 95% and 99% confidence limits and comments on use. *Am J Hum Genet,* 29**,** 94-7.

HOOK, E. B. 1981a. Prevalence of chromosome abnormalities during human gestation and implications for studies of environmental mutagens. *Lancet,* 2**,** 169-72.

HOOK, E. B. 1981b. Rates of chromosome abnormalities at different maternal ages. *Obstet Gynecol,* 58**,** 282-5.

HORNAK, M., HULINSKA, P., MUSILOVA, P., KUBICKOVA, S. & RUBES, J. 2009. Investigation of chromosome aneuploidies in early porcine embryos using comparative genomic hybridization. *Cytogenet Genome Res,* 126**,** 210-6.

HORNAK, M., ORACOVA, E., HULINSKA, P., URBANKOVA, L. & RUBES, J. 2012. Aneuploidy detection in pigs using comparative genomic hybridization: from the oocytes to blastocysts. *PLoS One,* 7**,** e30335.

HOWMAN, E. V., FOWLER, K. J., NEWSON, A. J., REDWARD, S., MACDONALD, A. C., KALITSIS, P. & CHOO, K. H. 2000. Early disruption of centromeric chromatin organization in centromere protein A (Cenpa) null mice. *Proc Natl Acad Sci U S A,* 97**,** 1148-53.

IWANAGA, Y., CHI, Y. H., MIYAZATO, A., SHELEG, S., HALLER, K., PELOPONESE, J. M., JR., LI, Y., WARD, J. M., BENEZRA, R. & JEANG, K. T. 2007. Heterozygous deletion of mitotic arrest-deficient protein 1 (MAD1) increases the incidence of tumors in mice. *Cancer Res,* 67**,** 160-6.

JACKSON, S. P. & BARTEK, J. 2009. The DNA-damage response in human biology and disease. *Nature,* 461**,** 1071-8.

JACOBS, P. A., MELVILLE, M., RATCLIFFE, S., KEAY, A. J. & SYME, J. 1974. A cytogenetic survey of 11,680 newborn infants. *Ann Hum Genet,* 37**,** 359-76.

JALLEPALLI, P. V. & PELLMAN, D. 2007. Cell biology. Aneuploidy in the balance. *Science,* 317**,** 904-5.

JAMES, R. M., KLERKX, A. H., KEIGHREN, M., FLOCKHART, J. H. & WEST, J. D. 1995. Restricted distribution of tetraploid cells in mouse tetraploid<==>diploid chimaeras. *Dev Biol,* 167**,** 213-26.

JAMIESON, M. E., COUTTS, J. R. & CONNOR, J. M. 1994. The chromosome constitution of human preimplantation embryos fertilized in vitro. *Hum Reprod,* 9**,** 709-15.

JANSEN, R. P., BOWMAN, M. C., DE BOER, K. A., LEIGH, D. A., LIEBERMAN, D. B. & MCARTHUR, S. J. 2008. What next for preimplantation genetic screening (PGS)? Experience with blastocyst biopsy and testing for aneuploidy. *Hum Reprod,* 23**,** 1476-8.

JANSSEN, A., VAN DER BURG, M., SZUHAI, K., KOPS, G. J. & MEDEMA, R. H. 2011. Chromosome segregation errors as a cause of DNA damage and structural chromosome aberrations. *Science,* 333**,** 1895-8.

JEDRUSIK, A., BRUCE, A. W., TAN, M. H., LEONG, D. E., SKAMAGKI, M., YAO, M. & ZERNICKA-GOETZ, M. 2010. Maternally and zygotically provided Cdx2 have novel and critical roles for early development of the mouse embryo. *Dev Biol,* 344**,** 66-78.

JEDRUSIK, A., PARFITT, D. E., GUO, G., SKAMAGKI, M., GRABAREK, J. B., JOHNSON, M. H., ROBSON, P. & ZERNICKA-GOETZ, M. 2008. Role of Cdx2 and cell polarity in cell allocation and specification of trophectoderm and inner cell mass in the mouse embryo. *Genes & Development,* 22**,** 2692-2706.

JEGANATHAN, K., MALUREANU, L., BAKER, D. J., ABRAHAM, S. C. & VAN DEURSEN, J. M. 2007. Bub1 mediates cell death in response to chromosome missegregation and acts to suppress spontaneous tumorigenesis. *J Cell Biol,* 179**,** 255-67.

JOHNSON, D. S., CINNIOGLU, C., ROSS, R., FILBY, A., GEMELOS, G., HILL, M., RYAN, A., SMOTRICH, D., RABINOWITZ, M. & MURRAY, M. J. 2010. Comprehensive analysis of karyotypic mosaicism between trophectoderm and inner cell mass. *Mol Hum Reprod,* 16**,** 944-9.

JOHNSON, M. H. & MARO, B. 1984. The distribution of cytoplasmic actin in mouse 8-cell blastomeres. *J Embryol Exp Morphol,* 82**,** 97-117.

JOHNSON, M. H. & MCCONNELL, J. M. 2004. Lineage allocation and cell polarity during mouse embryogenesis. *Semin Cell Dev Biol,* 15**,** 583-97.

JOHNSON, M. H. & ZIOMEK, C. A. 1983. Cell interactions influence the fate of mouse blastomeres undergoing the transition from the 16- to the 32-cell stage. *Dev Biol,* 95**,** 211-8.

JOHNSON, M. H. Z., C.A. 1981. The foundation of two distinct cell lineages within the mouse morula. *Cell,* 24**,** 71-80.

KALITSIS, P., EARLE, E., FOWLER, K. J. & CHOO, K. H. 2000. Bub3 gene disruption in mice reveals essential mitotic spindle checkpoint function during early embryogenesis. *Genes Dev,* 14**,** 2277-82.

KALITSIS, P., FOWLER, K. J., EARLE, E., HILL, J. & CHOO, K. H. 1998. Targeted disruption of mouse centromere protein C gene leads to mitotic disarray and early embryo death. *Proc Natl Acad Sci U S A,* 95**,** 1136-41.

KALOUSEK, D. K. & DILL, F. J. 1983. Chromosomal mosaicism confined to the placenta in human conceptions. *Science,* 221**,** 665-7.

KALOUSEK, D. K. & VEKEMANS, M. 1996. Confined placental mosaicism. *J Med Genet,* 33**,** 529-33.

KAWAMURA, Y., UCHIJIMA, Y., HORIKE, N., TONAMI, K., NISHIYAMA, K., AMANO, T., ASANO, T., KURIHARA, Y. & KURIHARA, H. 2010. Sirt3 protects in vitro-fertilized mouse preimplantation embryos against oxidative stress-induced p53-mediated developmental arrest. *J Clin Invest,* 120**,** 2817-28.

KERR, J. F., WYLLIE, A. H. & CURRIE, A. R. 1972. Apoptosis: a basic biological phenomenon with wide-ranging implications in tissue kinetics. *Br J Cancer,* 26**,** 239-57.

KHODJAKOV, A. & RIEDER, C. L. 2009. The nature of cell-cycle checkpoints: facts and fallacies. *J Biol,* 8**,** 88.

KING, R. W. 2008. When 2+2=5: the origins and fates of aneuploid and tetraploid cells. *Biochim Biophys Acta,* 1786**,** 4-14.

KLINE-SMITH, S. L., SANDALL, S. & DESAI, A. 2005. Kinetochore-spindle microtubule interactions during mitosis. *Curr Opin Cell Biol,* 17**,** 35-46.

KOLA, I. & WILTON, L. 1991. Preimplantation embryo biopsy: detection of trisomy in a single cell biopsied from a four-cell mouse embryo. *Mol Reprod Dev,* 29**,** 16-21.

KONINGS, P., VANNESTE, E., JACKMAERT, S., AMPE, M., VERBEKE, G., MOREAU, Y., VERMEESCH, J. R. & VOET, T. 2012. Microarray analysis of copy number variation in single cells. *Nat Protoc,* 7**,** 281-310.

KOPS, G. J., WEAVER, B. A. & CLEVELAND, D. W. 2005. On the road to cancer: aneuploidy and the mitotic checkpoint. *Nat Rev Cancer,* 5**,** 773-85.

KOTZOT, D. 2004. Advanced parental age in maternal uniparental disomy (UPD): implications for the mechanism of formation. *Eur J Hum Genet,* 12**,** 343-6.

KRIEG, S. A., LATHI, R. B., BEHR, B. & WESTPHAL, L. M. 2009. Normal pregnancy after tetraploid karyotype on trophectoderm biopsy. *Fertil Steril,* 92**,** 1169 e9-1169 e10.

KUBIAK, J. Z. & TARKOWSKI, A. K. 1985. Electrofusion of mouse blastomeres. *Experimental Cell Research,* 157**,** 561-566.

KWIATKOWSKI, N., JELLUMA, N., FILIPPAKOPOULOS, P., SOUNDARARAJAN, M., MANAK, M. S., KWON, M., CHOI, H. G., SIM, T., DEVERAUX, Q. L., ROTTMANN, S., PELLMAN, D., SHAH, J. V., KOPS, G. J., KNAPP, S. & GRAY, N. S. 2010. Small-molecule kinase inhibitors provide insight into Mps1 cell cycle function. *Nat Chem Biol,* 6**,** 359-68.

LAN, W. & CLEVELAND, D. W. 2010. A chemical tool box defines mitotic and interphase roles for Mps1 kinase. *J Cell Biol,* 190**,** 21-4.

LATHAM, K. E. & SCHULTZ, R. M. 2001. Embryonic genome activation. *Front Biosci,* 6**,** D748-59.

LAVON, N., NARWANI, K., GOLAN-LEV, T., BUEHLER, N., HILL, D. & BENVENISTY, N. 2008. Derivation of euploid human embryonic stem cells from aneuploid embryos. *Stem Cells,* 26**,** 1874-82.

LEDBETTER, D. H. 2009. Chaos in the embryo. *Nat Med,* 15**,** 490-1.

LEDBETTER, D. H., ZACHARY, J. M., SIMPSON, J. L., GOLBUS, M. S., PERGAMENT, E., JACKSON, L., MAHONEY, M. J., DESNICK, R. J., SCHULMAN, J., COPELAND, K. L. & ET AL. 1992. Cytogenetic results from the U.S. Collaborative Study on CVS. *Prenat Diagn,* 12**,** 317-45.

LEESE, H. J. 2002. Quiet please, do not disturb: a hypothesis of embryo metabolism and viability. *Bioessays,* 24**,** 845-9.

LEESE, H. J., BAUMANN, C. G., BRISON, D. R., MCEVOY, T. G. & STURMEY, R. G. 2008. Metabolism of the viable mammalian embryo: quietness revisited. *Mol Hum Reprod,* 14**,** 667-72.

LI, M., DEUGARTE, C. M., SURREY, M., DANZER, H., DECHERNEY, A. & HILL, D. L. 2005. Fluorescence in situ hybridization reanalysis of day-6 human blastocysts diagnosed with aneuploidy on day 3. *Fertil Steril,* 84**,** 1395-400.

LI, M., FANG, X., BAKER, D. J., GUO, L., GAO, X., WEI, Z., HAN, S., VAN DEURSEN, J. M. & ZHANG, P. 2010. The ATM-p53 pathway suppresses aneuploidy-induced tumorigenesis. *Proc Natl Acad Sci U S A,* 107**,** 14188-93.

LI, M., FANG, X., WEI, Z., YORK, J. P. & ZHANG, P. 2009. Loss of spindle assembly checkpoint-mediated inhibition of Cdc20 promotes tumorigenesis in mice. *J Cell Biol,* 185**,** 983-94.

LIGHTFOOT, D. A., KOUZNETSOVA, A., MAHDY, E., WILBERTZ, J. & HOOG, C. 2006. The fate of mosaic aneuploid embryos during mouse development. *Dev Biol,* 289**,** 384-94.

LIU, L., AOKI, V. W. & CARRELL, D. T. 2008. Evaluation of the developmental competence and chromosomal compliment of mouse oocytes derived from in-vitro growth and maturation of preantral follicles. *J Assist Reprod Genet,* 25**,** 107-13.

LIVAK, K. J. & SCHMITTGEN, T. D. 2001. Analysis of relative gene expression data using real-time quantitative PCR and the 2(-Delta Delta C(T)) Method. *Methods,* 25**,** 402-8.

LOS, F. J., VAN OPSTAL, D. & VAN DEN BERG, C. 2004. The development of cytogenetically normal, abnormal and mosaic embryos: a theoretical model. *Hum Reprod Update,* 10**,** 79-94.

LY, K. D., AGARWAL, A. & NAGY, Z. P. 2011. Preimplantation genetic screening: does it help or hinder IVF treatment and what is the role of the embryo? *J Assist Reprod Genet,* 28**,** 833-49.

LYLE, R., GEHRIG, C., NEERGAARD-HENRICHSEN, C., DEUTSCH, S. & ANTONARAKIS, S. E. 2004. Gene expression from the aneuploid chromosome in a trisomy mouse model of down syndrome. *Genome Res,* 14**,** 1268-74.

MACHTINGER, R. & RACOWSKY, C. 2013. Morphological systems of human embryo assessment and clinical evidence. *Reprod Biomed Online,* 26**,** 210-21.

MACKAY, G. E. & WEST, J. D. 2005. Fate of tetraploid cells in 4n<-->2n chimeric mouse blastocysts. *Mech Dev,* 122**,** 1266-81.

MACKLON, N. S., GERAEDTS J.P & B.C, F. 2002. Conception to ongoing pregnancy: the 'black box' of early pregnancy loss. *Human Reproduction Update,* 8**,** 333 - 343.

MAGLI, M. C., GIANAROLI, L., FERRARETTI, A. P., LAPPI, M., RUBERTI, A. & FARFALLI, V. 2007. Embryo morphology and development are dependent on the chromosomal complement. *Fertil Steril,* 87**,** 534-41.

MAGLI, M. C., JONES, G. M., GRAS, L., GIANAROLI, L., KORMAN, I. & TROUNSON, A. O. 2000. Chromosome mosaicism in day 3 aneuploid embryos that develop to morphologically normal blastocysts in vitro. *Human Reproduction,* 15**,** 1781-1786.

MANES, C. 1973. The participation of the embryonic genome during early cleavage in the rabbit. *Dev Biol,* 32**,** 453-9.

MANTIKOU, E., WONG, K. M., REPPING, S. & MASTENBROEK, S. 2012. Molecular origin of mitotic aneuploidies in preimplantation embryos. *Biochim Biophys Acta,* 1822**,** 1921-30.

MAO, R., ZIELKE, C. L., ZIELKE, H. R. & PEVSNER, J. 2003. Global up-regulation of chromosome 21 gene expression in the developing Down syndrome brain. *Genomics,* 81**,** 457-67.

MARANGOS, P. & CARROLL, J. 2012. Oocytes progress beyond prophase in the presence of DNA damage. *Curr Biol,* 22**,** 989-94.

MARTINEZ, M. C., MENDEZ, C., FERRO, J., NICOLAS, M., SERRA, V. & LANDERAS, J. 2010. Cytogenetic analysis of early nonviable pregnancies after assisted reproduction treatment. *Fertil Steril,* 93**,** 289-92.

MASTENBROEK, S., TWISK, M., VAN ECHTEN-ARENDS, J., SIKKEMA-RADDATZ, B., KOREVAAR, J. C., VERHOEVE, H. R., VOGEL, N. E., ARTS, E. G., DE VRIES, J. W., BOSSUYT, P. M., BUYS, C. H., HEINEMAN, M. J., REPPING, S. & VAN DER VEEN, F. 2007. In vitro fertilization with preimplantation genetic screening. *N Engl J Med,* 357**,** 9-17.

MCMANUS, K. J. & HENDZEL, M. J. 2005. ATM-dependent DNA damage-independent mitotic phosphorylation of H2AX in normally growing mammalian cells. *Mol Biol Cell,* 16**,** 5013-25.

MEILHAC, S. M., ADAMS, R. J., MORRIS, S. A., DANCKAERT, A., LE GARREC, J. F. & ZERNICKA-GOETZ, M. 2009. Active cell movements coupled to positional induction are involved in lineage segregation in the mouse blastocyst. *Dev Biol,* 331**,** 210-21.

MERALDI, P., DRAVIAM, V. M. & SORGER, P. K. 2004. Timing and checkpoints in the regulation of mitotic progression. *Dev Cell,* 7**,** 45-60.

MERTZANIDOU, A., WILTON, L., CHENG, J., SPITS, C., VANNESTE, E., MOREAU, Y., VERMEESCH, J. R. & SERMON, K. 2013. Microarray analysis reveals abnormal chromosomal complements in over 70% of 14 normally developing human embryos. *Hum Reprod,* 28**,** 256-64.

MESEGUER, M., HERRERO, J., TEJERA, A., HILLIGSOE, K. M., RAMSING, N. B. & REMOHI, J. 2011. The use of morphokinetics as a predictor of embryo implantation. *Hum Reprod,* 26**,** 2658-71.

MEYER, L. R., KLIPSTEIN, S., HAZLETT, W. D., NASTA, T., MANGAN, P. & KARANDE, V. C. 2009. A prospective randomized controlled trial of preimplantation genetic screening in the "good prognosis" patient. *Fertil Steril,* 91**,** 1731-8.

MICHEL, L. S., LIBERAL, V., CHATTERJEE, A., KIRCHWEGGER, R., PASCHE, B., GERALD, W., DOBLES, M., SORGER, P. K., MURTY, V. V. & BENEZRA, R. 2001. MAD2 haplo-insufficiency causes premature anaphase and chromosome instability in mammalian cells. *Nature,* 409**,** 355-9.

MOLEY, K. H., CHI, M. M., KNUDSON, C. M., KORSMEYER, S. J. & MUECKLER, M. M. 1998. Hyperglycemia induces apoptosis in pre-implantation embryos through cell death effector pathways. *Nat Med,* 4**,** 1421-4.

MOORE, N. W., ADAMS, C. E. & ROWSON, L. E. 1968. Developmental potential of single blastomeres of the rabbit egg. *J Reprod Fertil,* 17**,** 527-31.

MORRIS, S. A. 2011. Cell fate in the early mouse embryo: sorting out the influence of developmental history on lineage choice. *Reprod Biomed Online,* 22**,** 521-4.

MORRIS, S. A., GREWAL, S., BARRIOS, F., PATANKAR, S. N., STRAUSS, B., BUTTERY, L., ALEXANDER, M., SHAKESHEFF, K. M. & ZERNICKA-GOETZ, M. 2012a. Dynamics of anterior-posterior axis formation in the developing mouse embryo. *Nat Commun,* 3**,** 673.

MORRIS, S. A., GUO, Y. & ZERNICKA-GOETZ, M. 2012b. Developmental plasticity is bound by pluripotency and the Fgf and Wnt signaling pathways. *Cell Rep,* 2**,** 756-65.

MORRIS, S. A., TEO, R. T., LI, H., ROBSON, P., GLOVER, D. M. & ZERNICKA-GOETZ, M. 2010. Origin and formation of the first two distinct cell types of the inner cell mass in the mouse embryo. *Proc Natl Acad Sci U S A,* 107**,** 6364-9.

MU, X. F., JIN, X. L., FARNHAM, M. M., LI, Y. & O'NEILL, C. 2011. DNA damage-sensing kinases mediate the mouse 2-cell embryo's response to genotoxic stress. *Biol Reprod,* 85**,** 524-35.

MUNNE, S., CHEN, S., COLLS, P., GARRISI, J., ZHENG, X., CEKLENIAK, N., LENZI, M., HUGHES, P., FISCHER, J., GARRISI, M., TOMKIN, G. & COHEN, J. 2007. Maternal age, morphology, development and chromosome abnormalities in over 6000 cleavage-stage embryos. *Reprod Biomed Online,* 14**,** 628-34.

MUNNE, S., FISCHER, J., WARNER, A., CHEN, S., ZOUVES, C., COHEN, J. & REFERRING CENTERS, P. G. D. G. 2006. Preimplantation genetic diagnosis significantly reduces pregnancy loss in infertile couples: a multicenter study. *Fertil Steril,* 85**,** 326-32.

MUNNE, S., FRAGOULI, E., COLLS, P., KATZ-JAFFE, M., SCHOOLCRAFT, W. & WELLS, D. 2010. Improved detection of aneuploid blastocysts using a new 12-chromosome FISH test. *Reprod Biomed Online,* 20**,** 92-7.

MUNNE, S., LEE, A., ROSENWAKS, Z., GRIFO, J. & COHEN, J. 1993. Diagnosis of major chromosome aneuploidies in human preimplantation embryos. *Hum Reprod,* 8**,** 2185-91.

MUNNE, S., MAGLI, C., COHEN, J., MORTON, P., SADOWY, S., GIANAROLI, L., TUCKER, M., MARQUEZ, C., SABLE, D., FERRARETTI, A. P., MASSEY, J. B. & SCOTT, R. 1999. Positive outcome after preimplantation diagnosis of aneuploidy in human embryos. *Hum Reprod,* 14**,** 2191-9.

MUNNE, S., MARQUEZ, C., MAGLI, C., MORTON, P. & MORRISON, L. 1998. Scoring criteria for preimplantation genetic diagnosis of numerical abnormalities for chromosomes X, Y, 13, 16, 18 and 21. *Mol Hum Reprod,* 4**,** 863-70.

MUNNE, S., SANDALINAS, M., ESCUDERO, T., VELILLA, E., WALMSLEY, R., SADOWY, S., COHEN, J. & SABLE, D. 2003. Improved implantation after preimplantation genetic diagnosis of aneuploidy. *Reprod Biomed Online,* 7**,** 91-7.

MUNNE, S., VELILLA, E., COLLS, P., GARCIA BERMUDEZ, M., VEMURI, M. C., STEUERWALD, N., GARRISI, J. & COHEN, J. 2005. Self-correction of chromosomally abnormal embryos in culture and implications for stem cell production. *Fertil Steril,* 84**,** 1328-34.

MUSACCHIO, A. & SALMON, E. D. 2007. The spindle-assembly checkpoint in space and time. *Nat Rev Mol Cell Biol,* 8**,** 379-93.

NAGAOKA, S. I., HASSOLD, T. J. & HUNT, P. A. 2012. Human aneuploidy: mechanisms and new insights into an age-old problem. *Nat Rev Genet,* 13**,** 493-504.

NAGY, H., GERTSENSTEIN, M., VINTERSTEN, K. & BEHRINGER, R. 2003. Manipulating the mouse embryo.

NIAKAN, K. K., HAN, J., PEDERSEN, R. A., SIMON, C. & PERA, R. A. 2012. Human pre-implantation embryo development. *Development,* 139**,** 829-41.

NICHOLS, J., SILVA, J., ROODE, M. & SMITH, A. 2009. Suppression of Erk signalling promotes ground state pluripotency in the mouse embryo. *Development,* 136**,** 3215-22.

NIETZEL, A., ROCCHI, M., STARKE, H., HELLER, A., FIEDLER, W., WLODARSKA, I., LONCAREVIC, I. F., BEENSEN, V., CLAUSSEN, U. & LIEHR, T. 2001. A new multicolor-FISH approach for the characterization of marker chromosomes: centromere-specific multicolor-FISH (cenM-FISH). *Hum Genet,* 108**,** 199-204.

NORTHROP, L. E., TREFF, N. R., LEVY, B. & SCOTT, R. T., JR. 2010. SNP microarray-based 24 chromosome aneuploidy screening demonstrates that cleavage-stage FISH poorly predicts aneuploidy in embryos that develop to morphologically normal blastocysts. *Mol Hum Reprod,* 16**,** 590-600.

O'SULLIVAN, D. M., JOHNSON, M. H. & MCCONNELL, J. M. 1993. Staurosporine advances interblastomeric flattening of the mouse embryo. *Zygote,* 1**,** 103-12.

ORON, E. & IVANOVA, N. 2012. Cell fate regulation in early mammalian development. *Phys Biol,* 9**,** 045002.

ORTH, J. D., LOEWER, A., LAHAV, G. & MITCHISON, T. J. 2012. Prolonged mitotic arrest triggers partial activation of apoptosis, resulting in DNA damage and p53 induction. *Mol Biol Cell,* 23**,** 567-76.

PAMPFER, S. & DONNAY, I. 1999. Apoptosis at the time of embryo implantation in mouse and rat. *Cell Death Differ,* 6**,** 533-45.

PAPAIOANNOU, V. E. & EBERT, K. M. 1995. Mouse half embryos: viability and allocation of cells in the blastocyst. *Dev Dyn,* 203**,** 393-8.

PEDERSEN, R. A., WU, K. & BALAKIER, H. 1986. Origin of the inner cell mass in mouse embryos: cell lineage analysis by microinjection. *Dev Biol,* 117**,** 581-95.

PEURA, T., BOSMAN, A., CHAMI, O., JANSEN, R. P., TEXLOVA, K. & STOJANOV, T. 2008. Karyotypically normal and abnormal human embryonic stem cell lines derived from PGD-analyzed embryos. *Cloning Stem Cells,* 10**,** 203-16.

PFAU, S. J. & AMON, A. 2012. Chromosomal instability and aneuploidy in cancer: from yeast to man. *EMBO Rep,* 13**,** 515-27.

PICTON, H. M., ELDER, K., HOUGHTON, F. D., HAWKHEAD, J. A., RUTHERFORD, A. J., HOGG, J. E., LEESE, H. J. & HARRIS, S. E. 2010. Association between amino acid turnover and chromosome aneuploidy during human preimplantation embryo development in vitro. *Mol Hum Reprod,* 16**,** 557-69.

PIERCE, G. B., LEWELLYN, A. L. & PARCHMENT, R. E. 1989. Mechanism of programmed cell death in the blastocyst. *Proc Natl Acad Sci U S A,* 86**,** 3654-8.

PIOTROWSKA, K., WIANNY, F., PEDERSEN, R. A. & ZERNICKA-GOETZ, M. 2001. Blastomeres arising from the first cleavage division have distinguishable fates in normal mouse development. *Development,* 128**,** 3739-48.

PIOTROWSKA, K. & ZERNICKA-GOETZ, M. 2001. Role for sperm in spatial patterning of the early mouse embryo. *Nature,* 409**,** 517-21.

PLACHTA, N., BOLLENBACH, T., PEASE, S., FRASER, S. E. & PANTAZIS, P. 2011. Oct4 kinetics predict cell lineage patterning in the early mammalian embryo. *Nat Cell Biol,* 13**,** 117-23.

PLUSA, B., HADJANTONAKIS, A. K., GRAY, D., PIOTROWSKA-NITSCHE, K., JEDRUSIK, A., PAPAIOANNOU, V. E., GLOVER, D. M. & ZERNICKA-GOETZ, M. 2005. The first cleavage of the mouse zygote predicts the blastocyst axis. *Nature,* 434**,** 391-5.

PLUSA, B., PILISZEK, A., FRANKENBERG, S., ARTUS, J. & HADJANTONAKIS, A. K. 2008. Distinct sequential cell behaviours direct primitive endoderm formation in the mouse blastocyst. *Development,* 135**,** 3081-91.

PRACTICE COMMITTEE OF SOCIETY FOR ASSISTED REPRODUCTIVETECHNOLOGY & PRACTICE COMMITTEE OF AMERICAN SOCIETY FOR REPRODUCTIVE MEDICINE 2008. Preimplantation genetic testing: a Practice Committee opinion. *Fertil Steril,* 90**,** S136-43.

PUTKEY, F. R., CRAMER, T., MORPHEW, M. K., SILK, A. D., JOHNSON, R. S., MCINTOSH, J. R. & CLEVELAND, D. W. 2002. Unstable kinetochore-microtubule capture and chromosomal instability following deletion of CENP-E. *Dev Cell,* 3**,** 351-65.

QUIGNON, F., ROZIER, L., LACHAGES, A. M., BIETH, A., SIMILI, M. & DEBATISSE, M. 2007. Sustained mitotic block elicits DNA breaks: one-step alteration of ploidy and chromosome integrity in mammalian cells. *Oncogene,* 26**,** 165-72.

RABINOWITZ, M., RYAN, A., GEMELOS, G., HILL, M., BANER, J., CINNIOGLU, C., BANJEVIC, M., POTTER, D., PETROV, D. A. & DEMKO, Z. 2012. Origins and rates of aneuploidy in human blastomeres. *Fertil Steril,* 97**,** 395-401.

RACOWSKY, C., VERNON, M., MAYER, J., BALL, G. D., BEHR, B., POMEROY, K. O., WININGER, D., GIBBONS, W., CONAGHAN, J. & STERN, J. E. 2010. Standardization of grading embryo morphology. *Fertil Steril,* 94**,** 1152-3.

RAO, X., ZHANG, Y., YI, Q., HOU, H., XU, B., CHU, L., HUANG, Y., ZHANG, W., FENECH, M. & SHI, Q. 2008. Multiple origins of spontaneously arising micronuclei in HeLa cells: direct evidence from long-term live cell imaging. *Mutat Res,* 646**,** 41-9.

RIEDER, C. L., COLE, R. W., KHODJAKOV, A. & SLUDER, G. 1995. The checkpoint delaying anaphase in response to chromosome monoorientation is mediated by an inhibitory signal produced by unattached kinetochores. *J Cell Biol,* 130**,** 941-8.

RIEDER, C. L. & MAIATO, H. 2004. Stuck in division or passing through: what happens when cells cannot satisfy the spindle assembly checkpoint. *Dev Cell,* 7**,** 637-51.

RIEDER, C. L. & PALAZZO, R. E. 1992. Colcemid and the mitotic cycle. *J Cell Sci,* 102 (Pt 3)**,** 387-92.

ROBBERECHT, C., SCHUDDINCK, V., FRYNS, J. P. & VERMEESCH, J. R. 2009. Diagnosis of miscarriages by molecular karyotyping: benefits and pitfalls. *Genet Med,* 11**,** 646-54.

ROBERTS, C., LUTJEN, J., KRZYMINSKA, U. & O'NEILL, C. 1990. Cytogenetic analysis of biopsied preimplantation mouse embryos: implications for prenatal diagnosis. *Hum Reprod,* 5**,** 197-202.

ROBERTS, C. G. & O'NEILL, C. 1988. A simplified method for fixation of human and mouse preimplantation embryos which facilitates G-banding and karyotypic analysis. *Hum Reprod,* 3**,** 990-2.

ROSSANT, J. 1976. Postimplantation development of blastomeres isolated from 4- and 8-cell mouse eggs. *J Embryol Exp Morphol,* 36**,** 283-90.

RUANGVUTILERT, P., DELHANTY, J. D., RODECK, C. H. & HARPER, J. C. 2000. Relative efficiency of FISH on metaphase and interphase nuclei from non-mosaic trisomic or triploid fibroblast cultures. *Prenat Diagn,* 20**,** 159-62.

RUBIO, C., RODRIGO, L., MERCADER, A., MATEU, E., BUENDIA, P., PEHLIVAN, T., VILORIA, T., DE LOS SANTOS, M. J., SIMON, C., REMOHI, J. & PELLICER, A. 2007. Impact of chromosomal abnormalities on preimplantation embryo development. *Prenat Diagn,* 27**,** 748-56.

SABHNANI, T. V., ELAIMI, A., SULTAN, H., ALDURAIHEM, A., SERHAL, P. & HARPER, J. C. 2011. Increased incidence of mosaicism detected by FISH in murine blastocyst cultured in vitro. *Reprod Biomed Online,* 22**,** 621-31.

SANDALINAS, M., SADOWY, S., ALIKANI, M., CALDERON, G., COHEN, J. & MUNNE, S. 2001. Developmental ability of chromosomally abnormal human embryos to develop to the blastocyst stage. *Hum Reprod,* 16**,** 1954-8.

SANTAGUIDA, S., TIGHE, A., D'ALISE, A. M., TAYLOR, S. S. & MUSACCHIO, A. 2010. Dissecting the role of MPS1 in chromosome biorientation and the spindle checkpoint through the small molecule inhibitor reversine. *J Cell Biol,* 190**,** 73-87.

SANTOS, M. A., TEKLENBURG, G., MACKLON, N. S., VAN OPSTAL, D., SCHURING-BLOM, G. H., KRIJTENBURG, P. J., DE VREEDEN-ELBERTSE, J., FAUSER, B. C. & BAART, E. B. 2010. The fate of the mosaic embryo: chromosomal constitution and development of Day 4, 5 and 8 human embryos. *Hum Reprod,* 25**,** 1916-26.

SCHOOLCRAFT, W. B., FRAGOULI, E., STEVENS, J., MUNNE, S., KATZ-JAFFE, M. G. & WELLS, D. 2010. Clinical application of comprehensive chromosomal screening at the blastocyst stage. *Fertil Steril,* 94**,** 1700-6.

SCHULTZ, G. A. & HEYNER, S. 1992. Gene expression in pre-implantation mammalian embryos. *Mutat Res,* 296**,** 17-31.

SCHULTZ, R. M. 2002. The molecular foundations of the maternal to zygotic transition in the preimplantation embryo. *Hum Reprod Update,* 8**,** 323-31.

SCOTT, R. T., JR., FERRY, K., SU, J., TAO, X., SCOTT, K. & TREFF, N. R. 2012. Comprehensive chromosome screening is highly predictive of the reproductive potential of human embryos: a prospective, blinded, nonselection study. *Fertil Steril,* 97**,** 870-5.

SCRIVEN, P. N. & BOSSUYT, P. M. 2010. Diagnostic accuracy: theoretical models for preimplantation genetic testing of a single nucleus using the fluorescence in situ hybridization technique. *Hum Reprod,* 25**,** 2622-8.

SEGAL, D. & MCCOY, E. 1974. Studies on Down's syndrome in tissue culture. I. Growth rates and protein contents of fibroblast cultures. *J Cell Physiol,* 83**,** 85-90.

SERMON, K., VAN STEIRTEGHEM, A. & LIEBAERS, I. 2004. Preimplantation genetic diagnosis. *Lancet,* 363**,** 1633-41.

SHARIF, B. 2011. *M-phase kinases in mouse oocyte maturation and early embryo development.* PhD, University of Cambridge.

SHARIF, B., NA, J., LYKKE-HARTMANN, K., MCLAUGHLIN, S. H., LAUE, E., GLOVER, D. M. & ZERNICKA-GOETZ, M. 2010. The chromosome passenger complex is required for fidelity of chromosome transmission and cytokinesis in meiosis of mouse oocytes. *J Cell Sci,* 123**,** 4292-300.

SHELTZER, J. M., TORRES, E. M., DUNHAM, M. J. & AMON, A. 2012. Transcriptional consequences of aneuploidy. *Proc Natl Acad Sci U S A,* 109**,** 12644-9.

SHI, W., DIRIM, F., WOLF, E., ZAKHARTCHENKO, V. & HAAF, T. 2004. Methylation reprogramming and chromosomal aneuploidy in in vivo fertilized and cloned rabbit preimplantation embryos. *Biol Reprod,* 71**,** 340-7.

SIEGEL, J. J. & AMON, A. 2012. New insights into the troubles of aneuploidy. *Annu Rev Cell Dev Biol,* 28**,** 189-214.

SNOW, M. H. 1977. Gastrulation in the mouse: growth and regionalization of the epiblast. *J Embryol Exp Morphol,* 42**,** 293-303.

SPENCER, T. E., JOHNSON, G. A., BAZER, F. W. & BURGHARDT, R. C. 2004. Implantation mechanisms: insights from the sheep. *Reproduction,* 128**,** 657-68.

STAESSEN, C., PLATTEAU, P., VAN ASSCHE, E., MICHIELS, A., TOURNAYE, H., CAMUS, M., DEVROEY, P., LIEBAERS, I. & VAN STEIRTEGHEM, A. 2004. Comparison of blastocyst transfer with or without preimplantation genetic diagnosis for aneuploidy screening in couples with advanced maternal age: a prospective randomized controlled trial. *Hum Reprod,* 19**,** 2849-58.

STAESSEN, C., VERPOEST, W., DONOSO, P., HAENTJENS, P., VAN DER ELST, J., LIEBAERS, I. & DEVROEY, P. 2008. Preimplantation genetic screening does not improve delivery rate in women under the age of 36 following single-embryo transfer. *Hum Reprod,* 23**,** 2818-25.

STEPHENS, P. J., GREENMAN, C. D., FU, B., YANG, F., BIGNELL, G. R., MUDIE, L. J., PLEASANCE, E. D., LAU, K. W., BEARE, D., STEBBINGS, L. A., MCLAREN, S., LIN, M. L., MCBRIDE, D. J., VARELA, I., NIK-ZAINAL, S., LEROY, C., JIA, M., MENZIES, A., BUTLER, A. P., TEAGUE, J. W., QUAIL, M. A., BURTON, J., SWERDLOW, H., CARTER, N. P., MORSBERGER, L. A., IACOBUZIO-DONAHUE, C., FOLLOWS, G. A., GREEN, A. R., FLANAGAN, A. M., STRATTON, M. R., FUTREAL, P. A. & CAMPBELL, P. J. 2011. Massive genomic rearrangement acquired in a single catastrophic event during cancer development. *Cell,* 144**,** 27-40.

STEPTOE, P. C. & EDWARDS, R. G. 1978. Birth after the reimplantation of a human embryo. *Lancet,* 2**,** 366.

STETTEN, G., ESCALLON, C. S., SOUTH, S. T., MCMICHAEL, J. L., SAUL, D. O. & BLAKEMORE, K. J. 2004. Reevaluating confined placental mosaicism. *Am J Med Genet A,* 131**,** 232-9.

STUCKE, V. M., SILLJE, H. H., ARNAUD, L. & NIGG, E. A. 2002. Human Mps1 kinase is required for the spindle assembly checkpoint but not for centrosome duplication. *EMBO J,* 21**,** 1723-32.

SUWINSKA, A., CZOLOWSKA, R., OZDZENSKI, W. & TARKOWSKI, A. K. 2008. Blastomeres of the mouse embryo lose totipotency after the fifth cleavage division: expression of Cdx2 and Oct4 and developmental potential of inner and outer blastomeres of 16- and 32-cell embryos. *Dev Biol,* 322**,** 133-44.

TABANSKY, I., LENARCIC, A., DRAFT, R. W., LOULIER, K., KESKIN, D. B., ROSAINS, J., RIVERA-FELICIANO, J., LICHTMAN, J. W., LIVET, J., STERN, J. N., SANES, J. R. & EGGAN, K. 2013. Developmental bias in cleavage-stage mouse blastomeres. *Curr Biol,* 23**,** 21-31.

TAM, P. P. & ROSSANT, J. 2003. Mouse embryonic chimeras: tools for studying mammalian development. *Development,* 130**,** 6155-63.

TANG, P. C., RITCHIE, W. A., WILMUT, I. & WEST, J. D. 2000. The effects of cell size and ploidy on cell allocation in mouse chimaeric blastocysts. *Zygote,* 8**,** 33-43.

TANG, Z., BHARADWAJ, R., LI, B. & YU, H. 2001. Mad2-Independent inhibition of APCCdc20 by the mitotic checkpoint protein BubR1. *Dev Cell,* 1**,** 227-37.

TARKOWSKI, A. K. 1959. Experiments on the development of isolated blastomers of mouse eggs. *Nature,* 184**,** 1286-7.

TARKOWSKI, A. K. 1966. An air-drying method for chromosome preparations from mouse eggs. *Cytogenetic and Genome Research,* 5**,** 394-400.

TARKOWSKI, A. K., OZDZENSKI, W. & CZOLOWSKA, R. 2005. Identical triplets and twins developed from isolated blastomeres of 8- and 16-cell mouse embryos supported with tetraploid blastomeres. *Int J Dev Biol,* 49**,** 825-32.

TARKOWSKI, A. K., SUWINSKA, A., CZOLOWSKA, R. & OZDZENSKI, W. 2010. Individual blastomeres of 16- and 32-cell mouse embryos are able to develop into foetuses and mice. *Dev Biol,* 348**,** 190-8.

TARKOWSKI, A. K., WITKOWSKA, A. & OPAS, J. 1977. Development of cytochalasin in B-induced tetraploid and diploid/tetraploid mosaic mouse embryos. *J Embryol Exp Morphol,* 41**,** 47-64.

TARKOWSKI, A. K. & WROBLEWSKA, J. 1967. Development of blastomeres of mouse eggs isolated at the 4- and 8-cell stage. *J Embryol Exp Morphol,* 18**,** 155-80.

TERRADAS, M., MARTIN, M., HERNANDEZ, L., TUSELL, L. & GENESCA, A. 2012. Is DNA damage response ready for action anywhere? *Int J Mol Sci,* 13**,** 11569-83.

TERRADAS, M., MARTIN, M., TUSELL, L. & GENESCA, A. 2010. Genetic activities in micronuclei: is the DNA entrapped in micronuclei lost for the cell? *Mutat Res,* 705**,** 60-7.

TESHIMA, I. E., KALOUSEK, D. K., VEKEMANS, M. J., MARKOVIC, V., COX, D. M., DALLAIRE, L., GAGNE, R., LIN, J. C., RAY, M., SERGOVICH, F. R. & ET AL. 1992. Canadian multicenter randomized clinical trial of chorion villus sampling and amniocentesis. chromosome mosaicism in CVS and amniocentesis samples. *Prenat Diagn,* 12**,** 443-66.

THOMPSON, L. H. 2012. Recognition, signaling, and repair of DNA double-strand breaks produced by ionizing radiation in mammalian cells: the molecular choreography. *Mutat Res,* 751**,** 158-246.

THOMPSON, S. L., BAKHOUM, S. F. & COMPTON, D. A. 2010. Mechanisms of chromosomal instability. *Curr Biol,* 20**,** R285-95.

THOMPSON, S. L. & COMPTON, D. A. 2008. Examining the link between chromosomal instability and aneuploidy in human cells. *J Cell Biol,* 180**,** 665-72.

THOMPSON, S. L. & COMPTON, D. A. 2010. Proliferation of aneuploid human cells is limited by a p53-dependent mechanism. *J Cell Biol,* 188**,** 369-81.

THORNHILL, A. R., DEDIE-SMULDERS, C. E., GERAEDTS, J. P., HARPER, J. C., HARTON, G. L., LAVERY, S. A., MOUTOU, C., ROBINSON, M. D., SCHMUTZLER, A. G., SCRIVEN, P. N., SERMON, K. D., WILTON, L. & CONSORTIUM, E. P. 2005. ESHRE PGD Consortium 'Best practice guidelines for clinical preimplantation genetic diagnosis (PGD) and preimplantation genetic screening (PGS)'. *Hum Reprod,* 20**,** 35-48.

TORRES, E. M., DEPHOURE, N., PANNEERSELVAM, A., TUCKER, C. M., WHITTAKER, C. A., GYGI, S. P., DUNHAM, M. J. & AMON, A. 2010. Identification of aneuploidy-tolerating mutations. *Cell,* 143**,** 71-83.

TORRES, E. M., SOKOLSKY, T., TUCKER, C. M., CHAN, L. Y., BOSELLI, M., DUNHAM, M. J. & AMON, A. 2007. Effects of aneuploidy on cellular physiology and cell division in haploid yeast. *Science,* 317**,** 916-24.

TREFF, N. R., LEVY, B., SU, J., NORTHROP, L. E., TAO, X. & SCOTT, R. T., JR. 2010. SNP microarray-based 24 chromosome aneuploidy screening is significantly more consistent than FISH. *Mol Hum Reprod,* 16**,** 583-9.

TREFF, N. R. & SCOTT, R. T., JR. 2012. Methods for comprehensive chromosome screening of oocytes and embryos: capabilities, limitations, and evidence of validity. *J Assist Reprod Genet,* 29**,** 381-90.

TSUNODA, Y. & MCLAREN, A. 1983. Effect of various procedures on the viability of mouse embryos containing half the normal number of blastomeres. *J Reprod Fertil,* 69**,** 315-22.

TSURUMI, C., HOFFMANN, S., GELEY, S., GRAESER, R. & POLANSKI, Z. 2004. The spindle assembly checkpoint is not essential for CSF arrest of mouse oocytes. *J Cell Biol,* 167**,** 1037-50.

TWISK, M., MASTENBROEK, S., VAN WELY, M., HEINEMAN, M. J., VAN DER VEEN, F. & REPPING, S. 2006. Preimplantation genetic screening for abnormal number of chromosomes (aneuploidies) in in vitro fertilisation or intracytoplasmic sperm injection. *Cochrane Database Syst Rev***,** CD005291.

VAN ECHTEN-ARENDS, J., MASTENBROEK, S., SIKKEMA-RADDATZ, B., KOREVAAR, J. C., HEINEMAN, M. J., VAN DER VEEN, F. & REPPING, S. 2011. Chromosomal mosaicism in human preimplantation embryos: a systematic review. *Hum Reprod Update,* 17**,** 620-7.

VANNESTE, E., VOET, T., LE CAIGNEC, C., AMPE, M., KONINGS, P., MELOTTE, C., DEBROCK, S., AMYERE, M., VIKKULA, M., SCHUIT, F., FRYNS, J. P., VERBEKE, G., D'HOOGHE, T., MOREAU, Y. & VERMEESCH, J. R. 2009. Chromosome instability is common in human cleavage-stage embryos. *Nat Med,* 15**,** 577-83.

VERLINSKY, Y., CIESLAK, J., FREIDINE, M., IVAKHNENKO, V., WOLF, G., KOVALINSKAYA, L., WHITE, M., LIFCHEZ, A., KAPLAN, B., MOISE, J. & ET AL. 1995. Pregnancies following pre-conception diagnosis of common aneuploidies by fluorescent in-situ hybridization. *Hum Reprod,* 10**,** 1923-7.

VIUFF, D., GREVE, T., AVERY, B., HYTTEL, P., BROCKHOFF, P. B. & THOMSEN, P. D. 2000. Chromosome aberrations in in vitro-produced bovine embryos at days 2-5 post-insemination. *Biol Reprod,* 63**,** 1143-8.

VIUFF, D., PALSGAARD, A., RICKORDS, L., LAWSON, L. G., GREVE, T., SCHMIDT, M., AVERY, B., HYTTEL, P. & THOMSEN, P. D. 2002. Bovine embryos contain a higher proportion of polyploid cells in the trophectoderm than in the embryonic disc. *Mol Reprod Dev,* 62**,** 483-8.

VOULLAIRE, L., SLATER, H., WILLIAMSON, R. & WILTON, L. 2000. Chromosome analysis of blastomeres from human embryos by using comparative genomic hybridization. *Hum Genet,* 106**,** 210-7.

WANG, Q., LIU, T., FANG, Y., XIE, S., HUANG, X., MAHMOOD, R., RAMASWAMY, G., SAKAMOTO, K. M., DARZYNKIEWICZ, Z., XU, M. & DAI, W. 2004a. BUBR1 deficiency results in abnormal megakaryopoiesis. *Blood,* 103**,** 1278-85.

WANG, Q. T., PIOTROWSKA, K., CIEMERYCH, M. A., MILENKOVIC, L., SCOTT, M. P., DAVIS, R. W. & ZERNICKA-GOETZ, M. 2004b. A genome-wide study of gene activity reveals developmental signaling pathways in the preimplantation mouse embryo. *Dev Cell,* 6**,** 133-44.

WARBURTON, D., YU, C. Y., KLINE, J. & STEIN, Z. 1978. Mosaic autosomal trisomy in cultures from spontaneous abortions. *Am J Hum Genet,* 30**,** 609-17.

WATERSTON, R. H., LANDER, E. S. & SULSTON, J. E. 2002. On the sequencing of the human genome. *Proc Natl Acad Sci U S A,* 99**,** 3712-6.

WEI, Y., MULTI, S., YANG, C. R., MA, J., ZHANG, Q. H., WANG, Z. B., LI, M., WEI, L., GE, Z. J., ZHANG, C. H., OUYANG, Y. C., HOU, Y., SCHATTEN, H. & SUN, Q. Y. 2011. Spindle assembly checkpoint regulates mitotic cell cycle progression during preimplantation embryo development. *PLoS One,* 6**,** e21557.

WEISS, E. & WINEY, M. 1996. The Saccharomyces cerevisiae spindle pole body duplication gene MPS1 is part of a mitotic checkpoint. *J Cell Biol,* 132**,** 111-23.

WELLS, D. 2010. Embryo aneuploidy and the role of morphological and genetic screening. *Reprod Biomed Online,* 21**,** 274-7.

WELLS, D., ALFARAWATI, S. & FRAGOULI, E. 2008. Use of comprehensive chromosomal screening for embryo assessment: microarrays and CGH. *Mol Hum Reprod,* 14**,** 703-10.

WELLS, D. & DELHANTY, J. D. 2000. Comprehensive chromosomal analysis of human preimplantation embryos using whole genome amplification and single cell comparative genomic hybridization. *Mol Hum Reprod,* 6**,** 1055-62.

WHITTEN, W. K. 1956. Culture of tubal mouse ova. *Nature,* 177**,** 96.

WIANNY, F. & ZERNICKA-GOETZ, M. 2000. Specific interference with gene function by double-stranded RNA in early mouse development. *Nat Cell Biol,* 2**,** 70-5.

WILCOX, A. J., WEINBERG, C. R., O'CONNOR, J. F., BAIRD, D. D., SCHLATTERER, J. P., CANFIELD, R. E., ARMSTRONG, E. G. & NISULA, B. C. 1988. Incidence of early loss of pregnancy. *N Engl J Med,* 319**,** 189-94.

WILLADSEN, S. M. 1981. The development capacity of blastomeres from 4- and 8-cell sheep embryos. *J Embryol Exp Morphol,* 65**,** 165-72.

WILLADSEN, S. M. & POLGE, C. 1981. Attempts to produce monozygotic quadruplets in cattle by blastomere separation. *Vet Rec,* 108**,** 211-3.

WILLIAMS, B. R., PRABHU, V. R., HUNTER, K. E., GLAZIER, C. M., WHITTAKER, C. A., HOUSMAN, D. E. & AMON, A. 2008. Aneuploidy affects proliferation and spontaneous immortalization in mammalian cells. *Science,* 322**,** 703-9.

WILTON, L. 2002. Preimplantation genetic diagnosis for aneuploidy screening in early human embryos: a review. *Prenat Diagn,* 22**,** 512-8.

WILTON, L., WILLIAMSON, R., MCBAIN, J., EDGAR, D. & VOULLAIRE, L. 2001. Birth of a healthy infant after preimplantation confirmation of euploidy by comparative genomic hybridization. *N Engl J Med,* 345**,** 1537-41.

WOLSTENHOLME, J. 1996. Confined placental mosaicism for trisomies 2, 3, 7, 8, 9, 16, and 22: their incidence, likely origins, and mechanisms for cell lineage compartmentalization. *Prenatal Diagnosis,* 16**,** 511-524.

WONG, C. C., LOEWKE, K. E., BOSSERT, N. L., BEHR, B., DE JONGE, C. J., BAER, T. M. & REIJO PERA, R. A. 2010. Non-invasive imaging of human embryos before embryonic genome activation predicts development to the blastocyst stage. *Nat Biotechnol,* 28**,** 1115-21.

YAMANAKA, Y., LANNER, F. & ROSSANT, J. 2010. FGF signal-dependent segregation of primitive endoderm and epiblast in the mouse blastocyst. *Development,* 137**,** 715-24.

YOSHIZAWA, M., KONNO, H., ZHU, S., KAGEYAMA, S., FUKUI, E., MURAMATSU, S., KIM, S. & ARAKI, Y. 1999. Chromosomal diagnosis in each individual blastomere of 5- to 10-cell bovine embryos derived from in vitro fertilization. *Theriogenology,* 51**,** 1239-50.

YOSHIZAWA, M., NAKAMOTO, S., TSUNODA, Y. & MURAMATSU, T. 1990. A short-term hypotonic treatment for chromosome preparation of intact and zona-penetrated mouse embryos. *Theriogenology,* 33**,** 789-97.

YUAN, L., LIU, J. G., HOJA, M. R., WILBERTZ, J., NORDQVIST, K. & HOOG, C. 2002. Female germ cell aneuploidy and embryo death in mice lacking the meiosis-specific protein SCP3. *Science,* 296**,** 1115-8.

YUKAWA, M., ODA, S., MITANI, H., NAGATA, M. & AOKI, F. 2007. Deficiency in the response to DNA double-strand breaks in mouse early preimplantation embryos. *Biochem Biophys Res Commun,* 358**,** 578-84.

ZENZES, M. T. & CASPER, R. F. 1992. Cytogenetics of human oocytes, zygotes, and embryos after in vitro fertilization. *Hum Genet,* 88**,** 367-75.

ZENZES, M. T., WANG, P. & CASPER, R. F. 1992. Chromosome status of untransferred (spare) embryos and probability of pregnancy after in-vitro fertilisation. *Lancet,* 340**,** 391-4.

ZIEGLER-BIRLING, C., HELMRICH, A., TORA, L. & TORRES-PADILLA, M. E. 2009. Distribution of p53 binding protein 1 (53BP1) and phosphorylated H2A.X during mouse preimplantation development in the absence of DNA damage. *Int J Dev Biol,* 53**,** 1003-11.

ZINAMAN, M. J., CLEGG, E. D., BROWN, C. C., O'CONNOR, J. & SELEVAN, S. G. 1996. Estimates of human fertility and pregnancy loss. *Fertil Steril,* 65**,** 503-9.

ZIOMEK, C. A. & JOHNSON, M. H. 1982. The roles of phenotype and position in guiding the fate of 16-cell mouse blastomeres. *Dev Biol,* 91**,** 440-7.